



## The Otter Project

[www.otterproject.org](http://www.otterproject.org)

July 20, 2018

Central Coast Regional Water Quality Control Board  
895 Aerovista Place, Suite 101  
San Luis Obispo, CA 93401  
ATTN: Peter von Langen and Sheila Soderberg

Via email: [peter.vonlangen@waterboards.ca.gov](mailto:peter.vonlangen@waterboards.ca.gov)  
[Sheila.soderberberg@waterboards.ca.gov](mailto:Sheila.soderberberg@waterboards.ca.gov)

Re: **OPPOSE** Waste Discharge Requirements (R3-2018-0017) for Monterey One Water Regional Wastewater Treatment Plant

Dear Ms. Soderberg and Mr. von Langen:

Thank you for the opportunity to comment on the Waste Discharge Requirements (R3-2018-0017) for Monterey One Water Regional Wastewater Treatment Plant. The following comments are made on behalf of The Otter Project, our water quality program Monterey Coastkeeper, our ~2000 members, and our board of directors.

The Otter Project exists to protect our watersheds and coastal oceans for the benefit of California sea otters and humans through science-based policy and advocacy. California sea otters are listed as "threatened" under the Endangered Species Act. The primary threats to sea otters include contact with oil, loss of high quality habitat, fisheries interactions, and poor water quality.

The Otter Project supports the concept of the proposed project and permit but must respectfully oppose issuance of the permit until development of a time schedule order that requires denitrification of the plant's effluent.

The NPDES permit currently under discussion sets discharge limitations for both ocean discharge points (discharge 001) and inland discharge (002). [Note: The highly treated water injected to groundwater is not part of this permit]. This comment focuses on the proposed limitations at discharge point 001, ocean discharge.

Nutrient enrichment of inland and coastal ocean surface waters is a serious problem. Inland and coastal waters with enriched nutrients can become choked with growth and can become hypoxic, leading to temporary ecosystem collapse. Powerful toxins such as microcystin and domoic acid can be produced by algal blooms and can poison or kill pets and wildlife and can sicken or kill people. Coastal harmful algal blooms, caused by the discharge of nutrients, has

P.O. Box 269  
Monterey, CA 93942  
831/663-9460

closed entire multi-State commercial fishing seasons leading to family and community hardship and national declarations of economic disaster.

The proposed permit, based on the California Ocean Plan, sets an effluent limit (ocean discharge 001) of 87,000 pounds of ammonia (as N) per day (pg 7). Ammonia is only one part of the total nitrogen in the effluent. While every mix of waste effluent is unique, values for typical strength domestic wastewater as determined by Metcalf and Eddy, Inc, Wastewater Engineering Treatment, Disposal, and Reuse, Third Addition, 1991 are shown below:

Typical Composition of Domestic Wastewater

Parameter	Average Concentration (mg/l)	Typical Range (mg/l)
Ammonia nitrogen	25	12-50
Nitrate + Nitrite	0	0
Organic Nitrogen	15	8-35
Total Nitrogen	40	20-85

In addition to domestic wastewater, the Monterey One Water supply-water will be fortified with nitrate-rich agricultural return water.

The Central Coast Board has the ability, and should, set stricter limits to meet our local conditions.

Nationally, various workgroups and workshops have been convened to review the scientific information, evaluate tools to address nutrient pollution, identify barriers to progress, and outline next steps. In a March 2011 memorandum to the states, tribes, and territories, the EPA Acting Assistant Administrator for Water reiterated the need for action by stating: "States, EPA, and stakeholders, working in partnership, must make greater progress in accelerating the reduction of nitrogen and phosphorus loadings to our nation's waters."

US EPA [in the past] has taken aggressive steps to help WWTP reduce their harmful nutrient discharge. In 2015, EPA released a report entitled, "Case Studies on Implementing Low-Cost Modifications to Improve Nutrient Reduction at Wastewater Treatment Plants."<sup>1</sup> A link to this report was provided to Monterey One Water in 2015 when The Otter Project first advocated for improved nutrient treatment practices for this project. In addition to these low-cost nitrogen reducing operational suggestions, denitrification bio-reactors are widely used throughout the

<sup>1</sup> <http://www2.epa.gov/nutrient-policy-data/reports-and-research#reports>

United States. According to US EPA, a significant percentage, 43-percent, of California WWTP have nitrogen effluent limits as part of their permit (Hawaii leads with 50-percent)<sup>2</sup>.

Nitrate (and phosphate) pollution is of critical concern to sea otters. Nutrient enriched freshwater surface waters cause freshwater toxic blooms of the cyanobacteria *Microcystis*; the microcystin toxin is flushed downstream into the nearshore, concentrated by shellfish, eaten by otters, and ultimately leading to microcystin poisoning and death of the otter. Miller et. al. 2010. <http://journals.plos.org/plosone/article?id=10.1371/journal.pone.0012576> . We believe, nutrient discharges at discharge point 002 could lead to microcystin poisoning. However, as already noted, we are focusing this letter on discharge point 001.

Sea otters also die from exposure to domoic acid poisoning caused by nutrient enrichment and bloom of the marine toxic algae (actually a diatom) *Pseudo-nitzschia*. Domoic acid poisoning kills sea otters, scores of whales and dolphins, hundreds of sea lions, and thousands of marine birds. The massive “red tide” (popularly known by oceanographers as the red-blob) of 2015-2016 stretched from Santa Barbara to the Oregon border and closed the most commercially valuable fishery in California, Dungeness crab. According to Governor Brown’s disaster declaration, the closure caused by the domoic acid producing diatom *Pseudo-nitzschia* caused \$48.3 million of **direct** economic impact (ex-vessel value)<sup>3</sup>. Fishing families and communities of Santa Barbara, Morro Bay, Monterey, and Moss Landing were especially hard hit. Dr. Clarissa Anderson, Post-Doctoral Sea Grant Fellow at U.C. Santa Cruz had been studying toxic algal blooms along the California coast and gave this quote to Sea Grant Bulletin, “We have seen a 30- to 100-fold increase in domoic acid in water samples in the last decade or so.” (An overview of the issue including impacts on marine mammals and birds can be found in the nine-minute news report found at <https://vimeo.com/104728711>). We believe, nutrient discharges at discharge point 001 contribute to coastal toxic algal blooms.

The science of coastal toxic algal blooms is rapidly advancing. Only two decades ago, coastal upwelling was considered the predominant, or only, source of nutrients along the California Coast. The increasing frequency of toxic algal blooms, including in years and seasons of low-to no upwelling (such as 2015) stimulated current research. The emerging picture is complex: Any nutrient, including agricultural nutrients or upwelling can cause a “bloom” of algae and diatoms; but it is the presence of concentrations of urea – a common contaminant in WWTP effluent -- that causes an innocuous bloom to turn toxic. Like storms and climate change, it is difficult to say any single bloom has been triggered by human-caused discharges; but it is the increasing frequency, toxicity, and duration that is telling.

Recent (over the past five years) has shown that rivers and streams, and “submarine groundwater discharge” (groundwater originating inland and making its way to the ocean) are seasonally dominant sources of nutrients.

---

<sup>2</sup> [https://www.epa.gov/sites/production/files/2017-06/documents/potw\\_nutrient\\_lim\\_and\\_mon\\_as\\_of\\_2\\_5\\_2016\\_2.08.17.pdf](https://www.epa.gov/sites/production/files/2017-06/documents/potw_nutrient_lim_and_mon_as_of_2_5_2016_2.08.17.pdf) published in 2017 using 2016 data

<sup>3</sup> Governor Brown’s disaster declaration found at <https://nrm.dfg.ca.gov/FileHandler.ashx?DocumentID=116284&inline>

Lane, J. et. al. 2011. Assessment of river discharge as a source of nitrate-1 nitrogen to Monterey Bay, California. Submitted but unpublished.

Howard, M, et. al. 2014. Anthropogenic nutrient sources rival natural sources on small scales in the coastal waters of the Southern California Bight. *Limnol. Oceanogr.*, 59(1), 2014, 285–297.

Lecher, A. et. al. 2015. Nutrient Loading through Submarine Groundwater Discharge and Phytoplankton Growth in Monterey Bay, CA. *Environmental Science & Technology* 2015 49 (11), 6665-6673.

Finally, the link between anthropogenic nutrients and toxic algal blooms has been established.

Howard, M. et. al. 2007. Nitrogenous preference of toxigenic *Pseudo-nitzschia australis* (Bacillariophyceae) from field and laboratory experiments. *Harmful Algae* 6 (2007) 206–217.

Kudela, R. et. al. 2008. The potential role of anthropogenically derived nitrogen in the growth of harmful algae in California, USA. *Harmful Algae* 8 (2008) 103–110.

Lane, J. et. al. 2009. Development of a logistic regression model for the prediction of toxigenic *Pseudo-nitzschia* blooms in Monterey Bay, California. *Mar Ecol Prog Ser* 383: 37–51, 2009.

Anderson, C.R., Edwards, C.A., Goebel, N.L., Kudela, R.M., 2013. Forecasting the terrestrial influence on domoic acid production: A mechanistic approach. In: 7th Symposium on Harmful Algae in the US. Abstract is available at: <http://www.whoi.edu/fileserver.do?id=208984&pt=2&p=28786> .

Lecher, A. et. al. 2015. Ibid.

**Our recommendation for Discharge Point 001:** Harmful algal blooms are killing federally listed sea otters, closing commercial fisheries, and impacting commercial fishing dependent families and communities. Monterey One Water and its customers can afford denitrification technologies to stop the nutrient pollution of Monterey Bay and should be required to do so. Monterey One Water has the lowest rates in Monterey County and their rate of \$15.85 is well below the statewide average of \$44.10.<sup>4</sup> As stated on the Monterey One Water website, “M1W rates and charges continue to be among the lowest in California.”<sup>5</sup> The discharge of a nutrient enriched waste stream into the nearshore ocean environment should be avoided and

---

4

[https://www.waterboards.ca.gov/water\\_issues/programs/grants\\_loans/srf/docs/fy1617/fy1617ww\\_user\\_charge\\_survey.pdf](https://www.waterboards.ca.gov/water_issues/programs/grants_loans/srf/docs/fy1617/fy1617ww_user_charge_survey.pdf)

<sup>5</sup> [http://montereyonewater.org/billpay\\_rates\\_comparisons\\_process.html](http://montereyonewater.org/billpay_rates_comparisons_process.html).

not permitted. However, we understand Monterey One Water is asking for the Regional Board to permit a project that is already well underway. Therefore, we respectfully request:

- Starting immediately, Monterey One Water should monitor and report, on a monthly basis, total nitrogen, Kjeldahl nitrogen, and ammonia, both as concentrations and loads.
- We request that the current permit be revised to include a time schedule order for either:
  - Ocean discharge be entirely discontinued as has been the stated goal of Monterey One Water, or;
  - Monterey One Water attain a total nitrogen discharge limitation protective of commercial fisheries and endangered species beneficial use. This limitation should be set in consultation with independent scientists such as Dr. Clarissa Anderson, Dr. Mary Silver, and Dr. Raphe Kudela.

**In conclusion**

The Otter Project opposes the proposed permit but could support a permit that includes a time schedule order including monitoring and reporting requirements, discharge limitations protective of commercial fisheries and endangered species, and a date-certain for compliance.

Monterey County's ground and surface waters are critically impaired by nutrient pollution. Simply redistributing the pollution from one area to another – the nearshore ocean -- is inconsistent with the goals of the Regional Water Quality Control Board. Waste and fertilizer laden source waters will be carried to the very water treatment facility where treatment is possible, and it would be an abuse of this special opportunity to not deal with this county's – this State's -- nutrient pollution problem.

Please, feel free to contact me if you have questions or require clarifications.

Sincerely,



Steve Shimek  
Executive Director  
exec@otterproject.org

# Nitrogenous preference of toxigenic *Pseudo-nitzschia australis* (Bacillariophyceae) from field and laboratory experiments

Meredith D. Armstrong Howard<sup>a,\*</sup>, William P. Cochlan<sup>b</sup>,  
Nicolas Ladizinsky<sup>1</sup>, Raphael M. Kudela<sup>a</sup>

<sup>a</sup> Ocean Science Department, University of California, Santa Cruz, 1156 High Street, Santa Cruz, CA 95064, USA

<sup>b</sup> Romberg Tiburon Center for Environmental Studies, San Francisco State University,  
3152 Paradise Drive, Tiburon, CA 94920-1250, USA

Received 12 July 2005; received in revised form 19 June 2006; accepted 29 June 2006

## Abstract

Field and laboratory experiments were designed to determine the differential growth and toxin response to inorganic and organic nitrogen additions in *Pseudo-nitzschia* spp. Nitrogen enrichments of 50  $\mu\text{M}$  nitrate ( $\text{KNO}_3$ ), 10  $\mu\text{M}$  ammonium ( $\text{NH}_4\text{Cl}$ ), 20  $\mu\text{M}$  urea and a control (no addition) were carried out in separate carboys with seawater collected from the mouth of the San Francisco Bay (Bolinas Bay), an area characterized by high concentrations of macronutrients and iron. All treatments showed significant increases in biomass, with chlorophyll *a* peaking on days 4–5 for all treatments except urea, which maintained exponential growth through the termination of the experiment. *Pseudo-nitzschia australis* Frenguelli abundance was  $10^3$  cells  $\text{l}^{-1}$  at the start of the experiment and increased by an order of magnitude by day 2. Particulate domoic acid (pDA) was initially low but detectable ( $0.15 \mu\text{g l}^{-1}$ ), and increased throughout exponential and stationary phases across all treatments. At the termination of the experiment, the urea treatment produced more than double the amount of pDA ( $9.39 \mu\text{g l}^{-1}$ ) than that produced by the nitrate treatment ( $4.26 \mu\text{g l}^{-1}$ ) and triple that of the control and ammonium treatments ( $1.36 \mu\text{g l}^{-1}$  and  $2.64 \mu\text{g l}^{-1}$ , respectively). The mean specific growth rates, calculated from increases in chlorophyll *a* and from cellular abundance of *P. australis*, were statistically similar across all treatments.

These field results confirmed laboratory experiments conducted with a *P. australis* strain isolated from Monterey Bay, CA (isolate AU221-a) grown in artificial seawater enriched with 50  $\mu\text{M}$  nitrate, 50  $\mu\text{M}$  ammonium or 25  $\mu\text{M}$  of urea as the sole nitrogen source. The exponential growth rate of *P. australis* was significantly slower for cells grown on urea (*ca.*  $0.5 \text{ day}^{-1}$ ) compared to the cells grown on either nitrate or ammonium (*ca.*  $0.9 \text{ day}^{-1}$ ). However the urea-grown cells produced more particulate and dissolved domoic acid (DA) than the ammonium- or nitrate-grown cells. The field and laboratory experiments demonstrate that *P. australis* is able to grow effectively on urea as the primary source of nitrogen and produced more pDA when grown on urea in both natural assemblages and unialgal cultures. These results suggest that the influence of urea from coastal runoff may prove to be more important in the development or maintenance of toxic blooms than previously thought, and that the source of nitrogen may be a determining factor in the relative toxicity of west coast blooms of *P. australis*.

© 2006 Elsevier B.V. All rights reserved.

**Keywords:** Domoic acid; Harmful algae; Nitrogen; *Pseudo-nitzschia australis*; Urea

## 1. Introduction

The occurrence of harmful algal blooms (HABs) appears to be increasing in both frequency and intensity in recent years (e.g., see reviews by Hallegraeff, 1993;

\* Corresponding author. Tel.: +1 831 247 7206;  
fax: +1 831 459 4882.

E-mail address: [Meredith@pmc.ucsc.edu](mailto:Meredith@pmc.ucsc.edu) (M.D.A. Howard).

<sup>1</sup> Current address: U.S. Geological Survey, Menlo Park Campus,  
Bldg. 3, 345 Middlefield Rd., Menlo Park, CA 94025, USA.

Anderson et al., 2002; Glibert et al., 2005a). This is especially evident along the central California coast where amnesic shellfish poisoning (ASP) events caused by toxic blooms of the diatom *Pseudo-nitzschia* spp. have increased dramatically over the last decade (Buck et al., 1992; Scholin et al., 2000; Trainer et al., 2000). The first major ASP event identified in North America occurred in 1987 in eastern Prince Edward Island, Canada, where a toxic bloom of *Pseudo-nitzschia multiseries* Hasle (Bates et al., 1989) resulted in 107 illnesses and the deaths of three people after ingesting contaminated blue mussels (*Mytilus edulis*) (Perl et al., 1990). Blooms of *Pseudo-nitzschia australis* in Monterey Bay, California were first recorded during the fall months of 1989, 1990 and 1991 as well as the spring of 1990 and summer of 1991 (Buck et al., 1992). In September 1991, the first confirmed report of domoic acid poisoning on the U.S. west coast resulted in the mortality of more than 100 brown pelicans (*Pelecanus occidentalis*) and Brandt's cormorants (*Phalacrocorax penicillatus*) (Fritz et al., 1992; Work et al., 1993). In 1998 another bloom, which spanned the central California coast, resulted in the deaths of over 400 sea lions (*Zalophus californianus*) due to consumption of contaminated northern anchovies (*Engraulis mordax*) (Scholin et al., 2000; Trainer et al., 2000).

As a result of these events, a number of laboratory studies on *Pseudo-nitzschia* were initiated, which identified macronutrient limitation as an important factor affecting cellular toxicity (Pan et al., 1996a,b,c; Bates, 1998). Although initial studies focused on macronutrients, iron and copper limitation, as well as elevated copper conditions, have been shown in laboratory studies to induce toxin production in both *P. multiseries* and *P. australis* (Maldonado et al., 2002; Ladizinsky and Smith, 2003; Wells et al., 2005). Domoic acid (DA) has been shown to form chelates with both of these trace metals, potentially increasing the biological availability of iron and/or decreasing the toxicity of copper (Ladizinsky and Smith, 2000; Rue and Bruland, 2001). However, Bates et al. (2000) reported DA levels were 10 times lower in iron-stressed cultures relative to iron-replete cultures of *P. multiseries*.

Substantial variability in growth and toxicity has been shown among different *Pseudo-nitzschia* species as well as isolates of the same species in culture from the same geographical area (Bates, 1998; Kudela et al., 2003a). Macronutrient limitation (silicate and phosphate, but not nitrogen) is known to induce toxin production in *P. multiseries* (Pan et al., 1996a,b; Bates, 1998). Pan et al. (1996a,b) proposed two different stages in the production of DA under silicate limitation. The first occurs during

the late exponential phase, characterized by slower growth rates and moderate DA production. The second stage occurs during stationary phase and is distinguished by the depletion of silicate and a significant increase in toxin production per cell (an order of magnitude higher in batch culture). Similar results were found under phosphate limitation. Pan et al. (1996c) showed an increase in the production of domoic acid in *P. multiseries*, in both steady-state continuous culture and batch cultures, when phosphate concentrations were limiting and alkaline phosphatase activity was high. There have been fewer laboratory studies using strains of *P. australis*. Garrison et al. (1992) isolated *P. australis* from the Monterey Bay bloom in 1991, and conducted batch culture experiments with two strains that confirmed DA production by this species with maximum particulate DA concentrations of 37 pg cell<sup>-1</sup> and 12 pg cell<sup>-1</sup>.

Despite the many studies on toxin production and nutrient limitation, very few studies have evaluated the nutritional preference of *Pseudo-nitzschia* spp., particularly in terms of nitrogen sources. In laboratory experiments, Bates et al. (1993) grew cultures of *P. multiseries* with varying concentrations of ammonium and nitrogen, ranging from 55 μM to 880 μM, and found that at less than 110 μM N the growth of the cells and the production of DA were the same for nitrate- and ammonium-grown cultures. Hillebrand and Sommer (1996) also evaluated the nitrogenous preference of *P. multiseries* by using nitrate, ammonium and urea in batch cultures. In a batch culture with initial concentrations of 40 μM ammonium, the growth rate increased with increasing concentration of nitrate added to the culture, which the authors interpreted as an alleviation of ammonium inhibition of nitrate uptake, whereas at growth-saturating nitrate concentrations, ammonium additions decreased the growth rate of *P. multiseries*.

While there have been numerous laboratory studies using isolates of *P. multiseries*, this is the first study to examine the nitrogenous nutrition (including urea) of *P. australis*, the predominant DA producer in California waters. In contrast to previous nitrogen-based studies, the field and laboratory experiments reported here were designed to identify differential responses to ammonium, nitrate and urea enrichment using ecologically relevant nitrogen concentrations.

## 2. Materials and methods

### 2.1. Field experiment

Nutrient addition experiments were conducted aboard the R/V *Point Sur* during February 2003. Seawater was

collected in the vicinity of the San Francisco Bay (Bollinas Bay, 37°51.30'N, 122°39.13'W). At the time of collection, there was a broad chlorophyll maximum that ranged from 4 m to 14 m depth, a surface mixed layer temperature of 12.5 °C and a practical salinity of 31.5. Ten-liter PVC Niskin bottles (refitted with silicone rubber band springs) mounted on an instrumented rosette were used to collect seawater from 4 m depth. Although water was not collected using strict trace metal clean protocols, reasonable care was taken to reduce the risk of metal contamination. On the same cruise, water collected in the same fashion, but from a high nutrient low chlorophyll (HNLC) coastal region was apparently not contaminated by iron, as evidenced by the lack of enhanced phytoplankton growth under multi-day, deck incubation conditions (data not shown).

Four 9-liter acid-cleaned polycarbonate (Nalgene) carboys were rinsed three times and filled with seawater using multiple Niskin bottles. Carboys were then either unenriched (control) or enriched with nitrogen and placed in a deckboard incubator maintained at the ambient surface temperature (with running seawater) and *ca.* 50% surface irradiance (using neutral density screening). The ambient nitrogen concentration of the seawater collected for the experiment was 6.6 μM nitrate, 1.76 μM ammonium, and 0.9 μM urea. Three separate nutrient treatments were conducted where 42.4 μM nitrate (as KNO<sub>3</sub>) was added to the first carboy (total nitrate 49 μM), 10 μM ammonium (as NH<sub>4</sub>Cl) was added to the second carboy (total ammonium 11.76 μM) and 20 μM urea was added to the third carboy (total urea 20.9 μM). There was also a control (no addition). Reagent grade stocks and Milli-Q<sup>®</sup> water were used to prepare all nutrient enrichments. Incubations were maintained for 3 days at sea in a deckboard incubator (mean daily irradiance *ca.* 350 μmol photons m<sup>-2</sup> s<sup>-1</sup>), and subsequently transferred to a walk-in environmental chamber (15 °C and *ca.* 100 μmol photons m<sup>-2</sup> s<sup>-1</sup> irradiance using “cool-white” fluorescent lamps and a 12:12 light:dark cycle) at the University of California Santa Cruz (due to termination of the cruise) for the remainder of the experiment.

### 2.1.1. Analytical methods

Samples for chlorophyll *a* were collected daily in triplicate and filtered onto uncombusted glass-fiber filters (Whatman GF/F; nominal pore size 0.7 μm); separate samples for size fractionated chlorophyll *a* were determined using 1-μm and 5-μm polycarbonate filters (Poretics), frozen in liquid nitrogen and processed using the non-acidification method (Welschmeyer, 1994). Macronutrients (nitrate plus nitrite [hereafter referred

to as nitrate], silicate and *ortho*-phosphate) were sampled daily, stored frozen, and later analyzed with a Lachat Quick Chem 8000 Flow Injection Analysis system using standard colorimetric techniques (Knepel and Bogren, 2001; Smith and Bogren, 2001a,b). Ammonium and urea samples were collected using 60 ml low-density polyethylene (LDPE) centrifuge tubes (Corning<sup>®</sup>). Ammonium samples were stored refrigerated after the addition of the phenolic reagent; the addition of the phenolic reagent binds ammonium and eliminates the need to freeze samples (Degobbis, 1973). The remaining reagents were added within 120 h, and the samples were manually analyzed using a spectrophotometer equipped with a 10-cm cell (Solarzano, 1969). Urea samples were frozen at -20 °C, and subsequently thawed ashore at room temperature before manual analysis using the diacetyl monoxime thiosemicarbazide technique (Price and Harrison, 1987), modified to account for a longer time period (72 h) and lower digestion temperature (22 °C). Particulate domoic acid (pDA) samples were filtered onto uncombusted Whatman GF/F filters and processed according to the method of Pocklington et al. (1990), using high performance liquid chromatography with fluorescence detection. At two time points, *P. australis* was identified using large subunit rRNA-targeted fluorescent probes (whole cell) as described by Miller and Scholin (1998). The samples were also probed for *P. multiseriis* but this species was not present. Samples (10 ml) from each treatment were collected in triplicate, on days 0 and 2, filtered and immediately preserved in saline ethanol for later microscopic analysis in the laboratory. Because rRNA probes were not available for the remaining sample points, whole-water samples were collected on all days, to be preserved with acidified Lugol's solution; however, after inspecting the samples, it was apparent that 1% non-acidic Lugol's solution was erroneously used. Therefore, it was not possible to use these samples for phytoplankton floristic analysis. Visual examination of the positive whole-cell probe samples (which probes all phytoplankton) provided a record of dominant groups.

### 2.2. Laboratory experiments

*P. australis* was isolated from Monterey Bay, California (isolate AU221-a), and grown as batch cultures in filter-sterilized (0.2 μm), nutrient-enriched artificial seawater (modified ESAW; Harrison et al., 1980) at the Romberg Tiburon Center; modifications to this artificial seawater included reducing the nitrogen enrichment to 50 μM nitrate, 50 μM ammonium and 25 μM urea, respectively, for each treatment. Other

modifications are described in detail by Berges et al. (2003). Cultures were maintained at  $15 (\pm 0.3) ^\circ\text{C}$  with irradiance levels at  $100 \mu\text{mol photons m}^{-2} \text{s}^{-1}$  for a 12:12 light:dark cycle. Cell samples were fixed in 1% acidic Lugol's solution and counted using a Palmer-Maloney nanoplankton counter at  $100\times$  using a phase contrast microscope (Eclipse E4000, Nikon<sup>®</sup>). Chlorophyll *a* samples were collected during the late exponential phase; 20 ml of each treatment was filtered onto uncombusted Whatman GF/F filters, extracted in 90% acetone and analyzed as described for the field experiment. Particulate and dissolved DA samples were also taken towards the end (late exponential phase) of the experiment and analyzed using the ELISA method (Garthwaite et al., 2001). For particulate determinations, cells were filtered onto  $0.2\text{-}\mu\text{m}$  pore-sized polycarbonate filters (Nuclepore) that were placed in 4-ml vials containing 2-ml deionized water (Millipore). They were cycled through four freeze–thaw sequences using liquid nitrogen and boiling water to liberate the water-soluble DA molecule from the cellular matrix. After the samples were refiltered through a  $0.2\text{-}\mu\text{m}$  acrodisc syringe filter, aliquots of the supernatant were analyzed with appropriate dilutions. The  $0.2\text{-}\mu\text{m}$  filtrate was collected for measurement of dissolved DA and analyzed directly without dilution. *In vivo* chlorophyll *a* and the ratio of variable ( $F_v$ ) to maximum ( $F_m$ ) fluorescence measured during the dark cycle using DCMU (Cullen and Renger, 1979) were determined daily on a Turner Designs 10-AU fluorometer. All experiments were conducted in triplicate for each nitrogen source.

### 3. Results

#### 3.1. Field experiment

Seawater was collected during a period of minimal prior rainfall, low ambient nutrient levels, and a relatively homogenous water column to 50 m depth. Total biomass (as chlorophyll *a*) in the carboys was initially moderate ( $4.03 \mu\text{g l}^{-1}$  on day 0) and increased significantly with the addition of each nitrogen substrate as well as in the control (Fig. 1A). The maximum chlorophyll values were recorded on day 4 for the nitrate addition and the control ( $29.33 \mu\text{g l}^{-1}$  and  $19.9 \mu\text{g l}^{-1}$ , respectively) and on day 5 for the ammonium addition ( $28.48 \mu\text{g l}^{-1}$ ). The urea addition was still in exponential growth on day 7 ( $30.40 \mu\text{g l}^{-1}$ ) (Fig. 1B). Size fractionated chlorophyll indicated that most of the biomass was greater than  $1.0 \mu\text{m}$ .

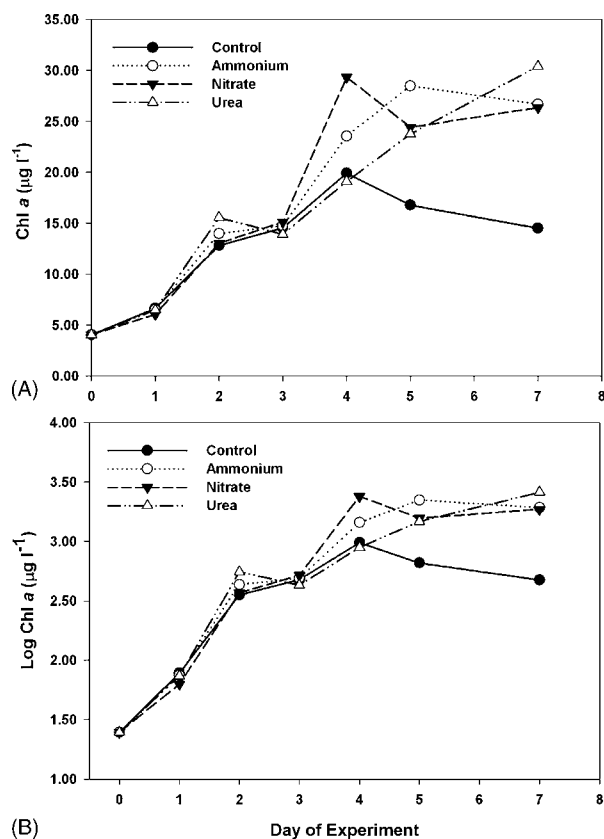


Fig. 1. (A) Total phytoplankton community chlorophyll *a* measured daily from the field experiment and (B) semi-log plot of growth of the same samples for each nitrogen treatment: control (●), ammonium (○), nitrate (▼) and urea (▽). Samples were not taken on day 6 of the experiment. Values are the mean of triplicate samples.

#### 3.1.1. Domoic acid

Initially, particulate domoic acid (pDA) was low but easily detectable,  $0.15 \mu\text{g l}^{-1}$  on day 0 (Fig. 2). However, by day 4 during exponential growth, the pDA of the community increased to the following: nitrate addition,  $0.41 \mu\text{g l}^{-1}$ ; ammonium addition (the highest on day 4),  $1.50 \mu\text{g l}^{-1}$ ; urea addition,  $1.04 \mu\text{g l}^{-1}$ ; the control,  $0.46 \mu\text{g l}^{-1}$ . By the end of the experiment (day 7), the urea treatment produced significantly more pDA ( $9.39 \mu\text{g l}^{-1}$ ) and was still in exponential growth, while the control was still the lowest at  $1.36 \mu\text{g l}^{-1}$  and it had entered stationary phase. Both the nitrate and ammonium additions were in stationary phase on day 7, when pDA increased to  $4.26 \mu\text{g l}^{-1}$  and  $2.64 \mu\text{g l}^{-1}$ , respectively. Using the days 0 and 2 *P. australis* specific cell counts, per-cell toxicity was  $43 \text{ pg cell}^{-1}$  on day 0. We do not have simultaneous whole-cell probe data and toxin data for other days; however, using chlorophyll as a proxy, pDA  $\text{chl}^{-1}$  was  $38.7 \text{ ng pDA chl}^{-1}$  on day 0. By day 4, the control and nitrate addition decreased to

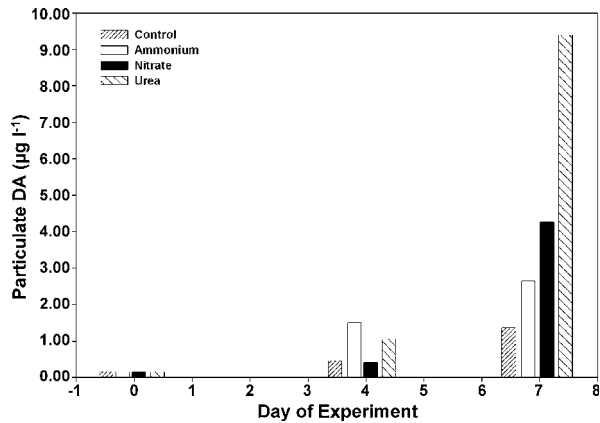


Fig. 2. Particulate domoic acid ( $\mu\text{g l}^{-1}$ ) sampled on days 0, 4, and 7 of the field experiment for each nitrogen treatment: control (lined bar), ammonium (white bar), nitrate (solid black bar), and urea (hatch bar).

23.5 ng pDA chl<sup>-1</sup> and 14.0 ng pDA chl<sup>-1</sup>, respectively, while the ammonium and urea treatments increased to 64.0 ng pDA chl<sup>-1</sup> and 54.7 ng pDA chl<sup>-1</sup>. Concentrations increased for all carboys by day 7 to 162.0 ng pDA chl<sup>-1</sup> in the nitrate addition, 99.3 ng pDA chl<sup>-1</sup> in the ammonium addition, 309.1 ng pDA chl<sup>-1</sup> in the urea addition and 94.3 ng pDA chl<sup>-1</sup> in the control carboy.

### 3.1.2. Inorganic and organic nitrogen

The ambient nitrogen concentration of the seawater used in the incubation experiments was 6.6  $\mu\text{M}$  nitrate, 1.7  $\mu\text{M}$  ammonium and 0.9  $\mu\text{M}$  urea. An additional 42.4  $\mu\text{M N}$  was added for the nitrate addition treatment, 10  $\mu\text{M N}$  for the ammonium treatment, and 20  $\mu\text{M}$  urea for the urea addition. For the ammonium treatment, the ammonium concentration was half of its initial value by day 2 and was depleted by day 5 (Fig. 3A).

The initial urea concentration did not change significantly in the nitrate (Fig. 3B) ammonium and control treatments (Fig. 3C), but decreased ~50% by day 5 in the urea treatment (Fig. 3D) which also corresponded to the time point at which nitrate was depleted. At the termination of the experiment there was still 6.6  $\mu\text{M}$  urea in the urea treatment.

Macronutrient depletion rates were calculated from a least-squares linear regression analysis of the exponential growth phase and an analysis of variance (ANOVA) determined from semi-log plots of nutrient concentration versus time (Guillard, 1973). The depletion of total nitrogen in each treatment was highest in the control treatment (Table 1) and lowest in the nitrate treatment. Because of the large amount of nitrate added (relative to the depletion rate) and due to issues associated with the

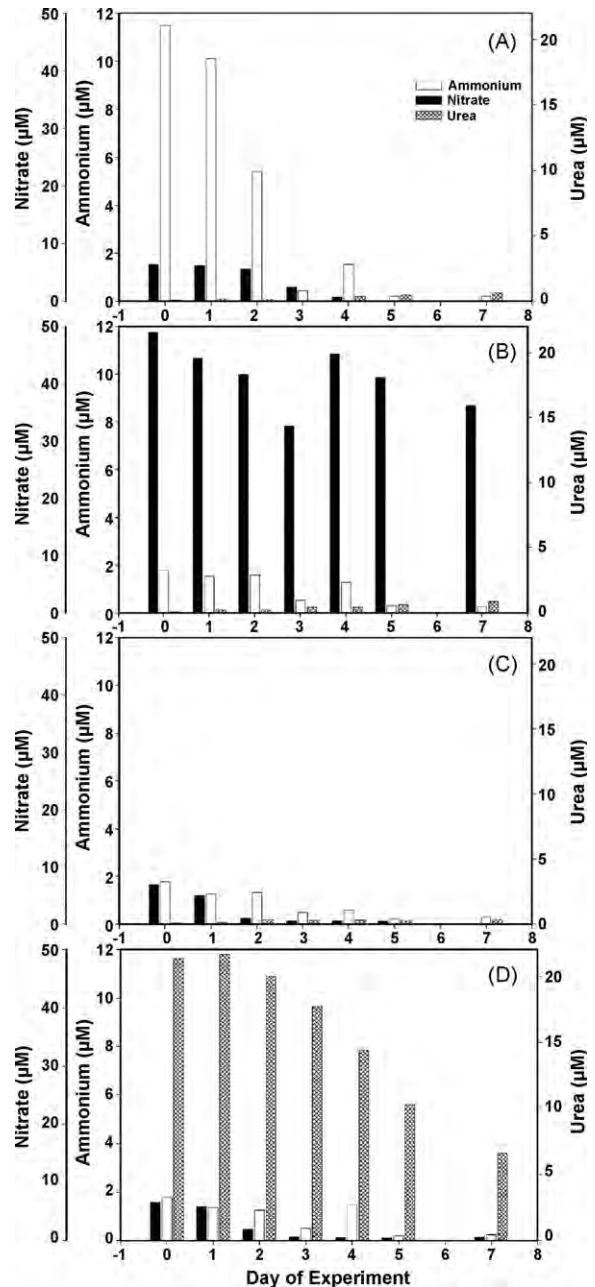


Fig. 3. Nitrate, ammonium and urea concentrations (in  $\mu\text{M}$ ) measured daily in the field experiment for each nitrogen treatment: (A) ammonium; (B) nitrate; (C) control; (D) urea. Nitrate concentration (solid black bar) on the far left axis, ammonium concentration (white bar) on the left axis and urea concentration (crosshatch bar) on the right axis. Samples were not taken on day 6 of the experiment.

analysis of these high values on the autoanalyzer, the analytical error associated with the estimate of nitrate drawdown precludes accurate estimation of nitrate depletion rates to compare with the drawdown of ammonium and urea. As a result, the depletion rates

Table 1  
Net nitrogen depletion rates for all treatments during the field experiment

Treatment	Depletion rates (day <sup>-1</sup> ) from days 0 to 3 (S.E.; n; r <sup>2</sup> )												
	Nitrate			Ammonium			Urea			Total nitrogen			
Nitrate	0.06	4	0.95	0.38	4	0.82	0.31	-0.47	4	0.92	0.06	4	0.95
Ammonium	0.30	4	0.83	0.88	4	0.88	0.61	0.13	4	0.34	0.45	4	0.89
Urea	0.35	4	0.96	0.28	4	0.90	0.05	0.06	4	0.89	0.07	4	0.96
Control	0.36	4	0.96	0.31	4	0.88	0.39	-0.48	4	0.88	0.16	4	0.98

Standard error (S.E.), number of days included in the rate calculation (*n*) and *r*-squared values (*r*<sup>2</sup>) are included in the table.

calculated for the nitrate treatment (total nitrogen and nitrate) do not accurately reflect the utilization of total nitrogen, as evidenced by the growth rates which are statistically indistinguishable across treatments. The highest net nitrate depletion rate (excluding the nitrate treatment) was in the control treatment and the lowest was in the ammonium treatment. For ammonium-based depletion rates, the ammonium treatment had the highest rate of depletion and the nitrate treatment was lowest. The ammonium-based depletion rates for the nitrate, urea and control treatments were not statistically indistinguishable ( $p < 0.05$ ). For urea depletion rates, the highest rates were observed in the ammonium treatment and lowest in the urea treatment, while the nitrate treatment and the control had positive depletion rates for urea, meaning there was an increase in urea with time, probably due to grazers.

### 3.1.3. Other nutrients

The silicate concentration was initially 23 μM and decreased to 2.7–3.5 μM in the nitrogen additions and to 8.7 μM in the control by the end of the 7-day experiment. Silicate decreased to half of the initial concentration in the nitrate and ammonium treatments by day 3, and in the urea and control treatments, by day 4. The concentration of phosphate was initially 0.8 μM and by day 3 was half of this concentration across all treatments. Phosphate was depleted by day 4 in the nitrogen additions but not until day 7 in the control treatment.

### 3.1.4. Growth rate

Growth rates for the whole phytoplankton community were calculated from a linear regression analysis of the exponential growth phase and ANOVA determined from semi-log plots of chlorophyll *a* versus time (Guillard, 1973). Growth rates were statistically

indistinguishable across all treatments ( $p > 0.05$ ): nitrate 0.48 day<sup>-1</sup> (calculated over 5 days, days 0–4); ammonium, 0.39 day<sup>-1</sup> (days 0–5); urea, 0.34 day<sup>-1</sup> (days 0–5); control, 0.40 day<sup>-1</sup> (days 0–4). Qualitative indicators of growth of *P. australis* were calculated over 2 days from enumeration of the whole cell probes taken on days 0 and 2. The ammonium treatment was the highest (1.19 day<sup>-1</sup>), followed by urea (1.16 day<sup>-1</sup>), then the control (1.08 day<sup>-1</sup>), and the lowest was the nitrate treatment (0.95 day<sup>-1</sup>) (Table 2). The growth rates of for *P. australis* were substantially higher than those calculated from the entire assemblage.

### 3.1.5. Community composition

The phytoplankton assemblage was initially diatom-dominated, with ca. 76% centric and 24% pennate

Table 2

Calculated growth rates based on the increase in phytoplankton community chlorophyll *a* (during exponential growth) and *Pseudo-nitzschia australis* cell abundance (days 0–2) during the field experiment off San Francisco Bay

Treatment	Chlorophyll growth rates (day <sup>-1</sup> ) (S.D.; n; r <sup>2</sup> )		Growth rate of <i>P. australis</i> (day <sup>-1</sup> )	
Nitrate	0.14	5	0.48	0.95
Ammonium	0.19	6	0.39	1.19
Urea	0.26	6	0.34	1.16
Control	0.16	5	0.40	1.08

Standard deviation (S.D.), number of days included in the rate calculation (*n*) and *r*-squared values (*r*<sup>2</sup>) are included in the table for chlorophyll-based rates.

forms (by number). Dominant genera included *Asterionellopsis*, *Chaetoceros*, and *Thalassiosira* spp.; other genera included *Skeletonema* and *Stephanopyxis* and, to a lesser extent, *Coscinodiscus* and *Eucampia*; dinoflagellates were negligible.

Despite the elevated growth rate for *P. australis* calculated from direct cell counts, there was a reduction from days 0 to 2 in pennate abundance (ca. 5–6.5% by number versus ca. 91–94% centrics and 0.5–2.1% dinoflagellates).

Although only two time points were available for *P. australis* enumeration (whole cell probe), *P. australis* was present in all samples. *P. australis* cell concentration was initially  $3.60 \times 10^3$  cells  $l^{-1}$  and by day 2 had increased by an order of magnitude in all treatments to the following: nitrate addition,  $2.77 \times 10^4$  cells  $l^{-1}$ ; ammonium addition,  $4.62 \times 10^4$  cells  $l^{-1}$ ; urea addition,  $4.32 \times 10^4$  cells  $l^{-1}$ ; the control,  $3.64 \times 10^4$  cells  $l^{-1}$ . At the start of the experiment, *P. australis* comprised 72% of all pennates and 17% of the whole phytoplankton community. By day 2, *P. australis* accounted for 41% of the pennates in the nitrate treatment, 86% in the ammonium treatment, 55% in the urea treatment and 69% in the control, but only 2.3–5.5% of the entire assemblage.

### 3.2. Laboratory experiment

#### 3.2.1. Growth rate

Specific growth rates during the exponential growth phase were determined from linear regressions of the natural log of cell abundance versus time (Fig. 4A and B). Comparisons of the mean ( $\pm 1$ S.D.) growth rates, using ANOVA (using post-hoc Tukey's test), indicate that the cells maintained on urea grew slower ( $0.52 \pm 0.09$  day $^{-1}$ ) than the cells grown on either nitrate ( $0.89 \pm 0.08$  day $^{-1}$ ) or ammonium ( $0.93 \pm 0.001$  day $^{-1}$ ), which both maintained significantly greater growth rates ( $p < 0.01$ ), but were indistinguishable from each other ( $p > 0.05$ ).

#### 3.2.2. Chlorophyll *a* and cellular fluorescence capacity

Chlorophyll *a* samples were collected during late exponential phase and the chlorophyll *a* per cell was statistically indistinguishable ( $p > 0.05$ ) for the nitrate and ammonium treatments ( $2.44 \pm 0.55$  pg cell $^{-1}$  and  $2.37 \pm 0.48$  pg cell $^{-1}$ , respectively). However, the urea treatment exhibited a significantly lower ( $p < 0.05$ ) mean cellular chlorophyll *a* concentration of  $0.99 \pm 0.43$  pg cell $^{-1}$ . The cellular fluorescence capacity for all nitrogen-substrate treatments, determined

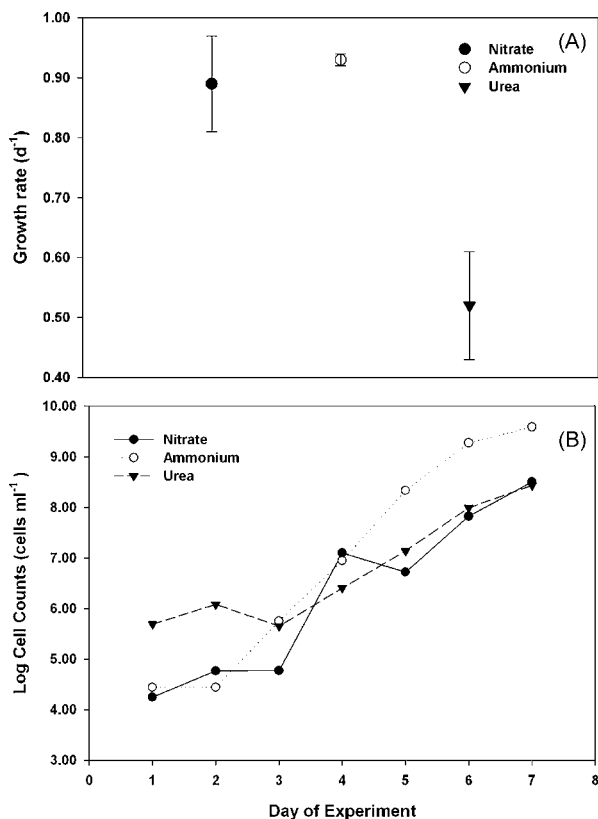


Fig. 4. (A) Growth rates derived from cell count measurements during exponential growth phase; (B) semi-log plot of cell counts measured daily from the laboratory experiment for each nitrogen treatment: (●), nitrate (○), ammonium (▼) and urea. Values are the mean of triplicate samples and error bars on the growth rate plot denote range of replicates.

using DCMU, was indistinguishable from one another during exponential growth;  $F_v/F_m$  averaged  $0.62 \pm 0.05$  ( $n = 16$ ). The  $F_v/F_m$  values did not decrease during the late exponential phase when samples were collected for chlorophyll *a* and DA.

#### 3.2.3. Domoic acid

Particulate DA was collected during late exponential growth for each culture and normalized to cell abundance; the mean ( $\pm 1$ S.D.) pDA per cell for each nitrogen treatment is presented here and graphically (Fig. 5A). The urea treatment had substantially greater pDA per cell,  $1.37 \pm 0.97$  fg cell $^{-1}$ , whereas the nitrate and ammonium treatments were lower,  $0.48 \pm 0.14$  fg cell $^{-1}$  and  $0.26 \pm 0.098$  fg cell $^{-1}$ , respectively. Overall, strain Au221-a was generally less toxic than the natural assemblages, which is consistent with previous laboratory experiments that demonstrate substantial strain-specific variability as well as a gradual loss of toxicity with time (e.g. Villac et al., 1993; Kudela et al., 2003b).

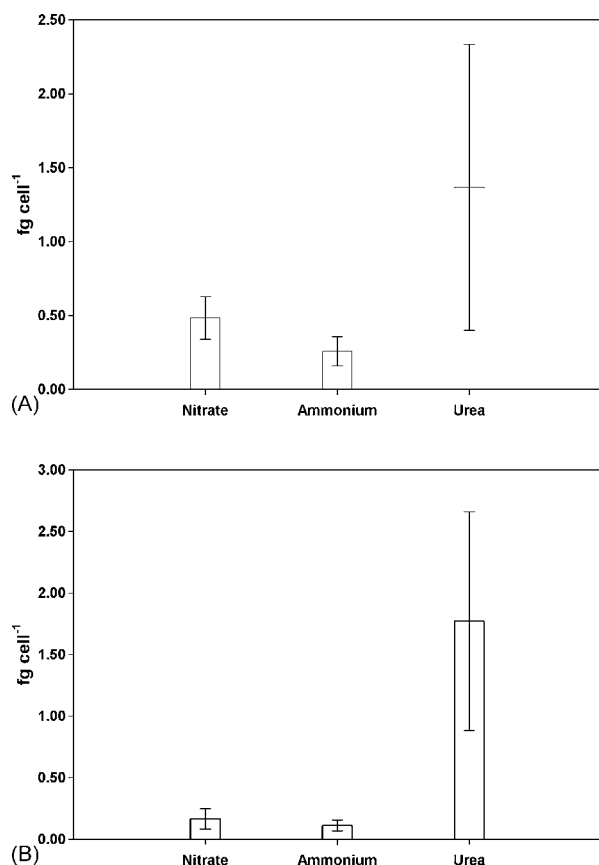


Fig. 5. Particulate (A) and dissolved (B) domoic acid per cell in the laboratory experiment. Values are means ( $n=3$ ) of domoic acid concentrations normalized to cellular abundance. Error bars represent  $\pm 1$ S.D.

Dissolved domoic acid (dDA), expressed either volumetrically (per ml of culture filtrate) or normalized to cellular abundance (Fig. 5B), was significantly greater ( $p < 0.05$ ) in the urea treatment ( $5.42 \pm 2.24 \text{ pg ml}^{-1}$ ;  $1.77 \pm 0.89 \text{ fg cell}^{-1}$ ), compared to either the nitrate treatment ( $0.80 \pm 0.34 \text{ pg ml}^{-1}$ ;  $0.165 \pm 0.082 \text{ fg cell}^{-1}$ ), or the ammonium treatment ( $1.51 \pm 0.74 \text{ pg ml}^{-1}$ ;  $0.112 \pm 0.045 \text{ fg cell}^{-1}$ ).

## 4. Discussion

### 4.1. Field experiment

The central California coast consists of a wide continental shelf characterized by seasonally high concentrations of upwelled macronutrients as well as the micronutrient iron. The supply of fine-grained sediment from river input, combined with upwelling occurring over the shelf, creates an iron-replete region ideal for diatom blooms (Bruland et al., 2001). The

phytoplankton assemblage in this region has previously been reported to be largely nitrogen and light limited during the winter (Kudela and Dugdale, 2000; Olivieri and Chavez, 2000). The oceanic conditions experienced during this experiment were typical of the winter season in central California (Wilkerson et al., 2000). Although the elevated ammonium and urea concentrations suggest the influence of San Francisco Bay outflow, Si:N ratios were relatively low ( $\sim 4:1$ ), substantially lower than reported during high-flow periods (Wilkerson et al., 2000). Consistent with these past observations, biomass (chlorophyll *a*) increased in all the field grow-out treatments, including the control, which suggests that the growth of the phytoplankton community was primarily limited by light availability and not initially limited by nitrogen.

The mean growth rates from our field data during the exponential phase were statistically indistinguishable across all nitrogen-substrate treatments, using either chlorophyll *a* concentrations or the *P. australis* cell abundance. It appears that *P. australis* does not exhibit a strong preference for any particular nitrogen source and can grow equally well on the organic substrate, urea. *P. australis*, initially present at a cell concentration of  $10^3 \text{ cells l}^{-1}$ , increased by an order of magnitude in all treatments to  $10^4 \text{ cells l}^{-1}$ , which is considered “bloom” conditions by monitoring agencies. At this cell concentration threshold, increased testing for domoic acid in coastal waters ensues (M. Silver, pers. commun.). This increase in *P. australis* across all treatments suggests that specific conditions such as stratification of the water column (alleviation of light limitation) can increase the growth of *P. australis* when nitrogen is available.

#### 4.1.1. Domoic acid

There is a wide reported range of DA concentrations for central California (Table 3). Buck et al. (1992) reported pDA concentrations in Monterey Bay of  $1.1\text{--}2.4 \text{ } \mu\text{g l}^{-1}$  in October 1991 and  $0.1\text{--}6.7 \text{ } \mu\text{g l}^{-1}$  in November 1991. *P. australis* abundances were  $(6.5\text{--}20) \times 10^4 \text{ cells l}^{-1}$  and  $(0.8\text{--}67) \times 10^4 \text{ cells l}^{-1}$ , respectively. Scholin et al. (2000) reported a range of  $7.2\text{--}31.2 \text{ pg DA per } P. australis \text{ cell}$  in Monterey Bay during the 1998 bloom. The calculated pDA in Monterey Bay on 20 May 1998, was  $0.36\text{--}9.75 \text{ } \mu\text{g l}^{-1}$ . Scholin et al. (2000) suggested that the increase in abundance of *P. australis* in the first half of May was a response to increased silicate concentrations, possibly in response to enhanced coastal runoff. El Niño conditions reduced the upwelling intensity signal along the California coast and record levels of rainfall were recorded in 1998 (Trainer

Table 3

Highest concentrations of particulate domoic acid reported in field observations for central California from 1991 to 2003 where *P. australis* was the dominant recorded organism

Location	DA ( $\mu\text{g l}^{-1}$ )	Date	Reference
Monterey Bay	1.1–2.4	October 1991	Buck et al. (1992)
Monterey Bay	0.1–6.7	November 1991	Buck et al. (1992)
Monterey Bay	9.75	May 1998	Scholin et al. (2000)
Santa Cruz Wharf	2.5	May 1998	Scholin et al. (2000)
Monterey Bay	0.36	May 1998	Scholin et al. (2000)
Point Lobos	0.18–0.27	June 1998	Trainer et al. (2000)
Morro Bay	1.3–3.8	June 1998	Trainer et al. (2000)
Point Arguello and Point Conception	2.2–7.3	June 1998	Trainer et al. (2000)
Santa Barbara	0.5–1.2	June 1998	Trainer et al. (2000)
Mouth of San Francisco Bay	0.13	June 1998	Trainer et al. (2000)
Above Point Ano Nuevo	0.44	June 1998	Trainer et al. (2000)
Monterey Bay and Point Lobos	0.38	June 1998	Trainer et al. (2000)
Bolinas Bay	0.15–9.39	February 2003	This study

Note that the values from Trainer et al. (2000) are whole water samples (particulate and dissolved domoic acid).

et al., 2000). However, even in May and June during the 1998 bloom, temperature and salinity measurements indicated oceanic conditions. Trainer et al. (2000) suggested upwelling, not enhanced river flow, as the source of nutrients that sustained the bloom. Concentrations of whole water DA on 3–5 June ranged from 1.3 to 3.8  $\mu\text{g l}^{-1}$  in Morro Bay and 2.2 to 6.3  $\mu\text{g l}^{-1}$  in Point Conception where *P. australis* was the dominant species, at abundances of  $4.9 \times 10^4$  cells  $\text{l}^{-1}$  and  $2.3 \times 10^5$  cells  $\text{l}^{-1}$ , respectively. The highest whole water DA concentrations (7.3  $\mu\text{g l}^{-1}$ ) were recorded in southern California, at Point Arguello (Trainer et al., 2000).

Results from this experiment (0.15–9.39  $\mu\text{g pDA l}^{-1}$ ) fall within the reported range for pDA values, with initial concentrations on the low end, increased concentrations across all treatments by day 4 and the highest levels achieved near the maximum pDA concentrations of 9.75  $\mu\text{g l}^{-1}$  reported by others (Scholin et al., 2000). All but the urea treatment entered stationary growth phase by the end of the experiment (day 7). The results of the urea treatment are especially significant since it produced the highest pDA on day 7, which was double the amount produced by the nitrate treatment and three times more than that of the control and ammonium treatments. The initial (days 0–2) quantitative indicators of growth of *P. australis* were similar in all of the treatments, and the mean specific growth rates calculated from community chlorophyll concentrations were also statistically indistinguishable from each other. Therefore, the large increase in pDA production cannot be explained simply by higher biomass or lower growth rates in the urea treatment. This suggests that the per-cell production of pDA was substantially greater when

grown on urea. Since the cells in the urea treatment were still growing exponentially when pDA was measured, and previous laboratory experiments have shown that the major increase in production of pDA is in stationary phase (at least for *P. multiseriis*; Pan et al., 1996a,b; Bates, 1998), one might expect pDA values to be conservative. The implications of these results are that elevated concentrations of urea from anthropogenic sources such as agricultural and urban runoff, or sewage discharge, could be a significant source of nitrogen for toxic bloom development or sustenance of *P. australis*.

#### 4.1.2. Utilization of more than one nitrogen source

The depletion of half of the initial concentration of ammonium and approximately 10% of the concentration of nitrate in the ammonium treatment by day 2, as well as the depletion of both nitrogen sources by day 5, demonstrates simultaneous utilization of more than one nitrogen source. In addition, there was no indication of any inhibitory effects of ammonium on nitrate uptake. Bates et al. (1993) showed that cultures grown at less than 110  $\mu\text{M}$  of nitrate and ammonium had equivalent growth rates and that there was no inhibition of nitrate uptake due to ammonium. As might be expected, ammonium addition stimulated ammonium depletion rates, whereas ammonium depletion rates were similar in the other treatments. Since these experiments utilized mixed phytoplankton assemblages, it is not possible to attribute these nitrogen uptake characteristics to *Pseudo-nitzschia* specifically, but *P. australis* remained the dominant pennate diatom (86%) in the ammonium treatment and accounted for 41% in the nitrate treatment.

In the urea treatment, the depletion of 6  $\mu\text{M}$  of the initial nitrate but only 2  $\mu\text{M}$  of the initial urea by day 2 indicates a slight preference for nitrate over urea. However, the depletion of nitrate by day 5 and the subsequent drawdown of urea indicate the sustained growth capabilities of the assemblage, including *P. australis*, when urea is the sole nitrogen source, particularly since this treatment was still growing exponentially on day 7. The lower depletion rates for urea across all treatments were expected since elevated ammonium concentrations ( $>1 \mu\text{M}$ ) have been shown to suppress the uptake mechanism for urea in unialgal cultures (e.g. Molloy and Syrett, 1988; Cochlan and Harrison, 1991). In addition, an increase in urea in the carboys can be attributed to grazers. Growth rates were not statistically different across treatments, but based on the growth and nitrogen depletion rates (Tables 1 and 2), there appears to be a slight preference for nitrate and ammonium relative to urea.

Although limitation by other macro- or micronutrients was not directly assessed, ambient silicate and phosphate conditions during the experiment suggest that these nutrients were not limiting (they were not completely depleted for most treatments). Iron limitation and copper toxicity were also not directly addressed; however, initial iron concentrations were elevated, as expected over this shallow shelf region (Bruland, pers. commun.). Copper concentrations can be expected to be similar across nutrient additions, so any changes in growth rate or toxin production are not directly attributable to changes in copper toxicity.

## 4.2. Laboratory experiment

### 4.2.1. Growth rates and chlorophyll *a*

Laboratory experiments indicated that the concentration of chlorophyll *a* per cell was two- to three-fold less in the urea treatment compared to the nitrate and ammonium treatments. The low chlorophyll *a* per cell in the urea treatment could indicate possible nutrient stress, but the cellular fluorescence capacity for each nitrogen treatment did not differ (mean  $F_v/F_m = 0.62$ , and did not decline with time), suggesting that the physiological status was unaffected by the nitrogen source supporting growth. However, the exponential growth rate (determined using cell abundance) of *P. australis* was significantly slower for cells grown on urea compared to those grown on nitrate and ammonium, which both maintained similar growth rates. These laboratory results demonstrate the capability of this diatom to grow equally well on oxidized and reduced forms of nitrogen, and that *P. australis* is

capable of using urea as the sole nitrogen source for growth, albeit at a somewhat slower rate than cultures grown on either nitrate or ammonium.

### 4.2.2. Domoic acid

The highest level of particulate domoic acid (pDA) per cell occurred in the urea treatment. As with the urea-amended field experiment, cells from the laboratory cultures were harvested in late logarithmic phase for particulate and dissolved domoic acid (dDA) analysis, and it is possible that urea-grown cells could potentially produce higher pDA cell<sup>-1</sup> once the cells enter stationary phase. In addition, the dDA (normalized to cell abundance) was  $\sim 140\%$  of the pDA in the urea treatment whereas in the ammonium and nitrate treatments dDA/pDA only averaged 40–50%. This ratio of dDA/pDA is unusually high for cells harvested in late logarithmic phase. However, there are no other published results at this concentration of ammonium. The results for the laboratory experiment were similar to those of the field experiment in that DA production as a function of nitrogen source was greatest when nitrogen was derived solely from urea, followed by nitrate and ammonium, which were statistically indistinguishable. Assuming that DA production would continue to increase as cells entered stationary phase, and that a considerable fraction of DA is dissolved, our estimates of enhanced toxicity when grown on urea are likely conservative.

## 5. Conclusions

In California coastal waters, *Pseudo-nitzschia* spp. represent only a minor constituent of the total phytoplankton assemblage during most of the year. Previous authors have suggested a number of potential environmental factors such as coastal runoff (Scholin et al., 2000), metal stress (Rue and Bruland, 2001; Maldonado et al., 2002; Ladizinsky and Smith, 2003; Wells et al., 2005) or macronutrient limitation (Pan et al., 1996a,b,c) that may trigger toxin production in *Pseudo-nitzschia* blooms. In the San Francisco Bay experiment, no conspicuous “triggers” of DA production, such as silicate or phosphate limitation, were observed. The phytoplankton assemblage, which included a large proportion of *P. australis*, did not exhibit a preference for any particular nitrogen substrate, and both inorganic and organic nitrogen sources could support the growth of this assemblage, while the unialgal cultures definitively show that *P. australis* can grow on all nitrogen substrates tested. Both the field and laboratory experiments demonstrate

that urea-grown cells were more toxic than cells utilizing either nitrate or ammonium. Given that this diatom blooms during both upwelling and non-upwelling conditions off the west coast of the U.S. (Buck et al., 1992; Fryxell et al., 1997; Trainer et al., 2000), substantial differences in the nitrogenous nutrition of *P. australis* can be expected, and anthropogenic inputs of reduced nitrogen substrates, such as urea, may be more important in harmful algal bloom development than previously thought, as suggested in a recent analysis by Glibert et al. (2005b). We conclude that *P. australis* is capable of using both inorganic and organic nitrogen sources and that nitrogenous source can influence toxin production in this species in central California.

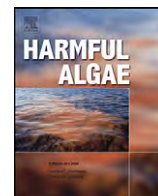
### Acknowledgements

This work was supported by the NOAA-ECO HAB grant NA96OP0475 awarded to RMK and WPC, and additional grants awarded to RMK and MDA, including C7-94085 (NOAA), OCE-138544 (NSF), and those from Dr. Earl H. and Ethyl M. Meyers Trust, Ida Benson Lynn Fellowship, the University of California, Santa Cruz Women's Club, and the Ocean Science Department. Ship time for the field component was made available by Dr. Kenneth W. Bruland, funded by NSF grant OCE-0238347. The authors thank Dr. Peter E. Miller, Dr. Chris Scholin, Mr. Rob Franks, Dr. Mary Silver, Mr. Julian Herndon and the captain and crew of the R/V *Point Sur*. In particular, we acknowledge the time and effort of Ms. Margaret P. Hughes and Dr. Mark L. Wells for their culturing assistance, domoic acid analyses, and for supplying the initial cultures. We also thank two anonymous reviewers and Dr. Ted Smayda who provided useful commentary on an earlier version of the manuscript.[TS]

### References

- Anderson, D.M., Glibert, P.M., Burkholder, J.M., 2002. Harmful algal blooms and eutrophication: nutrient sources, composition and consequences. *Estuaries* 25, 562–584.
- Bates, S.S., Bird, C.J., de Freitas, A.S.W., Foxall, R., Gilgan, M., Hanic, L.A., Johnson, G.R., McCulloch, A.W., Odense, P., Pocklington, R., Quilliam, M.A., Sim, P.G., Smith, J.C., Subba Rao, D.V., Todd, E.C.D., Walter, J.A., Wright, J.L.C., 1989. Pennate diatom *Nitzschia pungens* as the primary source of domoic acid, a toxin in shellfish from eastern Prince Edward Island, Canada. *Can. J. Fish. Aquat. Sci.* 46, 1203–1215.
- Bates, S.S., Worms, J., Smith, J.C., 1993. Effects of ammonium and nitrate on growth and domoic acid production by *Nitzschia pungens* in batch culture. *Can. J. Fish. Aquat. Sci.* 50, 1248–1254.
- Bates, S.S., 1998. Ecophysiology and metabolism of ASP toxin production. In: Anderson, D.M., Cembella, A.D., Hallegraeff, G.M. (Eds.), *The Physiological Ecology of Harmful Algal Blooms*. Springer-Verlag, Heidelberg, pp. 405–426.
- Bates, S.S., Leger, C., Satchwell, M., Boyer, G.L., 2000. The effects of iron on domoic acid production by *Pseudo-nitzschia multiseries*. In: Hallegraeff, G.A., Blackburn, S.I., Bolch, C.J., Lewis, R.J. (Eds.), *Harmful Algal Blooms 2000*. Intergov. Oceanogr. Comm., Paris, pp. 320–323.
- Berges, J.A., Franklin, D.J., Harrison, P.J., 2003. Evolution of an artificial seawater medium: Improvements in enriched seawater, artificial water over the last two decades. *J. Phycol.* 37, 1138–1145 [Correction addition 40 (2004) 619].
- Bruland, K.W., Rue, E.L., Smith, G.J., 2001. Iron and macronutrients in California coastal upwelling regimes: implications for diatom blooms. *Limnol. Oceanogr.* 46, 1661–1674.
- Buck, K.R., Uttal-Cooke, L., Pilskaln, C.H., Roelke, D.L., Villac, M.C., Fryxell, G.A., Cifuentes, L., Chavez, F.P., 1992. Autecology of the diatom *Pseudonitzschia australis* Frenguelli, a domoic acid producer, from Monterey Bay, California. *Mar. Ecol. Prog. Ser.* 84, 293–302.
- Cochlan, W.P., Harrison, P.J., 1991. Uptake of nitrate ammonium and urea by nitrogen-starved cultures of *Micomonas pusilla* (Prasinophyceae): transient responses. *J. Phycol.* 27, 673–679.
- Cullen, J.J., Renger, E.H., 1979. Continuous measurement of the DMCU-induced fluorescence response of natural phytoplankton populations. *Mar. Biol.* 53, 13–20.
- Degobbi, D., 1973. On the storage of sea water samples for ammonia determination. *Limnol. Oceanogr.* 18, 146–150.
- Fritz, L., Quilliam, M.A., Wright, J.L.C., Beale, A., Work, T.M., 1992. An outbreak of domoic acid poisoning attributed to the pennate diatom *Pseudo-nitzschia australis*. *J. Phycol.* 28, 439–442.
- Fryxell, G.A., Villac, M.C., Shapiro, L.P., 1997. The occurrence of the toxic diatom genus *Pseudonitzschia* (Bacillariophyceae) on the West Coast of the USA, 1920–1996: a review. *Phycologia* 36, 419–437.
- Garrison, D.L., Conrad, S.M., Eilers, P.P., Waldron, E.M., 1992. Confirmation of domoic acid production by *Pseudonitzschia australis* (Bacillariophyceae) cultures. *J. Phycol.* 28, 604–607.
- Garthwaite, I., Ross, K.M., Mile, C.O., Briggs, L.R., Towers, N.R., 2001. Integrated enzyme-linked immunosorbent assay screening system for amnesic, neurotoxic, diarrhetic, and paralytic shellfish poisoning toxins found in New Zealand. *J. AOAC Int.* 84, 1643–1648.
- Glibert, P.M., Anderson, D.M., Gentien, P., Granéli, E., Sellner, K.G., 2005a. The global, complex phenomena of harmful algal blooms. *Oceanography* 18, 136–147.
- Glibert, P.M., Harrison, J., Heil, C., Seitzinger, S., 2005b. Escalating worldwide use of urea—a global change contributing to coastal eutrophication. *Biogeochemistry* 77, 441–463.
- Guillard, R.R.L., 1973. Division rates. In: Stein (Eds.), *Handbook of Phycological Methods*, vol. VI. Cambridge University Press, Cambridge, pp. 289–312.
- Hallegraeff, G.M., 1993. A review of harmful algal blooms and their apparent global increase. *Phycologia* 32, 79–99.
- Harrison, P.J., Waters, R.E., Taylor, F.J.R., 1980. A broad spectrum artificial sea water medium for coastal and open ocean phytoplankton. *J. Phycol.* 16, 28–35.
- Hillebrand, H., Sommer, U., 1996. Nitrogenous nutrition of the potentially toxic diatom *Pseudonitzschia pungens* f. *multiseries* Hasle. *J. Plank. Res.* 18, 295–301.

- Knepel, K., Bogren, K., 2001. Determination of orthophosphorous by flow injection analysis in seawaters: QuickChem Method 31-115-01-1-H. In: Saline Methods of Analysis, Lachat Instruments, Milwaukee, WI, 14 pp.
- Kudela, R., Dugdale, R., 2000. Nutrient regulation of phytoplankton productivity in Monterey Bay, California. *Deep-Sea Res. II* 47, 1023–1053.
- Kudela, R., Cochlan, W., Roberts, A., 2003a. Spatial and temporal patterns of *Pseudo-nitzschia* spp. in central California related regional oceanography. In: Steidinger, K.A., Landsberg, J.H., Tomas, C.R., Vargo, G.A. (Eds.), *Harmful Algae 2002*. Florida and Wildlife Conservation Commission, Florida Institute of Oceanography, and Intergovernmental Oceanographic Commission of UNESCO, pp. 347–349.
- Kudela, R., Roberts, A., Armstrong, M., 2003b. Laboratory analyses of nutrient stress and toxin production in *Pseudo-nitzschia* spp. from Monterey Bay, California. In: Steidinger, K.A., Landsberg, J.H., Tomas, C.R., Vargo, G.A. (Eds.), *Harmful Algae 2002*. Florida and Wildlife Conservation Commission, Florida Institute of Oceanography, and Intergovernmental Oceanographic Commission of UNESCO, pp. 136–138.
- Ladizinsky, N., Smith, G.J., 2000. Accumulation of domoic acid by the coastal diatom *Pseudo-nitzschia multiseries*: a possible copper complexation strategy. *J. Phycol.* 36, 41.
- Ladizinsky, N., Smith, G.J., 2003. Copper influence on the production of domoic acid in toxic *Pseudo-nitzschia* spp. in Monterey Bay, CA: a field study. Poster. In: Proceedings of the Second Symposium on Harmful Marine Algae in the US, Woods Hole, MA.
- Maldonado, M.T., Hughes, M.P., Rue, E.L., 2002. The effect of Fe and Cu on growth and domoic acid production by *Pseudo-nitzschia multiseries* and *Pseudo-nitzschia australis*. *Limnol. Oceanogr.* 47, 515–526.
- Miller, P.E., Scholin, C.A., 1998. Identification and enumeration of cultured and wild *Pseudo-nitzschia* (Bacillariophyceae) using species-specific LSU rRNA-targeted fluorescent probes and filter-based whole cell hybridization. *J. Phycol.* 34, 371–382.
- Molloy, C.J., Syrett, P.J., 1988. Interrelationships between uptake of urea and uptake of ammonium by microalgae. *J. Exp. Mar. Biol. Ecol.* 118, 85–95.
- Olivieri, R.A., Chavez, F.P., 2000. A model of plankton dynamics for the coastal upwelling system of Monterey Bay, California. *Deep-Sea Res. II* 47, 1077–1106.
- Pan, Y., Subba Rao, D.V., Mann, K.H., Brown, R.G., Pocklington, R., 1996a. Effects of silicate limitation on production of domoic acid, a neurotoxin, by the diatom *Pseudo-nitzschia multiseries*. I. Batch culture studies. *Mar. Ecol. Prog. Ser.* 131, 225–233.
- Pan, Y., Subba Rao, D.V., Mann, K.H., Li, W.K.W., Harrison, W.G., 1996b. Effects of silicate limitation on production of domoic acid, a neurotoxin, by the diatom *Pseudo-nitzschia multiseries*. II. Continuous culture studies. *Mar. Ecol. Prog. Ser.* 131, 235–243.
- Pan, Y., Subba Rao, D.V., Mann, K.H., 1996c. Changes in domoic acid production and cellular chemical composition of the toxigenic diatom *Pseudo-nitzschia multiseries* under phosphate limitation. *J. Phycol.* 32, 371–381.
- Perl, T.M., Bedard, L., Kosatsky, T., Hockin, J.C., Todd, E.C.D., Remis, R.S., 1990. An outbreak of toxic encephalopathy by eating mussels contaminated with domoic acid. *New. Engl. J. Med.* 322, 1775–1780.
- Pocklington, R., Milley, J.E., Bates, S.S., Bird, C.J., de Freitas, A.S.W., Quilliam, M.A., 1990. Trace determination of domoic acid in seawater and phytoplankton by high-performance liquid chromatography of the fluorenylmethoxycarbonyl (FMOC) derivative. *Int. J. Environ. Anal. Chem.* 38, 351–368.
- Price, N.M., Harrison, P.J., 1987. A comparison of methods for the measurement of dissolved urea concentration in seawater. *Mar. Biol.* 92, 307–319.
- Rue, E.L., Bruland, K.W., 2001. Domoic acid binds iron and copper: a possible role for the toxin produced by the marine diatom *Pseudo-nitzschia*. *Mar. Chem.* 76, 127–134.
- Scholin, C.A., Gulland, F., Doucette, G.J., Benson, S., Busman, M., Chavez, F.P., Cordaro, J., DeLong, R., DeVogelaere, A., Harvey, J., Haulena, M., Lefebvre, K., Lipsomb, T., Loscutoff, S., Lowens-tine, L.J., Marin III, R., Miller, P.E., McLellan, W.A., Moeller, P.D.R., Powell, C.L., Rowles, T., Silvagni, P., Silver, M., Spraker, T., Trainer, V., Van Dolah, F.M., 2000. Mortality of sea lions along the central California coast linked to a toxic diatom bloom. *Nature* 403, 80–84.
- Smith, P., Bogren, K., 2001a. Determination of nitrate and/or nitrite in brackish or seawater by flow injection analysis colorimeter: QuickChem Method 31-107-04-1-E. In: Saline Methods of Analysis, Lachat Instruments, Milwaukee, WI, 12 pp.
- Smith, P., Bogren, K., 2001b. Determination of silicate in brackish or seawater by flow injection analysis colorimeter: QuickChem Method 31-114-27-1-C. In: Saline Methods of Analysis, Lachat Instruments, Milwaukee, WI, 12 pp.
- Solorzano, L., 1969. Determination of ammonium in natural waters by the phenolphthorite method. *Limnol. Oceanogr.* 14, 799–801.
- Trainer, V.L., Adams, N.G., Bill, B.D., Stehr, C.M., Wekell, J.C., Moeller, P., Busman, M., Woodruff, D., 2000. Domoic acid production near California coastal upwelling zones, June 1998. *Limnol. Oceanogr.* 45, 1818–1833.
- Villac, M.C., Roelke, D.L., Chavez, F.P., Cifuentes, L.A., Fryxell, G.A., 1993. *Pseudonitzschia australis* Frenguelli and related species from the west coast of the U.S.A.: occurrence and domoic acid production. *J. Shellfish Res.* 12, 457–465.
- Wells, M.L., Trick, C.G., Cochlan, W.P., Hughes, M.P., Trainer, V.L., 2005. Domoic acid: the synergy of iron, copper, and the toxicity of diatoms. *Limnol. Oceanogr.* 50, 1908–1917.
- Welschmeyer, N.A., 1994. Fluorometric analysis of chlorophyll *a* in the presence of chlorophyll *b* and pheopigments. *Limnol. Oceanogr.* 39, 1985–1992.
- Wilkerson, F.P., Dugdale, R.C., Chavez, F.P., Kudela, R.M., 2000. Biomass and productivity in Monterey Bay, CA: contribution of the larger autotrophs. *Deep-Sea Res. II* 47, 1003–1022.
- Work, T.M., Beale, A.M., Fritz, L., Quilliam, M.A., Silver, M., Buck, K., Wright, J.L.C., 1993. Domoic acid intoxication of brown pelicans and cormorants in Santa Cruz, California. In: Smayda, T.J., Shimizu, Y. (Eds.), *Toxic Phytoplankton Blooms in the Sea*. Elsevier, Amsterdam, pp. 643–650.



## The potential role of anthropogenically derived nitrogen in the growth of harmful algae in California, USA

Raphael M. Kudela<sup>a,\*</sup>, Jenny Q. Lane<sup>a</sup>, William P. Cochlan<sup>b</sup>

<sup>a</sup> Ocean Sciences Department, University of California Santa Cruz, 1156 High Street, Santa Cruz, CA 95064, USA

<sup>b</sup> Romberg Tiburon Center for Environmental Studies, San Francisco State University, 3152 Paradise Drive, Tiburon, CA 94920-1250, USA

### ARTICLE INFO

#### Article history:

Received 30 April 2007

Received in revised form 22 July 2007

Accepted 1 August 2008

#### Keywords:

Ammonium

Eutrophication

Nitrate

Nitrogen uptake kinetics

Urea

### ABSTRACT

Cultural eutrophication is frequently invoked as one factor in the global increase in harmful algal blooms, but is difficult to definitively prove due to the myriad of factors influencing coastal phytoplankton bloom development. To assess whether eutrophication could be a factor in the development of harmful algal blooms in California (USA), we review the ecophysiological potential for urea uptake by *Pseudo-nitzschia australis* (Bacillariophyceae), *Heterosigma akashiwo* (Raphidophyceae), and *Lingulodinium polyedrum* (Dinophyceae), all of which have been found at bloom concentrations and/or exhibited noxious effects in recent years in California coastal waters. We include new measurements from a large (Chlorophyll *a* > 500 mg m<sup>-3</sup>) red tide event dominated by *Akashiwo sanguinea* (Dinophyceae) in Monterey Bay, CA during September 2006. All of these phytoplankton are capable of using nitrate, ammonium, and urea, although their preference for these nitrogenous substrates varies. Using published data and recent coastal time series measurements conducted in Monterey Bay and San Francisco Bay, CA, we show that urea, presumably from coastal eutrophication, was present in California waters at measurable concentrations during past harmful algal bloom events. Based on these observations, we suggest that urea uptake could potentially sustain these harmful algae, and that urea, which is seldom measured as part of coastal monitoring programs, may be associated with these harmful algal events in California.

© 2008 Elsevier B.V. All rights reserved.

### 1. Introduction

The apparent worldwide increase in the occurrence and impact of harmful algal bloom (HAB) events (e.g., Anderson et al., 2002) has frequently been attributed to, either directly or indirectly, increased cultural eutrophication (Glibert et al., 2005, 2006; GEOHAB, 2006). Despite this link, there is a general perception that coastal California is relatively less impacted by cultural eutrophication, because of the dominance of upwelling and the relatively minor contribution of terrestrial runoff (Otero and Siegel, 2004). Coastal California has also historically been classified as being primarily nitrogen-limited (e.g., Eppley et al., 1979; Kudela and Dugdale, 2000), suggesting that phytoplankton (including potential harmful algal species) in California coastal waters would respond positively to increased nitrogen loading. However, there is only limited regional evidence to support this assertion, with increased phytoplankton biomass directly attributed to runoff in the Gulf of California, Baja Mexico (Beman et al., 2005), Southern California (Kudela and Cochlan, 2000) and central California

(Kudela and Chavez, 2004), while the importance of runoff as a potential nutrient source has been suggested by numerous investigators (e.g. Eppley et al., 1979; Warrick et al., 2005).

To assess the role of runoff and cultural eutrophication in California, several approaches could be taken. The most direct would be to assess the temporal trend of harmful algal events with nutrient concentration and rates of nutrient use by HAB species; unfortunately, the long-term records of ambient nutrient concentrations and harmful algae in California are not necessarily coincident, and there are relatively few time series of land-derived nutrient loads. As an alternative, we present data on the physiological capacity for several HAB species from coastal California to respond to nutrient enrichment on short time scales. We focus on urea, both because of its accelerated global use (Glibert et al., 2006) and because elevated urea concentrations in the coastal ocean are generally indicative of eutrophication, while elevated concentrations of other nutrients such as nitrate and phosphate are more difficult to attribute directly to eutrophication in upwelling-dominated systems such as California.

We present data from several HAB and potentially harmful species, including the pennate diatom genus *Pseudo-nitzschia*, the dinoflagellates *Akashiwo sanguinea*, *Lingulodinium polyedrum*, and *Cochlodinium* spp., and the raphidophyte *Heterosigma akashiwo*,

\* Corresponding author. Tel.: +1 831 4593290; fax: +1 831 4594882.  
E-mail address: [kudela@ucsc.edu](mailto:kudela@ucsc.edu) (R.M. Kudela).

using nitrogen uptake kinetics as a metric for the potential of these organisms to respond to urea and ammonium, proxies for eutrophication. All of these N uptake kinetics have been measured by our laboratories using either natural assemblages or culture isolates from U.S. west coast waters.

## 2. Methods

We primarily focus on a review of nitrogen uptake and ecophysiological data for HAB species from coastal waters of California, and refer the reader to the referenced literature for the details of specific sampling and experimental protocols. New N kinetic results are presented for the dinoflagellate *Akashiwo sanguinea* from a nearly mono-specific bloom event in Monterey Bay during September 9–14, 2006, and are described in more detail. Unless otherwise stated, similar methods were employed for the other phytoplankton species, as documented in the respective publications.

To assess the role of anthropogenic loading, time-series measurements were conducted in Monterey Bay and San Francisco Bay. In Monterey Bay, ambient concentrations of nitrate, ammonium, urea, and *P. australis* abundance were measured from Santa Cruz Municipal Wharf (36°57.48'N, 122°1.02'W) for March 2006–May 2007, and in San Francisco Bay, ambient concentrations of nitrate, ammonium, and urea were measured for May–September, 2005 from the northeastern (Paradise Cay: 37°N, 122°28.5'W) and southwestern (Richardson Bay: 37°53'N, 122°30.2'W) sides of the Tiburon Peninsula both within 10 km from the Golden Gate entrance to the open ocean.

### 2.1. Field experiments

Water was collected at two separate locations during a large red tide event, dominated by the dinoflagellate *Akashiwo sanguinea*, from the R/V John H. Martin, on September 7 and 8, 2006. At the time of collection, *A. sanguinea* was concentrated in a near-surface red tide, with chlorophyll *a* (Chl *a*) concentrations within the red tide in excess of 500 mg Chl *a* m<sup>-3</sup> at some locations (Table 1). Either 10-l, PVC Niskin bottles (refitted with silicone rubber band springs) mounted on an instrumented rosette or a clean polyethylene bucket was used to collect seawater from 2 m and 0–1 m depth, respectively. Nine-liter, acid-cleaned polycarbonate (Nalgene) carboys were rinsed three times and filled with seawater using multiple Niskin bottles or the homogenized bucket sample. The water was maintained at sea in a deckboard incubator cooled with flowing surface seawater to maintain ambient temperature of collection and darkened to avoid light shock during transport back to shore. For the first experiment, samples collected on 7 September were transferred to an environmental chamber (15.5 °C, 180 μmol photons m<sup>-2</sup> s<sup>-1</sup>) ashore and assayed for nutrient kinetics within 3 h of collection. On 8 September, 2 m samples were transferred to a walk-in environmental chamber (15–16 °C and ca. 100–250 μmol photons m<sup>-2</sup> s<sup>-1</sup> irradiance using “cool-white” fluorescent lamps and a 14:10 light:dark cycle) at the University of California Santa Cruz. Kinetics experiments were performed within 12 h of water collection, after

maintenance of the whole water under simulated *in situ* conditions. Field concentrations of 300 mg Chl *a* m<sup>-3</sup> in surface waters would result in approximately 10% surface irradiance at 2 m depth, or approximately 100–200 μmol photons m<sup>-2</sup> s<sup>-1</sup>. Additional nutrient samples were taken to coincide with the kinetics experiments, and were within the sampling error of the N concentrations reported in Table 1.

### 2.2. Analytical methods

Samples for Chl *a* were collected in triplicate and filtered onto uncombusted glass-fiber filters (Whatman GF/F; nominal pore size 0.7 μm) and processed using the non-acidification method (Welschmeyer, 1994). Macronutrients (nitrate plus nitrite [hereafter referred to as nitrate], silicate and ortho-phosphate) were stored frozen, and later analyzed with a Lachat Quick Chem 8000 Flow Injection Analysis system using standard colorimetric techniques (Knepel and Bogren, 2001; Smith and Bogren, 2001a,b). Ammonium and urea samples were collected using 50 mL, low-density polyethylene (LDPE) centrifuge tubes (Corning®); previous tests have confirmed that these tubes are contaminant free for both urea and ammonium. Ammonium samples were stored refrigerated and were manually analyzed using the fluorescence method of Holmes et al. (1999). Urea samples were frozen at –20 °C, and subsequently thawed at room temperature before manual analysis using the diacetyl monoxime thiosemicarbazide technique (Price and Harrison, 1987), modified to account for a longer time period (72 h) and lower digestion temperature (22 °C) as suggested by Goeyens et al. (1998). The time-series measurements of ambient N concentrations from San Francisco Bay were measured similarly, except for ammonium which was measured using the phenol hypochlorite technique (Solorzano, 1969) with a spectrophotometer equipped with a 10-cm cell.

### 2.3. Kinetics methods

Three nitrogen substrates (nitrate, ammonium, urea) were used to determine the uptake response kinetics. In the laboratory, water was dispensed into pre-cleaned, 70 mL polycarbonate flasks at the same time that nutrient and pigment samples were collected, and inoculated with either <sup>15</sup>N-ammonium chloride, (99 atom%; Cambridge Isotopes), <sup>15</sup>N-sodium nitrate (99 atom%) or <sup>13</sup>C-<sup>15</sup>N-urea (99.0 and 98.2 atom%) at a range of initial substrate concentrations. For the first experiment (7 September) 10 substrate levels were used, with duplicate measurements at the lowest concentrations; initial concentrations were 0.14, 0.29, 0.43, 0.58, 0.72, 1.01, 1.16, 1.45, 7.24, and 14.49 μg-at N L<sup>-1</sup> for ammonium and nitrate, 2× those concentrations for urea. The second experiment (8 September) used 0.20, 0.30, 0.40, 0.60, 0.80, 1.01, 2.02, 5.05, 10.10 and 20.20 μg-at N L<sup>-1</sup> (2× these concentrations for urea, except for 40.40, which was lost) with three replicates at 0.30 (0.60) μg-at N L<sup>-1</sup>. For both experiments, after inoculation the flasks were transferred to an environmental chamber maintained at the temperature of sample collection (15–16 °C), and incubated under 180–240 μmol photons m<sup>-2</sup> s<sup>-1</sup> irradiance using standard (GE “soft white”) fluorescence

**Table 1**  
Ambient conditions at the time of collection for the two sampling events in Monterey Bay, CA during 2006

Date	Urea	Ammonium	Nitrate (μg-at N L <sup>-1</sup> )	Phosphate (μM)	Silicate (μM)	Temperature (°C)	Salinity	Chl <i>a</i> (μg L <sup>-1</sup> )	<i>A. sanguinea</i> (cells L <sup>-1</sup> )
7 September	0.25	0.03	0.02	3.56	16.99	15.59	33.53	370.05	8.41 × 10 <sup>6</sup>
8 September	n.d.	n.d.	0.35	0.41	19.48	15.10	33.60	573.66	9.88 × 10 <sup>6</sup>

Water was collected from 0 and 2 m on 7 and 8 September, respectively. n.d., not determined.

illumination. Incubations were terminated after 30 min by filtration (<100 mm Hg) onto precombusted GF/F filters, immediately dried at 50 °C, and subsequently analyzed for total particulate nitrogen and isotopic enrichment using a Finnigan Delta XP mass spectrometer.

Particulate nitrogen specific uptake rates ( $V$ ,  $\text{h}^{-1}$ ) were estimated from the accumulation of  $^{15}\text{N}$  in the particulate material, and calculated as described in Dugdale and Wilkerson (1986). Rates were not corrected for the effects of isotopic dilution (Glibert et al., 1982) due to the short (30 min) incubation periods. Curve fitting was carried out using an iterative, non-linear least-squares technique (Kaleidagraph; Abelbeck Software), which utilizes the Levenberg-Marquardt algorithm (Press et al., 1992), to determine the half-saturation ( $K_s$ ,  $\mu\text{g-at N L}^{-1}$ ) and maximum uptake ( $V_{\text{max}}$ ,  $\text{h}^{-1}$ ) parameters of a Michaelis–Menten curve for nitrogen kinetics. The substrate affinity constant at low concentrations (i.e., ambient nutrients  $<K_s$ ) was determined from the initial slope ( $\alpha$ ) of the Michaelis–Menten plot; calculated as  $\alpha = V_{\text{max}}/K_s$ .

#### 2.4. Species enumeration

Ashore, freshly preserved (1% paraformaldehyde or acidic Lugol's solution) whole water samples were qualitatively inspected for species dominance and abundance using with a Fluid Imaging Technologies FlowCAM. Preserved samples were subsequently settled and enumerated on a Zeiss Axiovert microscope using the Utermöhl technique. For the time-series of *Pseudo-nitzschia* abundance presented in Fig. 2, weekly whole-water samples were collected and enumerated using a DNA-specific whole cell probe method as described by Miller and Scholin (1998) for *P. australis* and *P. multiseriis*. During this time interval, *P. multiseriis* was always absent or a very small fraction (<1%) of the total *Pseudo-nitzschia* abundance. Therefore, Fig. 2B only presents *P. australis* abundance, expressed as log-transformed cell counts [ $\log(\text{cells L}^{-1})$ ]. Particulate domoic acid concentrations were also measured for the April–May 2007 bloom event, following the methods described by Schnetzer et al. (2007).

### 3. Results

To assess the nutrient utilization capability of *Akashiwo sanguinea* found off California, we conducted nutrient uptake kinetics experiments during September 2006 using natural assemblages where *A. sanguinea* was the dominant organism. The ambient nitrogen concentrations of nitrate, ammonium, and urea of the seawater collected for these experiments were low to undetectable, while phosphate and silicate concentrations were still measurable (Table 1). Because we assessed N uptake kinetics on natural field assemblages, we cannot attribute our uptake rates and estimated kinetic parameters solely to *Akashiwo*; however, since it was dominant, we have assumed that the reported values are indicative of *Akashiwo sanguinea*. For both samples, *A. sanguinea* was found at concentrations in excess of  $8 \times 10^6$  cells  $\text{L}^{-1}$  (Table 1) and represented >86% and >88% numerically (7 and 8 September, respectively), and >90–95% by biomass (estimated from cell size), of the algal cells present; a near mono-culture of this dinoflagellate in the surface waters of the red tide blooms.

All three nitrogen substrates exhibited reasonable Michaelis–Menten responses (Fig. 1, Table 2), although the nitrate kinetics for 7 September were linear or nearly linear at substrate concentrations greater than  $2 \mu\text{g-at N L}^{-1}$ . This does not affect the determination of  $\alpha$ , the initial slope, but it precludes a true estimate of  $V_{\text{max}}$ . We therefore report the highest measured value for nitrate uptake as a conservative  $V_{\text{max}}$  estimate. There was variability in kinetics responses between the two sampling events.

Although these differences are relatively minor for the estimated maximal uptake rates of nitrate and urea, the affinity coefficients differed substantially between dates. However for ammonium, whereas the  $V_{\text{max}}$  ammonium differed by almost twofold, the  $\alpha$  values were similar.

At elevated nutrient concentrations, ammonium uptake is between two- and threefold higher than urea and nitrate uptake, respectively (Table 2). At low ( $<K_s$ ) concentrations, urea exhibits a much greater range of uptake affinities ( $\alpha$ : the initial slope of the uptake curve), with between two- and threefold higher affinities than nitrate or ammonium, while nitrate and ammonium are essentially equivalent when the kinetics parameters from the same experiment are compared for the respective nitrogen substrates.

Substrate preference is often assessed by comparing maximum uptake rates ( $V_{\text{max}}$ ) for one nitrogen source in the absence of other N substrates (e.g. Dortch, 1990). Based on these single substrate experiments, the N preference of *Akashiwo sanguinea* follows the order: ammonium  $\gg$  urea > nitrate during high ambient N conditions. However using the half-saturation constants, which are generally thought to be indicative of substrate utilization under nutrient-limited conditions, the order is urea > nitrate > ammonium, and while using the initial slope ( $\alpha$ ), *A. sanguinea* affinity order is urea  $\gg$  ammonium > nitrate. The inherent variability in the nutrient kinetics parameters demonstrates the difficulty of assessing N preference from natural assemblages; regardless of how nutrient preference is assessed, however, it is clear that *A. sanguinea* is capable of utilizing all three forms of nitrogen measured in this

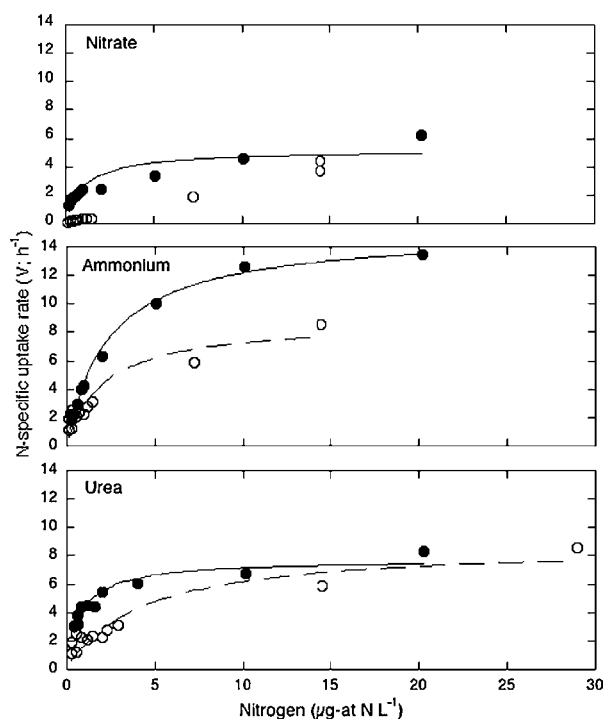


**Fig. 1.** Particulate N-specific uptake rates ( $V$ ,  $\text{h}^{-1}$ ) for nitrate (top), ammonium (middle), and urea (bottom) for natural assemblages dominated by *Akashiwo sanguinea* collected from Monterey Bay, California on 7 September (open circles), and 8 September (closed circles) plotted versus substrate concentrations ( $\mu\text{g-at N L}^{-1}$ ). Two replicates for nitrate and ammonium were conducted at the highest substrate concentration on 7 September, while three replicates were conducted at  $0.3 \mu\text{g-at N L}^{-1}$  on 8 September, and are presented as individual symbols (symbols are overlapping for ammonium and urea); replicates were not measured for other concentrations. The curves represent Michaelis–Menten kinetics for the data, except for the 7 September nitrate values, which are fitted to a linear regression. Curve parameters are summarized in Table 2.

**Table 2**  
Summary of literature values for nitrogen uptake kinetics of California natural assemblages and unialgal HAB cultures, and for non-HAB coastal assemblages

Species	Nitrate				Ammonium				References
	$V_{\max}$	$K_s$	$\alpha$	$r^2$ (n)	$V_{\max}$	$K_s$	$\alpha$	$r^2$ (n)	
<b>Cultures</b>									
<i>Heterosigma akashiwo</i>	18.0	1.47	12.2	0.92 (30)	28.0	1.44	19.4	0.81 (36)	Herndon and Cochlan (2007)
<i>Pseudo-nitzschia australis</i>	105.3	2.82	37.3	0.98 (19)	71.0	5.37	13.2	0.96 (20)	Cochlan et al. (2008)
<b>Natural HAB assemblages</b>									
Monterey Bay, CA ( <i>Cochlodinium bloom</i> )	0.9	1.01	0.89	0.85 (12)	>4.0	–	0.3	0.94 (12)	Kudela et al. (2008)
Southern California, USA ( <i>Lingulodinium polyedrum</i> )	3.85	0.467	0.82	0.56 (18)	8.09	0.586	1.3	0.92 (20)	Kudela and Cochlan (2000) <sup>a</sup>
<b>Monterey Bay (<i>A. sanguinea</i>)</b>									
7 September 2006	>4.0	–	0.04	0.99 (11)	8.78 (0.99)	2.05 (0.58)	4.28	0.86 (12)	This study <sup>b</sup>
8 September 2006	5.18 (0.50)	1.00 (0.22)	5.18	0.81 (12)	15.11 (0.50)	2.37 (0.22)	6.38	0.99 (12)	This study
<b>Coastal waters</b>									
Washington coast, USA	5.8	0.05	116	–	6.8	0.710	9.58	–	Dortch and Postel (1989)
Western New Zealand	13.8	1.1	12.5	–	20.7	0.5	41.4	–	Chang et al. (1995)
Neuse Estuary, NC, USA	3.98	0.54	7.37	–	52.9	2.38	22.2	–	Fan et al. (2003) <sup>c</sup>
Species	Urea				References				
	$V_{\max}$	$K_s$	$\alpha$	$r^2$ (n)					
<b>Cultures</b>									
<i>Heterosigma akashiwo</i>	2.89	0.42	6.88	0.67 (18)	Herndon and Cochlan (2007)				
<i>Pseudo-nitzschia australis</i>	>30	–	2.8	0.99 (18)	Cochlan et al. (2008) <sup>d</sup>				
<b>Natural HAB assemblages</b>									
Monterey Bay, CA ( <i>Cochlodinium bloom</i> )	0.19–0.22	1.57–6.56	0.35–1.24	0.94–0.96 (12)	Kudela et al. (2008)				
Southern California, USA ( <i>Lingulodinium polyedrum</i> )	10.6	0.99	1.07	0.73 (16)	Kudela and Cochlan (2000) <sup>a</sup>				
<b>Monterey Bay (<i>A. sanguinea</i>)</b>									
7 September 2006	8.77 (0.99)	4.13 (1.16)	2.13	0.86 (12)	This study				
8 September 2006	7.2 (0.34)	0.43 (0.07)	16.84	0.91 (11)	This study				
<b>Coastal waters</b>									
Washington coast, USA	4.6	0.78	5.89		Dortch and Postel (1989)				
Western New Zealand	12	0.5	24.0		Chang et al. (1995)				
Neuse Estuary, NC, USA	5.77	0.37	15.6		Fan et al. (2003) <sup>c</sup>				

Kinetic parameters are reported as  $\times 10^3 \text{ h}^{-1}$  for  $V_{\max}$ ,  $\mu\text{g-at N L}^{-1}$  for  $K_s$ , and  $(\times 10^3 \text{ h}^{-1})/(\mu\text{g-at N L}^{-1})$  for  $\alpha$ . When available, the coefficient of determination ( $r^2$ ) and number of samples ( $n$ ) used in the curve fits are reported. For *A. sanguinea*, the estimated standard error values of  $V_{\max}$  and  $K_s$  are given in parentheses.

<sup>a</sup>  $V_{\max}$  calculated from reported cell specific rates using cell abundance =  $3.57 \times 10^5 \text{ cells L}^{-1}$  (incorrectly reported in original paper) and PN concentration =  $44.5 \mu\text{g-at N L}^{-1}$ ,  $\alpha$  reported as  $(V_{\max}/K_s)$ .

<sup>b</sup>  $V_{\max}$  for nitrate determined from highest measured uptake rate.

<sup>c</sup>  $V_{\max}$  reported as  $\text{fg at-N (cell h}^{-1})$ ,  $\alpha$  reported as  $(V_{\max}/K_s)$ .

<sup>d</sup>  $V_{\max}$  estimated at  $[\text{urea}] = 40 \mu\text{g-at N L}^{-1}$  from linear fit of urea uptake vs. concentrations;  $\alpha$  reported from initial slope ( $[\text{urea}] < 2.4 \mu\text{g-at N L}^{-1}$ ) of linear fit.

study and routinely found in measurable concentrations in the coastal waters of California.

## 4. Discussion

### 4.1. Uptake kinetics by California HAB organisms

California has a long history of HAB monitoring. These efforts began in the early 1930s after discovery of saxitoxin (STX), the causative agent of paralytic shellfish poisoning (PSP), in San Francisco Bay. In 1991, a second major class of marine toxins was identified in California, responsible for Amnesic Shellfish Poisoning (ASP). A major mortality event of marine birds was linked to domoic acid, the causative agent of ASP, produced by several species of the pennate diatom *Pseudo-nitzschia* (Work et al., 1993). Since 1991, several more HAB organisms have been identified in California including causative organisms for diarrhetic shellfish poisoning (DSP; Kudela et al., 2005) and yessotoxin (YTX;

Armstrong and Kudela, 2006). There have also been frequent occurrences of potentially harmful red tides caused by several organisms, including *Cochlodinium* (Curtiss et al., 2008; Kudela et al., 2008). We include *Akashiwo sanguinea* (this study), which while not typically classified as an HAB, is indicative of the recent increase in potentially disruptive red tides in central California (Ryan et al., 2005; Curtiss et al., 2008) and within San Francisco Bay (Cloern et al., 2005). Of these organisms, *Heterosigma akashiwo* and *Lingulodinium polyedrum* have already been linked to elevated levels of anthropogenic N substrates and their preferential utilization in coastal waters (Kudela and Cochlan, 2000; Herndon et al., 2003; Herndon and Cochlan, 2007). Finally, *Pseudo-nitzschia* has previously been associated with both eutrophication and a reduction in the ratio of N:Si elsewhere (cf. review by Bates et al., 1998), an indirect consequence of cultural eutrophication. Field and lab studies of *P. australis* have also shown that this diatom increases its toxicity (production of domoic acid) when provided with urea as a nitrogen source (Howard et al., 2007) although this

trend was not observed in cultures of *Pseudo-nitzschia cuspidata* (Auro, 2007).

To assess the observed and potential role of urea (used here as a convenient metric for eutrophication), one can compare nutrient uptake kinetics for these organisms. Uptake kinetics can vary considerably as a function of strain variability, preconditioning of the cells (Fan et al., 2003), and enhanced short-term (surge) uptake in response to elevated nutrient concentrations when N starved (Conway et al., 1976; Goldman and Glibert, 1982). In the present study, we compare the kinetic parameters estimated for both natural assemblages and unialgal cultures, but in each case the methods employed to determine the N uptake kinetic parameters are very similar: multiple flask incubations where different concentrations of  $^{15}\text{N}$ -labeled substrate were added to each flask and the incubation times were consistently short and constant. Thus we feel that these parameters can be confidently compared to each other, bearing in mind the plasticity of kinetics parameters in response to environmental and incubation conditions.

Nutrient uptake kinetics parameters can be used to assess the relative preference and affinity of various substrates in low and high nutrient environments. Preference can be assessed by comparing maximum uptake rates ( $V_{\max}$ ) at high ambient nutrient concentrations, or by comparing either  $K_s$  or  $\alpha$ , the initial slope of the uptake kinetics curve. The initial slope ( $\alpha$ ) is generally considered to be a more robust indicator of preference at low ( $<K_s$ ) ambient nutrient concentrations, since it is not dependent on  $V_{\max}$ , unlike  $K_s$  (Healey, 1980).

Based on the nitrogen kinetics parameters of representative California HAB organisms (Table 2),  $V_{\max}$  values for ammonium or urea are greater than for nitrate for all of the organisms except *P. australis*, which exhibited a greater maximal uptake for nitrate, consistent with expectations for a diatom (e.g. Lomas and Glibert, 2000). The variability observed between sampling events (Table 2) could be due to the effect of holding the whole water for a longer period of time (12 h) with little to no ambient nitrogen prior to conducting the kinetics experiments, although other factors, such as sampling different water masses on different days, cannot be ruled out. Qualitative assessment of the status of the algal assemblage, determined as cell abundance, motility and morphology as well as changes in nutrients and pigments, indicated that holding the whole water for up to 12 h on 8 September did not result in obvious changes in the community. Note however that  $V_{\max}$  values are within about a factor of 2 for any given organism, and for all of these organisms, nitrate, ammonium, and urea are all capable of being used. At low ( $<K_s$ ) nutrient concentrations, the initial slopes ( $\alpha$ ) for the various nitrogen compounds exhibit more variability. *Pseudo-nitzschia australis* exhibits the highest affinity (i.e., preference at  $\ll K_s$ ) for nitrate, followed by ammonium then urea. *H. akashiwo* is similar, but with N affinity following the order: ammonium > nitrate > urea, while the dinoflagellates exhibit either similar affinities for all substrates (*L. polyedrum*), a slightly enhanced uptake rate at low substrate concentrations for nitrate and urea versus ammonium (*Cochlodinium*), or a preference for urea (*A. sanguinea*;  $\alpha = 2.13\text{--}16.84 (\times 10^3 \text{ h}^{-1})/(\mu\text{g-at N L}^{-1})$  for urea, versus  $0.04\text{--}6.38 (\times 10^3 \text{ h}^{-1})/(\mu\text{g-at N L}^{-1})$  for nitrate and ammonium). Note that 'preference' as discussed here is based on nutrient kinetics parameters, and should not be confused with the Relative Preference Index (RPI; McCarthy et al., 1977). For all of these organisms, the half-saturation values ( $K_s$ ) are reasonably high compared to more oceanic organisms (cf. review by Kudela and Cochlan, 2000) which is also consistent with these organisms being adapted to a neritic (high nutrient) environment. However, it is also important to note that the kinetics for these HAB organisms are not substantially different from non-HAB assemblages reported in the literature (Table 2). Thus, while there is clear

evidence that HABs can utilize multiple sources of nitrogen, this is not a unique characteristic, and does not imply that urea "selects for" HAB species. The exact mechanisms selecting for HAB versus non-HAB organisms is complex (cf. Smayda, 1997), and it is unrealistic to expect that nitrogen kinetics are the sole, or even dominant, factor.

#### 4.2. Availability of urea in coastal California

For anthropogenic nitrogen (urea) to be an important factor in the growth of harmful algal species, there must be both a physiological capacity to utilize organic nitrogen and a source of anthropogenic urea. Unfortunately, while the importance of urea as a nitrogen compound for phytoplankton growth and as an indicator of coastal runoff has long been recognized (e.g., McCarthy, 1972; Eppley et al., 1979), there are very few long-term measurements of urea concentrations in California (or in much of the global coastal oceans; cf. Glibert et al., 2006). Despite the lack of long-term data, limited observations suggest that urea is indeed directly supporting some HAB events in California. Kudela and Cochlan (2000) demonstrated that 38% of the nitrogen demand for an *L. polyedrum* red tide event in Southern California was supported by urea, despite relatively low (ca.  $0.5 \mu\text{g-at N L}^{-1}$ ) ambient urea concentrations, and relatively high ( $1 \mu\text{g-at N L}^{-1}$ ) ammonium concentrations; similarly, Kudela et al. (2008) showed that a dinoflagellate bloom dominated by *Cochlodinium* in Monterey Bay was acquiring approximately 55–62% of its nitrogen from urea. Howard et al. (2007) showed that *Pseudo-nitzschia* assemblages in the Gulf of the Farallones (outside San Francisco Bay) were using multiple N sources, and that urea accounted for approximately 17% of the ambient nitrogen substrates measured (nitrate, ammonium, urea); this same study demonstrated that natural assemblages of *Pseudo-nitzschia* (dominated by *P. australis*) can potentially double their toxin production when growing on urea-N compared to growth on either nitrate or ammonium.

To assess the relative contribution of urea to the coastal ocean, we focus on two regions where reasonably long-term monitoring of nitrogen loads have been conducted: Monterey Bay, California, and San Francisco Bay. In the Monterey region, urea measurements from fifteen terrestrial sampling sites (streams, rivers, wastewater discharge) have been assayed approximately monthly since 2001 by the Central Coast Long-term Environmental Assessment Network (CCLEAN) regional monitoring program, together with macronutrients (nitrate + nitrite, phosphate, silicate, ammonium [since 2003]), and other water quality parameters. Data presented are from the 2004 to 2005 annual report (CCLEAN, 2006). Since 2001–2002, the annual load of urea from seven gauged river collection sites and four urban wastewater discharges have increased annually, from  $<0.06 \times 10^5 \text{ kg/yr}$  to approximately  $0.23 \times 10^5 \text{ kg/yr}$  (2004–2005). During the same interval, urea load from rivers (versus wastewater) have gone from a small percentage (approximately 1%) to greater than half the total urea load. In comparison, the ammonium-nitrogen load is negligible in the gauged rivers compared to the wastewater discharge ( $8.0\text{--}10.0 \times 10^5 \text{ kg/yr}$ ), and nitrate remains the dominant source of nitrogen in rivers ( $3.5\text{--}6.0 \times 10^5 \text{ kg/yr}$ ), as well as a significant source in wastewater discharge ( $0.6\text{--}2.5 \times 10^5 \text{ kg/yr}$ ). Using the 2004–2005 data for seven gauged rivers, which account for most of the freshwater discharge into Monterey Bay, urea (by weight) accounts for approximately 2% of the nitrogen load, ammonium accounts for about 2.1% and the remainder of the N-load is as nitrate + nitrite.

Despite the small percentage of the total-N load accounted for by urea, it can nonetheless represent a significant source of nitrogen to the environment. Fig. 2 represents weekly nitrate,

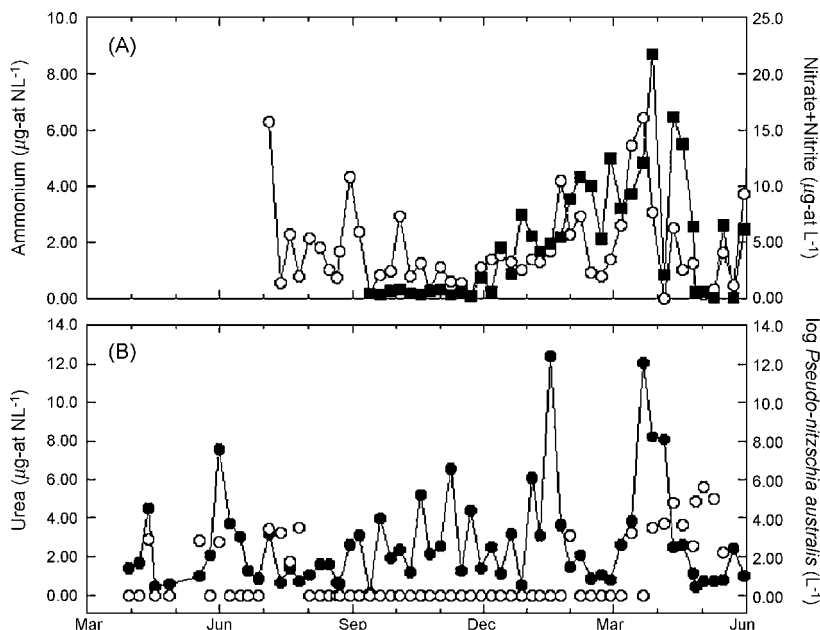


**Fig. 2.** Surface (0–2 m depth) nitrate + nitrite (filled squares), and ammonium (open circles) are plotted in Panel A, with urea (filled circles) concentrations from seawater and log-transformed values of *Pseudo-nitzschia australis* abundance [ $\log (\text{cells L}^{-1})$ ] plotted in Panel B. Samples were collected weekly from the Santa Cruz Municipal Wharf between March 2006 and May 2007.

ammonium, and urea concentrations from surface water samples collected at the Santa Cruz Municipal Wharf (note that nitrate concentrations were not available prior to September 2006). Values range from undetectable to  $12.38 \mu\text{g-at N L}^{-1}$  or an average of 38% of the total N, with some seasonality. In contrast, monthly surface samples collected from sites offshore in Monterey Bay during the same time period (data not shown) never exceeded  $0.74 \mu\text{g-at N L}^{-1}$ , or generally 10-fold lower than equivalent coastal concentrations. This, combined with the known loading from rivers and waste dischargers, strongly suggests that coastal urea concentrations in Monterey Bay are indicative of anthropogenic inputs. In the lower panel of Fig. 2, the dominant HAB organism from Monterey Bay, *P. australis* is plotted versus ambient urea concentrations. While these data are merely correlative, both *P. australis* and N loading (urea, nitrate, and ammonium) exhibit a seasonal increase in the late spring.

In San Francisco Bay, the monitoring of ambient concentrations of urea was initiated after the first recorded blooms of *H. akashiwo* in 2002 (Herndon, 2003; Herndon et al., 2003; O’Halloran et al., 2006). Time series from San Francisco Bay (Fig. 3) also exhibited measurable urea concentrations, which at times became the dominant nitrogen source in surface waters (e.g. early June 2005). Here we present data from May–October, 2005 from two sites in San Francisco Bay where *H. akashiwo* blooms have been seen previously; northeastern (Paradise Cay) and western (Richardson Bay) sides of the Tiburon Peninsula. Monthly, year-round concentrations of urea, ammonium and nitrate data are now being collected at a series of sites in San Francisco Bay as part of the National Estuarine Research Reserve and will be presented elsewhere. The mean urea surface concentrations in these two embayments close to the open ocean (<10 km) range from  $0.56$  to  $5.10 \mu\text{g-at N L}^{-1}$ , and represent between 3 and 42 percent (mean = 14%) of the total N (nitrate, ammonium and urea) available for phytoplankton growth. Recent urea measurements in the North Bay of San Francisco Bay also demonstrate strong seasonal variability, but ambient concentrations are much more elevated and concentrations exceeding  $>24 \mu\text{g-at N L}^{-1}$ , are commonly found (Cochlan and Herndon, unpublished data). Although urea concentrations in

San Francisco Bay often represent a relatively small proportion of the total ambient N, given the strong affinity demonstrated by California HAB species for urea at low concentrations, and the potential inhibitory effects of urea on nitrate uptake seen elsewhere (e.g., Molloy and Syrett, 1988; Cochlan and Harrison, 1991), the role of urea in HAB development in California may be more important than previously realized.

Despite the evidence for both physiological capacity and availability of urea in coastal waters, most previous investigations have been unable to make direct links between eutrophication and harmful algal blooms in California. For example, both Otero and Siegel (2004) and Warrick et al. (2005) suggest that maximum nutrient input occurs during the winter, out of phase with high

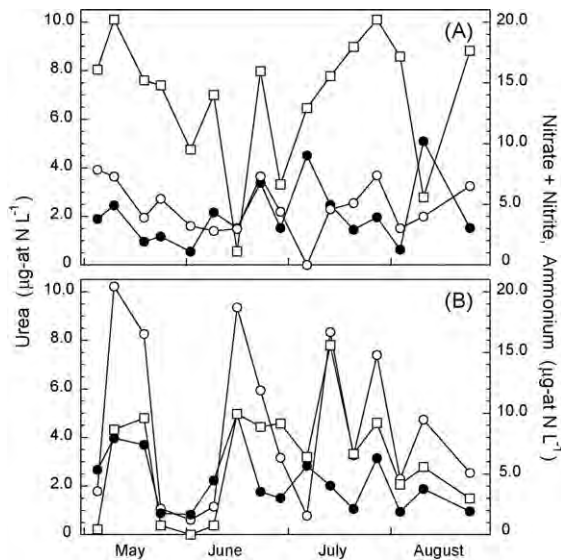


**Fig. 3.** Mean ( $n = 2$ ) surface (0–0.5 m depth) concentrations during May–Sept 2005 of urea (closed circles), ammonium (open circles) and nitrate + nitrite (open squares) on the (A) northeastern (adjacent to Paradise Cay) and (B) western (Richardson Bay) sides of the Tiburon Peninsula in San Francisco Bay, California.

coastal productivity, while Wilkerson et al. (2006) state that nutrient availability only secondarily controls productivity in the eutrophied San Francisco Bay, and dismiss the contribution of urea as insignificant due to its relative abundance compared to elevated nitrate concentrations. Similarly, a recent study by Schnetzer et al. (2007) demonstrated a negative correlation between runoff, nutrients, and a large *Pseudo-nitzschia* event in Southern California, while Kudela et al. (2004) could not find a direct correlation between runoff and *Pseudo-nitzschia* blooms in central California. We suggest that the lack of correlation between runoff and HAB events in California may be due in part to the lack of measurements of urea during these and most other studies, since there is at least a qualitative correlative relationship between urea concentrations and *P. australis* abundance for the Santa Cruz Municipal Wharf time-series (Fig. 2B). During the 2007 bloom event, particulate domoic acid concentrations ( $\text{ng DA L}^{-1}$ ) closely matched cell abundance, with maximum concentrations of  $236.4 \text{ ng L}^{-1}$  particulate domoic acid on 2 May 2007. Based on the reported findings, at minimum there is evidence that ambient urea concentrations can maintain (Kudela and Cochlan, 2000) or even exacerbate (Howard et al., 2007) HAB events.

#### 4.3. Summary and Implication for HABs in California

Based on these data and observations, there is good evidence for the availability of urea for both documented harmful algal bloom events (Kudela and Cochlan, 2000; Herndon et al., 2003; Howard et al., 2007; Kudela et al., 2008) and as a common source of nitrogen in coastal waters of California. All of the HAB organisms tested showed an ability to utilize urea, with generally higher affinity at low ( $<K_s$ ) ambient concentrations. As expected, the diatom *Pseudo-nitzschia* generally exhibited a preference (as determined by uptake kinetics parameters) for nitrate, and exhibited lower uptake and lower growth when given solely urea (Cochlan et al., 2008; Howard et al., 2007). In contrast, the three dinoflagellates compared herein exhibited higher  $V_{\text{max}}$  and  $\alpha$  values (greater preference) for ammonium and urea, or demonstrated little or no difference in kinetics parameters with nitrogen source (*L. polyedrum*). Finally, the raphidophyte *H. akashiwo* exhibited greater uptake and affinity for ammonium, then nitrate, and finally urea. Significantly, all of these HAB organisms exhibited flexibility in the ability to utilize whatever nitrogen compounds were provided. Kinetics data alone are not sufficient to identify urea or other anthropogenic nutrients as a direct cause for HAB blooms in California. Assuming that urea is a good indicator of eutrophication, there is clear evidence that the increase in high biomass, noxious, and/or toxic harmful algal blooms in California coastal waters would be capable of utilizing enhanced nutrient loading, and may be directly or indirectly responding (e.g. via enhanced toxin production) to anthropogenic impacts.

#### Acknowledgements

This manuscript developed from a presentation given as part of the GEOHAB HABs and Eutrophication workshop, and represents a contribution to the GEOHAB Core Science Project on Harmful Algal Blooms and Eutrophication. We thank the organizers, and in particular Dr. Patricia Glibert, for the opportunity to participate. A first version of the manuscript also benefited from the comments of Dr. Glibert and two anonymous reviewers. Data from CCLEAN were kindly provided by Mr. Dane Hardin. Dr. Tawnya Peterson kindly provided the cell enumeration data. Partial funding was provided by NOAA MERHAB grant NA04NOS4780239-02 and NOAA grant NA108H-C, the Center for Integrated Marine Technology through NOAA grant NA160C2936, and as a fellowship

(JQL) from an anonymous donor through the Center for the Dynamics and Evolution of the Land-Sea Interface (CELSI),[SS]

#### References

- Anderson, D., Glibert, P., Burkholder, J., 2002. Harmful algal blooms and eutrophication: nutrient sources, composition, and consequences. *Estuaries* 25, 704–726.
- Armstrong, M., Kudela, R., 2006. Evaluation of California isolates of *Lingulodinium polyedrum* for the production of yessotoxin. *African Journal of Marine Science* 28, 399–401.
- Auro, M.E., 2007. Nitrogen dynamics and toxicity of the pennate diatom *Pseudo-nitzschia cuspidata*: A field and laboratory study. M.S. Thesis, San Francisco State University, San Francisco, CA, USA, 91 pp.
- Bates, S., Garrison, D., Horner, R., 1998. Bloom dynamics and physiology of domoic acid producing *Pseudo-nitzschia* species. In: Anderson, D., Cembella, A., Hallegraeef, G. (Eds.), *Physiological ecology of harmful algal blooms*. Springer-Verlag, Heidelberg, pp. 267–292.
- Beman, M., Arrigo, K., Matson, P., 2005. Agricultural runoff fuels large phytoplankton blooms in vulnerable areas of the ocean. *Nature* 434, 211–214.
- CCLEAN, 2006. Central coast long-term environmental assessment network regional monitoring program annual report, 2004–2005: 125 pp.
- Cloern, J., Schraga, T., Lopez, C., Knowles, N., Labiosa, R., Dugdale, R., 2005. Climate anomalies generate an exceptional dinoflagellate bloom in San Francisco Bay. *Geophysical Research Letters* 32, L14608 doi:14610.11029/12005GL023321.
- Cochlan, W.P., Harrison, P.J., 1991. Inhibition of nitrate uptake by ammonium and urea in the eukaryotic picoflagellate *Micromonas pusilla*. *Journal of Experimental Marine Biology and Ecology* 153, 143–152.
- Cochlan, W.P., Herndon, J., Kudela, R.M., 2008. Inorganic and organic nitrogen uptake by the toxigenic diatom *Pseudo-nitzschia australis* (Bacillariophyceae). *Harmful Algae* 8, 111–118.
- Conway, H., Harrison, P., Davis, C., 1976. Marine diatoms grown in chemostats under silicate or ammonium limitation. II. Transient response of *Skeletonema costatum* to single addition of the limiting nutrient. *Marine Biology* 35, 187–199.
- Curtiss, C., Langlois, G., Busse, L., Mazzillo, F., Silver, M., 2008. The emergence of *Cochlodinium* along the California coast (USA). *Harmful Algae* 7, 337–346.
- Dortch, Q., Postel, J., 1989. Biochemical indicators of N utilization by phytoplankton during upwelling off the Washington coast. *Limnol Oceanogr* 34, 758–773.
- Dortch, Q., 1990. The interaction between ammonium and nitrate uptake in phytoplankton. *Marine Ecology Progress Series* 61, 183–201.
- Dugdale, R., Wilkerson, F., 1986. The use of  $^{15}\text{N}$  to measure nitrogen uptake in eutrophic oceans: experimental considerations. *Limnology and Oceanography* 31, 673–689.
- Eppley, R., Renger, E., Harrison, W., 1979. Nitrate and phytoplankton production in California coastal waters. *Limnology and Oceanography* 24, 483–494.
- Fan, C., Glibert, P., Burkholder, J., 2003. Characterization of the affinity for nitrogen, uptake kinetics, and environmental relationships for *Prorocentrum minimum* in natural blooms and laboratory cultures. *Harmful Algae* 2, 283–299.
- GEOHAB, 2006. Global ecology and oceanography of harmful algal blooms. *Harmful Algal Blooms in Eutrophic Systems* 74.
- Glibert, P.M., Lipschultz, F., McCarthy, J.J., Altabet, M.A., 1982. Isotope dilution models of uptake and remineralization of ammonium by marine plankton. *Limnology and Oceanography* 27, 639–650.
- Glibert, P., Anderson, D., Gentien, P., Graneli, E., Sellner, K., 2005. The global, complex phenomena of harmful algal blooms. *Oceanography* 18, 130–141.
- Glibert, P., Harrison, J., Heil, C., Seitzinger, S., 2006. Escalating worldwide use of urea—a global change contributing to coastal eutrophication. *Biogeochemistry* 77, 441–463.
- Goldman, J., Glibert, P., 1982. Comparative rapid ammonium uptake by four species of marine phytoplankton. *Limnology and Oceanography* 27, 814–827.
- Goeyens, L., Kindermans, N., Abu Yusuf, M., Elskens, M., 1998. A room temperature procedure for the manual determination of urea in seawater. *Estuarine, Coastal and Shelf Science* 47, 415–418.
- Healey, F., 1980. Slope of the Monod equation as an indicator of advantage in nutrient competition. *Microbial Ecology* 5, 245–336.
- Herndon, J., 2003. Nitrogen uptake by the raphidophyte *Heterosigma akashiwo*: a laboratory and field study. M.A. Thesis, San Francisco State University, San Francisco, CA, USA, 77 pp.
- Herndon, J., Cochlan, W.P., 2007. Nitrogen utilization by the raphidophyte *Heterosigma akashiwo*: Growth and uptake kinetics in laboratory cultures. *Harmful Algae* 6, 260–270.
- Herndon, J., Cochlan, W.P., Horner, R., 2003. *Heterosigma akashiwo* blooms in San Francisco Bay. Interagency Ecological Program for the San Francisco Estuary Newsletter 16, 46–48.
- Holmes, R.M., Aminot, A., Kerouel, R., Hooker, B.A., Peterson, B.J., 1999. A simple and precise method for measuring ammonium in marine and freshwater ecosystems. *Canadian Journal of Fisheries and Aquatic Science* 56, 1801–1808.
- Howard, M.D.A., Ladizinsky, N., Cochlan, W.P., Kudela, R.M., 2007. Nitrogenous preference of toxigenic *Pseudo-nitzschia australis* (Bacillariophyceae) from field and laboratory experiments. *Harmful Algae* 6, 206–217.
- Knepel, K., Bogren, K., 2001. Determination of orthophosphorus by flow injection analysis in seawaters. *QuickChem Method* 31-115-01-1-H, 14 pp.
- Kudela, R., Chavez, F., 2004. The impact of coastal runoff on ocean color during an El Niño year in central California. *Deep-Sea Research II* 51, 1173–1185.

- Kudela, R., Cochlan, W.P., 2000. Nitrogen and carbon uptake kinetics and the influence of irradiance for a red tide bloom off Southern California. *Aquatic Microbial Ecology* 21, 31–47.
- Kudela, R., Cochlan, W., Roberts, A., 2004. Spatial and temporal patterns of *Pseudo-nitzschia* spp. in central California related to regional oceanography. In: Steidinger, K., Lansberg, J., Tomas, C., Vargo, G. (Eds.), *Proceedings of the 10th International Conference on Harmful Algal Blooms*. Florida Environmental Research Institute and UNESCO, St. Petes Beach, FL, pp. 347–349.
- Kudela, R., Dugdale, R., 2000. Nutrient regulation of phytoplankton productivity in Monterey Bay, California. *Deep-Sea Research II* 47, 1023–1053.
- Kudela, R., Pitcher, G., Probyn, T., Figueiras, F., Moita, T., Trainer, V., 2005. Harmful algal blooms in coastal upwelling systems. *Oceanography* 18, 184–197.
- Kudela, R., Ryan, J., Blakely, M., Lane, J., Peterson, T., 2008. Linking the physiology and ecology of *Cochlodinium* to better understand harmful algal bloom events: a comparative approach. *Harmful Algae* 7, 278–292.
- Lomas, M.W., Glibert, P.M., 2000. Comparisons of nitrate uptake, storage and reduction in marine diatoms and flagellates. *Journal of Phycology* 36, 903–913.
- McCarthy, J.J., 1972. The uptake of urea by natural populations of marine phytoplankton. *Limnology and Oceanography* 17, 738–748.
- McCarthy, J., Taylor, W., Taft, J., 1977. Nitrogenous nutrition of the plankton in the Chesapeake Bay. 1. Nutrient availability and phytoplankton preferences. *Limnology and Oceanography* 22, 996–1011.
- Miller, P.E., Scholin, C.A., 1998. Identification and enumeration of cultured and wild *Pseudo-nitzschia* (Bacillariophyceae) using species-specific LSU rRNA-targeted fluorescent probes and filter-based whole cell hybridization. *Journal of Phycology* 34, 371–382.
- Molloy, C.J., Syrett, P.J., 1988. Effect of light and N deprivation on inhibition of nitrate uptake by urea in microalgae. *Journal of Experimental Marine Biology and Ecology* 118, 97–101.
- O'Halloran, C., Silver, M.W., Holman, T.R., Scholin, C.A., 2006. *Heterosigma akashiwo* in central California waters. *Harmful Algae* 5, 124–132.
- Otero, M.P., Siegel, D.A., 2004. Spatial and temporal characteristics of sediment plumes and phytoplankton blooms in the Santa Barbara Channel. *Deep-Sea Research II* 51, 1129–1149.
- Press, W., Teukolsky, S., Vetterling, A., Flannery, B., 1992. *Numerical Recipes in C: The Art of Scientific Computing*. Cambridge University Press.
- Price, N., Harrison, P., 1987. A comparison of methods for the measurement of dissolved urea concentration in seawater. *Marine Biology* 92, 307–319.
- Ryan, J., Dierssen, H., Kudela, R., Scholin, C., Johnson, K., Sullivan, J., Fischer, A., Rienecker, E., McEnaney, P., Chavez, F., 2005. Coastal ocean physics and red tides: an example from Monterey Bay, California. *Oceanography* 18 (2), 246–255.
- Schnetzler, A., Miller, P.E., Schaffner, R.A., Stauffer, B.A., Jones, B.H., Weisberg, S.B., DiGiacomo, P.M., Berelson, W.M., Caron, D.A., 2007. Blooms of *Pseudo-nitzschia* and domoic acid in the San Pedro Channel and Los Angeles harbor areas of the Southern California Bight. *Harmful Algae* 6, 372–387.
- Smayda, T., 1997. Harmful algal blooms: their ecophysiology and general relevance to phytoplankton blooms in the sea. *Limnology and Oceanography* 42, 1137–1153.
- Smith, P., Bogren, K., 2001a. Determination of nitrate and/or nitrite in brackish or seawater by flow injection analysis colorimeter: QuickChem Method 31-107-04-1-E, Saline Methods of Analysis. Lachat Instruments, Milwaukee, WI, 12 pp.
- Smith, P., Bogren, K., 2001b. Determination of silicate in brackish or seawater by flow injection analysis: QuickChem Method 31-114-27-1-C, Saline Methods of Analysis. Lachat Instruments, Milwaukee, WI, 12 pp.
- Solorzano, L., 1969. Determination of ammonia in natural waters by the phenol hypochlorite method. *Limnology and Oceanography* 14, 799–801.
- Warrick, J., Washburn, L., Brzezinski, M., Siegel, D., 2005. Nutrient contributions to the Santa Barbara Channel, California, from the ephemeral Santa Clara River. *Estuarine, Coastal and Shelf Science* 62, 559–574.
- Welschmeyer, N., 1994. Fluorometric analysis of Chlorophyll *a* in the presence of Chlorophyll *b* and pheopigments. *Limnology and Oceanography* 39, 1985–1992.
- Wilkerson, F.P., Dugdale, R.C., Hogue, V.E., Marchi, A., 2006. Phytoplankton blooms and nitrogen productivity in San Francisco Bay. *Estuaries and Coasts* 29, 401–416.
- Work, T., Beale, A., Fritz, L., Quilliam, M., Silver, M., Buck, K., Wright, J., 1993. Domoic acid intoxication of brown pelicans and cormorants in Santa Cruz. In: Smayda, T., Shimizu, Y. (Eds.), *Toxic Phytoplankton Blooms in the Sea*. Elsevier, California, pp. 643–650.



# Development of a logistic regression model for the prediction of toxigenic *Pseudo-nitzschia* blooms in Monterey Bay, California

Jenny Q. Lane<sup>1,\*</sup>, Peter T. Raimondi<sup>2</sup>, Raphael M. Kudela<sup>1</sup>

<sup>1</sup>Department of Ocean Sciences, University of California, 1156 High Street, Santa Cruz, California 95064, USA

<sup>2</sup>Department of Ecology and Evolutionary Biology, University of California, Center for Ocean Health, 100 Shaffer Road, Santa Cruz, California 95064, USA

**ABSTRACT:** Blooms of the diatom genus *Pseudo-nitzschia* have been recognized as a public health issue in California since 1991 when domoic acid, the neurotoxin produced by toxigenic species of *Pseudo-nitzschia*, was first detected in local shellfish. Although these blooms are recurring and recognized hazards, the factors driving bloom proliferation remain poorly understood. The lack of long-term field studies and/or deficiencies in the scope of environmental data included within them hinders the development of robust forecasting tools. For this study, we successfully developed predictive logistic models of toxigenic *Pseudo-nitzschia* blooms in Monterey Bay, California, from a multi-project dataset representing 8.3 yr of sampling effort. Models were developed for year-round (annual model) or seasonal use (spring and fall–winter models). The consideration of seasonality was significant: chlorophyll *a* (chl *a*) and silicic acid were predictors in all models, but period-specific inclusions of temperature, upwelling index, river discharge, and/or nitrate provided significant model refinement. Predictive power for 'unknown' (future) bloom cases was demonstrated at  $\geq 75\%$  for all models, out-performing a chl *a* anomaly model, and performing comparably to, or better than, previously described statistical models for *Pseudo-nitzschia* blooms or toxicity. The models presented here are the first to have been developed from long-term ( $>1.5$  yr) monitoring efforts, and the first to have been developed for bloom prediction of toxigenic *Pseudo-nitzschia* species. The descriptive capacity of our models places historical and recent observations into greater ecological context, which could help to resolve historical alternation between the implication of freshwater discharge and upwelling processes in bloom dynamics.

**KEY WORDS:** *Pseudo-nitzschia* · Predictive model · Logistic regression · Harmful algal bloom · Phytoplankton monitoring · Domoic acid

Resale or republication not permitted without written consent of the publisher

## INTRODUCTION

Harmful algal blooms (HABs) can have severe deleterious consequences for local industry (e.g. shellfish, tourism), public health, and ecosystem health. In addition, the incidence of HABs appears to be increasing in both frequency and intensity (Hallegraeff 1993, Anderson et al. 2002, Glibert et al. 2005). This trend, and its potential to inflict rising economic and societal costs, has encouraged the development of HAB forecasting tools in recent years (Schofield et al. 1999,

Johnsen & Sakshuag 2000, Fisher et al. 2003). Many of these efforts have focused on the prediction and monitoring of dinoflagellate blooms and associated red tides, and successful prediction models for these types of HABs span a wide range of modeling approaches and complexity. One of the simplest approaches utilizes satellite-derived chlorophyll anomalies to identify potentially harmful blooms (e.g. Allen et al. 2008) or even species-specific blooms (Tomlinson et al. 2004). Issues associated with satellite-derived models (non-specificity, infrequent data) can be overcome by com-

\*Email: jquay@ucsc.edu

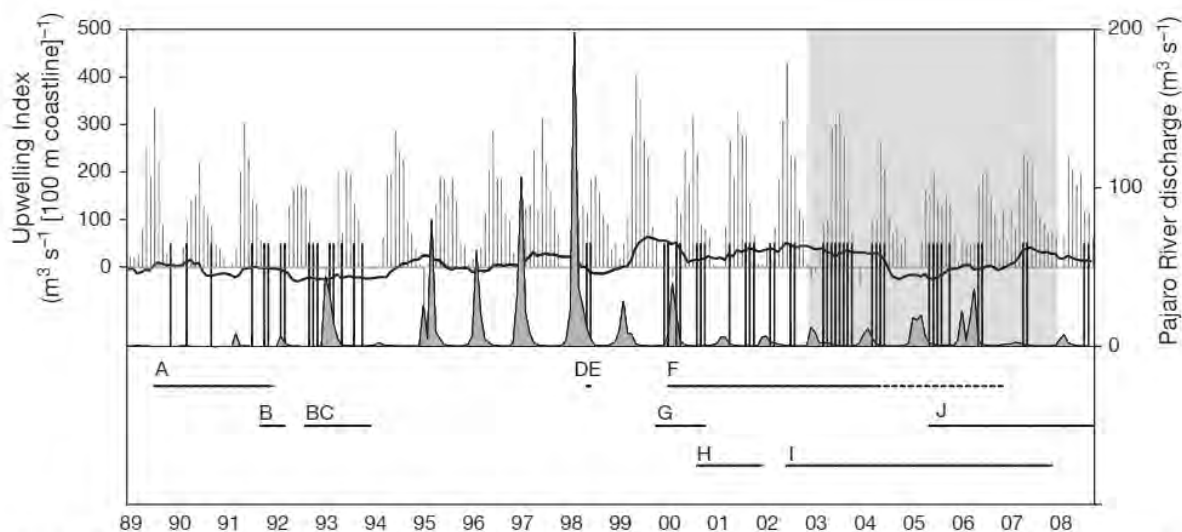


Fig. 1. Time series of bloom events, as reported in published literature and in the modeling dataset used here. The time periods addressed by the various studies are indicated below the plot and are as follows: A: Buck et al. (1992); B: Walz et al. (1994); C: Walz (1995); D: Scholin et al. (2000); E: Trainer et al. (2000); F: Jester et al. (2009); G: Lefebvre et al. (2002b); H: Goldberg (2003); I: Center for Integrated Marine Technologies model dataset (present study); J: California Program for Regional Enhanced Monitoring for PhycoToxins model dataset (present study). Grey shading: time-frame of data inclusion for the models developed in the present study. Vertical black bars: months for which blooms of toxigenic *Pseudo-nitzschia* (cell concentration  $\geq 10\,000$  cells  $\text{l}^{-1}$ ) were reported. A 12 mo moving average of monthly upwelling anomaly (black line), the monthly upwelling index for  $36^{\circ}\text{N}$ ,  $122^{\circ}\text{W}$  (grey bars), and monthly mean Pajaro River discharge (area plot) are shown. Within the time-frame of Jester et al. (2009) (F), note the negative values of the upwelling anomaly and the relatively high monthly mean river discharges over the span of summer 2004 through 2006 (F; dashed line); this period was identified by Jester et al. (2009) as a period of severely decreased *Pseudo-nitzschia* abundance

binning satellite data with other predictors, as is done in the Southwest Florida (USA) operational forecast for *Karenia brevis*. This model includes satellite data, wind predictions, and rule-based modeling to improve forecasting success (Stumpf et al. 2009). A similar approach integrating multiple environmental datasets was used for the European Harmful Algal Bloom Expert System (HABES); this predictive modeling approach uses 'fuzzy logic' to identify blooms of *Nodularia spumigena*, *Dinophysis* spp., *Alexandrium minutum*, *K. mikimotoi*, and *Phaeocystis globosa* (Blauw et al. 2006). The authors state that fuzzy logic bridges the gap between purely empirical (statistical) predictions and fully deterministic models. Finally, seasonal initiation of HAB events and spatial/temporal distribution have been successfully predicted using fully coupled deterministic physical-biological models in the Gulf of Maine (USA) for *A. fundyense* (McGillicuddy et al. 2005). In contrast to these and other efforts, relatively little predictive skill has been developed for HABs of diatom species.

Toxigenic species of the diatom *Pseudo-nitzschia* are producers of domoic acid, which can cause neurotoxic poisoning in humans (Addison & Stewart 1989, Bates et al. 1989), marine mammals (Lefebvre et al. 1999, 2002a, Scholin et al. 2000, Kreuder et al. 2005), and

birds (Fritz et al. 1992, Beltrán et al. 1997). Since initial documentation in 1991, HABs of toxigenic *Pseudo-nitzschia* have occurred in Monterey Bay, California, with regularity (Buck et al. 1992, Fritz et al. 1992, Work et al. 1993, Scholin et al. 2000, Trainer et al. 2001); the bulk of published *Pseudo-nitzschia* bloom data was generated through episodic, generally stand-alone, research projects undertaken in reaction to these periodic events (Fig. 1). Because these studies were relatively short and episodic in nature, they forcibly relied on circumstantial observations or single-variable correlations for identification of environmental conditions conducive to bloom formation; the constraints associated with this approach led to calls for long-term monitoring approaches (Trainer et al. 2000, Bates & Trainer 2006).

Despite the lack of long-term data, eutrophication via terrestrial freshwater runoff (Bird & Wright 1989, Trainer et al. 1998, Scholin et al. 2000), fluctuations in nutrient ratios (Marchetti et al. 2004), and upwelling processes (Buck et al. 1992, Trainer et al. 2000, Anderson et al. 2006) were implicated as prominent causative factors in historical literature, and our modeling design was developed with this historical ecological perspective in mind. While our data used for model development could not extend over the full time period

represented within the literature due to sampling and methodological inconsistencies, the range of ecological circumstances addressed are not unlike those encountered and implicated previously as triggers for HAB events (Fig. 1).

Our efforts follow 2 previous modeling studies that used shorter duration datasets. The first (Blum et al. 2006) was an attempt to model cellular domoic acid in a toxigenic strain of *Pseudo-nitzschia* (*Pseudo-nitzschia pungens f. multiseries*). In that study, 4 models were developed: 2 linear models demonstrated 'good predictive ability', but were developed from laboratory data that failed to address the scope of nutrient concentrations and ratios encountered in the field and were therefore not appropriate for use with field data. A third linear model and a logistic regression model were developed from combined laboratory data and field data collected from monospecific blooms of *P. pungens f. multiseries* off the coasts of Prince Edward Island (Canada), and Washington State (USA). Split-sample validations of these models (75% data used for model development; 25% reserved for model validation) demonstrated their 'adequate reliability', but the limited amount of field data (N = 46) and the predominance of restrictive laboratory data within the modeling dataset left the applicability of these models undetermined.

The second modeling study (Anderson et al. 2009) developed linear regression (hindcast) models of *Pseudo-nitzschia* blooms, particulate domoic acid, and cellular domoic acid, from: (1) a 'full' (remotely sensed and *in situ*) suite of predictor variables and (2) a 'remote-sensing only' suite of predictor variables. This study was limited in the amount of data available for model development (N = 72 to 89), but provided preliminary insight into *Pseudo-nitzschia* bloom mechanisms, including macronutrient control. Both model sets presented by Anderson et al. (2009) demonstrated high rates of false negative predictions, presumably due to the relatively limited dataset.

Here, we develop logistic regression models of toxigenic *Pseudo-nitzschia* blooms in Monterey Bay, California. This modeling exercise had 3 goals: (1) to develop *Pseudo-nitzschia* bloom models that are straightforward and useful in their application towards bloom monitoring, (2) through model development, to identify environmental variables that are significant factors in bloom incidence, and (3) to test the recurrence of these significant environmental variables in the previous *Pseudo-nitzschia* models described by Anderson et al. (2009) and Blum et al. (2006). The previous modeling efforts and this one are not wholly consistent in terms of scope, evaluated variables, or specific aim: Anderson et al. (2009) developed models of 'generic' *Pseudo-nitzschia* blooms, cellular domoic

acid, and particulate domoic acid from a 1.5 yr dataset collected from the Santa Barbara Channel, while Blum et al. (2006) developed models of particulate domoic acid from a mixture of experimental and field data. These previous studies and our efforts clearly differ in their region of interest and specific model subject. In the context of the present study, these disparities are an advantage, in that they allow for inter-model comparison capable of identifying factors that are likely to be universally significant to *Pseudo-nitzschia* bloom incidences and to the introduction of domoic acid into the marine environment through bloom proliferation. Thus, our model and the comparison of these 3 efforts should help to identify a common set of variables useful for predictive modeling of *Pseudo-nitzschia* in similar systems, such as major eastern boundary current regimes (Kudela et al. 2005).

We present 3 logistic regression models of toxigenic *Pseudo-nitzschia* blooms in Monterey Bay, California, as they occur throughout the year (annual model) and seasonally (spring and fall-winter models). A total of 31 environmental variables were evaluated, and 6 variables were identified as statistically significant for bloom prediction. This work is the first to present robust *Pseudo-nitzschia* bloom models developed from long-term monitoring data, and the first to evaluate eutrophication processes and seasonality in the prediction of *Pseudo-nitzschia* bloom incidences.

## MATERIALS AND METHODS

**Compilation of the model dataset.** We compiled a dataset from publications that included *Pseudo-nitzschia* cell counts for Monterey Bay (Buck et al. 1992, Walz et al. 1994, Walz 1995, Villac 1996, Scholin et al. 2000, Goldberg 2003, Lefebvre et al. 2002b). Additional unpublished datasets were provided by Moss Landing Marine Laboratories (MLML), and internally generated through the Center for Integrated Marine Technologies (CIMT) and through the California Program for Regional Enhanced Monitoring for PhycoToxins (Cal-PReEMPT). Details on sampling and analytical methods for internally generated datasets are provided.

We obtained 2099 discrete cases from the above sources, 1156 of which were from surface waters (depth  $\leq 5$  m). All of the data were assessed to ensure methodological consistency, specifically: (1) unbiased sample collection and (2) true concurrency in environmental and *Pseudo-nitzschia* sampling. Of the 1071 cases remaining, 576 contained cell counts of toxigenic *Pseudo-nitzschia*. Not all data contained the same suite of environmental variables. For finalization of the modeling dataset, it was necessary to evaluate which data

were sufficiently complete, i.e. evaluate the minimal combination of variables sufficient for the development of a successful model. The receiver operating characteristic (ROC) was used to conduct this evaluation. ROC is a measure of model fit that scales like a traditional (US) academic point system (<0.6 = poor; 0.6 to 0.7 = fair; 0.7 to 0.8 = good; 0.8 to 0.9 = very good; >0.9 = excellent). Models developed from single, single and universally available (i.e. river discharge, upwelling index), and pairs of predictor variables failed to achieve 'very good' model fit accuracy. To achieve this level of accuracy, model development required concurrent macronutrient, chlorophyll *a* (chl *a*), and temperature variables in combination (Tables 1 & 2). Final inclusion of cases for the models presented therefore required sample collection from Monterey Bay surface waters, and toxigenic *Pseudo-nitzschia* cell counts (*P. multiseriata* and/or *P. australis*) with concurrent environmental measurements of seawater temperature, chl *a*, and macronutrients.

**Internal data: sample collection.** Samples were collected monthly from June 2002 to November 2007 from 11 stations throughout Monterey Bay as part of the CIMT project. PVC Niskin bottles (10 l volume fitted with silicone rubber band strings) mounted on an instrumented rosette were used to collect water from 5 m depth. Surface samples were collected from 2 stations by PVC bucket. Temperature data were obtained from a Seabird SBE-19 CTD deployed concurrently with water sampling.

Table 1. Evaluations of independent variable(s) as predictor variables were performed using all compiled literature and field data of toxic *Pseudo-nitzschia* in Monterey Bay at a depth  $\leq 5$  m (N = 576). The receiver operating characteristic (ROC) is a measure of model fit accuracy, where <0.6 = poor, 0.6 to 0.7 = fair, 0.7 to 0.8 = good, 0.8 to 0.9 = very good, and >0.9 is considered excellent. Inclusion of macronutrient, seawater temperature, and chlorophyll *a* as predictor variables was necessary to achieve 'very good' model fit accuracy.

A key to variable names is provided in Table 2.

Independent variable	N (cases)	Cases omitted	ROC
Salinity	427	149	0.462
Temp	493	83	0.573
ln(silicic acid)	516	60	0.614
ln(chl <i>a</i> )	497	79	0.618
ln(chl <i>a</i> ), temp	473	103	0.638
ln(chl <i>a</i> ), upwelling	492	84	0.638
ln(silicic acid), upwelling	516	60	0.713
ln(silicic acid), ln(chl <i>a</i> )	444	132	0.757
ln(nitrate), temp, ln(chl <i>a</i> )	419	157	0.766
ln(silicic acid), temp	438	138	0.785
ln(silicic acid), temp, ln(chl <i>a</i> )	422	154	0.848

Table 2. Complete list of the variables evaluated as independent (predictor) variables in the logistic regression models. X: all environmental variables and ratios, excluding temperature

Independent variable	Abbreviation	Units
Seawater temperature	Temp	°C
Total chlorophyll <i>a</i>	Chl <i>a</i>	$\mu\text{g l}^{-1}$
Nitrate	Nitrate	$\mu\text{M}$
Silicic acid	Silicic acid	$\mu\text{M}$
Ortho-phosphate	Phosphate	$\mu\text{M}$
Silicic acid (nitrate) <sup>-1</sup>	Silicic acid:nitrate	
Nitrate (silicic acid) <sup>-1</sup>	Nitrate:silicic acid	
Ortho-phosphate (nitrate) <sup>-1</sup>	Phosphate:nitrate	
Nitrate (ortho-phosphate) <sup>-1</sup>	Nitrate:phosphate	
Ortho-phosphate (silicic acid) <sup>-1</sup>	Phosphate:silicic acid	
Silicic acid (ortho-phosphate) <sup>-1</sup>	Silicic acid:phosphate	
Pajaro River discharge	Pajaro River	$\text{m}^3 \text{s}^{-1}$
San Lorenzo River discharge	San Lorenzo River	$\text{m}^3 \text{s}^{-1}$
Soquel River discharge	Soquel River	$\text{m}^3 \text{s}^{-1}$
Salinas River discharge	Salinas River	$\text{m}^3 \text{s}^{-1}$
Bakun upwelling index	Upwelling	$\text{m}^3 \text{s}^{-1}$
Ln(X + 1)	Ln(X)	

Shore-based surface samples were collected weekly from May 2005 to April 2008 from the Santa Cruz Municipal Wharf (36° 57.48' N, 122° 1.02' W) as part of the Cal-PreEMPT project using a PVC bucket or by integration of water samples collected from 3 discrete depths (0, 1.5, and 3 m) with a FieldMaster 1.75 l basic water bottle. Temperature was measured in the field by digital thermometer immediately following sample retrieval.

River discharge rates for the Salinas, San Lorenzo, Soquel, and Pajaro Rivers were obtained from the United States Geological Survey National Water Information System (<http://waterdata.usgs.gov/nwis/>). Bakun daily upwelling index values for the Monterey Bay region (36°N, 122°W) were obtained from the National Oceanographic and Atmospheric Administration Pacific Environmental Research Division ([www.pfel.noaa.gov/products/PFEL/](http://www.pfel.noaa.gov/products/PFEL/)).

**Internal data: analytical methods.** Samples for chl *a* were collected in duplicate and filtered onto uncombusted glass-fiber filters (Whatman GF/F) and processed using the non-acidification method (Welschmeyer 1994). Macronutrients (Nitrate plus nitrite [hereafter referred to as nitrate], silicic acid and ortho-phosphate) were stored frozen prior to analysis with a Lachat Quick Chem 8000 Flow Injection Analysis system using standard colorimetric techniques (Knepel & Bogren 2001, Smith & Bogren 2001a,b). *Pseudo-nitzschia* species identification and enumeration utilized species-specific large subunit rRNA-targeted

probes following standard protocols (Miller & Scholin 1998). Samples were enumerated with a Zeiss Standard 18 compound microscope equipped with a fluorescence illuminator 100 (Zeiss). Duplicate filters were prepared for each species, and the entire surface area of each filter was considered in counting.

**Model development.** Logistic regression models were developed using MYSTAT Version 12.02.11. Logistic modeling is appropriate when the dependent variable is dichotomous (e.g. 0/1). Since our dataset contained continuous data of *Pseudo-nitzschia* abundance, logistic modeling required concatenation of *Pseudo-nitzschia* abundance data into a new dichotomous dependent variable (bloom\_nonbloom), using a defined bloom threshold of 10 000 toxigenic *Pseudo-nitzschia* cells  $l^{-1}$  (Lefebvre et al. 2002b, Fehling et al. 2006, Howard et al. 2007, Jester et al. 2009). Similar model results were obtained (not shown) when a criteria of 5000 cells  $l^{-1}$  was used.

Independent variables evaluated during model development are provided in Table 2. We used an automatic stepwise approach (forward, backward, and bidirectional) to identify the most significant subset. Variable selections were refined to: (1) maximize the rate at which blooms were successfully predicted, (2) minimize the rate of false negative predictions, and (3) maximize model fit accuracy (ROC), while controlling for covariance among the independent variables. Variables exhibiting severe covariation, as determined by variance inflation factors and condition indices, were considered mutually exclusive. Only significant variables ( $p < 0.05$ ) were included in the final models. For the development of the 2 seasonal models, the data were partitioned according to the seasonal periods previously described for Monterey Bay (Pennington & Chavez 2000), while the entire dataset was used for development of the annual model. The final 3 models

are as follows: (1) year-round (annual model), (2) February 14 to June 30 (spring model), and (3) July 1 to February 13 (fall-winter model).

We compare our models to a simple bloom prediction method using chl *a* anomalies. Data from June 2004 to July 2008 were obtained from the LOBOVIZ website ([www.mbari.org/lobo/loboviz.htm](http://www.mbari.org/lobo/loboviz.htm)) for a nearshore mooring in Monterey Bay (M0), and a 30 d median chl *a* anomaly was calculated according to methods previously described for 60 d mean anomalies (Tomlinson et al. 2004, Wynne et al. 2006). The LOBOVIZ website was selected as a data source due to its ease of access and applicability. A median was employed in lieu of a mean, since it has recently been recognized as the generally more appropriate value (R. Stumpf pers. comm.).

**Translating probability into prediction: prediction-point assignment.** When the model equation is solved, the user is presented with the probability of a bloom occurrence. The degree of probability that can be tolerated is referred to here as the 'prediction-point'. Where the model solution, bloom probability, is greater than the prediction-point the model predicts a bloom. Conversely, where the model solution is lower than the prediction-point, the probability of a bloom is considered sufficiently low to warrant a non-bloom prediction. The prediction-point must be pre-defined by either: (1) the model developer, for optimization of predictive power, or (2) the model user, for selective risk management. We provide optimized prediction-points for each model and offer guidance for their adjustment. Optimized prediction-points were determined by generating model prediction failure rates over the full range of potential prediction-point assignments (0.000 to 1.000) at 0.005 increments (Fig. 2). The overall failure rate is minimized when the failure to predict blooms and failure to predict non-blooms are simulta-

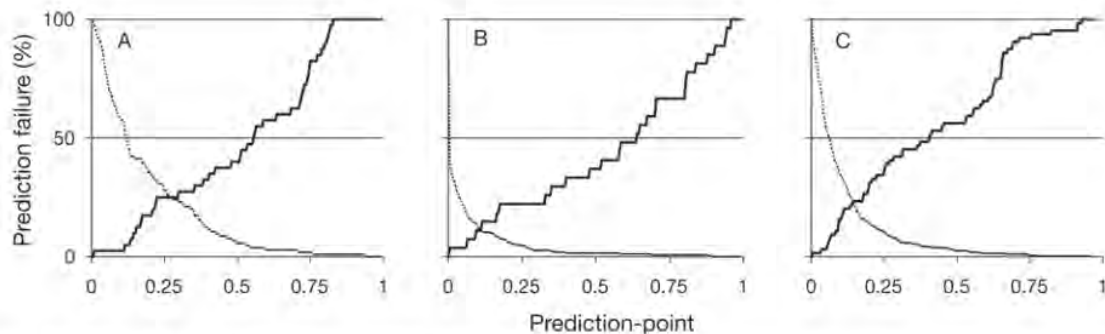


Fig. 2. Prediction failure rates for blooms (solid lines) and non-blooms (broken lines) for the spring (A), fall-winter (B), and annual model (C) along the range of possible prediction-points. The prediction failure rate is defined as the rate at which the model fails to predict a case type (bloom or non-bloom). The overall prediction failure rate is minimized at the optimized prediction-point, where the 2 lines cross

neously minimized. The optimized prediction-point values, therefore, occur where the failure rate curves intersect (Fig. 2).

**Model validation.** A jackknife cross-validation module was supplied by SYSTAT and used to validate model performance with respect to unknown (future) cases. This method is similar to the split-sample bootstrap validation approach taken by Blum et al. (2006) except that it does not reduce the dataset that can be used for initial model development, and it is an iterative process that allows for  $N$  instances of cross-validation against 'unknown' single cases. The cross-validation was run with the model-optimized prediction-points and with 'user-adjusted' prediction-points set according to the historical probability of blooms for Monterey Bay (2002 to 2005), calculated from an independent California Department of Public Health (CDPH) *Pseudo-nitzschia* bloom monitoring dataset. This historical probability is referred to as 'priors'.

## RESULTS

After removing those cases from the original ( $N = 2099$ ) dataset that did not fulfill the specified quality criteria, 506 cases from 2002 to 2008 remained, 74 of which were classified as bloom cases. There was clear seasonality in these data: the rate of bloom incidence was 28% during the spring model period, compared to a rate of 9% for the remainder of the year.

Logistic regression models are of the form:

$$\text{LOGIT}(p) = \ln[p/(1-p)] = \beta_0 + \beta_1 z_1 + \beta_2 z_2 + \dots + \beta_k z_k \quad (1)$$

where  $p$  is the probability of the condition being modeled; here,  $p$  represents the probability of a toxigenic *Pseudo-nitzschia* bloom.  $\beta_0$  is a constant, and  $\beta_1, \beta_2, \dots, \beta_k$  are the regression coefficients of  $z_1, z_2, \dots, z_k$ , respectively. The year-round (annual) and seasonal (spring and fall-winter) models are as follows:

### Annual model

$$\text{LOGIT}(p) = 9.763 - 1.700[\ln(\text{silicic acid})] + 1.132[\ln(\text{chl } a)] - 0.800(\text{temp}) + 0.006(\text{upwelling}) \quad (2)$$

### Spring model

$$\text{LOGIT}(p) = 5.835 + 1.398[\ln(\text{chl } a)] - 1.135[\ln(\text{silicic acid})] - 0.549(\text{temp}) \quad (3)$$

### Fall-Winter model

$$\text{LOGIT}(p) = 10.832 - 5.026[\ln(\text{Pajaro River})] - 3.893[\ln(\text{silicic acid})] + 1.972[\ln(\text{chl } a)] + 0.652(\text{nitrate}) \quad (4)$$

The regression curve for the spring model is presented for visualization of how the model solution [LOGIT ( $p$ )] translates into a bloom probability ( $p$ ) and, through the

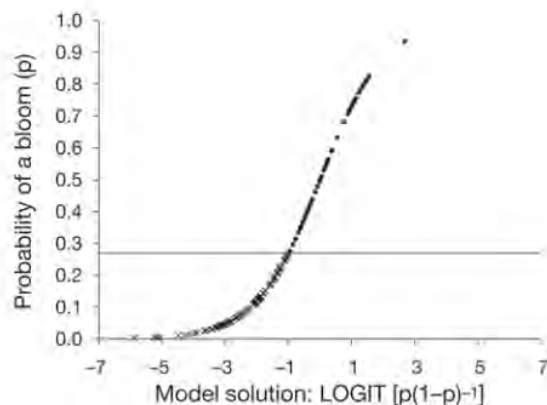


Fig. 3. The spring model logistic regression curve. Cases lying above the optimized prediction-point (probability = 0.275) are predicted as blooms (●); cases lying below the optimized prediction-point are predicted as non-blooms (×)

implementation of a prediction-point, into a bloom or non-bloom prediction (Fig. 3).

The models demonstrated 'very good' to 'excellent' model fit accuracy (Table 3). Other demonstrations of model proficiency include the determination of a model  $p$ -value through calculation and evaluation of a likelihood-ratio statistic, and the determination of adjusted  $R^2$  statistics, McFadden's  $\rho^2$  and Nagelkerke's  $R^2$ , for which values  $>0.2$  are indicative of very good model fit (Hensher & Johnson 1981) (Table 3). Each of the models achieved a high level of statistical proficiency with 4 or fewer predictive variables.

Two predictive variables,  $\ln(\text{chl } a)$  and  $\ln(\text{silicic acid})$ , were included in all models. The set of predictive variables used in the annual model and spring model were most similar, differing only in the inclusion of upwelling in the annual model. The fall-winter model is the most disparate of the 3 models with the variable set  $\ln(\text{Pajaro River})$ , nitrate,  $\ln(\text{silicic acid})$  and  $\ln(\text{chl } a)$ . Of particular note is the omission of temp and upwelling from the fall-winter model, and the inclusion of a river discharge variable,  $\ln(\text{Pajaro River})$ , and nitrate. All variables included in the models demonstrated extreme to maximum statistical significance.

The annual model did not emerge as an explicit sum of the 2 seasonal models. An annual model with  $\ln(\text{Pajaro River})$  and nitrate included (not shown) achieves results very similar to those of the presented annual model, but with slightly improved bloom and non-bloom prediction. These variables, however, were non-significant additions and caused inflation in the standard errors of the other (significant) variable coefficients; this is a general risk assumed when non-significant predictors are included in any model (Menard 1995). The inclusion of additional variables in the

annual model also resulted in unacceptable levels of covariance (condition indices > 30). Dueling complexity and covariance restrictions likely promoted the usefulness of a 'composite' variable, such as upwelling, as a predictor within this, the most temporally comprehensive of the models.

Analysis of model performance at the default prediction-point (0.500) is useful, because it allows for an even comparison of predictive success under equalizing but unrealistic assumptions that: (1) blooms are evenly distributed throughout the year and (2) blooms are expected to occur with as much frequency as non-bloom conditions. As shown in Table 4, the development of seasonal models significantly enhanced pre-

dictive ability: the rate at which blooms were successfully predicted was 16% (spring model) and 19% (fall-winter model) greater than for the annual model. The rates of false positive prediction were slightly improved in the seasonal models. The rates of false negative prediction were more unequal among the models, and ranged most significantly between the two seasonal models.

Model performance at optimized prediction-points is summarized in Table 4; the fall-winter model demonstrated the highest rates of case prediction, followed by the annual and spring models, respectively. As with the default prediction-point, the rates of false negative prediction are most disparate among the

seasonal models. The rates of false positive prediction are lowest for the seasonal models, but are increased overall with the implementation of the optimized prediction-points. The relatively high rates of false positive prediction result from a relatively low frequency of non-bloom predictions, which is an artifact of prediction-point optimization.

All of the models were assessed for predictive performance with unknown (future) cases by jackknife validation (Table 5). At the model-optimized prediction-points (Table 5), the rates at which blooms are successfully predicted are more comparable between the spring and annual models, and highest in the fall-winter model. Each model significantly out-performed a null model, improving bloom prediction by as much as 80%. This advantage does not extend to the prediction of non-bloom cases. The discrepancy in bloom versus non-bloom predictive improvement is a result of the model development, which focused on prediction of blooms. The Pearson's chi-squared test statistic for each model indicates extreme significance in the association of modeled predictions and the true outcome of future cases.

The models were also assessed by jackknife cross-validation under conditions simulating the application of 'user-adjusted' prediction-points. In Table 5, the application of 'low' prediction-points set by historical priors provides a demonstration of model performance in a period when future blooms occur with unexpectedly high frequency. The apparently conservative response is in part an artifact of logistic regression: logistic models generally guard against the misclassification of cases

Table 3. Model specifications and diagnostics for the logistic regression models presented in this study. The likelihood-ratio test is a test of the null hypothesis that the predictor variable coefficients are zero (i.e. have no predictive value), and can be evaluated for significance as a deviate chi-squared. McFadden's  $\rho^2$  is a transformation of the likelihood-ratio statistic to mimic an  $R^2$  statistic; values between 0.20 and 0.40 are considered very satisfactory (Hensher & Johnson 1981). The Nagelkerke's  $R^2$  is based on both log likelihood and sample size. ROC: receiver operating characteristic

	Spring	Fall-Winter	Annual
Predictor variables	ln(silicic acid) ln(chl a) Temp	ln(silicic acid) ln(chl a) ln(Pajaro River) Nitrate	ln(silicic acid) ln(chl a) Temp Upwelling
N (total cases)	144	289	422
N (bloom cases)	40	27	64
ROC	0.848	0.943	0.860
Likelihood-ratio statistic	45.885	96.859	102.377
p-value	0.000	0.000	0.000
McFadden's $\rho^2$	0.270	0.540	0.285
Nagelkerke's $R^2$	0.394	0.616	0.376

Table 4. Prediction success and failure rates (%) at the default prediction-point of 0.500 and at model-specific optimized prediction-points. A modeled bloom probability higher than the prediction-point results in a bloom prediction. 'False negative' is the rate at which non-bloom predictions were incorrect. 'False positive' is the rate at which bloom conditions were predicted where none existed

	Spring	Fall-Winter	Annual
<b>Default prediction-point</b>			
Prediction-point	0.500	0.500	0.500
Blooms successfully predicted	60	63	44
Non-blooms successfully predicted	94	99	98
False negative	14	4	9
False positive	20	19	24
<b>Model-optimized prediction-point</b>			
Prediction-point	0.275	0.110	0.145
Blooms successfully predicted	75	89	77
Non-blooms successfully predicted	75	89	78
False negative	11	1	5
False positive	46	55	62

Table 5. Jackknife validation results for the logistic regression models at optimized prediction-points, where overall prediction error is minimized and at prediction-points equal to the priors of an independent California Department of Public Health (CDPH) bloom monitoring dataset. Improvement in bloom prediction is relative to the performance of a null model. Square brackets: negative scores

	Spring	Fall–Winter	Annual
<b>Optimized prediction-points</b>			
Prediction-point	0.275	0.110	0.145
Blooms successfully predicted (%)	75	89	77
Non-blooms successfully predicted (%)	76	89	77
False negative (%)	11	1	5
False positive (%)	45	55	62
Improvement in bloom prediction (%)	47	80	62
Improvement in non-bloom prediction (%)	4	[2]	[8]
Pearson's chi-squared ( $\chi^2$ )	31.78	98.98	74.10
$\chi^2$ p-value	0.000	0.000	0.000
<b>CDPH priors prediction-points</b>			
Prediction-point (priors)	0.101	0.066	0.081
Blooms successfully predicted (%)	98	93	91
Non-blooms successfully predicted (%)	42	82	60
False negative (%)	2	1	3
False positive (%)	61	65	71
Improvement in bloom prediction (%)	70	84	76
Improvement in non-bloom prediction (%)	[30]	[9]	[25]
Pearson's chi-squared ( $\chi^2$ )	21.31	74.37	54.63
$\chi^2$ p-value	0.000	0.000	0.000

belonging to the under-represented case group, a quality that makes them especially attractive for application in high-risk predictive contexts such as environmental regulation and clinical health (Fan & Wang 1998). The use of the CDPH priors is therefore an appropriate but conservative approach, increasing the probability of correctly identifying blooms ( $\geq 91\%$  for all models), while reducing rates of false negative prediction ( $\geq 3\%$  for all models), but at a cost to non-bloom prediction.

## DISCUSSION

### Model application: prediction-point adjustment

We sought to develop and deliver robust predictive models of toxigenic *Pseudo-nitzschia* blooms that were straightforward in their application. Further, we hoped to lay a framework for future modeling studies and independent model application, since this is the first time logistic regression has been applied to *Pseudo-nitzschia* bloom prediction. Providing these models with predetermined, optimized prediction-points satisfies the former; application of the models without end-user adjustment provides a statistically robust method for bloom prediction. Optioning how, and when, the optimized prediction-points can be adjusted satisfies

the latter; the ability to modify the prediction-points grants an opportunity to consider and integrate local bloom ecology, specifically frequency, within the model design.

Statistical models should be developed and implemented while remaining mindful of the system under investigation. In particular, the model should be developed and implemented with consideration of: (1) the general frequency at which blooms occur (the priors), (2) the prediction error rates that are inherent to the model, and (3) the cost of prediction error to the model user. The first of these is taken into account by the designation of an optimized prediction-point. Consideration of Points 2 and 3 is left to the discretion of the model user, since it is only necessary when the risk of a *specific type* of predictive error, rather than *overall* predictive error, needs to be reduced.

Use of a shifted prediction-point, rather than the default prediction-point, should be implemented when-

ever the probabilities of the 2 outcomes are significantly unequal (Neter et al. 1989). At present, blooms of *Pseudo-nitzschia* are relatively rare occurrences (Fig. 1). Because the probability of a bloom is generally not near 50%, a default prediction-point of 0.500 cannot provide optimized predictive capability. By the same reasoning, if a system generally demonstrates priors that are overwhelmingly different from our assumptions, the prediction-point can be reduced (inflated) to account for the more infrequent (frequent) occurrence, and therefore likelihood, of blooms. Similarly, if the cost of a certain type of incorrect prediction (false positive or false negative) is disproportionately high, the prediction-point can be adjusted to protect from that exaggerated cost. Fig. 2 may be used as a guide for balancing the probability of these errors and controlling their relative costs.

Shifting a prediction-point affects the predictive behavior of the model, always forcing compromise: Fig. 4 illustrates the trade-off between minimizing the number of blooms that the model fails to predict and minimizing the number of non-blooms that are identified as blooms. Reducing the prediction-point minimizes overall failure to predict a bloom by relaxing the criteria for bloom prediction. Conversely, increasing the prediction-point means that the criteria for bloom prediction are more strenuous, and blooms will be forecasted only when they are extraordinarily likely to occur.

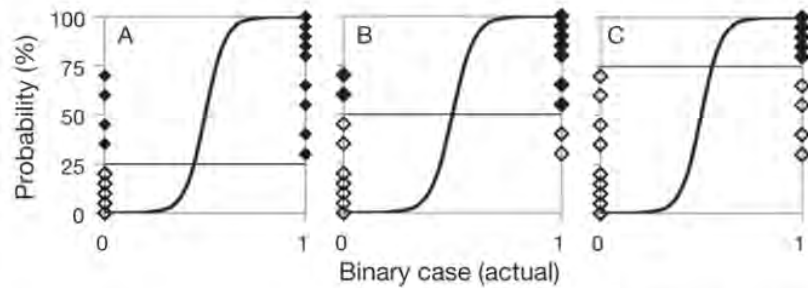


Fig. 4. A schematic diagram of a logistic regression with prediction-points of 0.250 (A), 0.500 (B), or 0.750 (C). Cases lying on the '0' vertical axis are actual non-bloom cases; cases lying on the '1' vertical axis are actual bloom cases. Filled symbols are predicted as blooms; open symbols are predicted as non-blooms. Reducing the prediction-point increases the number of cases that are predicted as blooms overall, maximizing the percent of actual blooms that are successfully predicted but reducing the percent of actual non-blooms that are successfully predicted (A). Increasing the prediction-point has the opposite effect (C)

### Comparative model performance

In Table 6, we present the predictive performance of our annual and seasonal models compared to those of: (1) a chl *a* anomaly, (2) linear hindcasting models developed for *Pseudo-nitzschia* blooms in the Santa Barbara Channel (Anderson et al. 2009), and (3) logistic regression models developed for pDA from a combination of field and experimental data (Blum et al. 2006).

Our logistic regression models were developed from the largest dataset to date, and demonstrate a relatively high level of predictive capacity. Our models out-perform the chl *a* anomaly model throughout the year and on a seasonal basis, although the predictive capacity of the chl *a* anomaly model was surprisingly comparable during the spring model period. Interestingly, the chl *a* anomaly model completely failed to predict blooms during the fall–winter model period. We suggest that dinoflagellate blooms, particularly common in Monterey Bay in the fall–winter model period, mask blooms of *Pseudo-nitzschia* otherwise identified by the chl *a* anomaly. Conversely, the chl *a* anomaly works well in the spring model period, when *Pseudo-nitzschia* is more likely to be the dominant bloom organism. It should be noted that the chl *a* anomaly model is advantageous in that it is generally applicable to all potential HABs, particularly 'red tides' (e.g. Kudela et al. 2008b, Ryan et al. 2008), and may therefore be a better model choice when not applied specifically for *Pseudo-nitzschia* bloom prediction.

Table 6. Performance comparisons (%) among the annual and seasonal models developed in the present study and in previous *Pseudo-nitzschia* modeling publications. 'Sensitivity' is the rate at which the binary value '1' cases (blooms or high toxicity) were successfully predicted. 'Specificity' is the rate at which the binary value '0' cases (non-blooms or low toxicity) were successfully predicted. Improvement in bloom prediction is relative to the performance of a null model. Square brackets: negative scores

Dependent variable	Toxigenic <i>Pseudo-nitzschia</i> bloom <sup>a</sup>	<i>Pseudo-nitzschia</i> toxicity <sup>b</sup>	Generic <i>Pseudo-nitzschia</i> bloom <sup>c</sup>	Toxigenic <i>Pseudo-nitzschia</i> bloom <sup>d</sup>
<b>Annual</b>				
Sensitivity	77	77	75	39
Specificity	78	75	93	72
False negative	5	–	25	5
False positive	62	–	7	88
Improvement in bloom prediction	61	–	–	31
N	422	139	75	182
<b>Spring</b>				
Sensitivity	75	–	–	50
Specificity	75	–	–	62
False negative	11	–	–	10
False positive	46	–	–	71
Improvement in bloom prediction	47	–	–	35
N	144	–	–	65
<b>Fall–Winter</b>				
Sensitivity	89	–	–	0
Specificity	89	–	–	77
False negative	1	–	–	3
False positive	55	–	–	100
Improvement in bloom prediction	80	–	–	(2.6)
N	289	–	–	117
<sup>a</sup> Present study				
<sup>b</sup> Blum et al. (2006)				
<sup>c</sup> Anderson et al. (2009)				
<sup>d</sup> Study of chl <i>a</i> anomaly (present study)				

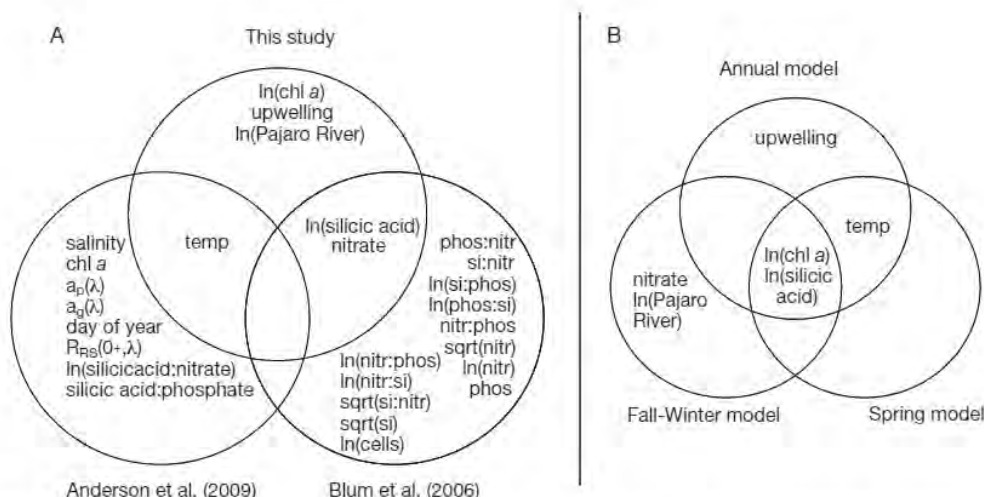


Fig. 5. Venn diagrams illustrating the shared and unique variables included in models of *Pseudo-nitzschia* ecophysiology shown within the present study, Anderson et al. (2009), and Blum et al. (2006) (A) and included in the annual, spring, and fall–winter models (B). Nutrient abbreviations for Blum et al. (2006) are as follows—phos: phosphate; si: silicic acid; nitr: nitrate. Variable abbreviations used in Anderson et al. (2009) are as follows—ap( $\lambda$ ): particulate absorption [412–665 nm]; ag( $\lambda$ ): CDOM absorption [412–665 nm]; RRS(0+, $\lambda$ ): remote-sensing reflectance [412–665 nm]. ‘Sqrt’: square-root operation

#### Inter-study patterning: recurrent predictor variables

Fig. 5A illustrates the predictor variables that are shared and not shared between the models developed by Blum et al. (2006), Anderson et al. (in press), and in the present study. While the regions of interest and, in some cases, the dependent variable differ between these studies, the similarities and differences shared between the models can provide insight into universal patterns of *Pseudo-nitzschia* ecophysiology and, in turn, indicate which variables may be fundamental to future monitoring and modeling.

Seawater temperature was identified as a significant predictor whenever it was included in a study for evaluation. In all cases, a negative relationship was demonstrated between temperature and the dependent variable. Cold surface temperatures are often associated with upwelling, one of the processes previously identified as a causative factor of *Pseudo-nitzschia* blooms. The direct assessment of the upwelling index was unique to the present study; where it emerged as a predictor variable, it had a weak positive association with *Pseudo-nitzschia* bloom incidence.

Silicic acid (ln-transformed) and nitrate both emerged as predictors in models developed for *Pseudo-nitzschia* toxicity (Blum et al. 2006) and in the models developed here. In both studies, the patterns agree: association with the dependent variable is negative for silicic acid and positive for nitrate. While neither variable emerged as an individual predictor in the models developed by Anderson et al. (2009), a negative relationship was demonstrated between the silicic acid to

nitrate ratio and blooms of *Pseudo-nitzschia*, indicating a possibly confounded negative and positive relationship between blooms and silicic acid and nitrate, respectively.

Additional recurrent patterns are suggested by variables that are related, but not explicitly shared, between the studies. Anderson et al. (2009) chose not to evaluate river discharge as a model variable, but presented a *Pseudo-nitzschia* bloom model and a cellular toxicity model that included particle absorption and absorption of chromophoric dissolved organic matter (CDOM), variables which are associated with significant recent river discharge events (Warrick et al. 2004, 2007). In both models, high particulate absorption was negatively associated with the dependent variable, suggesting a direct negative relationship between high river discharge and *Pseudo-nitzschia* blooms. Our fall–winter model, which addresses the time period in which ‘first flush’ and high discharge events generally occur, also demonstrates a direct negative relationship between river discharge and bloom incidence. The consideration of seasonality when modeling river discharge and blooms and the patterning of blooms and high discharge events through time reveal complexity in this relationship, as discussed in the next subsection.

#### Intra-study (seasonal) patterning: ecological context and implications

The predictor variables shared and not shared between the annual, spring, and fall–winter models

are presented in Fig. 5B, effectively 'zooming in' on the modeled relationships with a lens of added dimension and ecological context. The 2 most similar models are the annual and spring models; this is not entirely surprising, given that the majority of *Pseudo-nitzschia* blooms occur in the springtime (Fig. 1). Upwelling is the only predictor unique to the annual model; its omission from the spring model may arise from a general predominance of upwelling throughout the spring model period. The independent variables in the spring model exhibited particular propensity for covariation; this would further suggest that *Pseudo-nitzschia* bloom dynamics in Monterey Bay are largely dominated by a specific environmental forcing, i.e. upwelling, over the spring model period.

The fall–winter model includes oceanic periods that are not (by definition) generally dominated by upwelling processes. All of the models, including the fall–winter model, demonstrate that conditions of low silicic acid and concurrently high chl *a* are associated with blooms of toxigenic *Pseudo-nitzschia* in Monterey Bay. The fall–winter model, however, includes 2 unique predictor variables: nitrate (positive coefficient) and Pajaro River discharge (negative coefficient). The inclusion of nitrate in the fall–winter model suggests that the macronutrient control observed by Anderson et al. (2009), specifically the negative relationship between *Pseudo-nitzschia* blooms and the ratio of silicic acid to nitrate, may have been underscored by confounding seasonal relationships. Our results are therefore similar to those presented by Anderson et al. (2009), but are either more specific, due to the explicit assessment of seasonality, or representative of a similar relationship more heavily impacted by eutrophication. Annual dissolved inorganic nitrate loading via terrestrial storm runoff is relatively low in the region addressed by Anderson et al. (2009); however, nitrate input via storm runoff can be significant during winter runoff events (McPhee-Shaw et al. 2007).

The association of fall–winter blooms with conditions of high nitrate suggests that a nitrate eutrophication process is uniquely significant during this period. Notably, the Pajaro River in Monterey Bay introduces disproportionately high nitrate loads (CCLEAN 2006, 2007) on a strictly seasonal basis. In our dataset, blooms within the fall–winter model period occurred during periods of minimal freshwater discharge, while blooms within the spring model period occurred during periods of decreasing river discharge following a 'flush' event (Fig. 1). We also observed this pattern within the broader time-series, in which blooms are generally not associated with peak discharge events and occur either with the declining shoulder of a high river discharge event or within a period marked by minimal discharge (Fig. 1; note that a 4 yr period of

relatively high discharge between 1994 and 1998 accompanies an absence of data, not necessarily an absence of blooms). As described by the models, river discharge, through concentrated low-flow periods and 'load' events, may provide a eutrophic source of nitrate conducive to seasonal bloom formation, while allaying immediate bloom formation during periods of peak discharge.

Although not observed in the modeling dataset compiled here, one independent study recently reported 'a shift in toxin-producing species associated with an overall restructuring of the phytoplankton community' for Monterey Bay (Jester et al. 2009). Jester et al. (2009) used a similar dataset to ours (Monterey Bay, 2000 to 2006); the discrepancy in *Pseudo-nitzschia* abundance observations between the datasets may be due to differences in spatial coverage. The 'shift in toxin-producing species' was defined by a sharp decline in the incidence of toxigenic *Pseudo-nitzschia* in the summer of 2004, which persisted until the end of the study in 2006. This period was marked by anomalously low upwelling conditions and anomalously

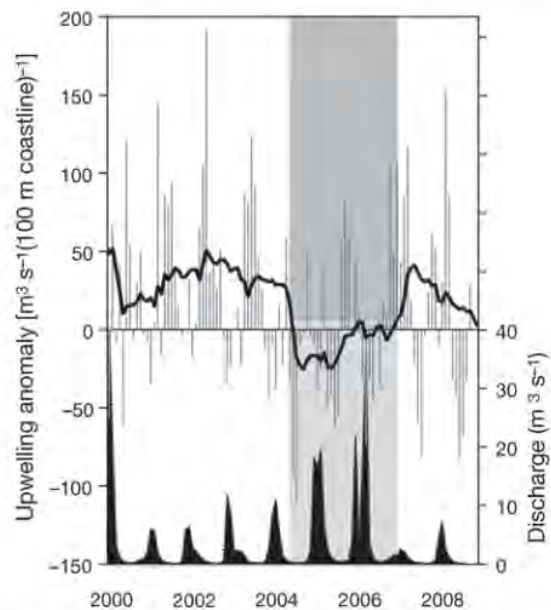


Fig. 6. Monthly upwelling anomaly for 36°N, 122°W (grey bars) with a 12 mo moving average trendline (black line), and the monthly mean discharge for the Pajaro River (area plot) are shown for the period from 2000 to 2008. An independent study addressing toxigenic *Pseudo-nitzschia* abundance in Monterey Bay for the period from 2000 to 2006 identified the summer 2004 period as a harmful species shifting-point (from *Pseudo-nitzschia* to *Alexandrium* and *Dinophysis*), and showed the summers from 2004 through 2006 to be periods of severely decreased *Pseudo-nitzschia* abundance (greyed area) (Jester et al. 2009). This 'shifted' period demonstrates relatively low upwelling and high river discharge activity

high periods of river discharge (Fig. 6), conditions which our models identify as non-conductive to toxigenic *Pseudo-nitzschia* blooms. Both of these conditions were alleviated in 2007, marked by a significant toxigenic *Pseudo-nitzschia* bloom event in Monterey Bay (Jester et al. 2009); a bloom of toxigenic *Pseudo-nitzschia* was also observed in 2008 (data not shown). According to the models and these observations, climatological conditions associated with low upwelling and high river discharge conditions may be conducive to suppressed toxigenic *Pseudo-nitzschia* bloom activity. The forecast of these conditions may now translate into the anticipation of large-scale shifts, such as the 'shift in toxin-producing species' described by Jester et al. (2009).

#### Bloom modeling versus toxin modeling

The monitoring of domoic acid for public health purposes is carried out continually by the CDPH and focuses, quite appropriately, on the protection of human health from domoic acid intoxication. This monitoring effort is more accurately described as the monitoring of domoic acid bioaccumulation in sentinel shellfish supplies (*Mytilus californianus*). Modeling or monitoring efforts that are focused on toxin load alone, while useful and appropriate for regulatory purposes, obviously do not allow for the estimation or monitoring of *Pseudo-nitzschia* blooms, which can be highly variable in their toxicity (Trainer et al. 2002, Marchetti et al. 2004, Anderson et al. 2006). This variability translates into a weak relationship between toxin bioaccumulation and toxigenic *Pseudo-nitzschia* abundance, evidenced here by CDPH/Cal-PReEMPT project data compiled from study sites in northern, central, and southern California over a 3 yr time period (Fig. 7). Note that there were cases where extreme bloom concentrations of toxigenic *Pseudo-nitzschia* were associated with sub-regulatory toxin levels ( $<20 \mu\text{g g}^{-1}$ ), but no observed cases where sub-bloom concentrations of toxigenic *Pseudo-nitzschia* were associated with toxin levels approaching the regulatory limit in shellfish. Logistic regression models developed for toxigenic *Pseudo-nitzschia* blooms can therefore be used for detection of both acute and sub-acute toxic bloom events, while models developed for domoic acid alone will fail to address the injection of toxin into the system via sub-acute bloom events. This is a significant failure inherent to all toxin models, since chronic or early life stage exposure to sub-lethal levels of domoic acid are increasingly being recognized as an emerging threat to both human health and wildlife (Kreuder et al. 2005, Goldstein et al. 2008, Grattan et al. 2008, Ramsdell & Zabka 2008, M. Miller pers. comm.). By providing

estimations of all toxigenic *Pseudo-nitzschia* bloom events, whether low or high in toxicity, *Pseudo-nitzschia* bloom models have the unique ability to address this emerging threat. Ideally, future models should be developed for both cell abundance (present study) and for toxin production (Blum et al. 2006, Anderson et al. 2009). While the domoic acid data associated with the cases used herein were insufficient for inclusion of a toxin component, a 2-step model would maximize both regulatory monitoring and our understanding of the ecophysiological conditions associated with toxin production.

#### CONCLUSIONS

The models presented here demonstrate toxigenic *Pseudo-nitzschia* bloom classification rates of  $\geq 75\%$ . These predictive success rates are comparable to, or improved over, those reported for previous models of toxicity and generic *Pseudo-nitzschia* blooms. The assessment of our model alongside a chl *a* anomaly model, a useful tool designed for the detection of HABs more generally, demonstrates the capacity for improved predictive ability through more rigorous model development. Although we have reported the largest modeling dataset to date, consisting of 506 cases from 2002 to 2008, the removal of approximately 75% of the full dataset highlights the need for more consistent data collection. The parameters common to the 3

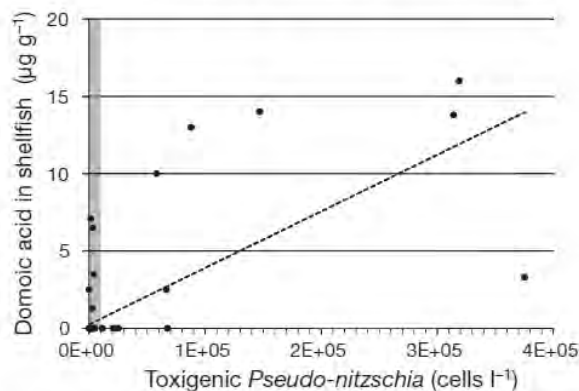


Fig. 7. Micrograms of domoic acid per gram shellfish plotted against counts of toxigenic *Pseudo-nitzschia*. Data are from study sites in northern, central, and southern California, monitored from 2005 to 2007 by Cal-PReEMPT in conjunction with the California Department of Public Health. Domoic acid never approached the regulatory limit of  $20 \mu\text{g domoic acid g}^{-1}$  shellfish when toxigenic *Pseudo-nitzschia* concentrations were at sub-bloom levels, i.e.  $\leq 10,000 \text{ cells l}^{-1}$  (shaded area), and only began to approach the regulatory limit at cell concentrations that were significantly higher than  $\leq 10,000 \text{ cells l}^{-1}$ . The dashed line shows the results of a linear regression for domoic acid toxicity versus cell abundance

regional models developed for the west coast of the United States (Fig. 5A) provide direction for the design of ongoing and future HAB monitoring. We note that several parameters identified as being important (e.g. urea [Howard et al. 2007, Kudela et al. 2008a]; lithium [Subba Rao et al. 1998]; ammonium [Trainer et al. 2007]; iron and copper [Rue & Bruland 2001, Maldonado et al. 2002, Wells et al. 2005]) were not included for evaluation and could potentially further improve model prediction. All models included macronutrient variables as predictors of toxigenic *Pseudo-nitzschia* blooms, indicating the influence of upwelling and possibly cultural eutrophication on toxigenic *Pseudo-nitzschia* bloom proliferation. The seasonal significance of river discharge during periods associated with weak upwelling suggests that both natural (upwelling) and cultural (freshwater discharge) eutrophication processes, and the timing and seasonality of these processes, are significant factors influencing toxigenic *Pseudo-nitzschia* bloom dynamics. Although our models are specific to Monterey Bay, we have identified several factors common to all 3 modeling efforts for *Pseudo-nitzschia*. Given appropriate validation data, we suggest that some variant of this reduced subset of environmental variables could be applied to other regions, particularly similar coastal upwelling systems where *Pseudo-nitzschia* is prevalent (e.g. the west coast of the United States and Baja, Mexico, the southern Benguela, and the Iberian peninsula; Bates et al. 1998, Kudela et al. 2005, Fawcett et al. 2007).

**Acknowledgements.** We thank P. E. Miller (University of California, Santa Cruz, UCSC) and the Cal-PreEMPT team for contributing to the modeling dataset. We gratefully acknowledge the significant contribution made by M. W. Silver (UCSC) to the CIMT dataset and thank CIMT participants for their efforts. We thank G. J. Smith and K. Hayashi for their contribution to the MLML dataset. Special thanks to G. W. Langlois (CDPH) for providing shellfish toxicity data and an independent *Pseudo-nitzschia* monitoring dataset. Three anonymous reviewers contributed significantly to the improvement of this manuscript. Partial funding was provided by NOAA MERHAB Award NA04NOS4780239 (Cal-PreEMPT), NOAA Award NA160C2936 (CIMT), and, as a fellowship (J.Q.L.), from an anonymous donor through the Center for the Dynamics and Evolution of the Land-Sea Interface (CDELSI). This contribution is part of the Global Ecology and Oceanography of Harmful Algal Blooms (GEOHAB) Core Research Project on Harmful Algal Blooms in Upwelling Systems, and is MERHAB (Monitoring and Event Response for Harmful Algal Blooms) Publication Number 70.

#### LITERATURE CITED

- ▶ Addison RF, Stewart JE (1989) Domoic acid and the eastern Canadian molluscan shellfish industry. *Aquaculture* 77: 263–269
- ▶ Allen I, Smyth T, Siddorn J, Holt M (2008) How well can we forecast high biomass algal bloom events in a eutrophic coastal sea? *Harmful Algae* 8:70–76
- ▶ Anderson DM, Glibert PM, Burkholder JM (2002) Harmful algal blooms and eutrophication: nutrient sources, composition, and consequences. *Estuaries* 25:704–726
- ▶ Anderson CR, Brzezinski MA, Washburn L, Kudela R (2006) Circulation and environmental conditions during a toxigenic *Pseudo-nitzschia* bloom in The Santa Barbara Channel, California. *Mar Ecol Prog Ser* 327:119–133
- Anderson CR, Siegel DA, Kudela RM, Brzezinski MA (2009) Empirical models of toxigenic *Pseudo-nitzschia* blooms: potential use as a remote detection tool in the Santa Barbara Channel. *Harmful Algae* 8:478–492
- Bates SS, Trainer VL (2006) The ecology of harmful diatoms. In: Granéli E, Turner J (eds) *Ecology of harmful algae*, Vol 189. Springer-Verlag, Heidelberg, p 81–93
- ▶ Bates SS, Bird CJ, de Freitas ASW, Foxall RA and others (1989) Pennate diatom *Nitzschia pungens* as the primary source of domoic acid, a toxin in shellfish from eastern Prince Edward Island, Canada. *Can J Fish Aquat Sci* 46: 1203–1215
- Bates SS, Garrison DL, Horner RA (1998) Bloom dynamics and physiology of domoic-acid-producing *Pseudo-nitzschia* species In: Anderson D, Cembella A, Hallegraeaf G (eds) *Physiological ecology of harmful algal blooms*. Springer-Verlag, Heidelberg, p 267–292
- ▶ Beltrán AS, Palafox-Urbe M, Grajales-Montiel J, Cruz-Villacorta A, Ochoa JL (1997) Sea bird mortality at Cabo San Lucas, Mexico: evidence that toxic diatom blooms are spreading. *Toxicon* 35:447–453
- Bird CJ, Wright JLC (1989) The shellfish toxin domoic acid. *World Aquac* 20:40–41
- Blauw AN, Anderson P, Estrada M, Johansen M and others (2006) The use of fuzzy logic for data analysis and modeling of European harmful algal blooms: results of the HABES project. *Afr J Mar Sci* 28:365–369
- Blum I, Subba Rao DV, Pan Y, Swaminathan S, Adams NG (2006) Development of statistical models for prediction of the neurotoxin domoic acid levels in the pennate diatom *Pseudonitzschia pungens* f. *multiseries* utilizing data from cultures and natural blooms. In: Subba Rao DV (ed) *Algal cultures, analogues of blooms and applications*. Science Publishers, Enfield, NH, p 891–916
- ▶ Buck KR, Uttal-Cooke L, Pilskaln CH, Roelke DL and others (1992) Autecology of the diatom *Pseudonitzschia australis*, a domoic acid producer, from Monterey Bay, California. *Mar Ecol Prog Ser* 84:293–302
- CCLEAN (Central Coast Long-Term Environmental Assessment Network) (2006) 2004–2005 annual report. Available at: [www.cclean.org/ftp/CCLEAN%20Final%2004-05.pdf](http://www.cclean.org/ftp/CCLEAN%20Final%2004-05.pdf)
- CCLEAN (Central Coast Long-Term Environmental Assessment Network) (2007) Program overview 2001–2006. Available at: [www.cclean.org/ftp/CCLEAN%2001-06%20Overview%20copy.pdf](http://www.cclean.org/ftp/CCLEAN%2001-06%20Overview%20copy.pdf)
- Fan X, Wang L (1998) Comparing linear discriminant function with logistic regression for the two-group classification problem. Annual Meeting of the American Educational Research Association, San Diego, CA (April 13–17, 1998)
- ▶ Fawcett A, Pitcher GC, Bernard S, Cembella A, Kudela RM (2007) Contrasting wind patterns and toxigenic phytoplankton in the southern Benguela upwelling system. *Mar Ecol Prog Ser* 348:19–31
- ▶ Fehling J, Davidson K, Bolch C, Tett P (2006) Seasonality of *Pseudo-nitzschia* spp. (Bacillariophyceae) in western Scottish waters. *Mar Ecol Prog Ser* 323:91–105
- ▶ Fisher WS, Malone TC, Giattina JD (2003) A pilot project to detect and forecast harmful algal blooms in the northern Gulf of Mexico. *Environ Monit Assess* 81:373–381

- Fritz L, Quilliam MA, Wright JLC, Beale AM, Work TM (1992) An outbreak of domoic acid poisoning attributed to the pennate diatom *Pseudonitzschia australis*. *J Phycol* 28: 439–442
- Glibert PM, Anderson DM, Gentien P, Granéli E, Sellner KG (2005) The global, complex phenomena of harmful algal blooms. *Oceanography (Wash DC)* 18:136–147
- Goldberg JD (2003) Domoic acid in the benthic food web of Monterey Bay, California. Master's thesis. California State University Monterey Bay, Monterey, CA
- Goldstein T, Mazet JAK, Zabka TS, Langlois G and others (2008) Novel symptomatology and changing epidemiology of domoic acid toxicosis in California sea lions (*Zalophus californianus*): an increasing risk to marine mammal health. *Proc R Soc Lond B Biol Sci* 275:267–276
- Grattan LM, Roberts S, Trainer V, Boushey C and others (2008) Domoic acid neurotoxicity in Native Americans in the Pacific Northwest: human health project methods and update. In: *Proc 4th Symp on harmful algae in the US*. US National Office for Harmful Algal Blooms
- Hallegraeff GM (1993) A review of harmful algal blooms and their apparent global increase. *Phycologia* 32:79–99
- Hensher DA, Johnson LW (1981) Applied discrete-choice modeling. Croom Helm, London
- Howard MA, Cochlan WP, Ladizinsky N, Kudela RM (2007) Nitrogenous preference of toxigenic *Pseudo-nitzschia australis* (Bacillariophyceae) from field and laboratory experiments. *Harmful Algae* 6:206–217
- Jester R, Lefebvre K, Langlois G, Vigilant V, Baugh K, Silver MW (2009) A shift in the dominant toxin-producing algal species in central California alters phycotoxins in food webs. *Harmful Algae* 8:291–298
- Johnsen G, Sakshuag E (2000) Monitoring of harmful algal blooms along the Norwegian coast using bio-optical methods. *S Afr J Mar Sci* 22:309–321
- Knepel K, Bogren K (2001) Determination of orthophosphorous by flow injection analysis in seawaters: QuickChem Method 31-113-01-1-H. In: *Saline methods of analysis*. Lachat Instruments, Milwaukee, WI
- Kreuder C, Miller MA, Lowensline LJ, Conrad PA, Carpenter TE, Jessup DA, Mazet JA (2005) Evaluation of cardiac lesions and risk factors associated with myocarditis and dilated cardiomyopathy in southern sea otters (*Enhydra lutris nereis*). *Am J Vet Res* 66:289–299
- Kudela R, Pitcher G, Probyn T, Figueiras F, Moita T, Trainer V (2005) Harmful algal blooms in coastal upwelling systems. *Oceanography (Wash DC)* 18:184–197
- Kudela RM, Lane JQ, Cochlan WP (2008a) The potential role of anthropogenically derived nitrogen in the growth of harmful algae in California, USA. *Harmful Algae* 8: 103–110
- Kudela RM, Ryan JP, Blakely MD, Lane JQ, Peterson TD (2008b) Linking the physiology and ecology of *Cochlodinium* to better understand harmful algal bloom events: a comparative approach. *Harmful Algae* 7:278–292
- Lefebvre KA, Powell CL, Busman M, Doucette GJ and others (1999) Detection of domoic acid in northern anchovies and California sea lions associated with an unusual mortality event. *Nat Toxins* 7:85–92
- Lefebvre KA, Barqu S, Kieckhefer T, Silver MW (2002a) From sanddabs to blue whales: the pervasiveness of domoic acid. *Toxicol* 40:971–977
- Lefebvre KA, Silver MW, Coale SL, Tjeerdema RS (2002b) Domoic acid in planktivorous fish in relation to toxic *Pseudo-nitzschia* cell densities. *Mar Biol* 140:625–631
- Maldonado MT, Hughes MP, Rue EL, Wells ML (2002) The effect of Fe and Cu on growth and domoic acid production by *Pseudo-nitzschia multiseriis* and *Pseudo-nitzschia australis*. *Limnol Oceanogr* 47:515–526
- Marchetti A, Trainer VL, Harrison PJ (2004) Environmental conditions and phytoplankton dynamics associated with *Pseudo-nitzschia* abundance and domoic acid in the Juan de Fuca eddy. *Mar Ecol Prog Ser* 281:1–12
- McGillicuddy Jr D, Anderson D, Lynch D, Townsend D (2005) Mechanisms regulating large-scale seasonal fluctuations in *Alexandrium fundyense* populations in the Gulf of Maine: results from a physical–biological model. *Deep Sea Res II* 52:2698–2714
- McPhee-Shaw EE, Siegel DA, Washburn L, Brzezinski MA, Jones JL, Leydecker A, Melack J (2007) Mechanisms for nutrient delivery to the inner shelf: observations from the Santa Barbara Channel. *Limnol Oceanogr* 52: 1748–1766
- Menard S (1995) Applied logistic regression analysis. Sage, Thousand Oaks, CA
- Miller PE, Scholin CA (1998) Identification and enumeration of cultured and wild *Pseudo-nitzschia* (Bacillariophyceae) using species-specific LSU rRNA-targeted fluorescent probes and filter-based whole cell hybridization. *J Phycol* 34:371–382
- Neter J, Wasserman W, Kutner M (1989) Applied linear regression models. Irwin, Homewood, IL
- Pennington JT, Chavez FP (2000) Seasonal fluctuations of temperature, salinity, nitrate, chlorophyll and primary production at station H3/M1 over 1989–1996 in Monterey Bay, California. *Deep Sea Res II* 47:947–973
- Ramsdell JS, Zabka TS (2008) *In utero* domoic acid toxicity: a fetal basis to adult disease in the California sea lion (*Zalophus californianus*). *Mar Drugs* 6:262–290
- Rue E, Bruland K (2001) Domoic acid binds iron and copper: a possible role for the toxin produced by the marine diatom *Pseudo-nitzschia*. *Mar Chem* 76:127–134
- Ryan JP, Gower JFR, King SA, Bissett WP and others (2008) A coastal ocean extreme bloom incubator. *Geophys Res Lett* 35, L12602, doi:10.1029/2008GL034081
- Schofield O, Grzymiski J, Bissett WP, Kirkpatrick GJ, Millie DF, Moline MA, Roesler CS (1999) Optical monitoring and forecasting systems for harmful algal blooms: possibility of pipe dream? *J Phycol* 35:1477–1496
- Scholin CA, Gulland F, Doucette GJ, Benson S and others (2000) Mortality of sea lions along the central California coast linked to a toxic diatom bloom. *Nature* 403:80–84
- Smith P, Bogren K (2001a) Determination of nitrate and/or nitrite in brackish or seawater by flow injection analysis colorimeter: QuickChem Method 31-107-04-1-E. In: *Saline methods of analysis*. Lachat Instruments, Milwaukee, WI
- Smith P, Bogren K (2001b) Determination of silicate in brackish or seawater by flow injection analysis colorimeter: QuickChem Method 31-114-27-1-C. In: *Saline methods of analysis*. Lachat Instruments, Milwaukee, WI
- Stumpf R, Tomlinson M, Calkins J, Kirkpatrick B and others (2009) Skill assessment for an operational algal bloom forecast system. *J Mar Syst* 76:151–161
- Subba Rao DVS, Pan Y, Mukhida K (1998) Production of domoic acid by *Pseudo-nitzschia multiseriis* Hasle, affected by lithium. *PSZN I: Mar Ecol* 19:31–36
- Tomlinson MC, Stumpf RP, Ranisbrahmanakul V, Truby EW and others (2004) Evaluation of the use of SeaWiFS imagery for detecting *Karenia brevis* harmful algal blooms in the eastern Gulf of Mexico. *Remote Sens Environ* 91: 293–303
- Trainer VL, Adams NG, Bill BD, Anulacion BF, Wekell JC (1998) Concentration and dispersal of a *Pseudo-nitzschia*

- bloom in Penn Cove, Washington, USA. *Nat Toxins* 6: 113–126
- Trainer VL, Adams NG, Bill BD, Stehr CM and others (2000) Domoic acid production near California coastal upwelling zones, June 1998. *Limnol Oceanogr* 45:1818–1833
- Trainer VL, Adams NG, Wekell JC (2001) Domoic acid producing *Pseudo-nitzschia* species off the U.S. west coast associated with toxification events. In: Hallegraeff GM, Blackburn SI, Bolch CJ, Lewis RJ (eds) *Harmful algal blooms 2000*. Intergovernmental Oceanographic Commission of UNESCO, Paris, p 46–49
- Trainer VL, Hickey BM, Horner RA (2002) Biological and physical dynamics of domoic acid production off the Washington coast. *Limnol Oceanogr* 47:1438–1446
- ▶ Trainer VL, Cochlan WP, Erickson A, Bill BD, Cox FH, Borchert JA, Lefebvre KA (2007) Recent domoic acid closures of shellfish harvest areas in Washington State inland waterways. *Harmful Algae* 6:449–459
- Villac MC (1996) Synecology of the genus *Pseudo-nitzschia* H. Peragallo from Monterey Bay, California, USA. PhD dissertation, Texas A&M University, College Station
- Walz PM (1995) *Pseudo-nitzschia* species and domoic acid in Monterey Bay, CA. PhD dissertation, University of California, Santa Cruz
- ▶ Walz PM, Garrison DL, Graham WM, Cattery MA, Tjeerdema RS, Silver MW (1994) Domoic acid-producing diatom blooms in the Monterey Bay, California: 1991–1993. *Nat Toxins* 2:271–279
- ▶ Warrick JA, Mertes LAK, Siegel DA, Mackenzie C (2004) Estimating suspended sediment concentrations in turbid coastal waters of the Santa Barbara Channel with SeaWiFS. *Int J Remote Sens* 25:1995–2002
- ▶ Warrick JA, DiGiacomo PM, Weisberg SB, Nezlín NP and others (2007) River plume patterns and dynamics within the Southern California Bight. *Cont Shelf Res* 27:2427–2448
- Wells ML, Trick CG, Cochlan WP, Hughes MP, Trainer VL (2005) Domoic acid: the synergy of iron, copper, and the toxicity of diatoms. *Limnol Oceanogr* 50:1908–1917
- Welschmeyer NA (1994) Fluorometric analysis of chlorophyll *a* in the presence of chlorophyll *b* and pheopigments. *Limnol Oceanogr* 39:1985–1992
- Work TM, Beale AM, Fritz L, Quilliam MA, Silver M, Buck K, Wright JLC (1993) Domoic acid intoxication of brown pelicans and cormorants in Santa Cruz, California. In: Smayda TJ, Shimizu Y (eds) *Toxic phytoplankton blooms in the sea*. Elsevier Science Publication B.V., Amsterdam, p 643–650
- ▶ Wynne T, Stumpf R, Richardson A (2006) Discerning resuspended chlorophyll concentrations from ocean color satellite imagery. *Cont Shelf Res* 26:2583–2597

Editorial responsibility: Matthias Seaman,  
Oldendorf/Luhe, Germany

Submitted: September 25, 2008; Accepted: March 5, 2009  
Proofs received from author(s): April 21, 2009

1 Assessment of river discharge as a source of nitrate-nitrogen to Monterey Bay, California

2  
3 Jenny Q. Lane<sup>1</sup>, David M. Paradies<sup>2</sup>, Karen R. Worcester<sup>3</sup>, Raphael M. Kudela<sup>1</sup>

4  
5  
6  
7  
8  
9  
10  
11  
12  
13  
14  
15  
16  
17 Running head: Nitrogen loading: rivers vs. upwelling  
18

---

<sup>1</sup> Department of Ocean Sciences, University of California Santa Cruz, 1156 High Street, Santa Cruz, California 95064

<sup>2</sup> Bay Foundation of Morro Bay, 601 Embarcadero, Suite 11, Morro Bay, California 93442

<sup>3</sup> Central Coast Water Quality Control Board, 895 Aerovista Place, Suite 101, San Luis Obispo, California 93401

18 Acknowledgements

19 We thank Dane Hardin (Applied Marine Sciences) and Marc Los Huertos (CSU Monterey Bay)  
20 for their guidance and suggestions. We appreciate the assistance of Gary Conley and Bridget  
21 Hoover (Monterey Bay National Marine Sanctuary), Melissa Blakely (UCSC), Larry Breaker  
22 (Moss Landing Marine Laboratories), and the staff and volunteers of the Pathogens Pollution  
23 (P3) Project and the Central Coast Ambient Monitoring Program (CCAMP). This manuscript  
24 was substantially improved by the comments from two anonymous reviewers. Partial funding  
25 was provided as a Benjamin and Ruth Hammett Award for Research on Climate Change; a  
26 Science, Technology, Engineering, Policy and Society (STEPS) Institute graduate student  
27 research award; and a Center for the Dynamics and Evolution of the Land-Sea Interface  
28 (CDELSI) graduate student research award. Additional funding was provided as a fellowship  
29 (JQL) from an anonymous donor through CDELSI and from National Science Foundation  
30 project OCE-9912361 (RMK) and NOAA Awards NA04NOS4780239 and NA08NOS4730382.  
31 This contribution is part of the Global Ecology and Oceanography of Harmful Algal Blooms  
32 (GEOHAB) Core Research Project on Harmful Algal Blooms in Upwelling Systems, and is  
33 Monitoring and Event Response to Harmful Algal Blooms (MERHAB) Publication #XXX.

34 Abstract

35 Characterizations of coastal regions as ‘upwelling-dominated’ have promoted a concomitant  
36 assumption that, relative to upwelling, river contributions of nitrogen-nitrate ( $N_{NO_3}$ ) to these  
37 systems are insignificant. Here, we use 10 years (2000 – 2009) of daily load estimates to evaluate  
38 the relativity of river and upwelling  $N_{NO_3}$  loads introduced to Monterey Bay, an open embayment  
39 located along the central coast of California, United States (i.e. within a coastal upwelling  
40 regime). The characterization of Monterey Bay as ‘upwelling dominated’ is affirmed at low  
41 temporal resolutions (upwelling loads exceed river loads by two orders-of-magnitude), but is  
42 inconsistent at higher-resolution timescales which are also of ecological relevance (days and  
43 weeks): river  $N_{NO_3}$  loading, compared to upwelling  $N_{NO_3}$  loading, can predominate across short  
44 timescales and does so with significant frequency (28% of days in a given year). There is a clear  
45 onshore-offshore gradient in river  $N_{NO_3}$  load influence even at low (annual) temporal resolution,  
46 demonstrating that a failure to refine spatial resolution may alternately preclude an accurate  
47 characterization of river  $N_{NO_3}$  load relevance. We observe an upward trend in river  $N_{NO_3}$  loads  
48 and no trend in upwelling  $N_{NO_3}$  loads, indicating that the relativity and influence of river  $N_{NO_3}$   
49 loads as described may be expected to increase under environmental conditions observed during  
50 the study period. The positive trending of  $N_{NO_3}$  river loads suggests that the eutrophic  
51 conditioning of Monterey Bay’s high-discharge rivers, identified here according to the Indicator  
52 for Coastal Eutrophication Potential (N-ICEP), may become more severe and should be  
53 monitored at multiple temporal resolutions within a local and global context.

54

54 Introduction

55 Historically, freshwater nitrogen delivery to Monterey Bay CA, has been presumed to be  
56 non-significant due to the much greater magnitude and spatial scale of nitrate introduction by  
57 wind-driven upwelling (Kudela and Chavez 2004), and pivotal investigations of its hydrography  
58 either omit the consideration of fluvial impacts or determine them to be minor (Bolin and Abbott  
59 1963; Breaker and Broenkow 1994; Olivieri and Chavez 2000; Pennington and Chavez 2000;  
60 Ramp et al. 2005; Rosenfeld et al. 1994; Shulman et al. 2010). Regional blooms of the toxigenic  
61 diatom *Pseudo-nitzschia*, however, have alternately been linked to river discharge and upwelling  
62 processes, suggesting that river discharge may influence the ecology of this region. A recently  
63 published model for toxigenic *Pseudo-nitzschia* blooms in Monterey Bay, California (Lane et al.  
64 2009) reconciles these viewpoints through the consideration of seasonality: seasonal modeling  
65 identified Pajaro River discharge and nitrate concentration as significant predictors specific to  
66 the period of the year when local oceanographic conditions are not dominated by upwelling  
67 processes (Bolin and Abbott 1963; Pennington and Chavez 2000). As described by the models,  
68 river discharge may provide a source of nitrogen conducive to seasonal bloom formation, while  
69 allaying immediate bloom formation during periods of peak discharge. This empirically-derived  
70 description indicates a relationship between river discharge events and bloom incidence that is  
71 biphasic: blooms are immediately dissociated from high-discharge ('flush') events, but  
72 subsequently promoted by the high nitrate/declining discharge conditions which follow. The  
73 Pajaro River introduces disproportionately large nitrate loads on a highly seasonal basis, and is  
74 frequently paired with nitrate in descriptions of changing regional water quality: nitrate  
75 concentration in the Pajaro River has risen from <0.1 mM in the 1950's to levels that regularly  
76 exceed the drinking-water standard of 0.714 mM in more recent years (Ruehl et al. 2007). As a

77 result of this conditioning, the Pajaro and Salinas rivers and their vicinities are now designated as  
78 impaired for nitrate by the Clean Water Act [303 (d)]. The identification of river discharge as a  
79 seasonally significant factor in *Pseudo-nitzschia* bloom formation, and the recognition of  
80 substantially elevated nitrate concentrations in rivers such as the Pajaro and the Salinas, suggest  
81 that the historical perspectives on the relative significance (or insignificance) of freshwater  
82 nitrogen loading to the Monterey Bay system may be based on assumptions that no longer apply.  
83 The present study is in part a reevaluation of the temporal and spatial scales over which those  
84 assumptions may or may not be valid.

85 Since the necessity for a reevaluation of riverine nitrate paradigm was determined from an  
86 empirical (statistical) model linking nitrate, wind-driven upwelling, and river discharge, it  
87 clearly did not account for all possible sources of nitrogen. We acknowledge the limitations  
88 introduced through our approach [e.g. we do not address  $N_{NO_3}$  input from sources such as  
89 advection, atmospheric deposition, internal tide flux, or nitrification (Mackey et al. 2010;  
90 Rosenfeld et al. 1994; Shea and Broenkow 1982; Wankel et al. 2007; Ward 2005)] but we  
91 emphasized the utility of a simple first-order comparison. This paper provides a first-order  
92 comparison of how inviolate the omission of rivers as a component in complex modeling  
93 building or nutrient budgets may be, and is intended to provide a framework for evaluation. A  
94 comprehensive nutrient budget for Monterey Bay is beyond the scope of this study. Similarly,  
95 while we index the eutrophication risk of Monterey Bay rivers according their potential to  
96 promote new production of non-siliceous algae through nutrient delivery (a particularly relevant  
97 exercise in Monterey Bay, where dinoflagellate blooms occur with regularity), the investigation  
98 of how this potential may or may not be fulfilled is beyond the scope of this paper and is

99 addressed elsewhere (Armstrong et al. 2007; Kudela and Chavez 2004; Kudela et al. 2004;  
100 Kudela et al. 2008a; Kudela and Peterson 2009; Kudela et al. 2008b; Ryan et al. 2008).

101 A comparison of annual nitrate loading by freshwater discharge versus upwelling has  
102 previously been described for the Santa Barbara Channel (Warrick et al. 2005). In that study, the  
103 authors recognized that “although [river nutrient] contributions are significantly less than  
104 upwelling inputs to the channel, they are highly pulsed and supply nutrients in significantly  
105 different proportions and at different times of the year compared to upwelling”. At the northern  
106 extreme of the California Current System (CCS), similar comparative studies of the Columbia  
107 River also describe river nitrate contributions that are relatively small, but indicate that “despite  
108 the relatively small contributions on a seasonal basis, the Columbia River can be important as a  
109 local source during periods of downwelling or weak upwelling winds” (Hickey and Banas 2008).  
110 While the significance of river nitrate supply and cultural eutrophication in non-upwelling  
111 coastal systems is well-documented (Billen and Garnier 2007; Bricker et al. 2007; Cloern 2001;  
112 Conley et al. 2009; Heisler et al. 2008; Howarth 2008; Howarth et al. 2000; Justic et al. 1995a;  
113 Justic et al. 1995b; Li et al. 2007; Ludwig et al. 2009; Spruill and Bratton 2008; Turner and  
114 Rabalais 1991; Turner and Rabalais 1994), the Santa Barbara Channel and the Columbia River  
115 region provide unique examples of river/upwelling nitrate input comparisons from an upwelling-  
116 dominated system. These previous studies were constrained to river/upwelling load assessments  
117 at coarse (annual or seasonal) temporal resolution; nonetheless, these comparisons either suggest  
118 or demonstrate the significance of temporality as opposed to consideration of load magnitude  
119 alone. Here we present the first comparative study of river nitrate supply relative to that of  
120 upwelling at a temporal resolution higher than seasonal, and the first comparative study from the  
121 central region of the CCS.

122 We compare annual, monthly and daily nitrate-nitrogen ( $N_{NO_3}$ ) loads introduced to Monterey  
123 Bay by rivers and by wind-driven upwelling over a 10 y period (Jan 2000 – Aug 2009). We  
124 describe  $N_{NO_3}$  input to Monterey Bay by wind-driven upwelling using two methods to calculate  
125 the upwelling index (UI): (1) the Pacific Fisheries Environmental Laboratory (PFEL) UI for 36N  
126 122W, based on the offshore component of Ekman transport (Bakun 1973), and (2) UI from  
127 wind velocities observed at the Monterey Bay Aquarium Research Institute (MBARI) M1  
128 mooring, also using the offshore component of Ekman transport. We describe  $N_{NO_3}$  input to  
129 Monterey Bay by rivers according to load models developed for seven Central California  
130 Ambient Monitoring Program (CCAMP) Coastal Confluences monitoring sites within Monterey  
131 Bay (Figure 1), and compare our annual  $N_{NO_3}$  load estimates to those developed through a  
132 simpler modeling approach used by the Central Coast Long-term Environmental Assessment  
133 Network (CCLEAN). Upwelling  $N_{NO_3}$  loading and river  $N_{NO_3}$  loading are compared through  
134 time for the identification of load trending across the 10 y period for which data are available. To  
135 understand and recognize the influence of river  $N_{NO_3}$  loading and upwelling  $N_{NO_3}$  loading across  
136 the marine receiving waters of Monterey Bay, we describe the generalized patterns of river and  
137 upwelling  $N_{NO_3}$  loading through a hydrological year (i.e. as annual climatologies), and compare  
138 them to analogous patterns of surface nitrate concentration at the Santa Cruz Municipal Wharf  
139 (SCMW), and at moorings M0 (8 km offshore), M1 (18 km offshore), and M2 (56 km offshore).

140 We further analyze two independent data sets to characterize nutrient source waters and  
141 nutrient receiving waters according to their nutrient stoichiometry. Nitrogen species omitted in  
142 our analysis include urea-nitrogen ( $N_{UREA}$ ) and ammonium-nitrogen ( $N_{NH_4}$ ). While the  
143 contribution of nitrogen as  $N_{UREA}$  and  $N_{NH_4}$  loading is generally less than the contribution of  
144 nitrogen as  $N_{NO_3}$ , the introduction of  $N_{UREA}$  and  $N_{NH_4}$  may have a disproportionate influence on

145 harmful algal bloom (HAB) dynamics: recent studies indicate that *Pseudo-nitzschia* growth  
146 dynamics and toxicity vary according to N-substrate supplied for growth (Armstrong et al. 2007;  
147 Radan 2008). In recognition of their potentially differential impact, the stoichiometries for  $N_{\text{UREA}}$   
148 and  $N_{\text{NH}_4}$  relative to  $N_{\text{NO}_3}$  are provided.

149 Lastly, Monterey Bay rivers are further characterized using the Indicator of Coastal  
150 Eutrophication Potential (N-ICEP) index, which summarizes in a single figure the relevant  
151 information provided both by the absolute and relative values of the nitrogen and silica fluxes  
152 delivered by large river systems to identify systems susceptible to or impacted by eutrophication  
153 (Billen and Garnier 2007).

154

## 155 Methods

156 *Estimation of daily  $N_{\text{NO}_3}$  loads: upwelling*—Upwelling nitrate load was calculated by  
157 taking the product of an upwelling index (UI; vertical mass transport of upwelling source water  
158 per day) and the nitrate concentration of upwelling source water (estimated from daily average  
159 water temperature, described below). Both components of this approach [(1) the load calculation  
160 as a product of mass transport and nitrate concentration, and (2) the estimation of nitrate  
161 concentration from temperature] conjointly allow for derivation of upwelling nitrate supply or  
162 surface nitrate concentration estimates, often for the approximation of new production (Chavez  
163 and Toggweiler 1995; Dugdale et al. 1989; Garside and Garside 1995; Kamykowski 1987;  
164 Kamykowski and Zentara 1986; Kudela and Chavez 2000; Kudela and Dugdale 1996; Messie et  
165 al. 2009; Olivieri 1996; Olivieri and Chavez 2000; Pennington et al. 2010; Toggweiler and  
166 Carson 1995). We use two independent time series of UI estimates to generate two comparative  
167 (local and regional) estimates of  $N_{\text{NO}_3}$  upwelling loading to Monterey Bay. The first series of UI

168 estimates were obtained from the National Oceanographic and Atmospheric Administration  
169 Pacific Fisheries Environmental Laboratory (PFEL; [www.pfel.noaa.gov](http://www.pfel.noaa.gov)). The PFEL derives UI  
170 for 26 positions along the Eastern Pacific coast; the PFEL UI for 36N 122W (Figure 1) is readily  
171 available and represents variations in coastal upwelling for the Monterey Bay region. The second  
172 series of UI estimates was calculated from wind vector data (using a MATLAB [Mathworks  
173 Inc.] script originally developed by L. Breaker) using daily averaged wind velocities at mooring  
174 M1 (<http://dods.mbari.org/lasOASIS>). As with the PFEL UI estimates, UI at M1 is an estimate of  
175 vertical mass transport derived according to Ekman's theory of mass transport due to wind stress  
176 (Smith 1995). The derivations of PFEL UI and M1 UI differ, however, according to: (1) the  
177 location at which the UI is derived (PFEL UI is for an offshore site located south of Monterey  
178 Bay while M1 is centrally located within Monterey Bay; Figure 1), and (2) the source of the  
179 wind stress data/estimates used for the calculation of Ekman transport (the PFEL UI is calculated  
180 from geostrophic wind stresses derived from surface atmospheric pressure fields provided by the  
181 U.S. Navy Fleet Numerical Meteorological and Oceanographic Center, while the M1 UI is  
182 calculated from observed winds at mooring M1).

183         The UI describes the quantity (mass) of source water being upwelled from depth; the  
184 delivery of nitrate load through this transport process is calculated by taking the product of UI  
185 (vertical mass transport) and the nitrate concentration of upwelling source water. This requires,  
186 then: (1) a definition of upwelling source (i.e. depth) in Monterey Bay, and (2) estimation of the  
187 nitrate concentration of the upwelling source water. In Monterey Bay and for the California  
188 Current System, the depth of upwelling source water has been described and validated elsewhere  
189 as 60 m (Kudela and Chavez 2000; Messie et al. 2009; Olivieri 1996). We use this  
190 approximation to satisfy the two requirements specified above, as follows: (1) the characteristics

191 of upwelling source water are those of water at 60 m depth, and (2) the nitrate concentration of  
192 upwelling source water ( $[\text{NO}_3]$ ) can be estimated according to the 60 m temperature record from  
193 MBARI mooring M1 (<http://dods.mbari.org/lasOASIS>) and the following temperature-nitrate  
194 relationship, established previously from 6 y of M1 mooring data (Olivieri and Chavez 2000):

195

$$196 \quad [\text{NO}_3] = 0.6075(T)^2 - 19.078(T) + 149.436$$

197

198 The product of a concentration (daily average nitrate in upwelling source water,  
199 estimated from source-water temperature measurements and an established temperature-nitrate  
200 relationship) and a flux (daily average vertical mass transport: UIs by PFEL and from observed  
201 wind stress at M1) is a load – here, daily average nitrate load according to regional and local  
202 upwelling indices.

203 *Estimation of daily  $N_{\text{NO}_3}$  loads: rivers*—All major stream and river discharges to the  
204 ocean from southern San Mateo County to Santa Barbara County have been monitored monthly  
205 since 2001 through CCAMP coastal confluences monitoring, characterizing the primary sources  
206 of freshwater discharge to the ocean in this area. The resulting dataset is unique in its capability  
207 to identify long-term trends in water quality, to estimate total river loads of pollutants to the  
208 ocean, and to provide benchmark data for flow model validation. Related but simpler modeling  
209 efforts utilizing CCAMP data have been employed in previous studies, including  
210 epidemiological evaluations of spatial risk to marine mammals (or their food items) of various  
211 land-based pathological diseases, based on animal location relative to freshwater outflows and  
212 other pollution sources (Miller et al. 2002; Miller et al. 2006; Miller et al. 2005; Stoddard et al.  
213 2008).

214 Daily  $N_{NO_3}$  loads (and Si loads, where available for the purpose of N-ICEP calculations)  
215 were calculated by application of a CCAMP stream flow model to macronutrient concentrations  
216 derived to daily resolution for the following streams and rivers: San Lorenzo River, Soquel  
217 Creek, Aptos Creek, Pajaro River, Salinas River, Carmel River, and Big Sur River (Figure 1).  
218 Salinas River  $N_{NO_3}$  load estimates include those introduced to Monterey Bay through the Moss  
219 Landing Harbor entrance.

220 The CCAMP stream flow estimation model was developed to enhance stream flow  
221 information presented within the National Hydrography Dataset Plus (NHD+) geospatial  
222 framework (U.S. Environmental Protection Agency and the U.S. Geological Survey 2005) The  
223 CCAMP model uses Unit Runoff Model (UROM) estimates provided in the NHD+ geospatial  
224 framework to develop more spatially and temporally explicit estimates of flow (i.e. it describes  
225 flow at CCAMP Coastal Confluence monitoring sites at daily resolution). Unmodified, the  
226 NHD+ UROM model can provide annual average daily flows for each medium resolution  
227 hydrographic stream reach. The underlying NHD+ approach uses five United States Geological  
228 Survey (USGS) stream gages from the Hydro-Climatic Data Network (HCDN) within a 322 km  
229 (200 mile) radius as calibration gages to produce an estimation of average daily flows for each  
230 stream reach, accounting for upstream watershed area and other climatic and hydrologic features.  
231 The CCAMP stream flow model reconciles the following issues inherent in the NHD+ UROM  
232 model, which otherwise disqualifies its application for CCAMP purposes: (1) a spatial scale of  
233 322 km is insufficient to resolve California hydrologic climate regimes, (2) anthropogenic  
234 influences on stream and river flows are beyond the scope of the NHD+ effort, (3) USGS gage  
235 network measurements provide high temporal data density and low spatial data density, while (4)

236 stream transect method measurements provide low temporal data density, high accuracy and  
237 improved spatial density.

238 CCAMP enhancements to the NHD+ UROM model include selection of one to three  
239 USGS gages that more directly represent localized flow conditions at the site of interest. In some  
240 cases the gage may reside on the same stream system. Ratios are developed between gaged daily  
241 flow measurements and the UROM mean daily flow at each gage location, and if more than one  
242 gage is used these ratios are averaged. Mean daily flow ratios are then multiplied by the NHD+-  
243 derived annual mean daily flow at the discharge location of interest to estimate flow at that  
244 location and point in time. Gage choice is optimized by evaluating performance against CCAMP  
245 measured stream flows collected monthly along a ten-point cross section using a Marsh-  
246 McBirney conductive probe flow meter and setting rod. Modeled and observed flow estimates  
247 match closely (data not shown) and linear correlation of modeled and observed flow demonstrate  
248 an excellent model representation of observed flow variability ( $R^2 > 0.94$  for the seven Coastal  
249 Confluence sites addressed in this study).

250 Monthly macronutrient data were collected by CCAMP in accordance with California  
251 State Board's Surface Water Ambient Monitoring Program Quality Assurance Program Plan  
252 ([www.waterboards.ca.gov/water\\_issues/programs/swamp/](http://www.waterboards.ca.gov/water_issues/programs/swamp/)). Depth-integrated samples are  
253 collected into 1 L plastic bottles from the center of the stream flow or thalweg and immediately  
254 placed in cold ice chests (4 °C) for transport to the analyzing laboratory (BC Laboratories, Inc.).  
255 Macronutrient concentration estimates were derived to daily resolution by linear interpolation of  
256 monthly measurements.

257 Error associated with linear interpolation of monthly macronutrient measurements was  
258 examined in more detail as part of the CCAMP monitoring program using high frequency nitrate

259 concentration data from an in-situ ultraviolet spectrophotometer sensor, deployed by Monterey  
260 Bay Aquarium Research Institute through its Land Ocean Biogeochemical Observatory (LOBO)  
261 network. The L03 sensor is located at the lower end of the Old Salinas River in Moss Landing  
262 Harbor. This instrument collects nitrate readings continuously at an hourly interval and has been  
263 in operation since 1994. Its location in a tidal area presents additional sources of variability that  
264 would not be encountered were the sensor located in a non-tidal riverine environment. We  
265 adapted this data for use by selecting daily measurements collected at salinity low points. We  
266 extracted monthly interval measurements from this dataset and used the subset to create a daily  
267 linear interpolation of nitrate concentrations. Linear regression between the measured and  
268 interpolated daily concentrations produced a significant relationship ( $p < 0.001$ ,  $R^2 = 0.53$ ).  
269 When averaged daily interpolated concentrations were compared to averaged measured  
270 concentrations for the period of record, the interpolated values underestimated average  
271 concentrations by 3%. An additional round of validation was performed for the CCAMP  $N_{NO_3}$   
272 daily load estimates using an independent data set (P3 Project, described below). This exercise  
273 allowed for validation of the CCAMP-modeled  $N_{NO_3}$  daily loads with  $N_{NO_3}$  loads calculated from  
274 direct measurement of macronutrients (UCSC) and discharge rates (USGS) and demonstrated  
275 high precision of CCAMP  $N_{NO_3}$  load estimation (RMSD = 10.7%,  $N = 100$ ).

276 *Non-CCAMP confluence monitoring and coastal sampling*—River and creek samples  
277 were collected by volunteers and staff at the California Department of Fish and Game (CDFG) as  
278 part of the Pathogens Pollution Project (P3 Project). Sampling was conducted monthly (May  
279 2007 – Sept 2008) at six CCAMP Coastal Confluences monitoring locations described  
280 previously (all except Aptos Creek), and from 2 additional sites (Waddell Creek and Scott Creek;  
281 Figure 1). Macronutrient grab samples were collected into acid-washed polyethylene

282 terephthalate (PTEG) bottles and transported to the analyzing laboratory (UCSC) in a cooler with  
283 blue ice. The grab samples were filtered upon arrival either by syringe-filtration (Whatman<sup>®</sup> 0.2  
284  $\mu\text{m}$  GD/X) or canister-filtration (Poretics<sup>®</sup> 0.6  $\mu\text{m}$  polycarbonate membrane; <100mm Hg).  
285 Filtrates for ammonium and urea analyses were collected into 50 mL polypropylene (PP)  
286 centrifuge tubes (Corning<sup>®</sup>); previous tests have confirmed that these tubes are contaminant free  
287 for both urea and ammonium. Filtrates for macronutrient analysis [nitrate plus nitrite, silicic acid,  
288 and ortho-phosphate (hereafter referred to as phosphate)] were collected in 20 mL low-density  
289 polyethylene (LDPE) scintillation vials and stored frozen at -20 °C until analysis. Macronutrients  
290 were analyzed with a Lachat Quick Chem 8000 Flow Injection Analysis system using standard  
291 colorimetric techniques (Knepel and Bogren 2001; Smith and Bogren 2001a; Smith and Bogren  
292 2001b). Ammonium samples were manually analyzed using a fluorescence method (Holmes et  
293 al. 1999). Urea samples were manually analyzed using the diacetylmonoxime thiosemicarbazide  
294 technique (Price and Harrison 1987) modified to account for a longer time period and lower  
295 digestion temperature (Goeyens et al. 1998).

296 Shore-based macronutrient sampling was conducted weekly at SCMW (Figure 1) as part  
297 of the California Program for Regional Enhanced Monitoring for PhycoToxins (Cal-PReEMPT)  
298 project. Samples were collected from the surface with a PVC bucket (Jan – Aug 2006) or were  
299 mixtures of water samples collected from three discrete depths (0, 1.5 and 3 m) with a  
300 FieldMaster 1.75 L basic water bottle (Aug 2006 – Nov 2009). Offshore macronutrient sampling  
301 was conducted approximately monthly June 2002 – November 2007 at eleven stations  
302 throughout Monterey Bay as part of the Center for Integrated Marine Technology (CIMT)  
303 program. Ten-liter PVC Niskin bottles (refitted with silicone rubber band strings) mounted on an  
304 instrumented rosette were used to collect water from 0, 5, 10 and 25 m depth. At two of the

305 stations surface (0 m) samples were collected using a PVC bucket. All Cal-PReEMPT and CIMT  
306 grab samples were processed and analyzed for macronutrients at UCSC as described for P3  
307 Project macronutrient samples. For the development of nitrate-salinity mixing curves, CIMT  
308 cruises were categorized *a priori* according to concurrent Pajaro River discharge (USGS  
309 11159000) as either (a) ‘high river flow’ ( $\geq 80$  CFS), or (b) ‘ambient’.

310 Data used for the development of monthly climatologies of nearshore/offshore nitrate at  
311 three MBARI moorings (M0, M1, M2; Figure 1) were obtained from the LOBOViz 3.0 LOBO  
312 Network Data Visualization website, which is managed and maintained as a public data source  
313 by MBARI ([www.mbari.org/lobo/loboviz](http://www.mbari.org/lobo/loboviz)). Surface nitrate data were obtained at hourly  
314 resolution for the timeframes over which they were available [M0 (Aug 2004 – Jul 2009), M1  
315 (Oct 2009 – Jun 2010), M2 (Jul 2002 – Jun 2010)].

316 *River basin characterization per the Indicator for Coastal Eutrophication Potential*  
317 *(ICEP) index*—In addition to nutrient stoichiometries, we characterize the Pajaro and Salinas  
318 rivers according to their ICEP indices for nitrogen export. The ICEP index for nitrogen export  
319 (hereafter referred to as N-ICEP) is defined as

320

$$321 \text{ N-ICEP} = [\text{NFlx} / (14 \times 16) - \text{SiFlx} / (28 \times 20)] \times 106 \times 12 \quad (1)$$

322

323 where NFlx and SiFlx are the mean specific fluxes of total nitrogen and dissolved silica (Si),  
324 respectively, delivered at the outlet of the river basin, expressed in  $\text{kg N km}^{-2} \text{ d}^{-1}$  and  $\text{kg Si km}^{-2}$   
325  $\text{d}^{-1}$ . The N-ICEP index is expressed in  $\text{kg C km}^{-2} \text{ d}^{-1}$ ; the scaling of the index according to  
326 watershed area allows unbiased comparisons between large river systems (Billen and Garnier  
327 2007). Si daily loads were available in the CCAMP data as a partial record (November 2007 –

328 July 2009). The daily average  $N_{NO_3}$  and Si loads were used for the calculation of monthly  
329 average N-ICEP. Annual N-ICEP for the Pajaro and Salinas Rivers are provided for hydrological  
330 years (July – June) 2004 and 2005 based on annual loads previously reported by CCLEAN  
331 (CCLEAN 2006; CCLEAN 2007) and from CCAMP load data for hydrological year 2008 (July  
332 2008 – June 2009).

333

### 334 Results

335 *N<sub>NO3</sub> from rivers and upwelling: load comparison* — $N_{NO_3}$  loading into Monterey Bay by  
336 rivers and by wind-driven upwelling is shown in Figure 2 at annual (Figure 2A), monthly (Figure  
337 2B), and daily (Figure 2C) resolution;  $N_{NO_3}$  loading statistics are presented in Table 1. River  
338  $N_{NO_3}$  input from rivers is 2 orders-of-magnitude lower than  $N_{NO_3}$  input by wind-driven upwelling  
339 at lower (annual and monthly) temporal resolutions, timescales over which previous comparative  
340 analyses have been conducted (e.g. Warrick et al. 2005). The 2 orders-of-magnitude difference  
341 between river and upwelling  $N_{NO_3}$  input is not consistently observed at higher (daily and weekly)  
342 resolution (Figure 3), where  $N_{NO_3}$  input from rivers is maintained while  $N_{NO_3}$  input by wind-  
343 driven upwelling is relatively lower or zero during some winter months. These 2-4 week periods  
344 of comparatively higher river  $N_{NO_3}$  input coincide with periods of southerly winds and/or wind  
345 relaxation, when river flows and river  $N_{NO_3}$  input remain positive (river loading is switched ‘on’)  
346 while daily mean upwelling is essentially zero (loading by upwelling is switched ‘off’). The day-  
347 to-day recurrence of this circumstance throughout our 10 y time series is 28%; this statistic  
348 generally reflects the proportion of days for which daily mean upwelling was zero (or negative,  
349 in instances of downwelling). River input is generally not significant compared to upwelling N-

350 loading when the analysis is constrained to days where upwelling wind stress is positive, and  
351 when only load magnitude (but not temporality) is considered (Table 1).

352 In addition to their constancy as a source of  $N_{NO_3}$ , rivers differ from upwelling in their  
353 annual loading character; the greater proportion of river  $N_{NO_3}$  load is introduced over relatively  
354 short periods during the rainy season, and the summarization of river  $N_{NO_3}$  loading into  
355 cumulative sum profiles across hydrological years demonstrates the ‘stepped’ character of river  
356 loading (Figure 4). Upwelling contributes most significantly towards its cumulative load total in  
357 the early and late periods of the hydrological year, when the percent contribution from rivers is  
358 relatively small. Conversely, plateaus in the upwelling annual cumulative load profiles coincide  
359 with periods of the year when rivers are contributing the bulk of their annual cumulative  $N_{NO_3}$   
360 load, generally across the mid-point of the hydrological year (i.e. winter). The characteristics  
361 described for the cumulative sum  $N_{NO_3}$  loading profiles are consistent across years: the profiles  
362 in Figure 4B (cumulative sum, in percentage units) are similar for all years, even those which  
363 precede and follow years of relatively high absolute loading, e.g. 2004 and 2005 (Figure 4A).

364 Linear salinity-nitrate mixing curves developed for CIMT cruises categorized *a priori*  
365 according to concurrent river discharge as either (a) ‘high flow’ or (b) ‘ambient’ showed a  
366 reversal in the salinity-nitrate relationship according to river state, although linear correlations  
367 were not statistically significant in either case. Under conditions of high river flow, the  
368 relationship between nitrate and salinity was inverse ( $\alpha = -0.3047$ ), counter the relationship  
369 identified for ‘ambient’ conditions ( $\alpha = 1.130$ ). Based on the ‘high-flow’ mixing curve  
370 developed from the regional cruise data, we would expect the freshwater endmember to  
371 Monterey Bay (i.e. the freshwater source of nitrate) to have a nitrate concentration of 13.58  $\mu M$ ;

372 this agrees well with average nitrate concentrations of ‘typical’ Monterey Bay rivers, calculated  
373 from P3 Project data (e.g. San Lorenzo: 16.45  $\mu\text{M}$ , Scotts Creek: 7.16  $\mu\text{M}$ ).

374 Using monthly climatological data for surface nitrate concentrations and  $\text{N}_{\text{NO}_3}$  loading by  
375 upwelling, a significant correlation exists at the two moorings located furthest offshore (M1 and  
376 M2; Figure 5C-D); the correlations between  $\text{N}_{\text{NO}_3}$  loading and surface nitrate weaken and  
377 become statistically non-significant at the more inshore stations M0 and SCMW (Figure 5A-B).  
378 The correlation between river  $\text{N}_{\text{NO}_3}$  loading and surface nitrate is strongest at the most inshore  
379 location, SCMW, and maintains statistical significance at the next most inshore station (M0), but  
380 is not significant at the offshore moorings (Figure 5E-H).

381  *$\text{N}_{\text{NO}_3}$  from rivers and upwelling: trend comparison* —As the longest continual monitoring  
382 program addressing nutrient loading to central California coastal waters, the 10 y of CCAMP  
383  $\text{N}_{\text{NO}_3}$  load data used for this study provided a unique opportunity to assess the presence of intra-  
384 decadal load trending. Mann-Kendall trend analysis of  $\text{N}_{\text{NO}_3}$  loading by rivers and by wind-  
385 driven upwelling revealed a difference in trends for the 10 y loading record used in this study.  
386 River  $\text{N}_{\text{NO}_3}$  loading demonstrated a significant upward trend with a slope of 0.012; upwelling  
387 loading trend was non-negative, but its slope was zero (Table 2). Trend results for upwelling  
388  $\text{N}_{\text{NO}_3}$  load estimates were the same whether the load estimates were based on UI at Monterey Bay  
389 mooring M1 (UI according to locally observed winds) or PFEL estimates for 36N 122W (UI  
390 according to wind stress derived from mean surface atmospheric pressure fields). The absence of  
391 a trend in upwelling  $\text{N}_{\text{NO}_3}$  loading over the time-period addressed in our study (2001-2009) is  
392 consistent with observations of intra-annual oceanographic and climatic variability in Monterey  
393 Bay (e.g. phase changes, regime shifts) which would preclude monotonic trending, including (1)

394 increased nitrate at 60 m from 1998-2005, with (2) increased water column stratification after  
395 2003 and a concomitant reduction in near-surface nitrate (Chavez et al. 2006).

396 While our trend analysis for upwelling is an accounting of changes in its strength and  
397 potential (i.e. wind-stress, thermocline depth, etc.), our use of a static temperature-nitrate  
398 relationship, albeit with precedent, would prevent the identification of a trend caused by  
399 interchange of the water mass (and its properties) from which source waters are drawn. Since our  
400 focus is the contextualization of riverine  $N_{NO_3}$  loading (positive trend), failure here would be the  
401 non-recognition of an matching (positive) trend in the upwelling  $N_{NO_3}$  loading. According to two  
402 parameters which are representative of the temperature-nitrate relationship, the Nitrate Depletion  
403 Temperature (NDT; (Kamykowski and Zentara 2003; Kamykowski et al. 2002) and the  
404 coefficient of the linear nitrate-temperature regression ( $\alpha$ ), calculated for each year from 2000 –  
405 2010 from daily averages of temperature and nitrate at MBARI mooring M1 (Figure 1), there is a  
406 significant trend in the nitrate-temperature relationship across this period ( $p < 0.05$ ), but one  
407 which would translate to decreasing  $N_{NO_3}$  loading (and a progressive over-estimation of  
408 upwelling  $N_{NO_3}$  loads) across the decade. According to our trend analysis and this preliminary  
409 evaluation of inter-annual variability in the temperature-nitrate relationship at M1, we find no  
410 evidence of a positive trend in upwelling  $N_{NO_3}$  loading and the suggestion that in fact a negative  
411 trend, potentially masked by our use of a single nitrate-temperature across years, may exist. The  
412 trend differential of upwelling to river  $N_{NO_3}$  loading is therefore as stated according to our load  
413 estimates (no-trend for upwelling versus positive trend for rivers) or more extreme (negative for  
414 upwelling versus positive trend for rivers). While specification of this differential is sufficient for  
415 our purposes of context and comparison, a comprehensive evaluation of upwelling  $N_{NO_3}$  load

416 trending requires multi-decadal-to-centennial scale data and their careful analysis according to  
417 the specific purpose of long-term trend identification.

418 *Differential loading: nutrient source stoichiometry*—If we assess the stoichiometry of  
419 Monterey Bay rivers and streams nutrient concentrations according to the Redfield-Brzezinski  
420 ratio of 106:16:15:1 (Brzezinski 1985; Redfield 1934), six of the eight fluvial sources would be  
421 enriched according to  $Si \gg P > N$  (Table 3). The remaining 2 rivers, the Pajaro and Salinas,  
422 would be enriched according to  $N > Si > P$  with the Salinas demonstrating extreme nitrogen  
423 enrichment ( $N \gg Si > P$ ). All rivers are enriched with Si relative to P; this proportionality is  
424 especially pronounced in the 2 southernmost rivers (Carmel and Big Sur). The Salinas and the  
425 Pajaro Rivers have their outfalls in the mid-Bay region, making them distinct from the other  
426 rivers in terms of both nutrient stoichiometry (as relatively nitrogen-enriched) and outfall locale  
427 (Figure 1). The prevalence of additional nitrogen species ( $N_{UREA}$  and  $N_{NH_4}$ , collectively referred  
428 to as  $N_X$ ) was also evaluated; for all rivers,  $N_{NO_3}$  is the most prevalent of the 3 nitrogen species  
429 that were quantified ( $N_{NO_3}$ ,  $N_{UREA}$ ,  $N_{NH_4}$ ).

430 The nutrient stoichiometry of Monterey Bay waters from shipboard sampling (0, 5, 10  
431 and 25 m) shows relatively low surface  $N_{NO_3}$  with values approaching the Redfield-Brzezinski  
432 ratio with increased depth (Table 3). Ratios of  $N_{NO_3}:N_X$  in surface waters measured throughout  
433 Monterey Bay are low compared to  $N_{NO_3}:N_X$  ratios of the major rivers (Pajaro and Salinas), and  
434 equivalent to  $N_{NO_3}:N_X$  ratios for the northernmost rivers (e.g. Waddell Creek). Nutrient  
435 stoichiometry in integrated water (0, 1.5, 3 m) from SCMW resembled that of Monterey Bay  
436 surface waters, but with relatively lower  $N_{NO_3}$  for all ratios. Unlike rivers and offshore Monterey  
437 Bay,  $N_{NO_3}$  was not the predominant nitrogen species at SCMW:  $N_{UREA}$  was generally 3-fold  
438 higher than  $N_{NO_3}$ , while  $N_{NO_3}:N_{NH_4}$  approached 1:1 (Table 3).

439 *Eutrophication risk assessment*—Monthly N-ICEP values for the Pajaro and Salinas  
440 rivers are shown in Figure 6. While there is clear variability in monthly N-ICEP, the Pajaro River  
441 was characterized by positive N-ICEP values from early- to mid-year (Jan – Aug 2008, Mar – Jul  
442 2009) while N-ICEP for the Salinas River was significantly positive only for 2 months in early  
443 2009 (February and March). This monthly comparison of the Pajaro River and Salinas River N-  
444 ICEP indexes is necessarily limited, and the monitoring of Si and N should be adjusted (or  
445 implemented) within water quality assessment programs to afford the regular determination of  
446 N-ICEP at sub-annual resolution. Annual N-ICEP indices for the hydrological years 2004 and  
447 2005 were positive for the Salinas River ( $0.15 \text{ kg C km}^{-2} \text{ d}^{-1}$  in both years). These annual N-  
448 ICEP figures, determined from annual loads reported by CCLEAN, are in agreement with the  
449 annual N-ICEP determined from CCAMP data for the hydrological year 2008 ( $0.12 \text{ kg C km}^{-2} \text{ d}^{-1}$ ).  
450 Annual N-ICEP indices for the Pajaro River were consistently negative in the hydrological  
451 years 2004 and 2005, as determined from CCLEAN load data (-2.08 and -1.07, respectively),  
452 and in the hydrological year 2008, as determined from CCAMP load data ( $-0.05 \text{ kg C km}^{-2} \text{ d}^{-1}$ ).

453

#### 454 Discussion

455 *Riverine  $N_{NO_3}$  loading along an 'upwelling-dominated' coastline*—The comparative  
456 subject of this study is not unprecedented:  $N_{NO_3}$  load comparisons are available for the Columbia  
457 and Santa Clara rivers, near the northern and southern termini of the California Current System,  
458 respectively (Hickey and Banas 2008; Hickey et al. 2010; Warrick et al. 2005). These studies  
459 provide reference points from opposite ends of the eastern boundary current system in which  
460 Monterey Bay is centrally located, and from regions which differ significantly in hydrological  
461 setting and climate. The Columbia River is a significant source of freshwater discharge,

462 contributing 77% of the drainage along the west coast of the United States of America north of  
463 San Francisco (Barnes et al. 1972). Nitrate input by the Columbia River is an order-of-magnitude  
464 lower than nitrate input by coastal upwelling in the outfall region, but has been shown to  
465 maintain the ecosystem during periods when upwelling is depressed (Hickey and Banas 2008;  
466 Hickey et al. 2010; Kudela et al. 2010). To the south, the Santa Clara River drains a much  
467 smaller and drier watershed, but one which is heavily influenced by patterns of land-use  
468 (agricultural and urban). For this relatively dry system in the southern CCS, river nitrate input is  
469 2-3 orders of magnitude lower than nitrate input by upwelling, but nutrient contributions from  
470 the river are regarded as significant due to differences in nutrient quality (i.e. Si:N:P for  
471 upwelled waters was 16:5:1; the same ratio for rivers was 13:10:1), and input timing.

472 Our evaluation of  $N_{NO_3}$  loading to Monterey Bay by rivers and by wind-driven upwelling  
473 confirms the significance of river  $N_{NO_3}$  load timing and indicates that the consideration of  
474 temporality, and not simply magnitude, must be taken into consideration – even in a region  
475 identified as one that is dominated by coastal upwelling. Our comparison of river and upwelling  
476  $N_{NO_3}$  loads on annual and monthly timescales affirms the classification of Monterey Bay as an  
477 upwelling-dominated region (the minimum differences between nitrate input from rivers and  
478 from upwelling were 2 orders of magnitude for annual and monthly timescales), but also affirms  
479 this classification as a generality. Most water quality monitoring programs cannot afford the  
480 opportunity to describe river nitrate loading on a daily basis, and the present study is the first to  
481 compare river and upwelling nitrate inputs at sub-seasonal resolution. As such, this study is the  
482 first to describe nitrate inputs within a region of the CCS at the temporal resolution at which  
483 regional discharge and upwelling events are often defined (e.g. wind-relaxation events, ‘first  
484 flush’ discharge events) and relevance to phytoplankton response has been described by others

485 (Malej et al. 1995; Small and Menzies 1981; Walsh et al. 1977). We note that only when our  
486 order-of-magnitude load comparison was conducted at this ecologically relevant temporal  
487 resolution (Beman et al. 2005) did the rate at which rivers exceed wind-driven upwelling as a  
488 nitrate source become apparent (28%; Figure 3). Similarly, the refined development of salinity-  
489 nitrate mixing curves from region-wide cruise data according to river flow status ('high flow'  
490 versus 'ambient') demonstrates: (1) regional riverine influence sufficient to cause a reversal in  
491 the salinity-nitrate mixing curve, i.e. a negative correlation between nitrate and salinity in Bay  
492 waters when river flow is high, and (2) further evidence for regional riverine  $N_{NO_3}$  source  
493 predominance under high flow conditions, per the agreement of average nitrate concentrations in  
494 'typical' Monterey Bay rivers with the freshwater  $N_{NO_3}$  endmember concentration predicted by  
495 the 'high flow' salinity-nitrate mixing curve.

496 *Onshore-to-offshore gradient in  $N_{NO_3}$  source climatology correlations*—Our comparison  
497 of upwelling and river  $N_{NO_3}$  loading was designed to address  $N_{NO_3}$  loading for Monterey Bay. In  
498 our comparison, the refinement of temporal scale (annual to monthly to weekly/daily) allowed  
499 for the recognition of periods when  $N_{NO_3}$  loads from rivers surpassed those introduced by  
500 upwelling across an entire region, while the climatological comparisons from nearshore to  
501 offshore (Figure 5) provide some indication of the cross-shelf gradient. The development of  
502 surface nitrate climatologies at discrete locations spanning the onshore-to-offshore distance  
503 encompassed by Monterey Bay (SCMW, M0, M1, M2; Figure 1) indicates the predominance of  
504 river  $N_{NO_3}$  loading even on a broad temporal scale at discrete nearshore (but still  
505 'oceanographic') observational locations. While there is strong correlation between the  
506 climatology of surface nitrate and the climatology of  $N_{NO_3}$  loading by upwelling at the offshore  
507 stations M1 and M2, the correlation becomes non-significant further inshore. Conversely, the

508 correlation between the climatologies for surface nitrate and  $N_{NO_3}$  loading by rivers is strongest  
509 at the most inshore station (SCMW), and weakens with increasing distance offshore. These  
510 onshore/offshore correlation gradients for river  $N_{NO_3}$  loading and for  $N_{NO_3}$  loading by upwelling  
511 suggest that the relative significance of  $N_{NO_3}$  river loading cannot be ignored, even without  
512 regard to temporality, at inshore locations such as SCMW and M0. The relative importance of  
513 this loading suggests an enhanced capacity to influence algal growth and harmful algal bloom  
514 dynamics within the onshore coastal zone, nearest to coastal communities and economies  
515 (Anderson et al. 2008; Anderson et al. 2002; Glibert et al. 2005a; Glibert et al. 2005b; Howarth  
516 2008; Kudela et al. 2006; Kudela et al. 2008a).

517         The southward advection of upwelling waters from an upwelling center immediately to  
518 the north of Monterey Bay has been observed during upwelling events (Ramp et al. 2009; Ramp  
519 et al. 2005; Rosenfeld et al. 1994), but this delivery requires sustained winds of  $10 \text{ m s}^{-1}$  on the  
520 order of a week (Ramp et al. 2005). More recently, a publication synthesizing the results of two  
521 Autonomous Ocean Sampling Network field experiments described in one case (August 2006) a  
522 failure to simulate salinity and temperature fields (demonstrated successfully for August 2003)  
523 using a nested, data assimilating model supported by focused, high-resolution sampling of the  
524 upwelling center. New consideration of minor, but evidently important,  $N_{NO_3}$  sources to  
525 Monterey Bay (Mackey et al. 2010; Wankel et al. 2007), have demonstrated circumstances when  
526 these processes exert significant influence within an ‘upwelling dominated’ regime. Our  
527 correlation of surface  $N_{NO_3}$  climatologies to river and upwelling  $N_{NO_3}$  loading climatologies  
528 (Figure 5) indicates the predominance of river  $N_{NO_3}$  loading on a *broad temporal scale* at  
529 nearshore locations. Under circumstances of high river flow, we identify evidence of this  
530 predominance on a *broad spatial scale*: the development of salinity-nitrate mixing curves from

531 regional cruise data according to river flow condition ('high-flow' versus 'ambient')  
532 demonstrates a sign reversal in the salinity-nitrate relationship (i.e. an inverse relationship  
533 between nitrate and salinity) during periods of high river flow.

534 *Implications for water quality monitoring programs*—While there are several ongoing  
535 water quality monitoring programs in the Monterey Bay region, the CCAMP dataset was used  
536 for this study because (1) it afforded estimates of river nitrate loads at daily resolution, and (2) it  
537 had been generated from continual monitoring over the longest timespan (2000 – 2009). In these  
538 two respects, the CCAMP data are relatively unique. While a long-term, high resolution dataset  
539 was necessary for the primary purpose of this study (upwelling/river  $N_{NO_3}$  load comparison), it is  
540 useful to consider whether the higher precision modeling required to generate daily river load  
541 estimates is necessary to inform annual estimates of riverine  $N_{NO_3}$  loads. For the hydrological  
542 years 2004 (July 2004 – June 2005) and 2005 (July 2005 – June 2006), annual load estimates  
543 from six monitoring locations are available for comparison from CCAMP and CCLEAN [Aptos  
544 Creek (2005 only), San Lorenzo River, Soquel Creek, Pajaro River, Carmel River, Big Sur River  
545 (2004 only); Figure 1]. Across these sites, annual  $N_{NO_3}$  load estimates agreed in both years to  
546 within an order-of-magnitude. The largest discrepancies between the annual load estimates  
547 occurred for the rivers with relatively small drainage areas (Carmel River and Big Sur River in  
548 2004; Aptos Creek and Soquel Creek in 2005); for all other rivers, the factor difference between  
549 CCLEAN and CCAMP annual load estimates ranged from < 1 to 3. In both 2004 and 2005, the  
550 CCLEAN estimates of total  $N_{NO_3}$  river load to Monterey Bay were lower than the estimates from  
551 CCAMP, and this difference is not wholly unexpected: annual loading figures generated by  
552 CCLEAN were presumed to be underestimates since CCLEAN estimates were generated by  
553 calculating daily loads from each monthly grab sample (from measured  $N_{NO_3}$  and  $NHD^+$

554 modeled discharge), averaging the daily loads across the hydrological year, and multiplying the  
555 average by the number of days in the hydrological year (365). While the approach taken by  
556 CCLEAN is simple and less time-intensive, the resulting annual load calculations were reported  
557 as “estimates, based on individual grab samples, (which) may underestimate actual loads because  
558 high loads associated with episodic storm events are not consistently sampled” (CCLEAN 2007).  
559 Since CCAMP annual load estimates are annual sums of daily loads, they have the potential to  
560 more precisely resolve and represent  $N_{NO_3}$  loads introduced during episodic high-flow (‘flush’)  
561 events. Our comparison of CCAMP annual load estimates with those generated by CCLEAN  
562 suggests that the simpler approach (CCLEAN) is adequate for large-scale (Bay-wide, annual)  
563 estimates. Where higher precision is required, large-scale estimates generated by programs such  
564 as CCLEAN could be augmented with data provided by programs designed to characterize river  
565 contributions during episodic events (e.g. ‘First Flush’ monitoring, with the addition of flow  
566 measurement or estimation). The significance of local water quality data may be more effectively  
567 extended to the coastal environment if, either individually or in concert, water quality programs  
568 include the parameters required for calculation of N-ICEP (and the analogous index for ortho-  
569 phosphate, P-ICEP) on daily, weekly, monthly, and annual timescales.

570 *Differential loading among Monterey Bay rivers*—In most years, the annual  $N_{NO_3}$  loads  
571 introduced by the Pajaro and the Salinas rivers comprise >95% of total annual river  $N_{NO_3}$  load to  
572 Monterey Bay (Figure 7). While the relative contribution from the Pajaro and Salinas is  
573 consistently large, the relative contribution from each of the two rivers is variable. Within the  
574 2001 – 2009 timeframe, 2005 and 2006 stand out as years of relatively high freshwater  
575 discharge: mean annual discharge from the Salinas River was an order-of-magnitude higher in  
576 2005 – 2006 than across the other years (16.7 versus 1.7  $m^3 s^{-1}$ ). In these high discharge years,

577 the Salinas River dominated the relatively high total  $N_{NO_3}$  load (Figure 7). Conversely, in years  
578 of low to moderate discharge, the Pajaro River tends to dominate. The unusually high  
579 contribution of  $N_{NO_3}$  from the Big Sur River in 2009 is unexplained, but presumed to be an  
580 artifact of severe wildfires that affected the region in the summer of 2008, and the drainage of  
581 burned landscape over the 2009 rainy season.

582 While we can illustrate disproportionate  $N_{NO_3}$  loading by the Pajaro and Salinas Rivers by  
583 comparing annual  $N_{NO_3}$  load contributions (Figure 7) and nutrient ratios (Table 3), the N-ICEP  
584 index provides added insight into the character of the Salinas and Pajaro River basins. The N-  
585 ICEP refers to the potential for new primary production (non-siliceous algae only) based upon  
586 the nutrient fluxes delivered by a river system. Designed as a summary characterization index,  
587 the N-ICEP represents the relevant information contained in both absolute and relative values of  
588 nitrogen and silica fluxes delivered by large river systems (Billen and Garnier 2007). The  
589 damming of rivers and reservoir construction (increased retention of biogenic silica),  
590 urbanization (increased discharge of low Si:N wastewater) and agriculture (increased nitrogen,  
591 thereby decreasing Si:N) all promote positive N-ICEP values, while rivers draining pristine  
592 watersheds are rich in silica and low in nitrogen (Billen and Garnier 2007; Table 3, this study),  
593 resulting in negative N-ICEP values. Our analysis of N-ICEP is constrained to the Salinas and  
594 Pajaro rivers since (1) the ICEP was formulated for the characterization of relatively large-scale  
595 river systems, and (2)  $N_{NO_3}$  loading by the Pajaro and Salinas regularly contributes >95% of total  
596 river  $N_{NO_3}$  loading on a consistent basis (Figure 7). Although the N-ICEP indices of the 5  
597 additional rivers included in the CCAMP dataset are unavoidably inflated in terms of absolute  
598 value [an artifact of inserting a small drainage area into the N-ICEP calculation], they trend  
599 strongly negative in the winter months and trend to less negative values through the remainder of

600 the year. As expected, the most consistent and extreme negative N-ICEP indices are observed in  
601 rivers that drain relatively pristine watersheds (e.g. Big Sur River; data not shown).

602 The monthly N-ICEP figures reveal extended periods during which the Pajaro River is  
603 characterized by positive N-ICEP (e.g. Jan – Aug 2008, Figure 6) while on an annual basis (e.g.  
604 for the 2008 hydrological year) the Pajaro River was characterized by negative N-ICEP. As with  
605 our comparisons between  $N_{NO_3}$  loading from upwelling and from river discharge, considerable  
606 information is gained by comparing annual and monthly patterns. Billen and Garnier (2007)  
607 recommended calculation of the N-ICEP on varying timescales (daily, monthly, yearly)  
608 according to the surface area of the impacted coastal marine zone and the residence time of  
609 freshwater masses within it. A thorough evaluation of N-ICEP for Monterey Bay rivers will  
610 require a more extensive collection of high-resolution Si and  $N_{NO_3}$  loading data than were  
611 available for this study, and future assessments should be undertaken across various temporal  
612 resolutions selected according to the question and conditions under consideration.

613 *Broad implications*—Our preliminary assessment of N-ICEP for Monterey Bay rivers  
614 identifies it as a useful and appropriate index for the characterization of large rivers within the  
615 Monterey Bay region, one which allows comparison of Monterey Bay rivers to rivers from  
616 different climatic regions of the world now and into the future. A recent collection of N-ICEP  
617 values based upon measured (versus modeled) load data demonstrates a general association of  
618 positive N-ICEP for river basins draining to the Mediterranean Sea, Black Sea, Baltic Sea and  
619 the North Atlantic and negative N-ICEP for rivers draining to the North and South Pacific, South  
620 Atlantic, the Arctic, and the Indian Ocean (Garnier et al. 2010). Our identification of the Salinas  
621 River as consistently positive N-ICEP highlights the Salinas River as an exception to these  
622 general patterns. Worldwide, N-ICEP generally increases with population density, and shifts to a

623 positive value in river basins with >30% agricultural land (Garnier et al. 2010). The Pajaro River  
624 N-ICEP appears to be shifting towards a positive value (-2.08, -1.07, and -0.05 kg C km<sup>-2</sup> d<sup>-1</sup> in  
625 2004, 2005 and 2008, respectively), in agreement with previous observations of increasing  
626 agricultural activity and water quality impairment within the watershed (Los Huertos et al. 2001;  
627 Ruehl et al. 2007). The positive trend identified in Monterey Bay river N<sub>NO3</sub> loads (CCAMP;  
628 2000 – 2009), and the increasing N-ICEP values in the Pajaro River both suggest that N-ICEP  
629 values will continue trending positive in the absence of intervention. Industrialized countries in  
630 Europe and the United States have seen N-ICEP values stabilize or decrease as a result of  
631 nitrogen removal in wastewater treatment and increases in the efficiency of agricultural nitrogen  
632 use; positive trends for Monterey Bay river N-ICEP values suggest a trajectory more similar to  
633 areas such as the Japanese and Chinese Seas, Indian and South African coasts, where rapidly  
634 increasing agricultural production and fast urbanization have led to increased N-ICEP across a  
635 30 year period (1970 – 2000; Garnier et al. 2010).

636         There is increasing scientific consensus that eutrophication plays a role in the  
637 development, persistence, and expansion of HABs in the United States and worldwide (Anderson  
638 et al. 2008; Heisler et al. 2008; Kudela et al. 2008a). More generally, regions that are not  
639 typically strongly influenced by riverine nutrient sources may exhibit strong responses by the  
640 phytoplankton community to relatively small changes in loading and stoichiometry; for example,  
641 the Washington and Oregon coast appear to be poised to shift from N-limitation to P or Si-  
642 limitation with very moderate increases in N-loading to the Columbia River (Kudela and  
643 Peterson 2009). This susceptibility can be introduced or augmented by climatological events  
644 such as El Niño, when river outflows provide significant macronutrient loads to nutrient-deplete  
645 surface coastal waters (Castro et al. 2002; Wilkerson et al. 2002); these conditions can induce a

646 significant phytoplankton response (Friederich et al. 2002; Kudela and Chavez 2004) and have  
647 been implicated in HAB conditions leading to mass wildlife mortality (Scholin et al. 2000).  
648 While toxigenic blooms of *Pseudo-nitzschia* in Monterey Bay are predominantly associated with  
649 upwelling conditions on an annual basis, the influence of river discharge becomes apparent on a  
650 seasonal basis (Lane et al. 2009). Our demonstration here of the predominance of river  $N_{NO_3}$   
651 loading on short timescales (~28% of the time), the onshore-offshore gradient of its influence,  
652 and its upward temporal trend, indicate that rivers are exerting significant (and increasing)  
653 influence within a coastal upwelling system. Based on previous descriptions of the linkage  
654 between HABs and eutrophication (Anderson et al. 2008; Heisler et al. 2008; Kudela et al.  
655 2008a; Lane et al. 2009), this influence, and its strengthening, should be expected to enhance the  
656 development, persistence and expansion of phytoplankton blooms, including HABs, in coastal  
657 waters of the present day and of the future.  
658  
659

659 Table 1. Comparative statistics for nitrogen as nitrate ( $N_{NO_3}$ ) loading by rivers monitored as part  
 660 of the Central Coast Ambient Monitoring Program (CCAMP; Coastal Confluences) and by wind-  
 661 driven upwelling according to observed daily mean winds at Monterey Bay mooring M1 (36.75N  
 662 122.03W) and according to daily mean upwelling index (UI) estimates issued by the Pacific  
 663 Fisheries Environmental Laboratory (PFEL) for 36N 122W.

	Rivers (CCAMP)	Upwelling (M1 / PFEL)
664 Average $N_{NO_3}$ load ( $\times 10^9$ kg $y^{-1}$ )	0.001	0.3 / 0.7
665 Days of positive $N_{NO_3}$ load	100%	73% / 87%
666 Days (river load > UI load)	28%	-- / --
667 Days (river load > UI load); UI > 0	1%	-- / --
668 Mean relative contribution ( $\% y^{-1}$ )	0.4 (range: 0.1–1.3)	>99 / --
669		
670		

670 Table 2. Sen's slope estimates from Mann-Kendall trend analysis of 10 y (01 Jan 2000 through  
 671 06 Aug 2009) of daily nitrogen loadings (nitrogen as nitrate; kg) to Monterey Bay by rivers  
 672 monitored as part of the Central Coast Ambient Monitoring Program (CCAMP; Coastal  
 673 Confluences), and by wind-driven upwelling according to observed daily mean winds at  
 674 Monterey Bay mooring M1 (36.75N 122.03W) and according to daily mean upwelling index  
 675 (UI) estimates issued by the Pacific Fisheries Environmental Laboratory (PFEL) for 36N 122W.

	Rivers (CCAMP)	Upwelling (M1 and PFEL)
676 Upward	0.012 ( $p = 0.000$ )	0.000 ( $p = 0.000$ )
678 Downward	$p > 0.05$	$p > 0.05$
679 $n$	3506	3503
680		
681		

681 Table 3. Nutrient ratios, expressed in phosphate (P), silica (Si), and nitrogen [urea-nitrogen  
682 ( $N_{UREA}$ ) nitrate-nitrogen ( $N_{NO_3}$ ); ammonium-nitrogen ( $N_{NH_4}$ )]. Ratios were determined from river  
683 and creek grab samples collected monthly (May 2007 – Sept 2008) from rivers and creeks  
684 throughout Monterey Bay as part of the Pathogens Pollution Project. Stoichiometries for  
685 onshore/offshore receiving waters are provided from cruise samples collected monthly at stations  
686 throughout Monterey Bay (Center for Integrated Marine Technology; 2002 – 2007);  
687 stoichiometries for inshore receiving waters are from integrated-depth (0, 1.5, 3 m) samples  
688 collected weekly at the Santa Cruz Municipal Wharf (SCMW; 2005 – 2009). For comparison,  
689 nutrient ratios for the Mississippi River, Santa Clara River, and upwelled water in the Santa  
690 Barbara (SB) Channel are included (Justic et al. 1995a; Warrick et al. 2005).

	Si:P	Si: $N_{NO_3}$	$N_{NO_3}$ :P	$N_{NO_3}$ : $N_{UREA}$	$N_{NO_3}$ : $N_{NH_4}$
691 Waddell Creek	291	50	3	4	5
692 Scott Creek	213	56	5	4	2
693 San Lorenzo River	108	24	5	8	5
694 Soquel Creek	175	133	2	6	7
695 Pajaro River	290	0.4	356	100	34
696 Salinas River	228	0.1	3277	424	884
697 Carmel River	443	55	7	18	29
698 Big Sur River	673	128	3	9	28
700 — —					
701 Mississippi River	14	0.9	15	n/a	n/a
702 Santa Clara River	16	3	5	n/a	n/a
703 — —					
704 Monterey Bay (0 m)	23	2	9	5	5
705 Monterey Bay (5 m)	20	2	9	4	7
706 Monterey Bay (10 m)	14	1	10	38	11
707 Monterey Bay (25 m)	13	1	12	54	28
708 SB Channel upwelling	13	1	10	n/a	n/a
709 — —					
710 SCMW	30	6	5	0.3	0.8
711					

711 Figure Legends

712 Figure 1. Map of the Monterey Bay region, annotated with Coastal Confluences Ambient  
713 Monitoring Project (CCAMP) river and creek coastal confluences (San Lorenzo River, Soquel  
714 Creek, Aptos Creek, Pajaro River, Salinas River, Carmel River, Big Sur River) which  
715 contributed to estimates of daily river nitrate-nitrogen ( $N_{NO_3}$ ) loading to Monterey Bay, the  
716 coastal confluences sampled through the Pathogens Pollution Project for their characterization  
717 according to nutrient stoichiometry (same as CCAMP coastal confluence sites, omitting Aptos  
718 Creek and including Waddell Creek), the Monterey Bay Aquarium Research Institute (MBARI)  
719 offshore moorings (M0, M1, M2), the location of 36N 122W for which daily upwelling index  
720 (UI) is generated by the Pacific and Fisheries Environmental Laboratory (PFEL), and the  
721 location of the Santa Cruz Municipal Wharf (SCMW). Filled symbols denote river monitoring  
722 sites (versus sites used for coastal monitoring).

723

724 Figure 2. Nitrate-nitrogen ( $N_{NO_3}$ ) loads introduced to Monterey Bay by rivers (grey bars) and by  
725 wind-driven upwelling estimated from observed winds at the Monterey Bay Aquarium Research  
726 Institute (MBARI) mooring M1 (filled circles) and from an upwelling index (UI) provided by the  
727 Pacific and Fisheries Environmental Laboratory (PFEL) for 36N 122W (open diamonds). The  
728 same  $N_{NO_3}$  load data are presented in each panel but at increasing temporal resolution, as  
729 follows: annual (A), monthly (B), and daily (C; daily  $N_{NO_3}$  loads are from M1 winds only). Note  
730 the unit difference between upwelling loads (plotted on the left vertical axis) and river loads  
731 (plotted on the right vertical axis).

732

733 Figure 3. Daily nitrate-nitrogen ( $N_{NO_3}$ ) loads introduced to Monterey Bay by rivers (grey bars)  
734 and by wind-driven upwelling estimated from observed winds at the Monterey Bay Aquarium  
735 Research Institute (MBARI) mooring M1 (black bars) across periods for which  $N_{NO_3}$  loads  
736 introduced by rivers were consistently higher than  $N_{NO_3}$  loads introduced by upwelling (i.e.  
737 upwelling winds were effectively turned ‘off’, while river loading remained switched ‘on’). This  
738 figure illustrates the relativity of river  $N_{NO_3}$  loading for only 3 select timeframes across which  
739 river loads are particularly competitive; across the entire study period (2000 – 2009), daily loads  
740 of  $N_{NO_3}$  from rivers exceed daily loads of  $N_{NO_3}$  from upwelling at a rate of 28%.

741

742 Figure 4. Nitrate-nitrogen ( $N_{NO_3}$ ) loading by rivers (grey fill) and by wind-driven upwelling  
743 estimated from observed winds at the Monterey Bay Aquarium Research Institute (MBARI)  
744 mooring M1 (black line), as expressed in absolute cumulative sum (A), and percent cumulative  
745 sum (B). The cumulative sums are calculated and displayed according to hydrological year (July  
746 – June). Note in (A) the unit difference between upwelling loads (plotted on the left vertical axis)  
747 and river loads (plotted on the right vertical axis).

748

749 Figure 5. The surface nitrate climatology for Santa Cruz Municipal Wharf (SCMW; A and E),  
750 mooring M0 (B and F), mooring M1 (C and G), and mooring M2 (D and H) are shown; the  
751 climatologies are arranged top-to-bottom according to offshore distance (i.e. SCMW is a pier-  
752 based monitoring location; the M0, M1, and M2 moorings are located 8, 18, and 56 km offshore,  
753 respectively. The climatology of  $N_{NO_3}$  loading to Monterey Bay by upwelling is repeated through  
754 panels A-D for its comparison with the onshore (top panel) to offshore (bottom panel) series of  
755 surface nitrate climatology. The climatology for  $N_{NO_3}$  loading to Monterey Bay by rivers is

756 repeated through panels E-H for its comparison with the onshore (top panel) to offshore (bottom  
757 panel) series of surface nitrate climatology. The correlation coefficient ( $r$ ) for each pair of  
758 climatologies is shown. Light grey bars (surface nitrate climatology), black lines (upwelling load  
759 climatology) and dark grey lines (river load climatology) denote standard deviation for each  
760 month's climatological average.

761

762 Figure 6. Monthly values of the Indicator for Coastal Eutrophication Potential with respect to  
763 nitrogen (N-ICEP) for the Pajaro and Salinas Rivers. The N-ICEP refers to the potential for new  
764 primary production (non-siliceous algae only) based upon the nutrient fluxes delivered by a river  
765 system. Designed as a summary characterization index, the N-ICEP encompasses and represents  
766 the relevant information contained in both absolute and relative values of nitrogen and silica  
767 fluxes delivered by large river systems (Billen and Garnier 2007). A negative value of the N-  
768 ICEP indicates silica delivery in excess over nitrogen delivery and the prevalence of relatively  
769 pristine conditions (i.e. the absence of eutrophication problems). A positive value of the N-ICEP  
770 indicates the reverse circumstance (nitrogen delivery in excess of silica delivery); positive values  
771 are generally indicative of eutrophication problems exerting their influence within the river  
772 basin.

773

774 Figure 7. Relative percent nitrate-nitrogen ( $N_{NO_3}$ ) load contribution (bars) from each of the rivers  
775 and creeks monitored by the Central Coast Ambient Monitoring Program (CCAMP). The total  
776 (absolute)  $N_{NO_3}$  load introduced to Monterey Bay in each year is shown (white circles) to  
777 illustrate the differential between the Pajaro and Salinas load contributions across years of  
778 moderate  $N_{NO_3}$  loading (corresponding to years of dry to normal hydrology) and years when

779  $N_{NO_3}$  loading was enhanced (i.e. the relatively wet years of 2005 and 2006).

780 References

- 781 Anderson, D. M. and others 2008. Harmful algal blooms and eutrophication: Examining linkages from  
782 selected coastal regions of the United States. *Harmful Algae* **8**: 39-53.
- 783 Anderson, D. M., P. M. Glibert, and J. M. Burkholder. 2002. Harmful algal blooms and eutrophication:  
784 nutrient sources, composition, and consequences. *Estuaries* **25**: 704-726.
- 785 Armstrong, M. D., W. P. Cochlan, N. Ladizinsky, and R. M. Kudela. 2007. Nitrogenous preference of  
786 toxigenic *Pseudo-nitzschia australis* (Bacillariophyceae) from field and laboratory experiments  
787 *Harmful Algae* **6**: 206-217.
- 788 Bakun, A. 1973. Coastal upwelling indices, west coast of North America, 1946-71. NOAA Technical  
789 Report. United States Department of Commerce.
- 790 Barnes, C. A., A. C. Duxbury, and B. A. Morse. 1972. Circulation and selected properties of the  
791 Columbia River effluent at sea, p. 41-80. *In* A. T. Pruter and D. L. Alverson [eds.], *The*  
792 *Columbia River Estuary and Adjacent Ocean Waters*. University of Washington Press.
- 793 Beman, J. M., K. R. Arrigo, and P. A. Matson. 2005. Agricultural runoff fuels large phytoplankton  
794 blooms in vulnerable areas of the ocean. *Nature* **434**: 211-214.
- 795 Billen, G., and J. Garnier. 2007. River basin nutrient delivery to the coastal sea: Assessing its potential to  
796 sustain new production of non-siliceous algae. *Mar Chem* **106**: 148-160.
- 797 Bolin, R. L., and D. P. Abbott. 1963. Studies on the marine climate and phytoplankton of the central  
798 coastal area of California, 1954-1960, p. 23-45. California Cooperative Oceanic Fisheries  
799 Investigations Report. Hopkins Marine Station of Stanford University.
- 800 Breaker, L. C., and W. W. Broenkow. 1994. The Circulation of Monterey Bay and Related Processes.  
801 *Oceanogr Mar Biol* **32**: 1-64.
- 802 Bricker, S. B. and others 2007. Effects of nutrient enrichment in the nation's estuaries: a decade of  
803 change. *Harmful Algae* **8**.
- 804 Brzezinski, M. A. 1985. The Si:C:N ratio of marine diatoms: interspecific variability and the effect of  
805 some environmental variables. *J Phycol* **21**: 347-357.
- 806 Castro, C. G. and others 2002. Nutrient variability during El Nino 1997-98 in the California current  
807 system off central California. *Prog Oceanogr* **54**: 171-184.
- 808 CCLEAN. 2006. Central Coast Long-term Environmental Assessment Network (CCLEAN): annual  
809 report 2004-2005.
- 810 ---. 2007. Central Coast Long-term Environmental Assessment Network (CCLEAN): regional monitoring  
811 program overview 2001-2006.
- 812 Chavez, F. and others 2006. Seeing the future in a stratified sea. Monterey Bay Aquarium Research  
813 Institute 2006 annual report.
- 814 Chavez, F. P., and J. R. Toggweiler. 1995. Physical estimates of global new production: the upwelling  
815 contribution. *In* C. P. Summerhayes, K. C. Emeis, M. V. Angel, R. L. Smith and B. Zeitzschel  
816 [eds.], *Upwelling in the Ocean: Modern Processes and Ancient Records*. J. Wiley and Sons.
- 817 Cloern, J. E. 2001. Our evolving conceptual model of the coastal eutrophication problem. *Mar Ecol-Prog*  
818 *Ser* **210**: 223-253.
- 819 Conley, D. J. and others 2009. Controlling eutrophication: nitrogen and phosphorus. *Science* **323**: 1014-  
820 1015.
- 821 Dugdale, R. C., A. Morel, A. Bricaud, and F. P. Wilkerson. 1989. Modeling new production in upwelling  
822 centers: A case study of modeling new production from remotely sensed temperature and color.  
823 *Journal of Geophysical Research* **94**: 18119-18132.
- 824 Friederich, G. E., P. M. Walz, M. G. Burczynski, and F. P. Chavez. 2002. Inorganic carbon in the central  
825 California upwelling system during the 1997-1999 El Nino-La Nina event. *Prog Oceanogr* **54**:  
826 185-203.
- 827 Garnier, J., A. Beusen, V. Thieu, G. Billen, and L. Bouwman. 2010. N:P:Si nutrient export ratios and  
828 ecological consequences in coastal seas evaluated by the ICEP approach. *Global Biogeochem Cy*  
829 **24**: -.

- 830 Garside, C., and J. C. Garside. 1995. Euphotic-zone nutrient algorithms for the Nabe and EqPac study  
831 sites. *Deep-Sea Research Part II: Topical Studies in Oceanography* **42**: 335-347.
- 832 Glibert, P. M., D. M. Anderson, P. Gentien, E. Granéli, and K. G. Sellner. 2005a. The global, complex  
833 phenomena of harmful algal blooms. *Oceanography* **18**: 136-147.
- 834 Glibert, P. M. and others 2005b. The role of eutrophication in the global proliferation of harmful algal  
835 blooms: new perspectives and new approaches. *Oceanography* **18**: 198-209.
- 836 Goeyens, L., N. Kindermans, M. A. Yusuf, and M. Elskens. 1998. A room temperature procedure for the  
837 manual determination of urea in seawater. *Estuarine, Coastal and Shelf Science* **47**: 415-418.
- 838 Heisler, J. and others 2008. Eutrophication and harmful algal blooms: A scientific consensus. *Harmful*  
839 *Algae* **8**: 3-13.
- 840 Hickey, B. M., and N. S. Banas. 2008. Why is the Northern End of the California Current System So  
841 Productive? *Oceanography* **21**: 90-107.
- 842 Hickey, B. M. and others 2010. River Influences on Shelf Ecosystems: Introduction and synthesis. *J*  
843 *Geophys Res-Oceans* **115**: -.
- 844 Holmes, R. M., A. Aminot, R. Kerouel, B. A. Hooker, and B. J. Peterson. 1999. A simple and precise  
845 method for measuring ammonium in marine and freshwater ecosystems. *Canadian Journal of*  
846 *Fisheries and Aquatic Sciences* **56**: 1801-1808.
- 847 Howarth, R. W. 2008. Coastal nitrogen pollution: A review of sources and trends globally and regionally.  
848 *Harmful Algae* **8**: 14-20.
- 849 Howarth, R. W. and others 2000. Nutrient pollution of coastal rivers, bays, and seas. *Issues in Ecology* **7**:  
850 1-15.
- 851 Justic, D., N. N. Rabalais, and R. E. Turner. 1995a. Stoichiometric Nutrient Balance and Origin of  
852 Coastal Eutrophication. *Mar Pollut Bull* **30**: 41-46.
- 853 Justic, D., N. N. Rabalais, R. E. Turner, and Q. Dortch. 1995b. Changes in Nutrient Structure of River-  
854 Dominated Coastal Waters - Stoichiometric Nutrient Balance and Its Consequences. *Estuar Coast*  
855 *Shelf S* **40**: 339-356.
- 856 Kamykowski, D. 1987. A Preliminary Biophysical Model of the Relationship between Temperature and  
857 Plant Nutrients in the Upper Ocean. *Deep-Sea Res* **34**: 1067-1079.
- 858 Kamykowski, D., and S. J. Zentara. 1986. Predicting plant nutrient concentrations from temperature and  
859 sigma-T in the upper kilometer of the world ocean. *Deep-Sea Res* **33**: 89-105.
- 860 ---. 2003. Can phytoplankton community structure be inferred from satellite-derived sea surface  
861 temperature anomalies calculated relative to nitrate depletion temperatures? *Remote Sens Environ*  
862 **86**: 444-457.
- 863 Kamykowski, D., S. J. Zentara, J. M. Morrison, and A. C. Switzer. 2002. Dynamic global patterns of  
864 nitrate, phosphate, silicate, and iron availability and phytoplankton community composition from  
865 remote sensing data. *Global Biogeochem Cy* **16**: -.
- 866 Knepel, K., and K. Bogren. 2001. Determination of orthophosphorous by flow injection analysis in  
867 seawaters: QuickChem Method 31-113-01-1-H. *Saline Methods of Analysis*. Lachat Instruments.
- 868 Kudela, R., and F. Chavez. 2004. The impact of coastal runoff on ocean color during an El Nino year in  
869 Central California. *Deep-Sea Res Pt II* **51**: 1173-1185.
- 870 Kudela, R., W. Cochlan, and A. Roberts. 2004. Spatial and temporal patterns of *Pseudo-nitzschia* species  
871 in central California related to regional oceanography *In* J. H. L. K.A. Steidinger, C.R. Tomas,  
872 and G.A. Vargo [ed.], *Harmful Algae 2002*. Florida Fish and Wildlife Conservation Commission,  
873 Florida Institute of Oceanography and Intergovernmental Oceanographic Commission of  
874 UNESCO, Paris.
- 875 Kudela, R. M., and F. P. Chavez. 2000. Modeling the impact of the 1992 El Niño on new production in  
876 Monterey Bay, California. *Deep-Sea Research II* **47**: 1055-1076.
- 877 Kudela, R. M., W. P. Cochlan, T. D. Peterson, and C. G. Trick. 2006. Impacts on phytoplankton biomass  
878 and productivity in the Pacific Northwest during the warm ocean conditions of 2005. *Geophys*  
879 *Res Lett* **33**.

- 880 Kudela, R. M., and R. C. Dugdale. 1996. Estimation of new production from remotely-sensed data in a  
881 coastal upwelling regime. *Adv Space Res* **18**: 791-797.
- 882 Kudela, R. M. and others 2010. Multiple trophic levels fueled by recirculation in the Columbia River  
883 plume. *Geophys Res Lett* **37**: -.
- 884 Kudela, R. M., J. Q. Lane, and W. P. Cochlan. 2008a. The potential role of anthropogenically derived  
885 nitrogen in the growth of harmful algae in California, USA *Harmful Algae* **8**: 103-110.
- 886 Kudela, R. M., and T. D. Peterson. 2009. Influence of a buoyant river plume on phytoplankton nutrient  
887 dynamics: What controls standing stocks and productivity? *J Geophys Res-Oceans* **114**: -.
- 888 Kudela, R. M., J. P. Ryan, M. D. Blakely, J. Q. Lane, and T. D. Peterson. 2008b. Linking the physiology  
889 and ecology of *Cochlodinium* to better understand harmful algal bloom events: A comparative  
890 approach. *Harmful Algae* **7**: 278-292.
- 891 Lane, J. Q., P. T. Raimondi, and R. M. Kudela. 2009. Development of a logistic regression model for the  
892 prediction of toxigenic *Pseudo-nitzschia* blooms in Monterey Bay, California. *Marine Ecology*  
893 *Progress Series* **383**: 37-51.
- 894 Li, M. T., K. Q. Xu, M. Watanabe, and Z. Y. Chen. 2007. Long-term variations in dissolved silicate,  
895 nitrogen, and phosphorus flux from the Yangtze River into the East China Sea and impacts on  
896 estuarine ecosystem. *Estuar Coast Shelf S* **71**: 3-12.
- 897 Los Huertos, M., L. E. Gentry, and C. Shennan. 2001. Land use and stream nitrogen concentrations in  
898 agricultural watersheds along the central coast of California. *ScientificWorldJournal* **1 Suppl 2**:  
899 615-622.
- 900 Ludwig, W., E. Dumont, M. Meybeck, and S. Heussner. 2009. River discharges of water and nutrients to  
901 the Mediterranean and Black Sea: Major drivers for ecosystem changes during past and future  
902 decades? *Prog Oceanogr* **80**: 199-217.
- 903 Mackey, K. R. M. and others 2010. Influence of atmospheric nutrients on primary productivity in a  
904 coastal upwelling region. *Global Biogeochem Cy* **24**: -.
- 905 Malej, A., P. Mozetic, V. Malacic, S. Terzic, and M. Ahel. 1995. Phytoplankton responses to freshwater  
906 inputs in a small semi-enclosed gulf (Gulf of Trieste, Adriatic Sea). *Marine Ecology Progress*  
907 *Series* **120**: 111-121.
- 908 Messie, M., J. Ledesma, D. D. Kolber, R. P. Michisaki, D. G. Foley, and F. P. Chavez. 2009. Potential  
909 new production estimates in four eastern boundary upwelling ecosystems. *Prog Oceanogr* **83**:  
910 151-158.
- 911 Miller, M. A. and others 2002. Coastal freshwater runoff is a risk factor for *Toxoplasma gondii* infection  
912 of southern sea otters (*Enhydra lutris nereis*). *Int J Parasitol* **32**: 997-1006.
- 913 Miller, W. A. and others 2006. *Salmonella* spp., *Vibrio* spp., *Clostridium perfringens*, and *Plesiomonas*  
914 *shigelloides* in marine and freshwater invertebrates from coastal California ecosystems. *Microb*  
915 *Ecol* **52**: 198-206.
- 916 ---. 2005. New genotypes and factors associated with *Cryptosporidium* detection in mussels (*Mytilus*  
917 spp.) along the California coast. *Int J Parasitol* **35**: 1103-1113.
- 918 Olivieri, R. A. 1996. Plankton dynamics and the fate of primary production in the coastal upwelling  
919 ecosystem of Monterey Bay, California. University of California Santa Cruz.
- 920 Olivieri, R. A., and F. P. Chavez. 2000. A model of plankton dynamics for the coastal upwelling system  
921 of Monterey Bay. *Deep-Sea Research II* **47**: 1077-1106.
- 922 Pennington, J. T., and F. P. Chavez. 2000. Seasonal fluctuations of temperature, salinity, nitrate,  
923 chlorophyll and primary production at station H3/M1 over 1989-1996 in Monterey Bay,  
924 California. *Deep-Sea Research II* **47**: 947-973.
- 925 Pennington, J. T., G. E. Friederich, C. G. Castro, C. A. Collins, W. E. Wiley, and F. P. Chavez. 2010. The  
926 northern and central California coastal upwelling system. *In* K. Liu, L. Atkinson, R. Quiñones  
927 and L. Talaue-McManus [eds.], *Carbon and nutrient fluxes in continental margins*. Springer.
- 928 Price, N. M., and P. J. Harrison. 1987. Comparison of Methods for the Analysis of Dissolved Urea in  
929 Seawater. *Mar Biol* **94**: 307-317.

- 930 Radan, R. 2008. Nutrient uptake and toxicity of *Pseudo-nitzschia cuspidata*: a laboratory and field based  
931 experiment. San Francisco State University.
- 932 Ramp, S. R. and others 2009. Preparing to predict: The Second Autonomous Ocean Sampling Network  
933 (AOSN-II) experiment in the Monterey Bay. *Deep-Sea Res Pt II* **56**: 68-86.
- 934 Ramp, S. R., J. D. Paduan, I. Shulman, J. Kindle, F. L. Bahr, and F. Chavez. 2005. Observations of  
935 upwelling and relaxation events in the northern Monterey Bay during August 2000. *J Geophys*  
936 *Res-Oceans* **110**: -.
- 937 Redfield, A. C. 1934. On the proportions of organic derivations in sea water and their relation to the  
938 composition of plankton, p. 177-192. *In* R. J. Daniel [ed.], James Johnstone Memorial Volume.  
939 University Press of Liverpool.
- 940 Rosenfeld, L. K., F. B. Schwing, N. Garfield, and D. E. Tracy. 1994. Bifurcated flow from an upwelling  
941 center: a cold water source for Monterey Bay. *Cont Shelf Res* **14**: 931-964.
- 942 Ruehl, C. R. and others 2007. Nitrate dynamics within the Pajaro River, a nutrient-rich, losing stream. *J N*  
943 *Am Benthol Soc* **26**: 191-206.
- 944 Ryan, J. P. and others 2008. A coastal ocean extreme bloom incubator. *Geophys Res Lett* **35**.
- 945 Scholin, C. A. and others 2000. Mortality of sea lions along the central California coast linked to a toxic  
946 diatom bloom. *Nature* **403**: 80-84.
- 947 Shea, R. E., and W. W. Broenkow. 1982. The role of internal tides in the nutrient enrichment of Monterey  
948 Bay, California. *Estuarine, Coastal and Shelf Science* **15**: 57-66.
- 949 Shulman, I., S. Anderson, C. Rowley, S. Derada, J. Doyle, and S. Ramp. 2010. Comparisons of upwelling  
950 and relaxation events in the Monterey Bay area. *J Geophys Res-Oceans* **115**: -.
- 951 Small, L. F., and D. W. Menzies. 1981. Patterns of primary productivity and biomass in a coastal  
952 upwelling region. *Deep-Sea Research (a): Oceanographic Research Papers* **28**: 123-149.
- 953 Smith, P., and K. Bogren. 2001a. Determination of nitrate and/or nitrite in brackish or seawater by flow  
954 injection analysis colorimeter: QuickChem method 31-107-04-1-E. *Saline Methods of Analysis*.  
955 Lachat Instruments.
- 956 ---. 2001b. Determination of silicate in brackish or seawater by flow injection analysis colorimeter:  
957 QuickChem Method 31-114-27-1-C. *Saline Methods of Analysis*. Lachat Instruments.
- 958 Smith, R. L. 1995. The physical processes of coastal ocean upwelling systems. *In* C. P. Summerhayes, K.  
959 C. Emeis, M. V. Angel, R. L. Smith and B. Zeitzschel [eds.], *Upwelling in the Ocean: Modern*  
960 *Processes and Ancient Records*. J. Wiley and Sons.
- 961 Spruill, T. B., and J. F. Bratton. 2008. Estimation of groundwater and nutrient fluxes to the Neuse River  
962 estuary, North Carolina. *Estuar Coast* **31**: 501-520.
- 963 Stoddard, R. A. and others 2008. Risk factors for infection with pathogenic and antimicrobial-resistant  
964 fecal bacteria in northern elephant seals in California. *Public Health Rep* **123**: 360-370.
- 965 Toggweiler, J. R., and S. Carson. 1995. What are upwelling systems contributing to the ocean's carbon  
966 and nutrient budgets? *In* C. P. Summerhayes, K. C. Emeis, M. V. Angel, R. L. Smith and B.  
967 Zeitzschel [eds.], *Upwelling in the Ocean: Modern Processes and Ancient Records*. J. Wiley and  
968 Sons.
- 969 Turner, R. E., and N. N. Rabalais. 1991. Changes in Mississippi River Water-Quality This Century.  
970 *Bioscience* **41**: 140-147.
- 971 ---. 1994. Coastal Eutrophication near the Mississippi River Delta. *Nature* **368**: 619-621.
- 972 U.S. Environmental Protection Agency and the U.S. Geological Survey. 2005. National Hydrography  
973 Dataset Plus - NHDPlus.
- 974 Walsh, J. J., T. E. Whitledge, J. C. Kelley, S. A. Huntsman, and R. D. Pillsbury. 1977. Further transition-  
975 states of Baja California upwelling ecosystem. *Limnol Oceanogr* **22**: 264-280.
- 976 Wankel, S. D., C. Kendall, J. T. Pennington, F. P. Chavez, and A. Paytan. 2007. Nitrification in the  
977 euphotic zone as evidenced by nitrate dual isotopic composition: Observations from Monterey  
978 Bay, California. *Global Biogeochem Cy* **21**: -.
- 979 Ward, B. B. 2005. Temporal variability in nitrification rates and related biogeochemical factors in  
980 Monterey Bay, California, USA. *Marine Ecology Progress Series* **292**: 97-109.

981 Warrick, J. A., L. Washburn, M. A. Brzezinski, and D. A. Siegel. 2005. Nutrient contributions to the  
982 Santa Barbara Channel, California, from the ephemeral Santa Clara River. *Estuarine, Coastal and*  
983 *Shelf Science* **62**: 559-574.  
984 Wilkerson, F. P., R. C. Dugdale, A. Marchi, and C. A. Collins. 2002. Hydrography, nutrients and  
985 chlorophyll during El Nino and La Nina 1997-99 winters in the Gulf of the Farallones, California.  
986 *Prog Oceanogr* **54**: 293-310.  
987  
988

Figure 1

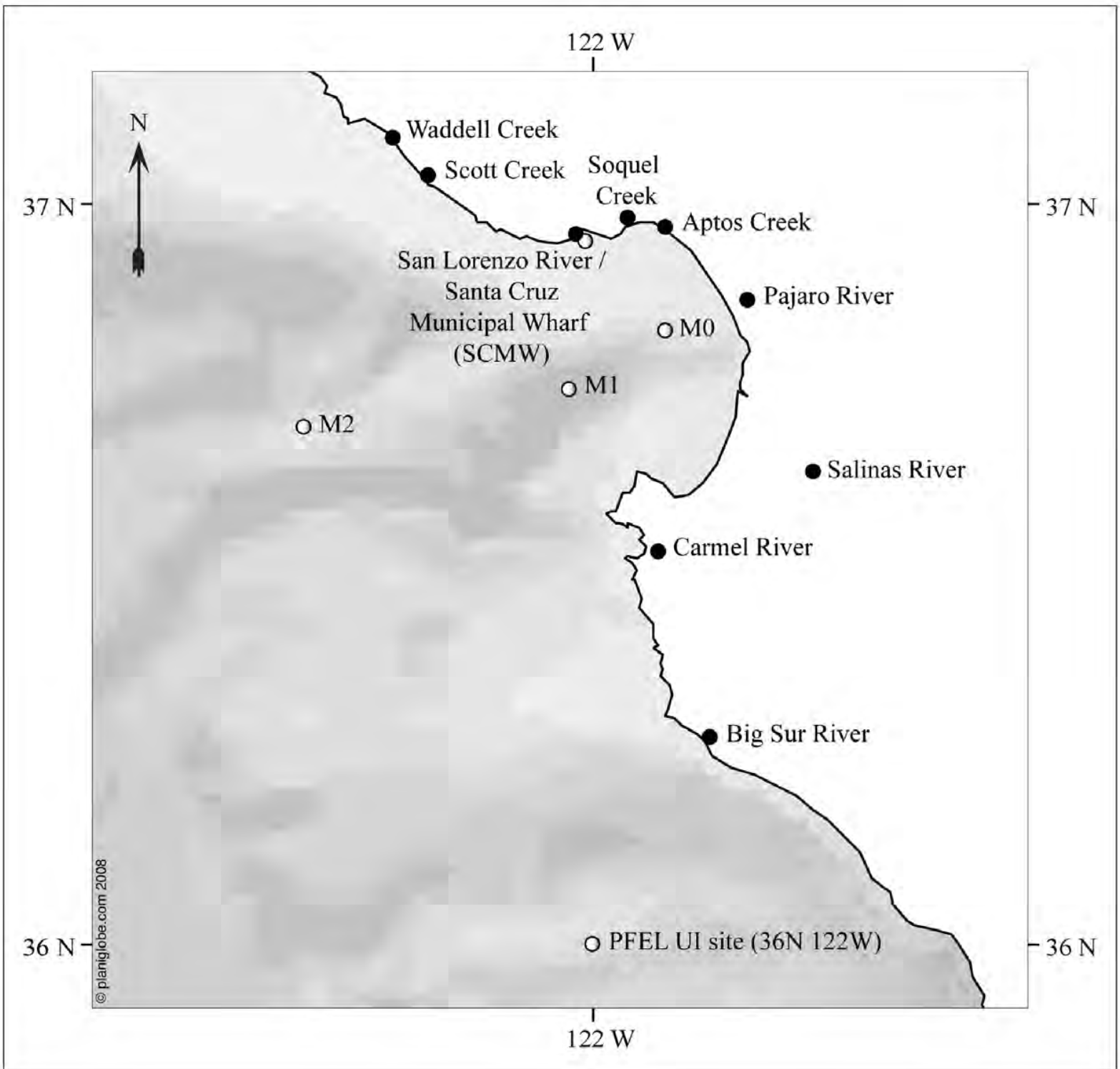


Figure 2

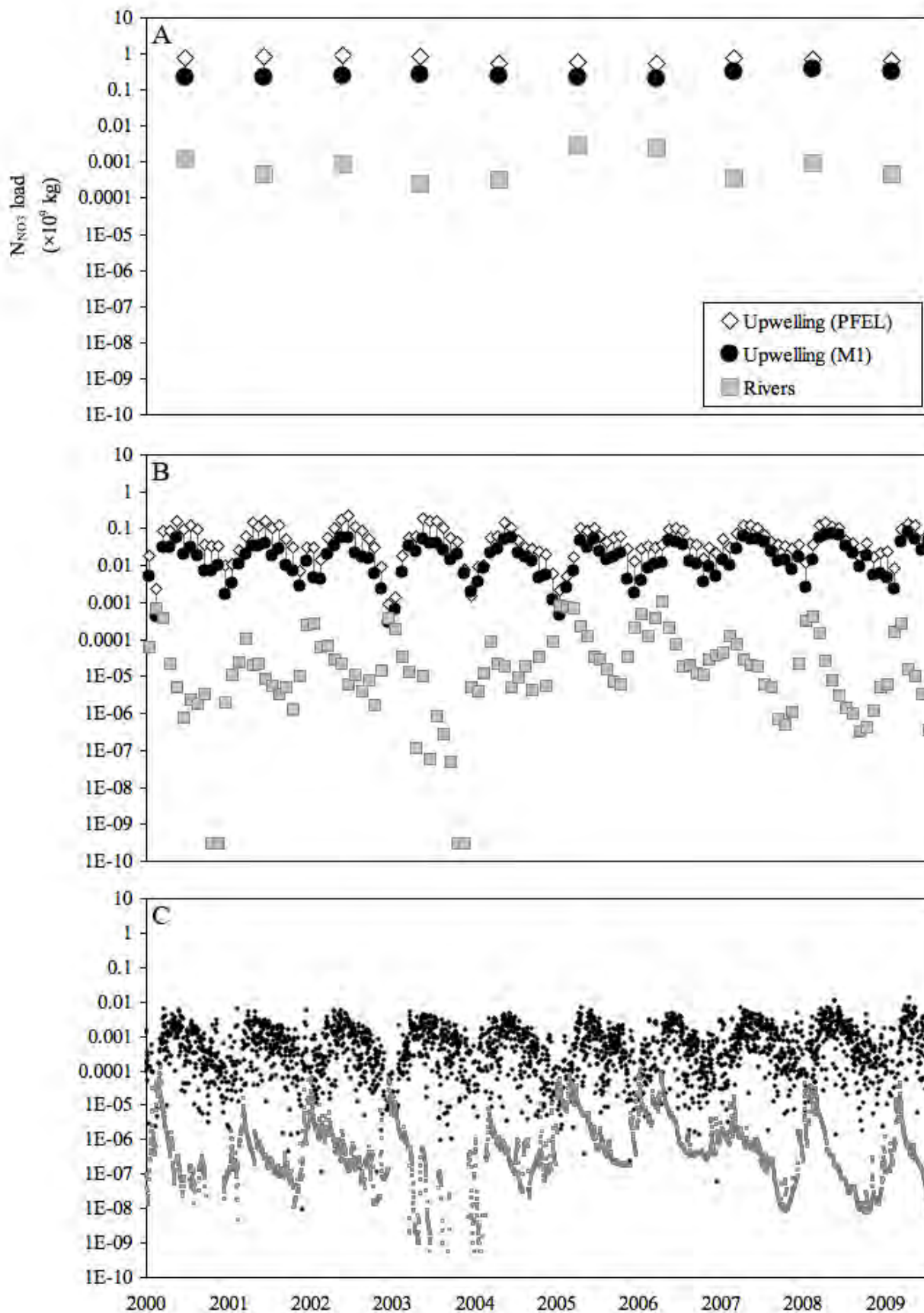


Figure 3

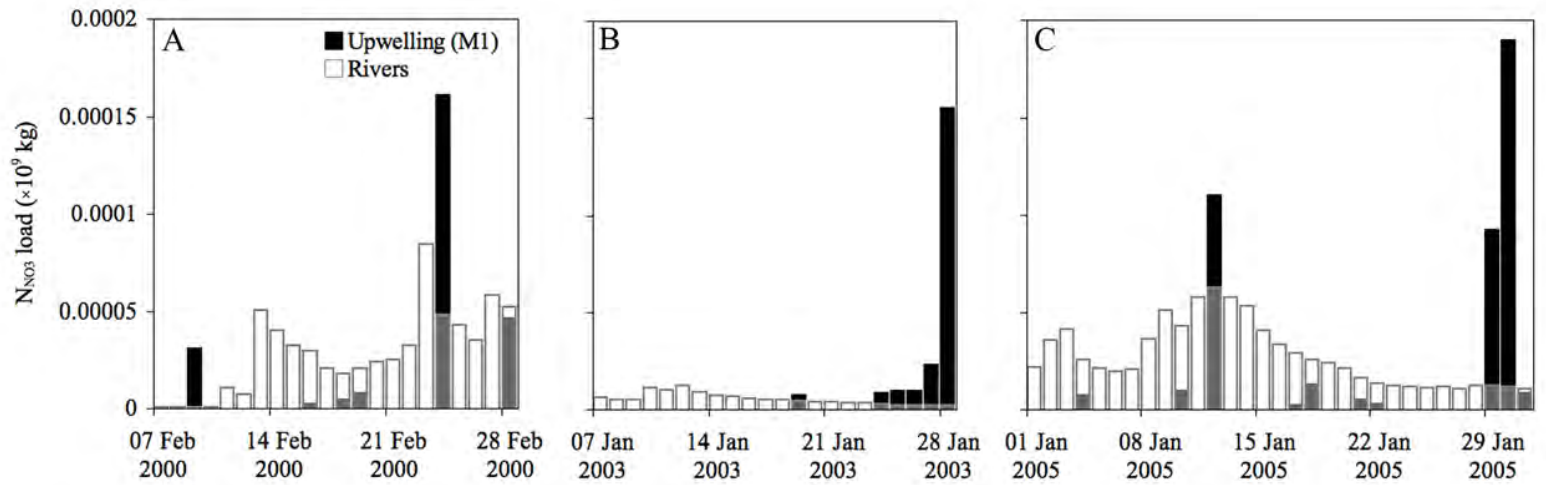


Figure 4

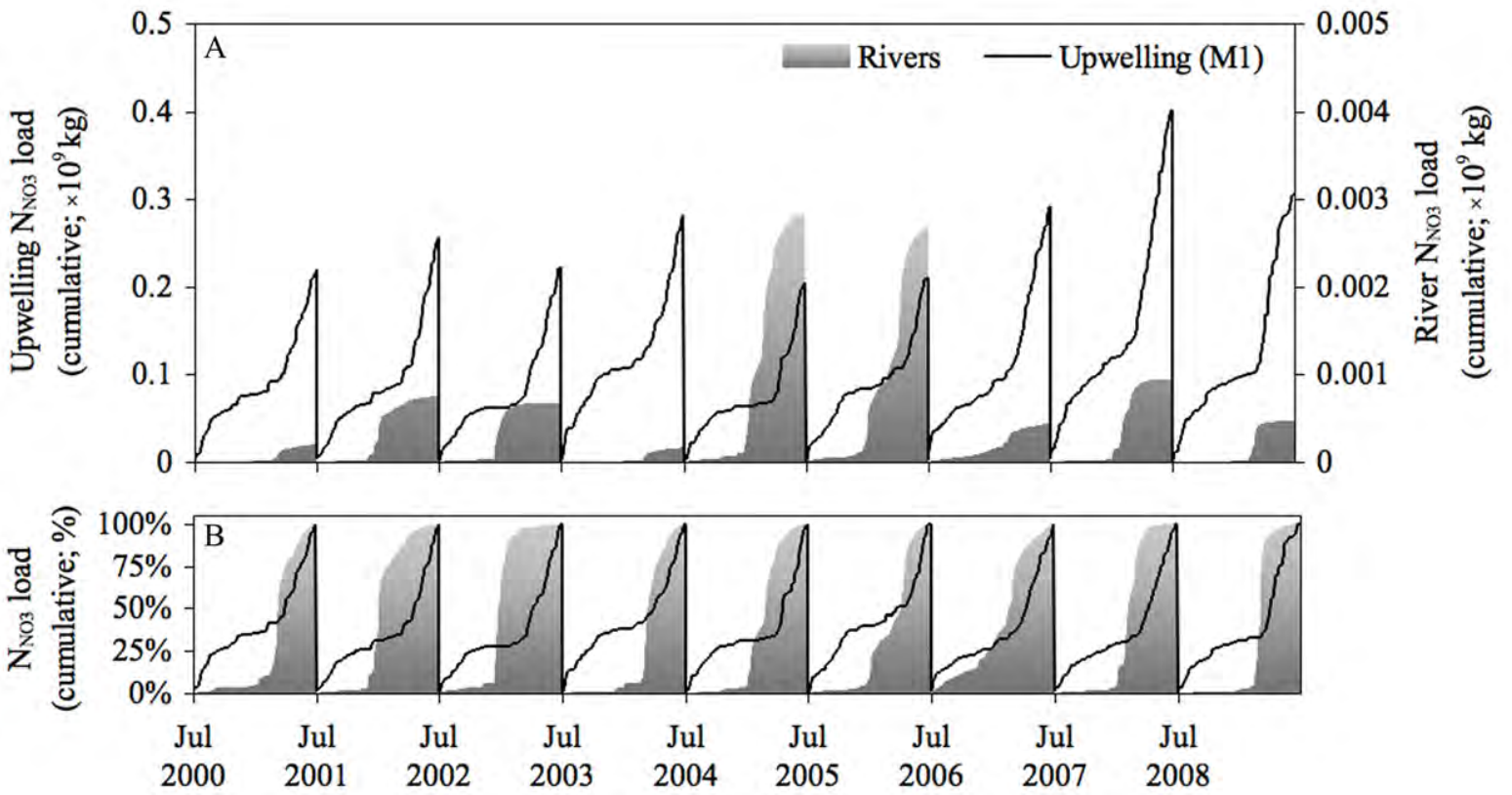


Figure 5

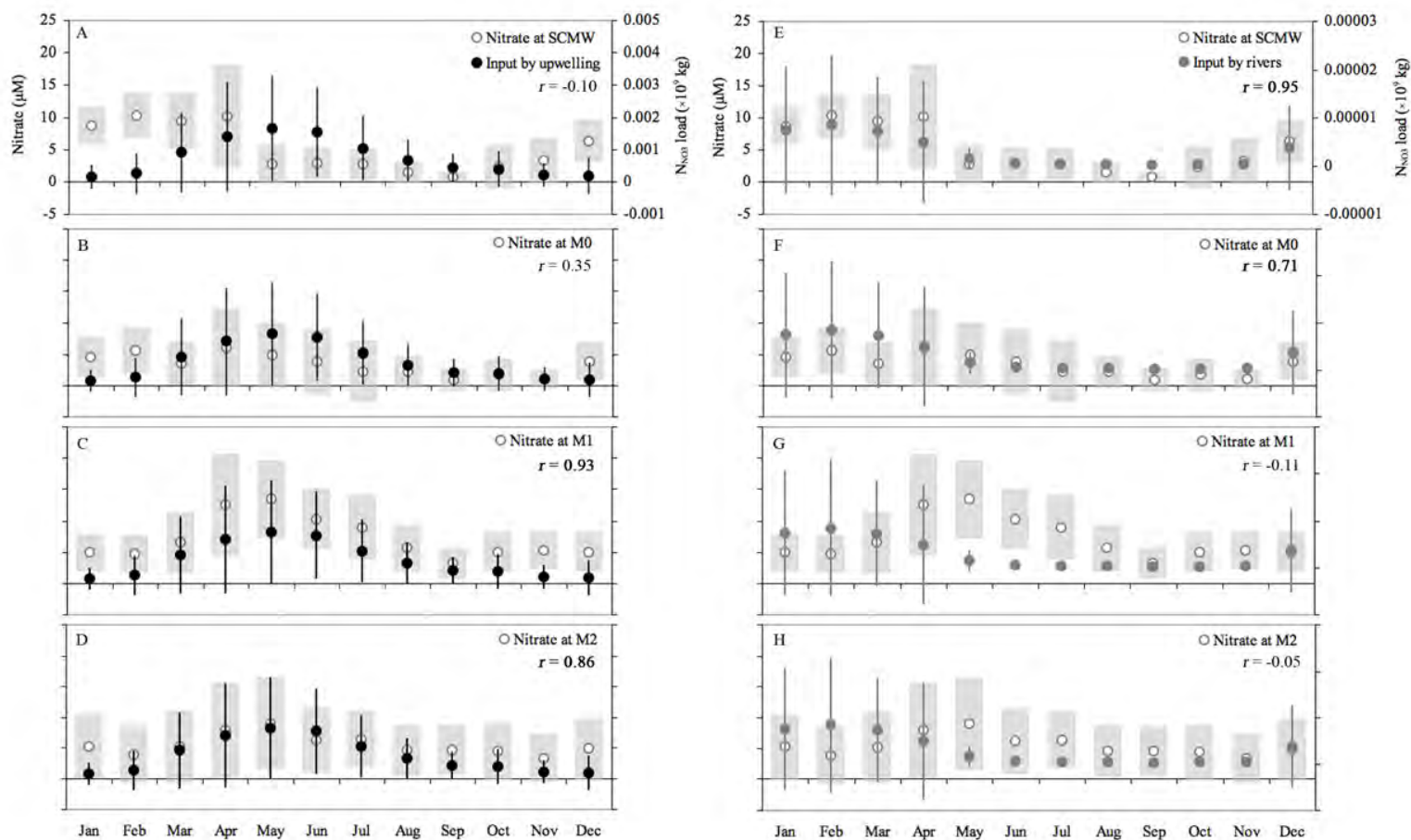


Figure 6

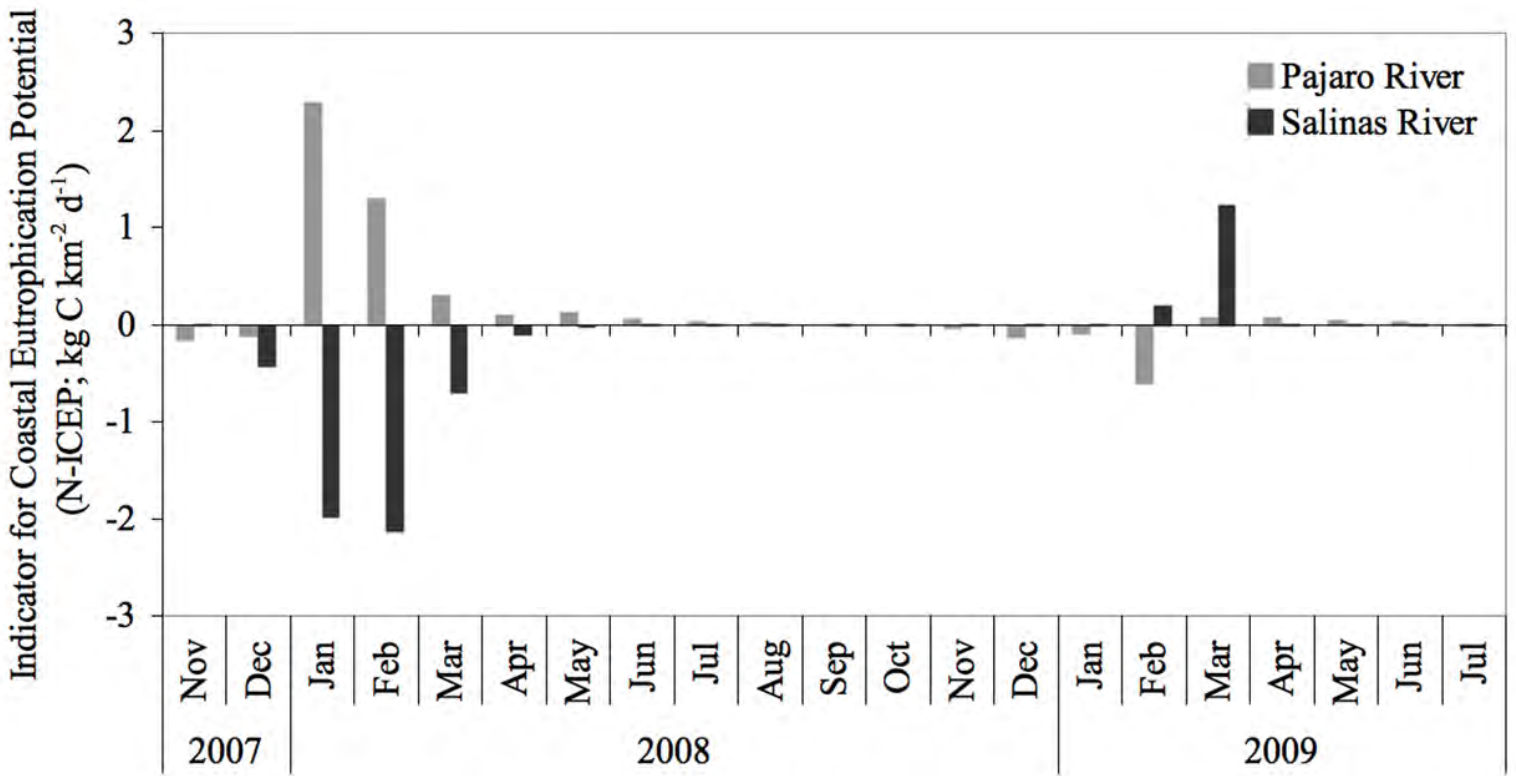
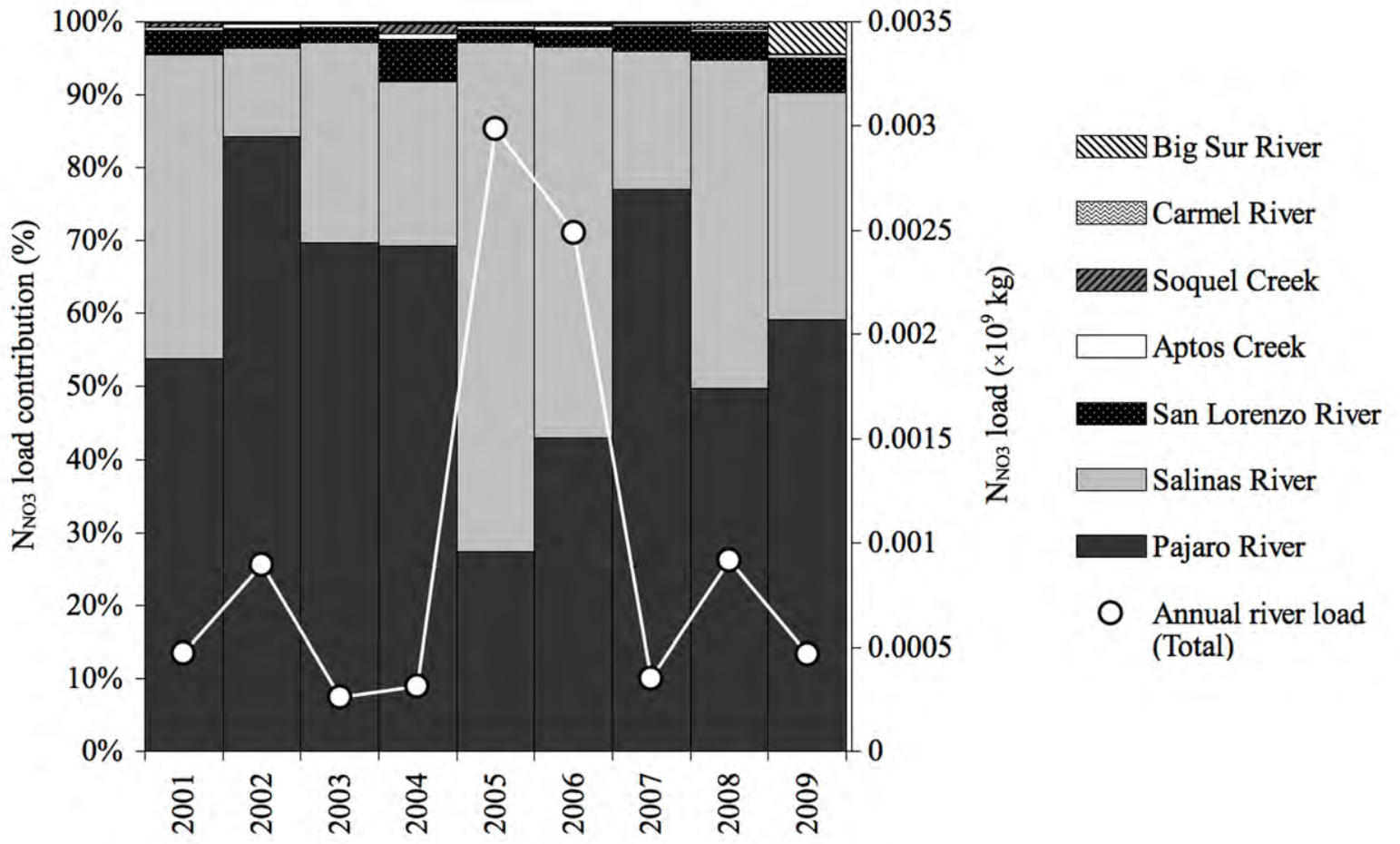
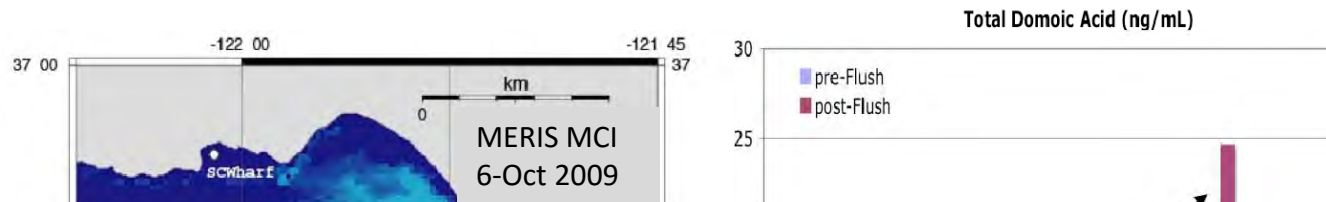


Figure 7

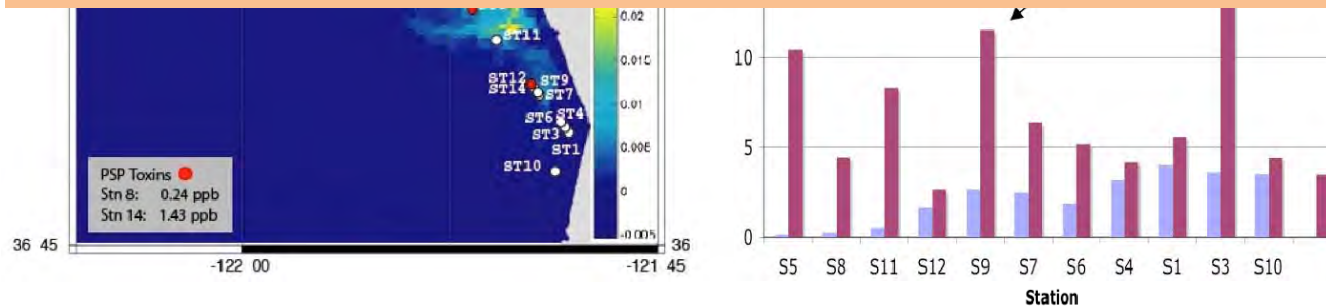


# Forecasting the Terrestrial Influence on Domoic Acid Production: A Mechanistic Approach

Clarissa Anderson, Chris Edwards, Nicole Goebel, and Raphe Kudela  
UC Santa Cruz



How well can we currently predict these Fall blooms?



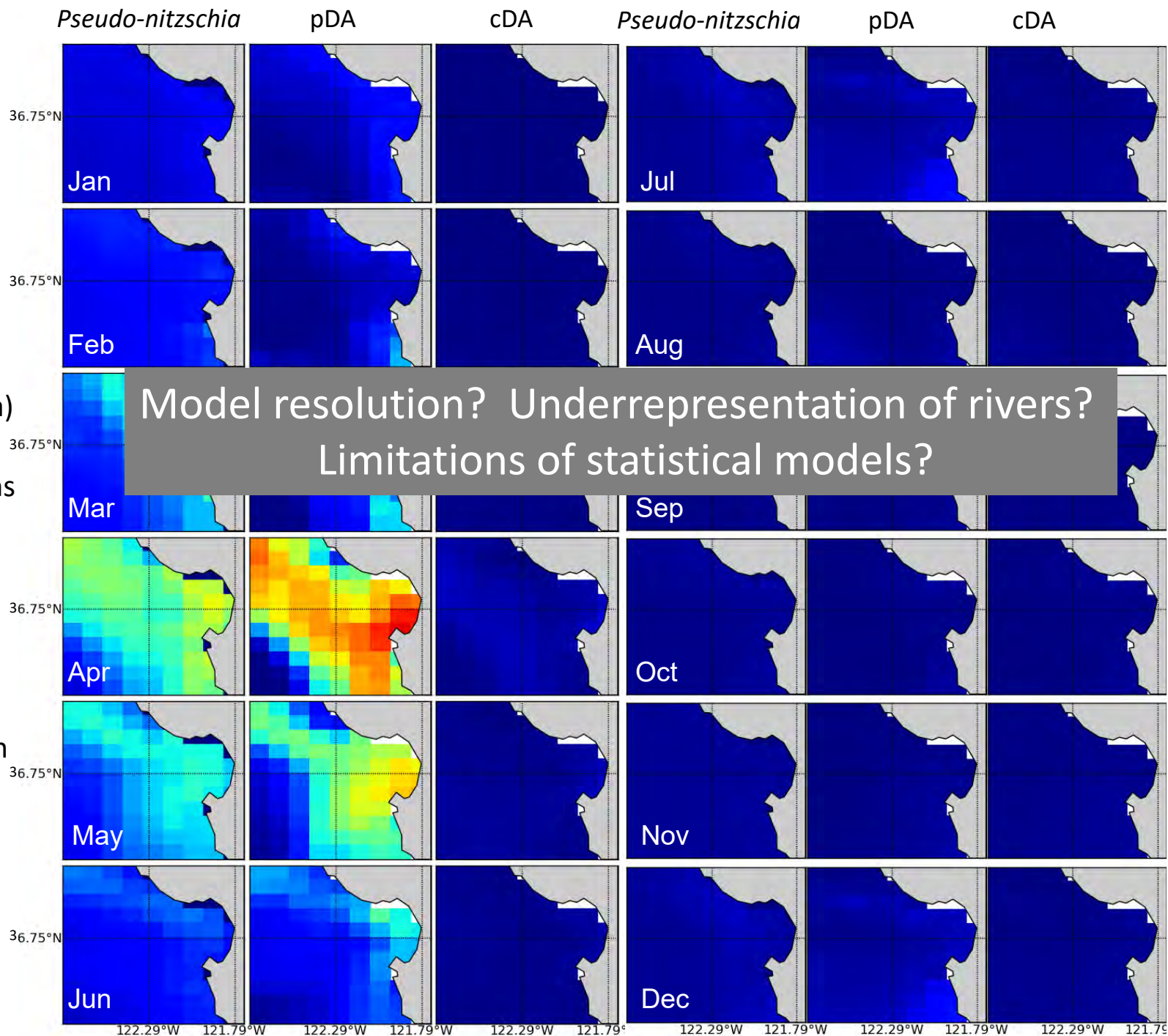
Field observations of increased domoic acid production by *Pseudo-nitzschia* following the FIRST FLUSH storm event of the rainy season

# 2008 Bloom Predictions

- ❖ NCOM CCS circulation model for MB coupled with modified CoSiNE and IOP module (Shulman & Penta)

- ❖ HAB predictions generated from statistical models forced with NCOM-COSiNE output

- ❖ Poor prediction of blooms and Domoic Acid in fall rainy season



# MODEL FORMULATION

What *does* a phytoplankton model look like anyway ???



$$\text{DA Production} = \alpha \mu P$$

$P$  = *Pseudo-nitzschia* biomass  
 $\mu$  = growth rate  
 $\alpha$  = DA production factor

$$\mu = \mu_{\max} * N_{\text{Lim}}$$

## Michaelis-Menten Nutrient Limitation

$$Si_{\text{Lim}} = Si(OH)_4 / [K_{Si} + Si(OH)_4]$$

$$NO_{3\text{Lim}} = NO_3 / [K_{NO3} + NO_3]$$

$$N_{\text{Lim}} = \min(NO_{3\text{Lim}}, Si_{\text{Lim}})$$

# MODEL FORMULATION

$$\text{DA Production} = \alpha \mu P$$

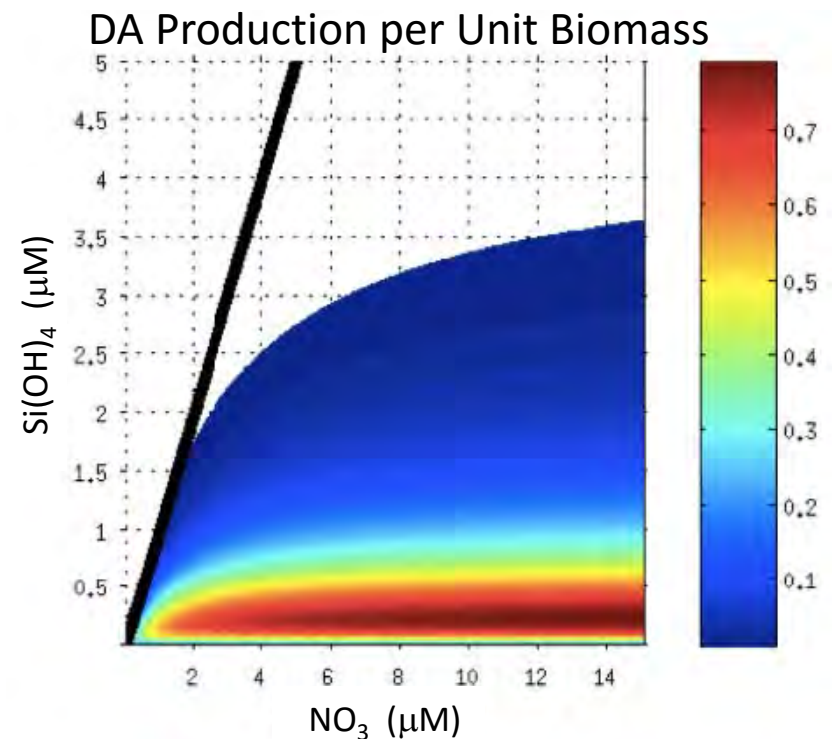
Based on results from statistical modeling exercises and laboratory experiments, we model DA production as a function of the Si:N ratio.

This can be tested with an adjustment to  $\alpha$ :

$$\alpha = (1 - \min(\text{SiLim}/\text{NO}_3\text{Lim}), 1)$$

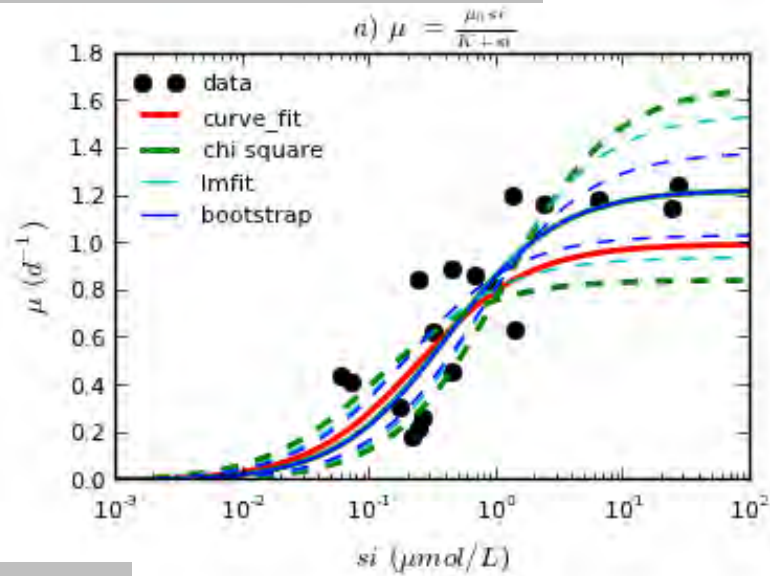
$\beta$  sets the maximum rate of DA production

$\gamma$  determines rate at which DA production declines with increasing Si levels

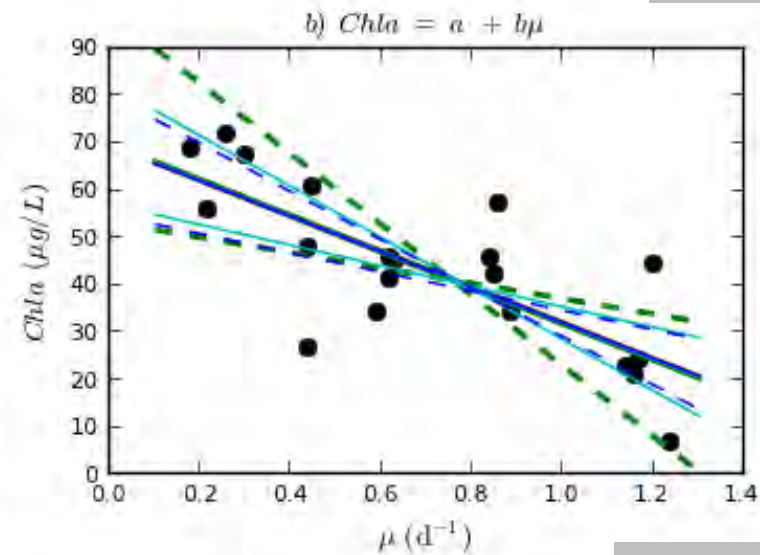


# FITTING MODEL TO CHEMOSTAT DATA

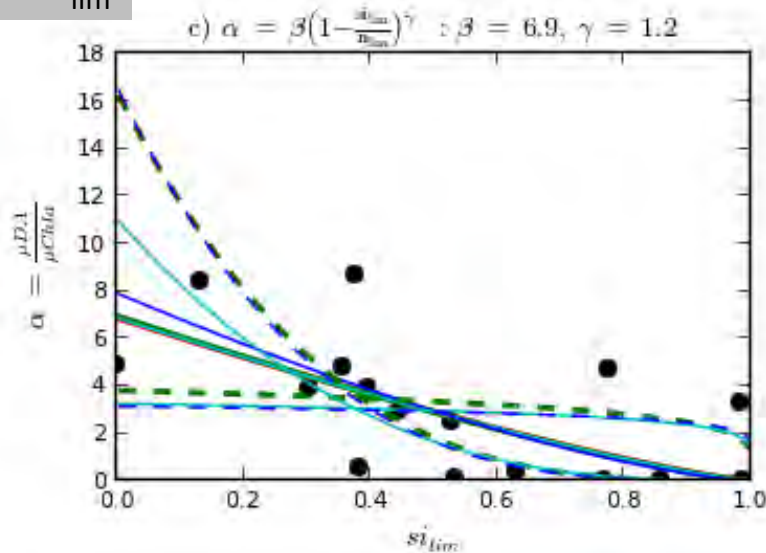
Michaelis-Menten Model for  $\mu$



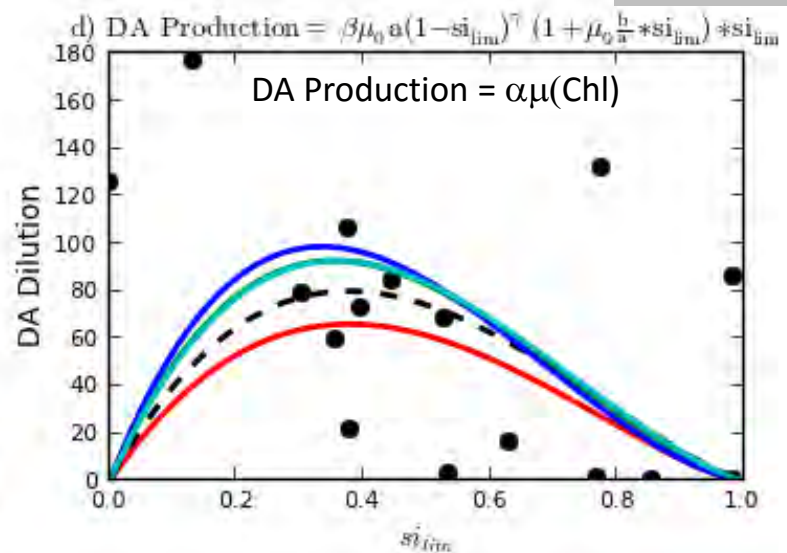
Chl-*a* vs.  $\mu$



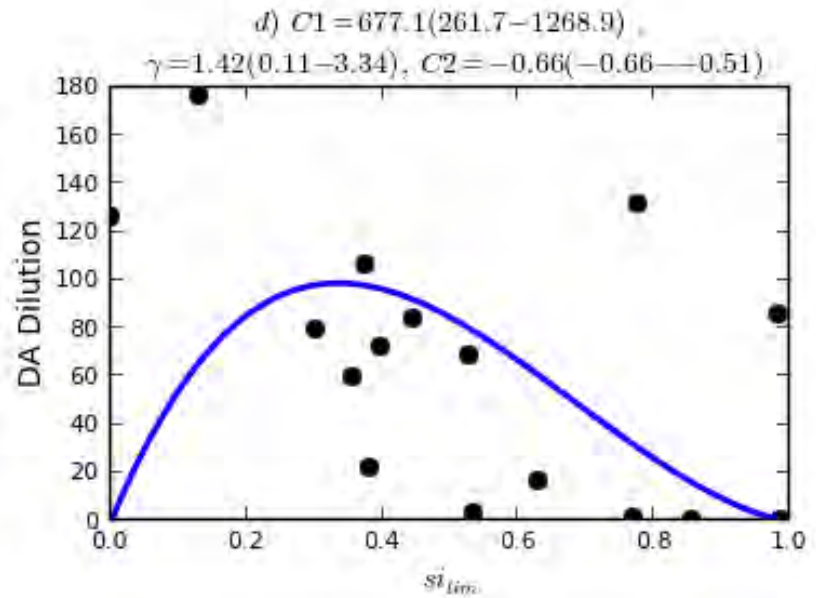
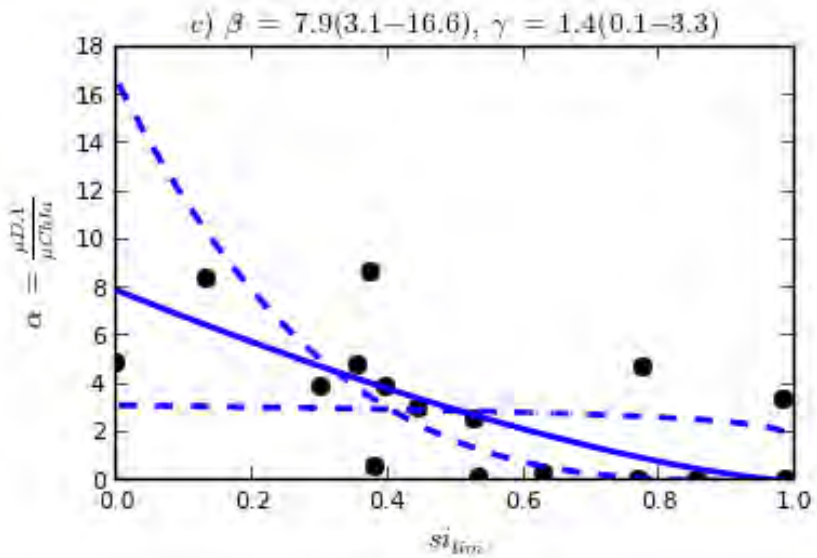
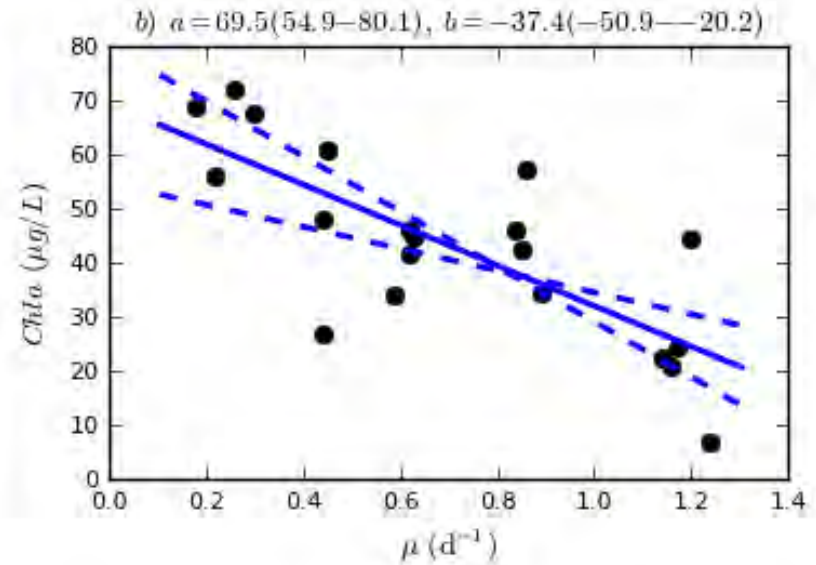
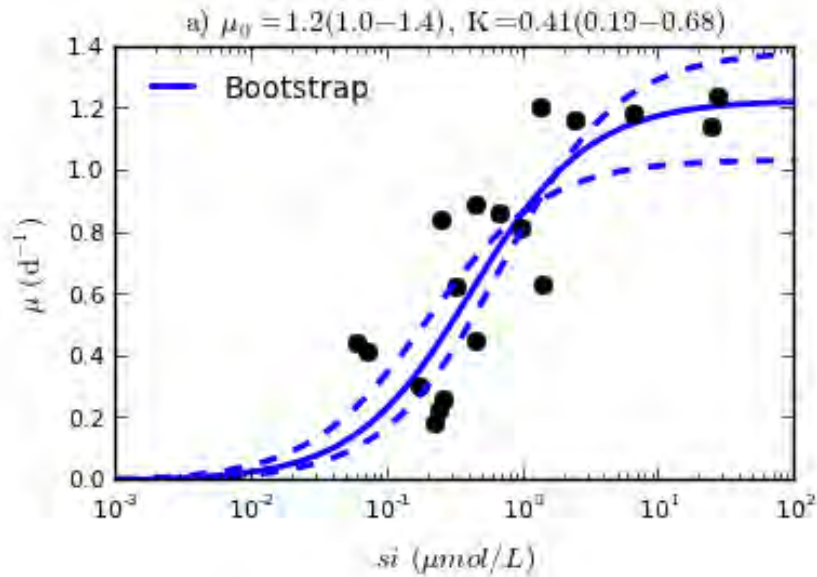
$\alpha$  vs.  $Si_{lim}$



DA vs.  $Si_{lim}$



# BOOTSTRAP PARAMETERIZATION LOOKED BEST!



1000 iterations



## Factors controlling the production of domoic acid by *Pseudo-nitzschia* (Bacillariophyceae): A model study

Nathan Terseleer\*, Nathalie Gypens, Christiane Lancelot

Université Libre de Bruxelles, Écologie des Systèmes Aquatiques, CP-221, Bd du Triomphe, B-1050 Brussels, Belgium

### ARTICLE INFO

#### Article history:

Received 28 June 2012

Received in revised form 28 January 2013

Accepted 28 January 2013

#### Keywords:

Harmful algal blooms

*Pseudo-nitzschia*

Domoic acid

Mechanistic modelling

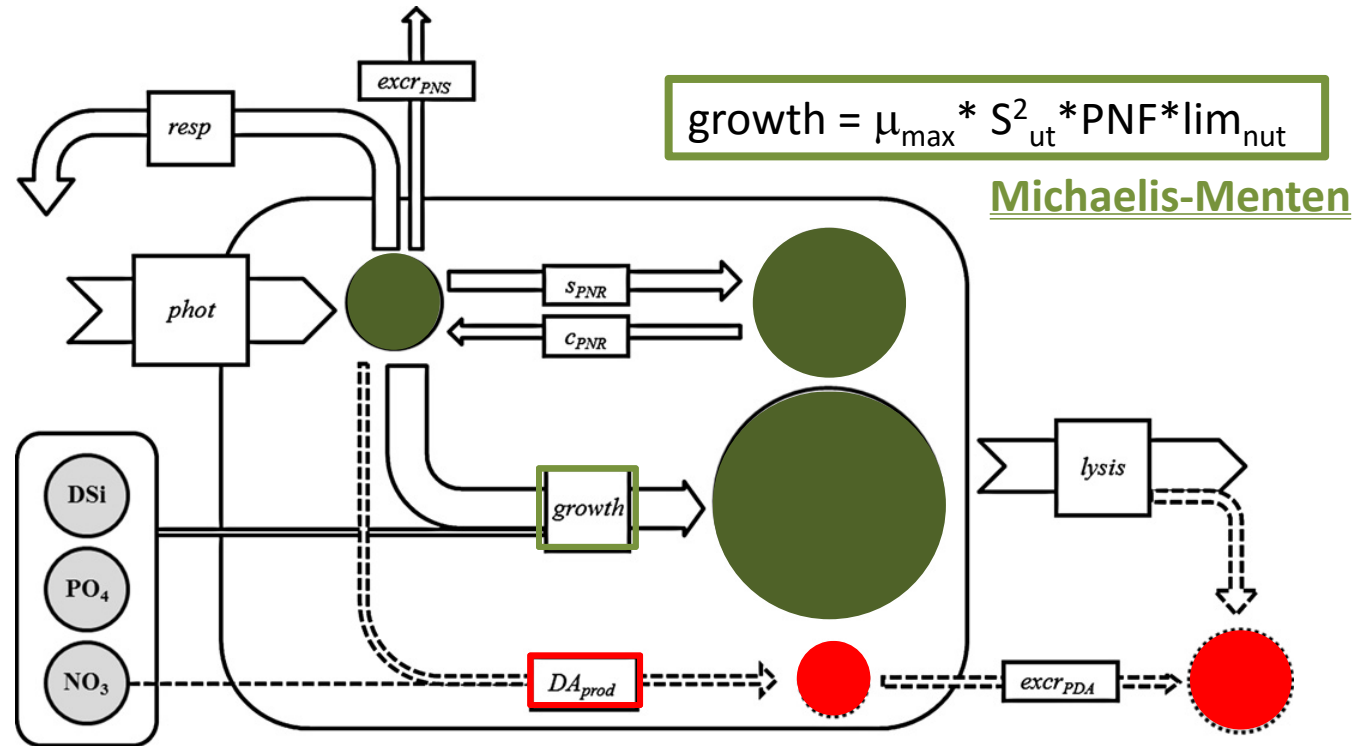
### ABSTRACT

A mechanistic model has been developed to explore the factors controlling the production of domoic acid (DA) by the pennate diatom *Pseudo-nitzschia*. The idealized model allows consideration of the uncoupling between photosynthesis and growth, while DA production has been set as a secondary metabolism sharing common precursors with growth. Under growth limitation, these precursors can accumulate, resulting in an increased DA production. The model was first evaluated based on its ability to simulate the observed DA production by either silicon (Si) or phosphorus (P) limited batch cultures of *Pseudo-nitzschia* available in the literature. Sensitivity tests were further performed to explore how the ambient nutrients and the light regime (intensity and photoperiod length) are possibly directing the *Pseudo-nitzschia* toxicity. The general pattern that emerged is that excess light, in combination with Si or P limitation, favours DA production, provided nitrogen (N) is sufficient. Model simulations with varying nutrient stocks supporting *Pseudo-nitzschia* blooms under non-limiting light suggest two potential ways for nutrients to control DA production. First, N excess in comparison to available Si and P relieves DA production from its limitation by N, an absolute requirement of the DA molecule. Second, increased nutrient stocks amplify the DA production phase of the blooms (in addition to enhancing *Pseudo-nitzschia* biomass) which leads to an even more toxigenic bloom. Simulations investigating the light regime suggest a light threshold below which an important delay in DA production could be expected in *Pseudo-nitzschia* cultures. In the natural environment, the monitoring of light conditions during *Pseudo-nitzschia* blooms might help to anticipate the magnitude of the toxic event. *Pseudo-nitzschia* toxicity is indeed linked to the excess of primary carbon that accumulates during photosynthesis under growth limitation by nutrients.

© 2013 Elsevier B.V. All rights reserved.

# Terseleer Model

$$DA_{prod} = k_{DA} * PNS * lim_N$$



**PNS:** Precursors to macromolecule Synthesis

$$\frac{dPNS}{dt} = phot - growth - resp - lysis_{PNS} - lysis_{PNS} - excr_{PNS} - S_{PNR} + C_{PNR} - DA_{prod}$$

**PNF:** Structural & Functional Macromolecules

$$\frac{dPNF}{dt} = growth - lysis_{PNF}$$

**PNR:** Reserves (polysaccharides/lipids)

$$\frac{dPNR}{dt} = S_{PNR} - C_{PNR} - lysis_{PNR}$$

**PDA:** Intracellular (Particulate) Domoic Acid

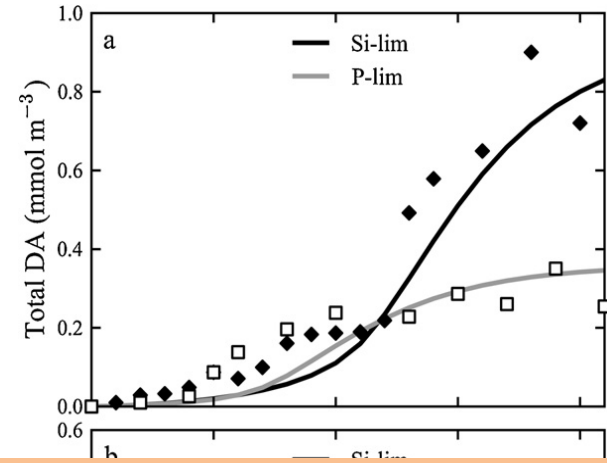
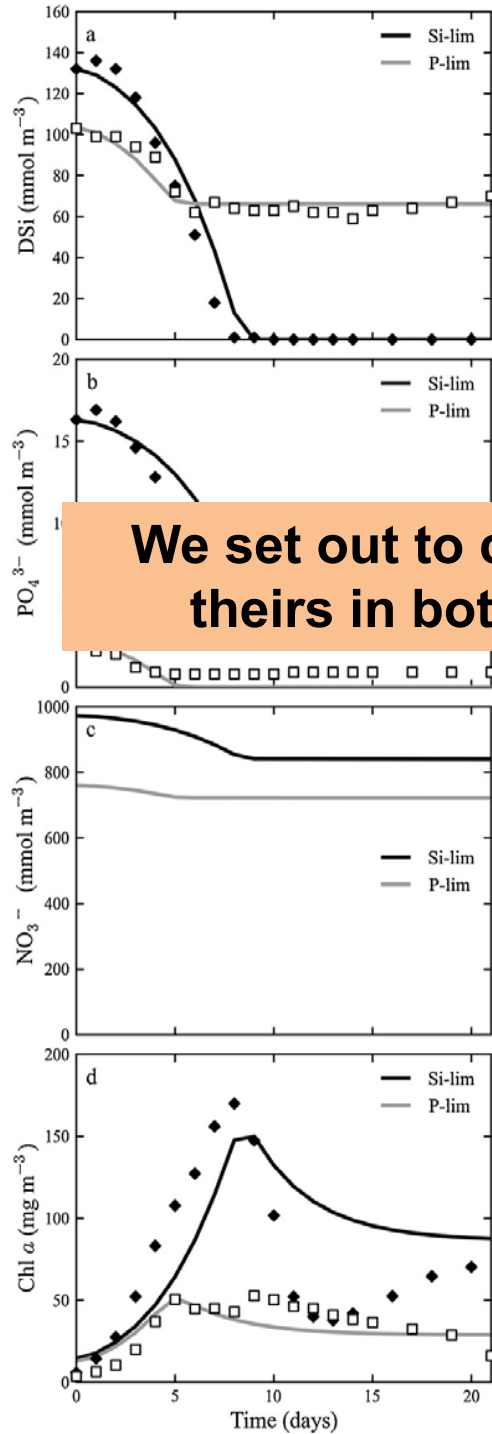
$$\frac{dPDA}{dt} = DA_{prod} - excr_{PDA} - lysis_{PDA}$$

**DDA:** Extracellular (Dissolved) Domoic Acid

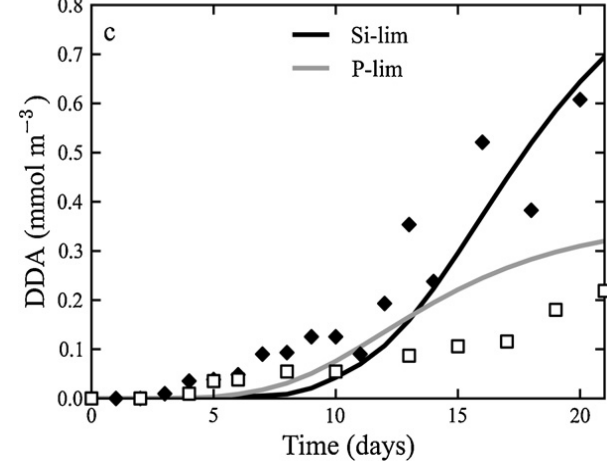
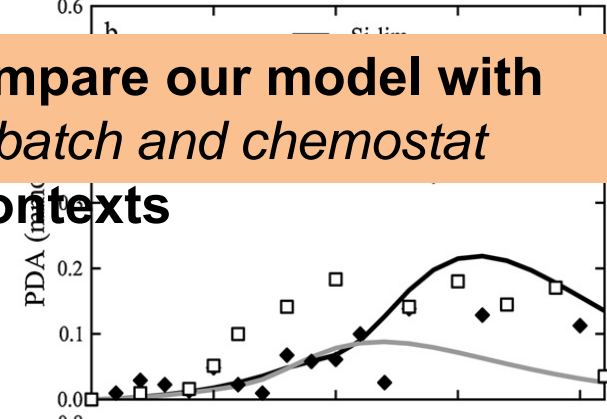
$$\frac{dDDA}{dt} = excr_{PDA} + lysis_{PDA}$$

# Terseleer Model Results

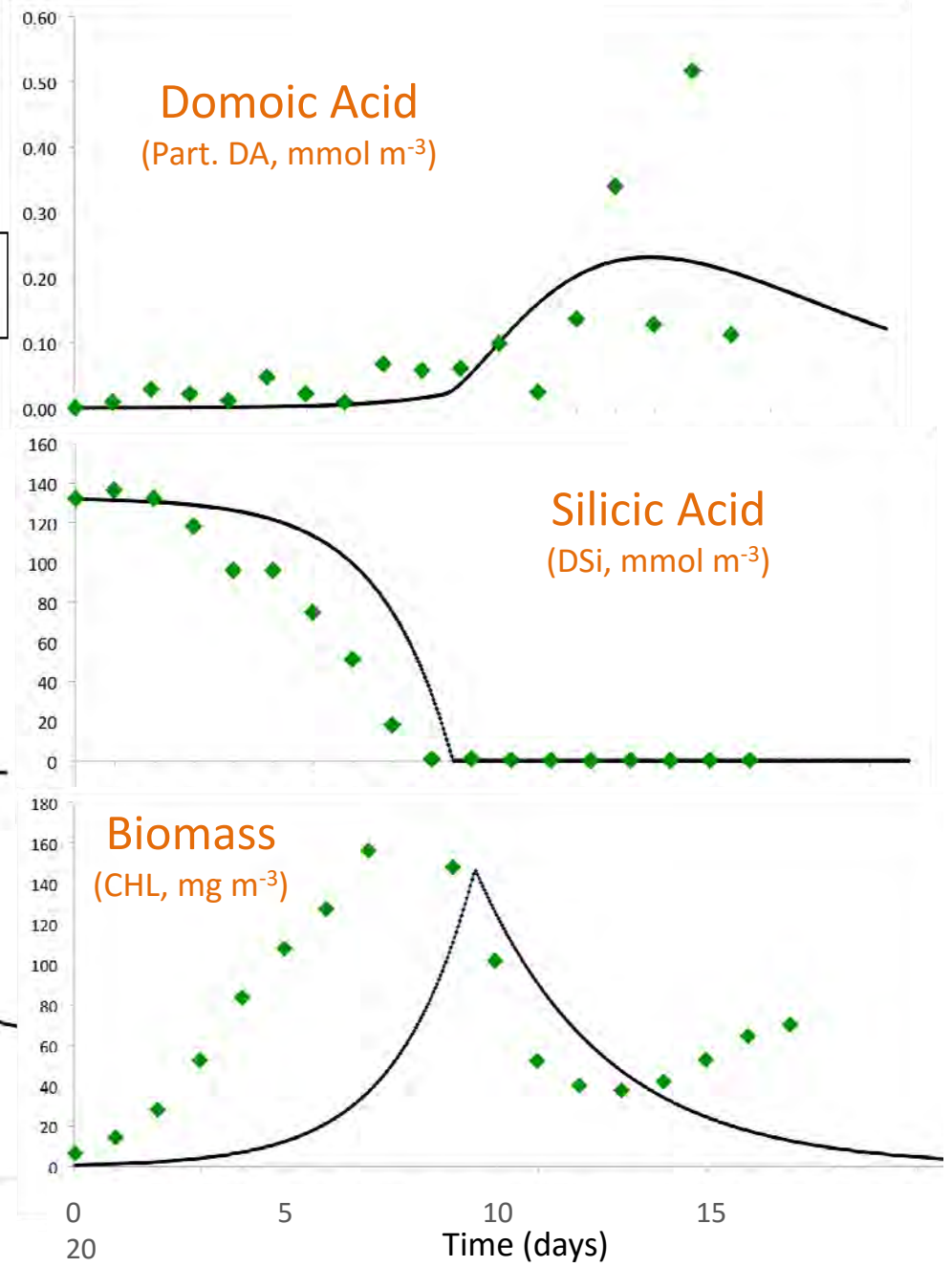
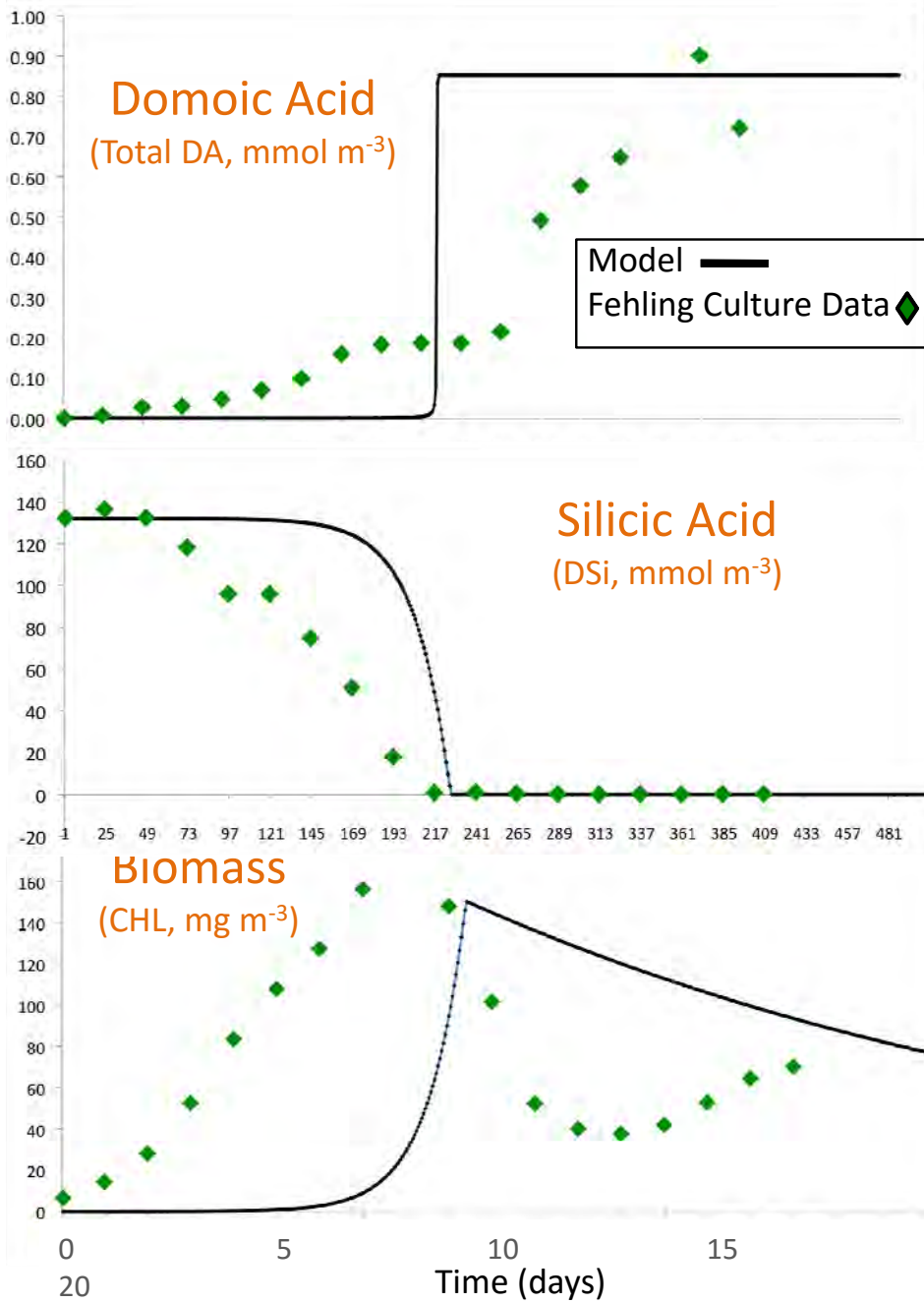
They compared their model with Si-limited and P-limited batch culture data for *P. seriata* from Fehling et al. (2004)

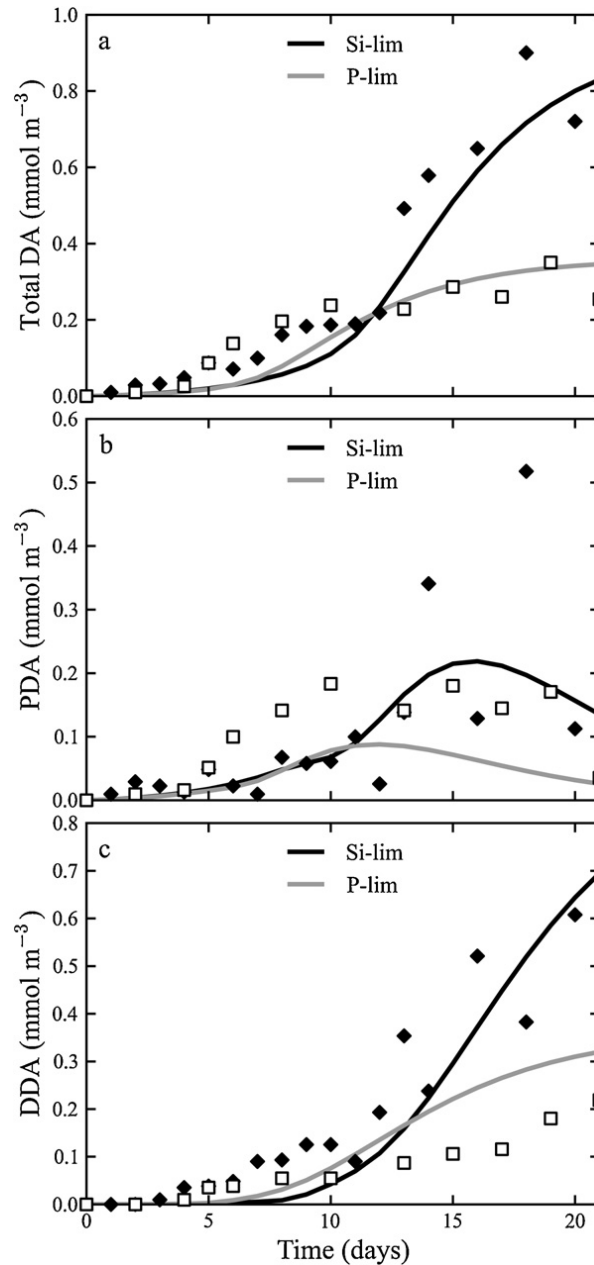
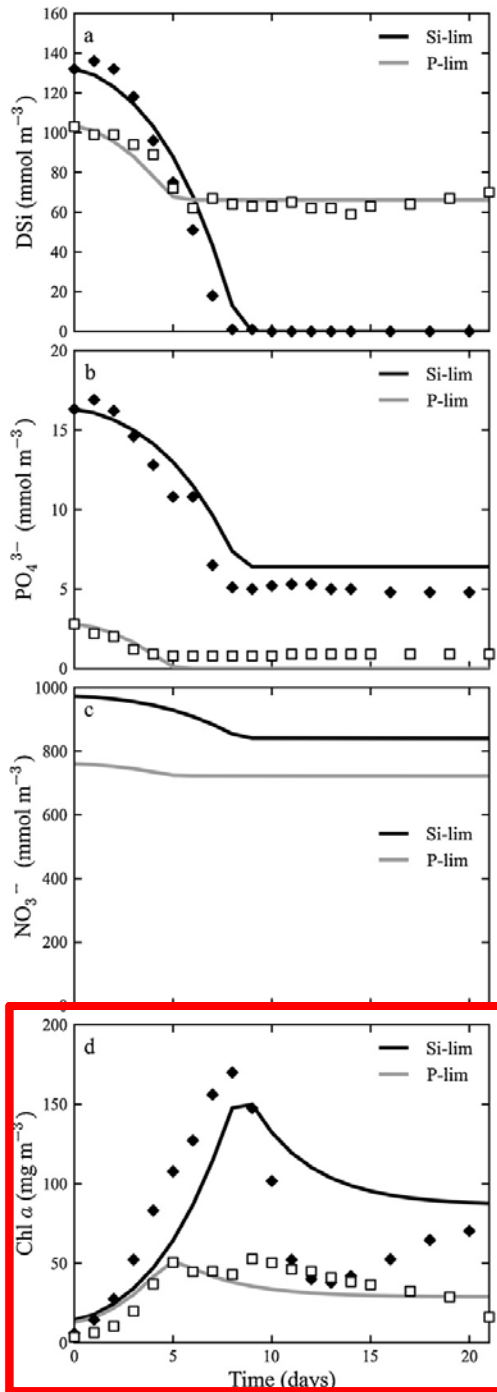


**We set out to compare our model with theirs in both *batch and chemostat* contexts**



Our MODEL \*\*\*\*\* BATCH CULTURE TEST \*\*\*\*\* Terseleer MODEL





## Terseleer MODEL

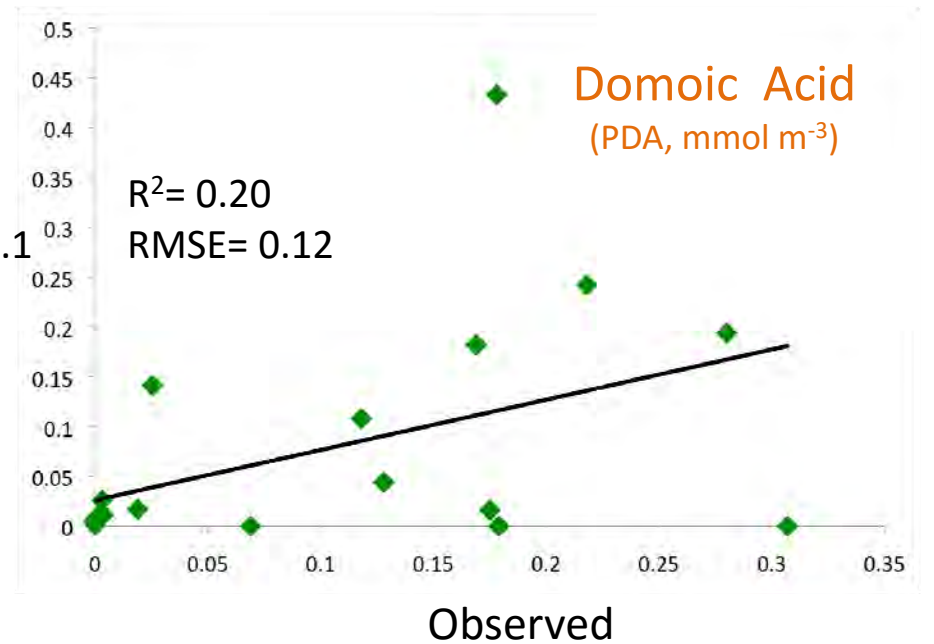
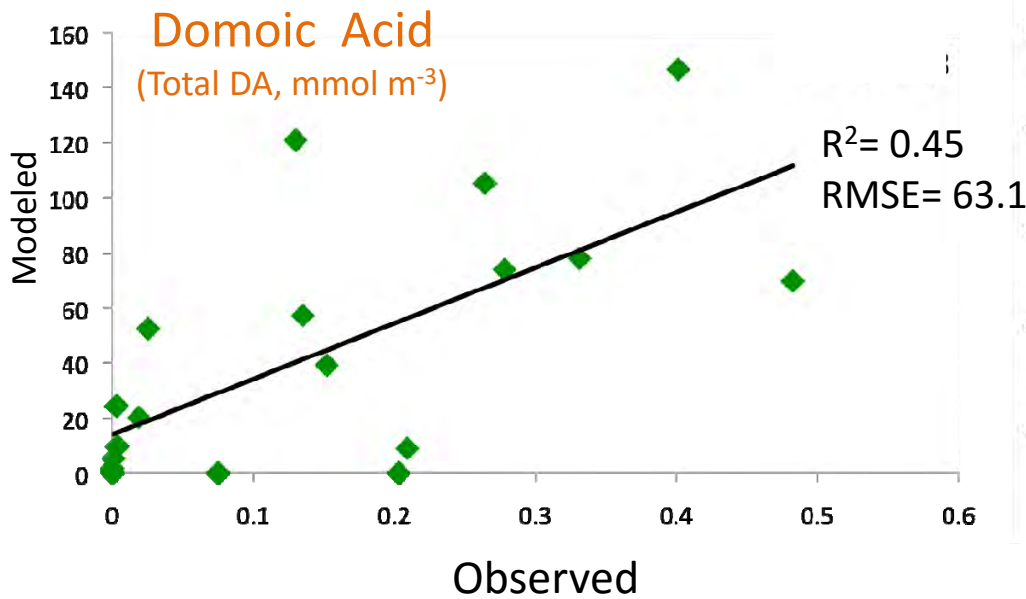
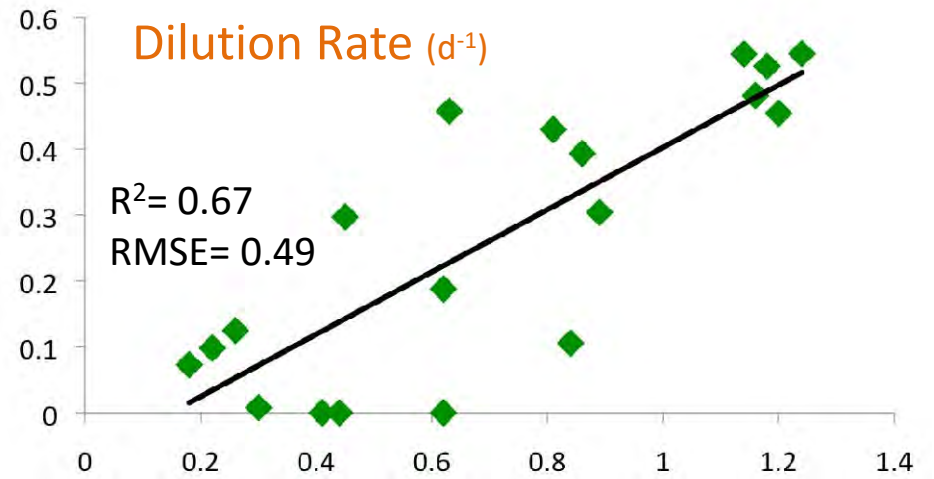
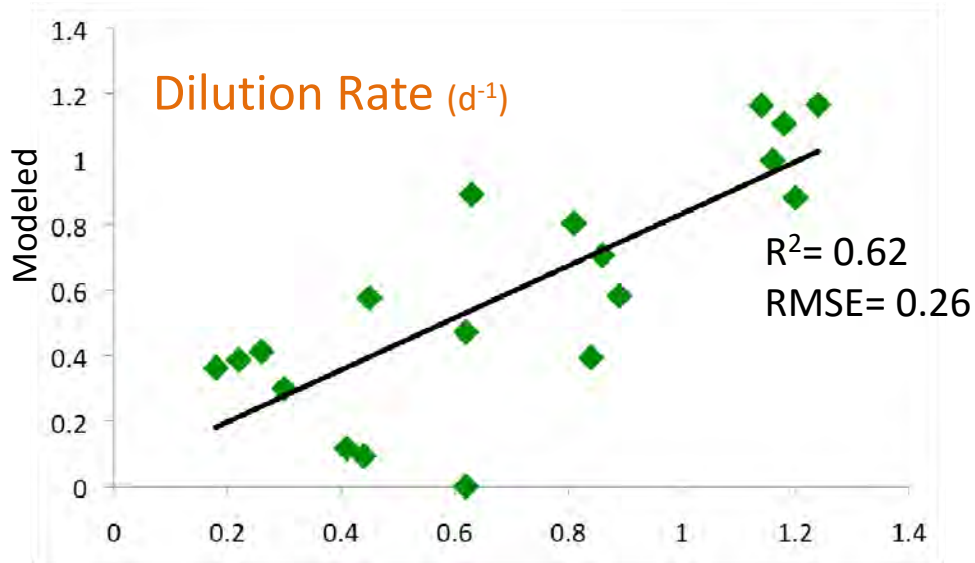
**Chlorophyll:**  
*better model fit shown in their paper*

*We could not reproduce their model 100% accurately*

*Initial conditions?*

Our MODEL \*\*\*\*\* CHEMOSTAT TEST (n=18) \*\*\*\*\* Terseleer MODEL  
 BOOTSTRAPPED PARAMETERS

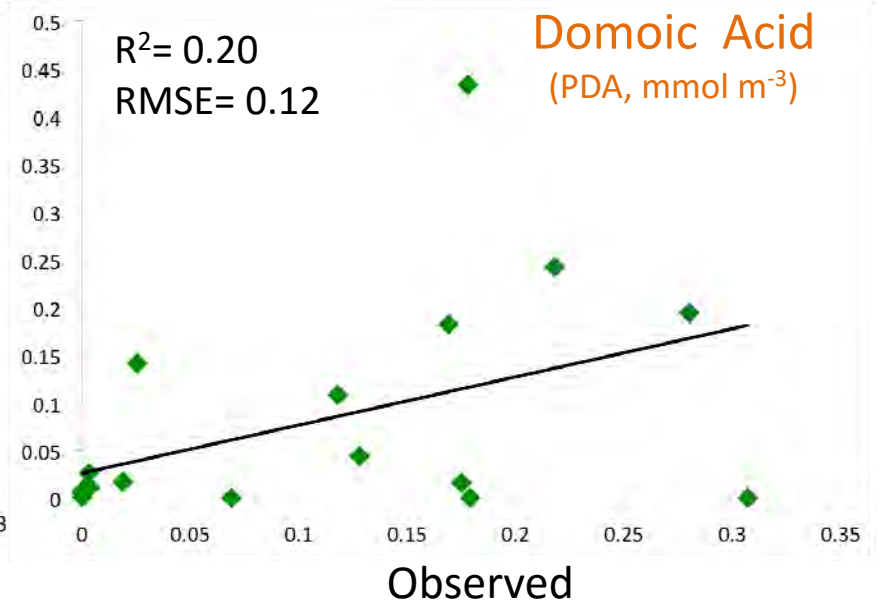
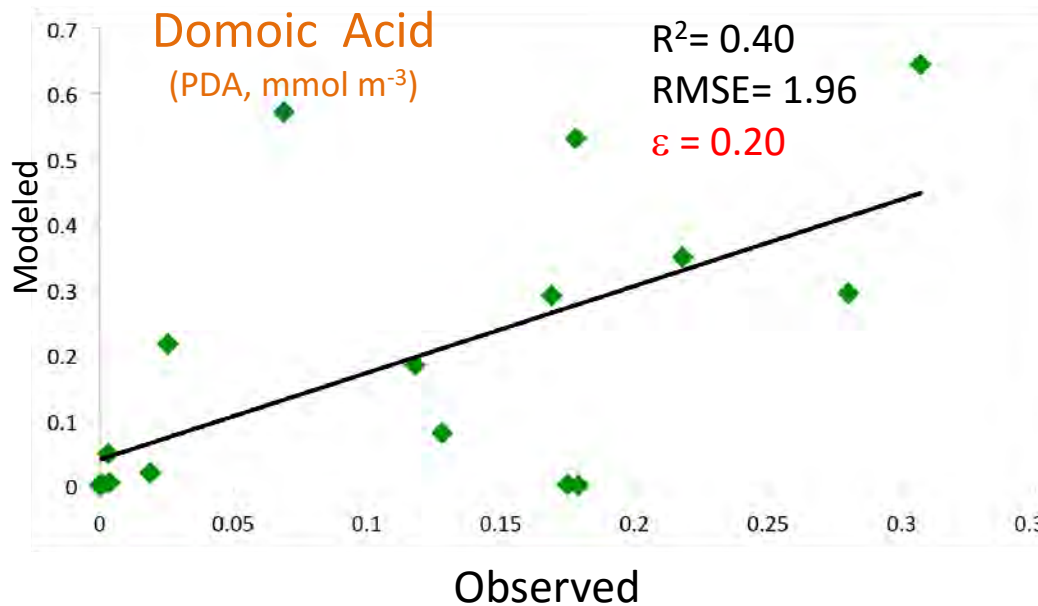
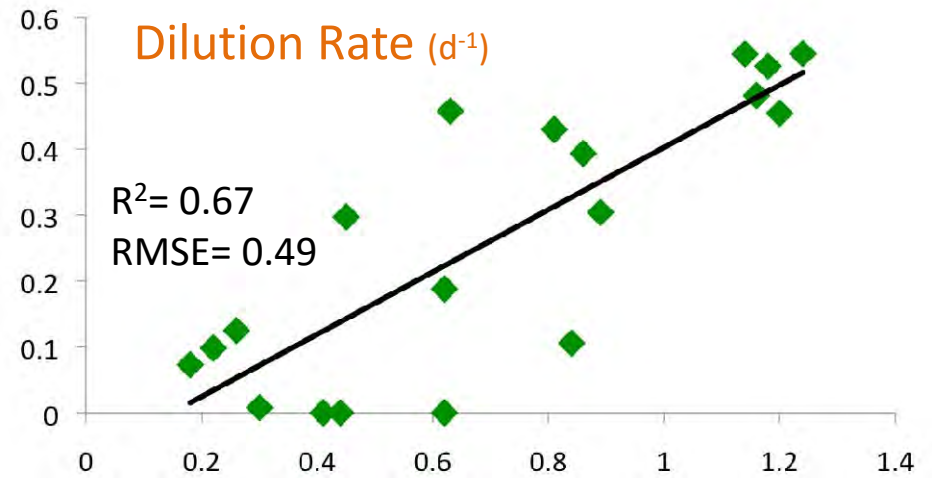
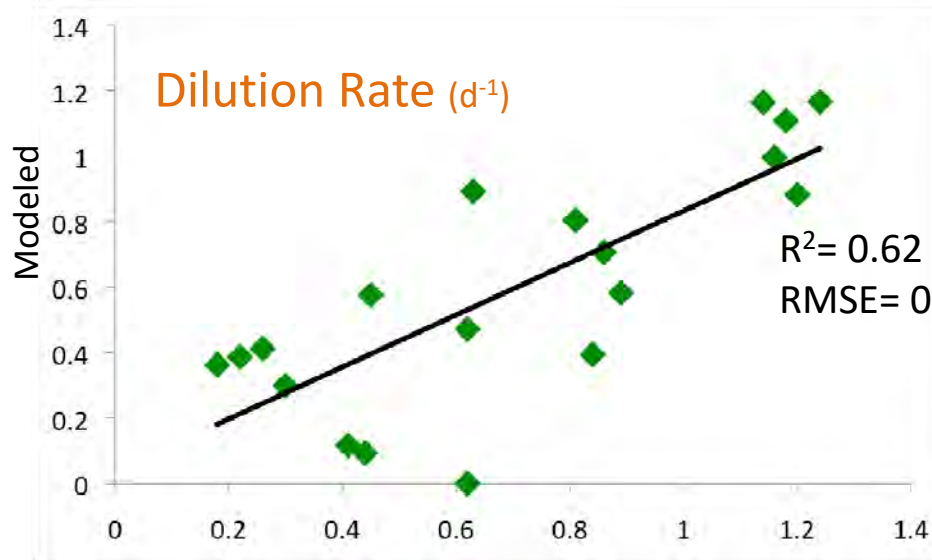
dN/dt=0 DA Loss =0 dil rate = *mod dil*



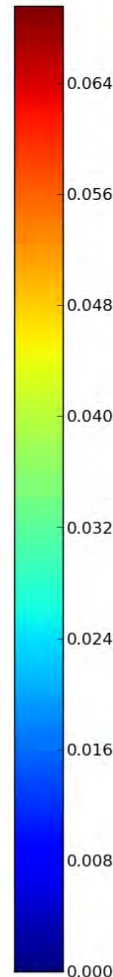
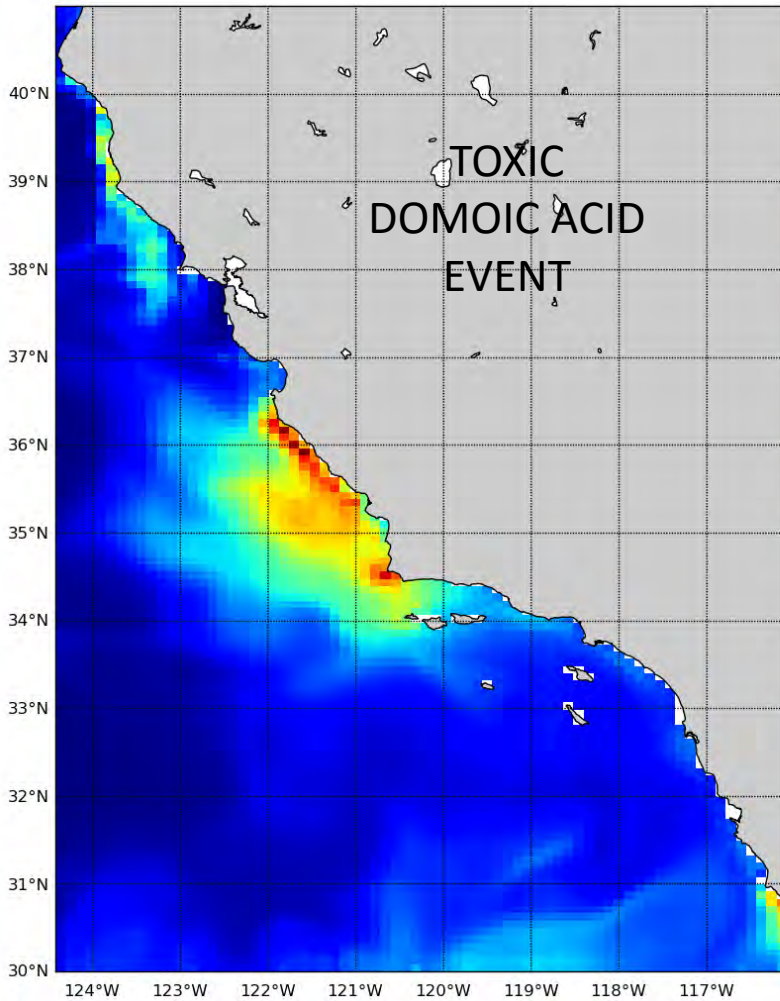
Our MODEL \*\*\*\*\* CHEMOSTAT TEST (n=18) \*\*\*\*\* Terseleer MODEL

MANUAL ADJUSTMENT TO PARAMETERS ( $\beta$ ,  $\gamma$ )

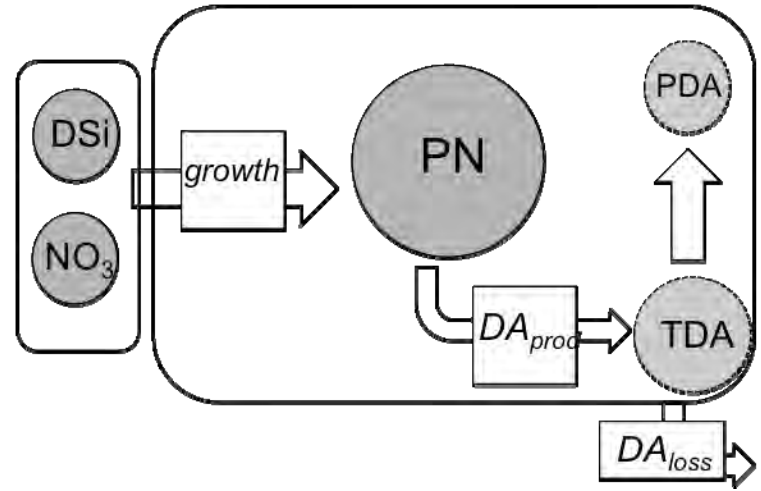
$dN/dt=0$   $DA_{loss} = \epsilon DA_{prod}$  dil rate = *mod dil*



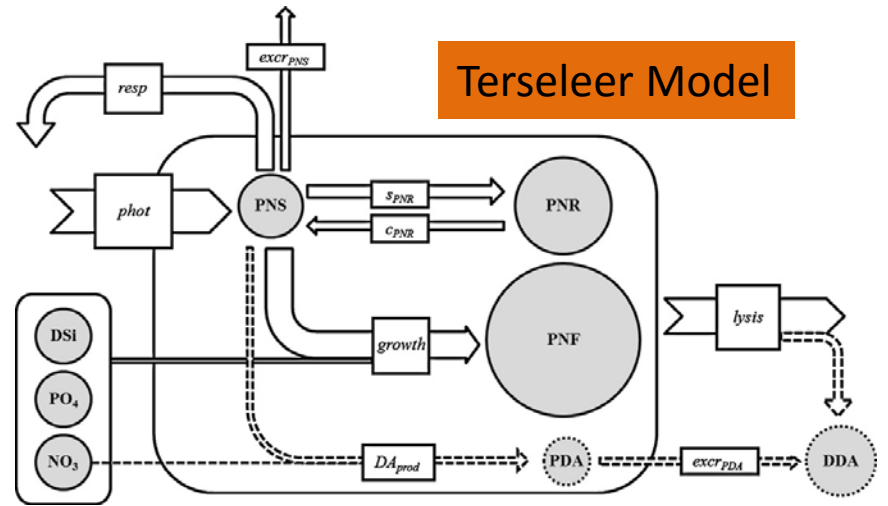
**END GOAL:** Create realistic simulations of DA events in coastal California -  
Is more model complexity really better?



**Our Model**



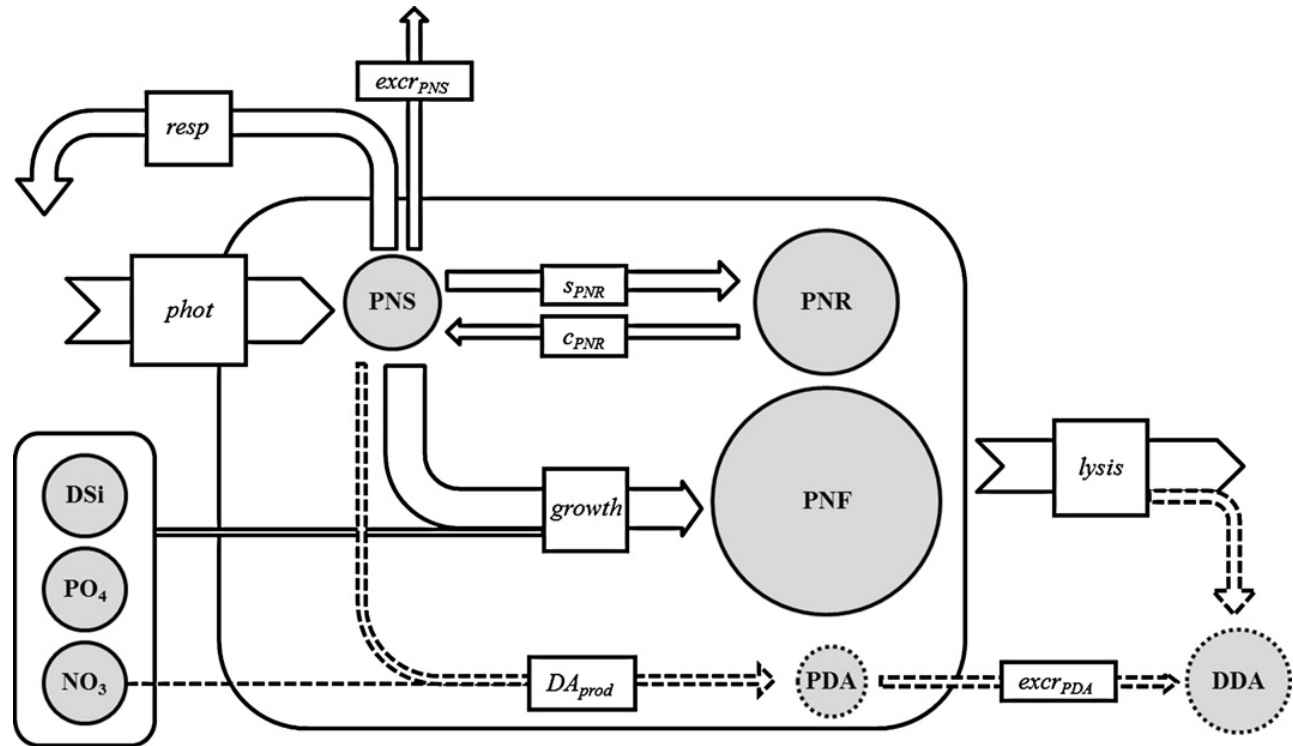
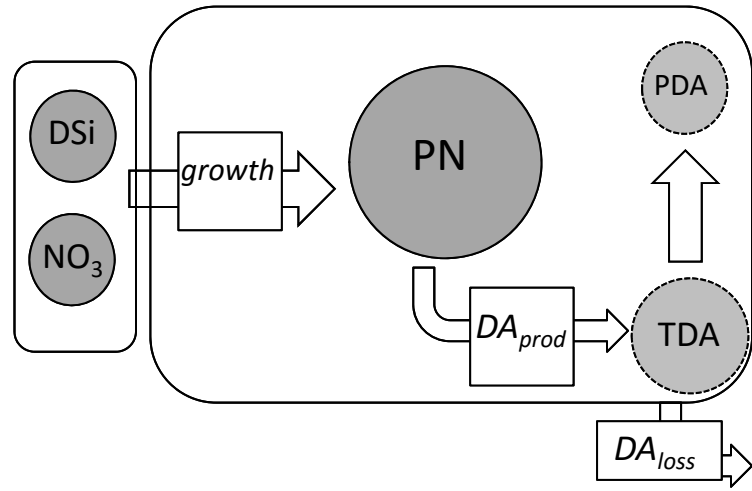
**Terseleer Model**



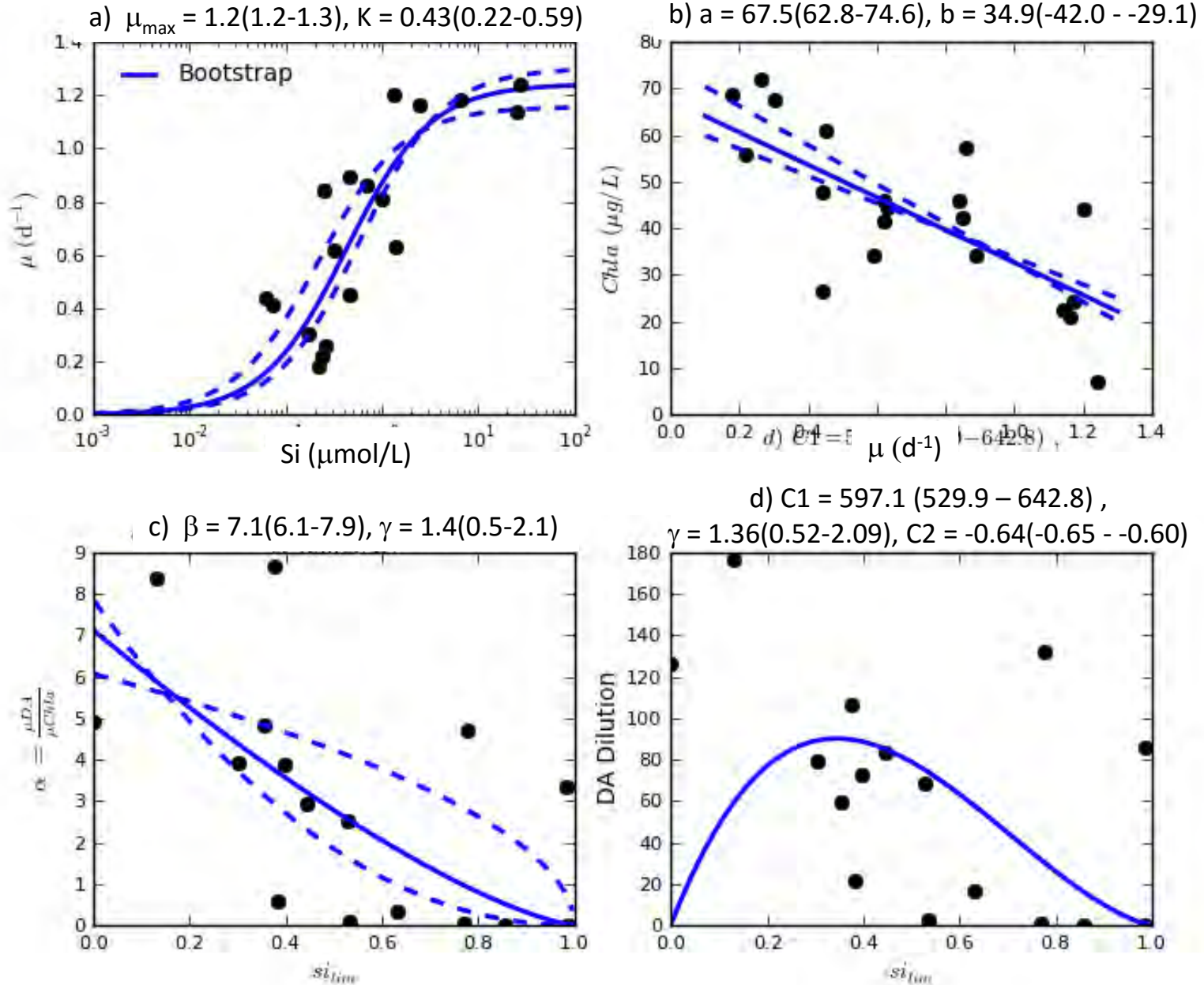
*THANK YOU, EPOC!*

FUNDING:  
Packard Foundation  
CA Sea Grant New Investigator Award





# BOOTSTRAP PARAMETERIZATION LOOKED BEST!



## Anthropogenic nutrient sources rival natural sources on small scales in the coastal waters of the Southern California Bight

Meredith D. A. Howard,<sup>1,\*</sup> Martha Sutula,<sup>1</sup> David A. Caron,<sup>2</sup> Yi Chao,<sup>3,a</sup> John D. Farrara,<sup>3</sup> Hartmut Frenzel,<sup>4,b</sup> Burton Jones,<sup>2,c</sup> George Robertson,<sup>5</sup> Karen McLaughlin,<sup>1</sup> and Ashmita Sengupta<sup>1</sup>

<sup>1</sup>Southern California Coastal Water Research Project, Costa Mesa, California

<sup>2</sup>Department of Biological Sciences, University of Southern California, Los Angeles, California

<sup>3</sup>Joint Institute for Regional Earth System Science and Engineering, University of California, Los Angeles, Los Angeles, California

<sup>4</sup>Department of Atmospheric and Oceanic Sciences, University of California, Los Angeles, Los Angeles, California

<sup>5</sup>Orange County Sanitation District, Fountain Valley, California

### Abstract

Anthropogenic nutrients have been shown to provide significant sources of nitrogen (N) that have been linked to increased primary production and harmful algal blooms worldwide. There is a general perception that in upwelling regions, the flux of anthropogenic nutrient inputs is small relative to upwelling flux, and therefore anthropogenic inputs have relatively little effect on the productivity of coastal waters. To test the hypothesis that natural sources (e.g., upwelling) greatly exceed anthropogenic nutrient sources to the Southern California Bight (SCB), this study compared the source contributions of N from four major nutrient sources: (1) upwelling, (2) treated wastewater effluent discharged to ocean outfalls, (3) riverine runoff, and (4) atmospheric deposition. This comparison was made using large regional data sets combined with modeling on both regional and local scales. At the regional bight-wide spatial scale, upwelling was the largest source of N by an order of magnitude to effluent and two orders of magnitude to riverine runoff. However, at smaller spatial scales, more relevant to algal bloom development, natural and anthropogenic contributions were equivalent. In particular, wastewater effluent and upwelling contributed the same quantity of N in several subregions of the SCB. These findings contradict the currently held perception that in upwelling-dominated regions anthropogenic nutrient inputs are negligible, and suggest that anthropogenic nutrients, mainly wastewater effluent, can provide a significant source of nitrogen for nearshore productivity in Southern California coastal waters.

Eutrophication of coastal waters has greatly increased in the last several decades throughout the world, with demonstrated linkages to anthropogenic nutrient loads (*see reviews* Howarth 2008; Paerl and Piehler 2008). Human population growth, development of coastal watersheds, agricultural and aquaculture runoff into the coastal oceans, and burning of fossil fuels are among the many factors contributing to increased eutrophication of coastal waters (Anderson et al. 2002; Howarth 2008). Anthropogenic inputs of agricultural runoff, wastewater and sewage discharge, and groundwater discharge have all been shown to provide significant sources of nitrogen (N) that have been linked to increased primary and macroalgal production (Lapointe et al. 2004, 2005) and harmful algal blooms (HABs) (Anderson et al. 2002; Glibert et al. 2005; Heisler et al. 2008). Anthropogenic nutrient inputs are considered the most significant factor contributing to the global increase in the frequency and intensity of HABs (Hallegraeff 2004; Glibert et al. 2005). Although many studies have focused on agricultural runoff, wastewater has also been found to promote HABs and increase primary productivity (Jaubert et al. 2003); in some regions, wastewater has been shown to

be more important than upwelling as a N source (Chisholm et al. 1997; Thompson and Waite 2003; Lapointe et al. 2005).

Nitrogen has been the focus of most coastal eutrophication studies because it has been shown to be the primary limiting macronutrient for algae in coastal waters (Dugdale 1967; Ryther and Dunstan 1971) including California (Eppley et al. 1979). However, previous research has shown that the N form, not just quantity, is important for HABs and algal blooms (Glibert et al. 2006), particularly in California coastal waters (Howard et al. 2007; Cochlan et al. 2008; Kudela et al. 2008).

Recent studies within the Southern California Bight (SCB) have documented chronic algal bloom hot spots that coincide with areas that have potentially significant anthropogenic nutrient inputs (Nezlin et al. 2012). Before 2000, toxic outbreaks of *Pseudo-nitzschia* (an algal diatom that produces domoic acid) were considered rare (Lange et al. 1994); however, in recent years, frequent occurrences (Seubert et al. 2013) and high concentrations of this toxin have been documented in the SCB (Trainer et al. 2000; Schnetzer et al. 2007; Caron et al. 2010) and have been attributed to upwelling (Lewitus et al. 2012; Schnetzer et al. 2013). Increased awareness of toxic HAB events served as the primary motivation for establishment of the Harmful Algae and Red Tide Regional Monitoring Program by the Southern California Coastal Ocean Observing System (SCCOOS). This ongoing program collects weekly HAB species and toxin information from five pier locations in Southern California (SC; data available online, <http://www.sccoos.org/data/habs/index.php>).

\* Corresponding author: [mhoward@sccwrp.org](mailto:mhoward@sccwrp.org)

### Present addresses:

<sup>a</sup> Remote Sensing Solutions, Pasadena, California

<sup>b</sup> University of Washington, Seattle, Washington

<sup>c</sup> King Abdullah University of Science and Technology, Thuwal Kingdom of Saudi Arabia

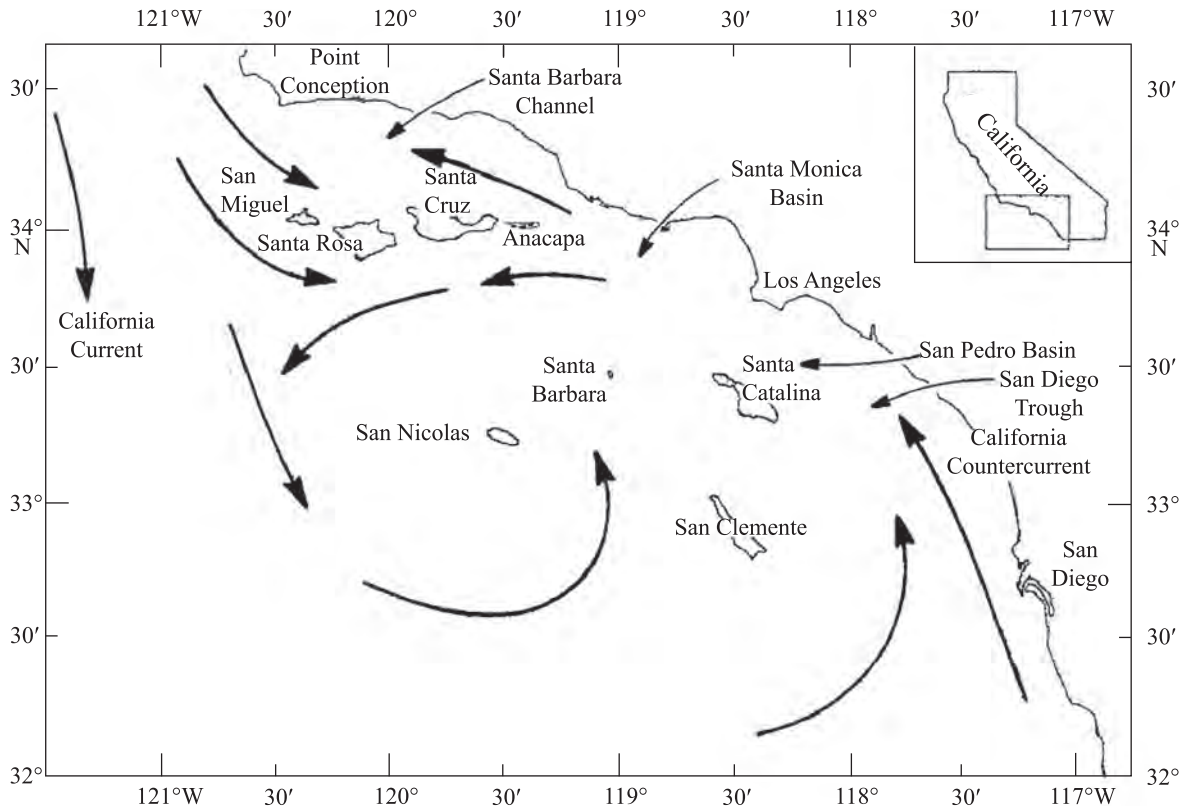


Fig. 1. The circulation patterns in the SCB (adapted from Hickey 1992).

There is a general perception that in upwelling regions, such as coastal California, the flux of anthropogenic nutrient inputs is insignificant relative to upwelling flux, and therefore anthropogenic inputs have relatively little effect on the productivity of coastal waters. Upwelling is the process by which vertical currents transport deep nutrient-rich water to the surface, displacing nutrient-depleted surface water. No studies to date have quantified and compared the natural and anthropogenic inputs on regional and local scales in the SCB to verify the accuracy of this perception. However, a growing number of studies have suggested a linkage between anthropogenic N sources and algal blooms (including HABs) in California (Kudela and Cochlan 2000; Beman et al. 2005; Kudela et al. 2008). Additionally, physiological studies have shown that several common California HAB species are capable of utilizing anthropogenic N forms, such as urea (Cochlan et al. 2008; Kudela et al. 2008), for growth, and toxin production can be increased under these conditions (Howard et al. 2007).

To test the hypothesis that natural sources (e.g., upwelling) greatly exceed anthropogenic nutrient sources to the SCB, this study compared the contributions of N from four major nutrient sources, (1) upwelling, (2) treated wastewater effluent discharged to ocean outfalls, (3) riverine runoff, and (4) atmospheric deposition. This comparison was made using large regional empirical data sets combined with modeling on both regional (SCB-wide) and subregional scales. This is the first study to make this comparison on the U.S. West Coast.

## Methods

*Study area and circulation patterns*—The SCB lies along the southern part of the Pacific coast of the continental United States. The continental coastline generally runs along a north–south gradient beginning at Cape Flattery, Washington (~48°23'N), until Cape Mendocino in northern California (~40°15'N), then turns toward a south–southeast direction. Figure 1 shows the generalized circulation patterns in the SCB. The continuum is broken by a bend or curvature in the coastline between Point Conception (~34°34'N) and the Mexico international border (~32°32'N). The SCB includes an ocean area of 78,000 km<sup>2</sup> (Dailey et al. 1993) and numerous islands offshore. The bottom topography consists of submarine mountains and valleys, neither of which could be considered a classical continental shelf nor a classical continental slope.

A ring of coastal mountain ranges defines SC and shelters the coastal area from dominating northwesterly winds, which create a “coastal basin” where cool, dense air is trapped, resulting in much weaker wind and sea patterns than over the open ocean (Dorman and Winant 1995). SC’s climate exhibits relatively dry summer and wet winter seasons. During the dry season a semipermanent eastern Pacific high-pressure area dominates SC. The marine layer is a prominent feature from late spring through early fall. Beginning late fall to early spring (October through March) the high-pressure ridge is displaced and the southern margin of the polar jet stream affects SC. Over 90% of the precipitation generally occurs during this time period.

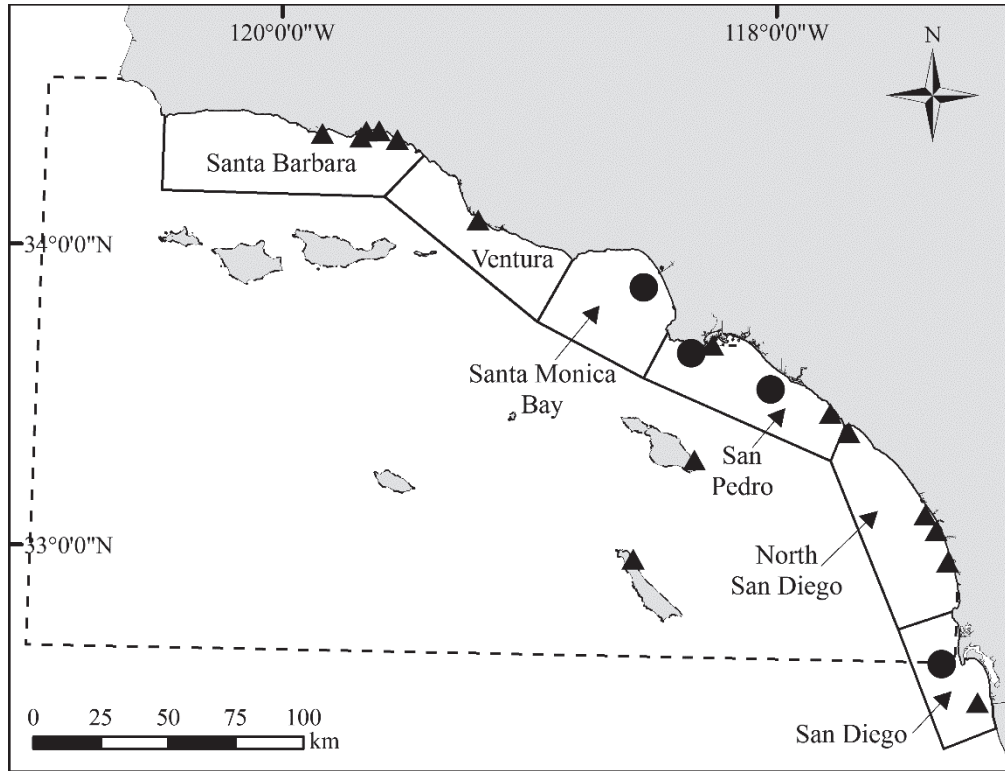


Fig. 2. Regional and subregional SCB boundaries used to calculate fluxes of each of the four major sources. The area used for regional estimates is outlined in a dashed black line; subregions are labeled and outlined in a solid black line. The POTW outfalls that discharge wastewater effluent are represented by black circles for large (> 100 MGD) and black triangles for small (< 25 MGD).

The migratory nature of the region’s storm fronts causes alternating periods of dry and wet weather during the rainy season.

The ocean region within the SCB is dominated by the equatorward California Current (CC). The CC is a typical broad eastern boundary current (Hickey 1979) that transports cold subarctic water from north to south throughout the year along a typically narrow (3 to 6 km) coastal continental shelf (Fig. 1). The CC is not steady but migrates seasonally onshore and offshore, producing a rich eddy field (Burkov and Pavlova 1980). As the CC passes Point Conception, it turns south-southeast along SC’s outer continental slope, then a portion branches (~32°N) eastward to northward along the coast (Hickey 1992), forming a large gyre known as the Southern California Eddy (Fig. 1). The poleward current along the coast is called the Southern California Countercurrent (SCC) (Sverdrup and Fleming 1941). It transports warm southern water into Santa Monica Bay and the Santa Barbara Channel.

Surface current flows may not reflect subpycnocline currents (Hamilton et al. 2006). During spring, the intensity of the equatorward CC increases compared with the poleward SCC. The CC jet migrates onshore, and the eastward branches penetrate into the SCB through the Santa Barbara Channel and onward south of the Channel Islands (Hickey 1979). The islands act as barriers to deflect surface currents in different directions. Near shore, over the continental shelf and borderland slope, the

near-surface flow is commonly equatorward, whereas the California Undercurrent is poleward (Hickey 1992).

*Estimation and comparison of nutrient sources*—The N fluxes into the SCB from four potential sources were estimated: (1) upwelling, (2) wastewater effluent discharge, (3) riverine runoff, and (4) atmospheric deposition. A combination of field measurements and modeling over a 1-yr period (January–December 2010) was used to estimate the contribution of each nutrient source on a bight-wide scale (51,686 km<sup>2</sup>) as well as for six smaller subregional areas (Fig. 2) including: Santa Barbara (2405 km<sup>2</sup>), Ventura (1449 km<sup>2</sup>), Santa Monica Bay (1571 km<sup>2</sup>), San Pedro (1641 km<sup>2</sup>), North San Diego (1837 km<sup>2</sup>), and San Diego (1020 km<sup>2</sup>). The combined area of all of the subregions makes up 20% of the total bight-wide area of the SCB. Nutrient inputs were estimated as annual loads for the bight-wide scale (reported in kg N yr<sup>-1</sup>) as well as annual fluxes for the six subregional areas (reported as kg N km<sup>-2</sup> yr<sup>-1</sup>).

*Modeling to estimate upwelling*—The upwelling contribution of N was estimated using the regional oceanic modeling system (ROMS), a three-dimensional ocean circulation model for the U.S. West Coast (Marchesiello et al. 2003), coupled with an nutrient–phytoplankton–zooplankton–detritus (NPZD)-type ecosystem–biogeochemistry model (Gruber et al. 2006) to generate a reanalysis of the ocean environment from January to December 2010. This model

integration resulted in highly time-resolved output of the three-dimensional physical and biogeochemical parameters. The ROMS model saves output of the daily averages of all advection terms in Eq. 1 (Gruber et al. 2006) and the output was integrated over time and space.

$$\frac{\partial B}{\partial t} = \nabla \cdot K \nabla B - \vec{u} \cdot \nabla_h B - (w + w^{\text{sink}}) \frac{\partial B}{\partial z} + J(B) \quad (1)$$

where  $K$  is the eddy kinematic diffusivity tensor, and where  $\nabla$  and  $\nabla_h$  are the three-dimensional (3-D) and horizontal gradient operators, respectively. The horizontal and vertical velocities of the fluid are represented by  $\vec{u}$  and  $w$ , respectively. The  $w^{\text{sink}}$  represents the vertical sinking rate of the biogeochemical components and  $J(B)$  represents the source minus sink term. All of these terms are described in detail in Gruber et al. (2006). From this detailed output, periods of upwelling were determined using vertical velocity, lateral advection, and temperature fields, and then the net mass of nitrate ( $\text{NO}_3$ ) and ammonium ( $\text{NH}_4$ ) from lateral and vertical fluxes to the euphotic zone was calculated. The total vertical flux assimilated by the model includes advection and diffusion, whereas the total lateral flux was assimilated for advection only. Daily estimates were summed to provide an annual estimate. The total flux of N ( $\text{NO}_3$  and  $\text{NH}_4$ ) estimates were made over a range of spatial scales, from a light-wide scale (Fig. 2 black dotted line) to smaller subregional scales (Fig. 2 black solid line).

*Model description*—ROMS is a free-surface, hydrostatic, 3-D primitive equation regional ocean model (Marchesiello et al. 2003; Shchepetkin and McWilliams 2005). A description and validation of the ROMS model at the 15-km spatial scale has been published (Gruber et al. 2006). This ROMS 3-D model provided both 6 hourly “nowcasts” obtained via assimilation of satellite sea-surface temperature, high-frequency radar surface current velocity, subsurface temperatures, and salinities profiled from Argo floats and gliders as well as daily 72-h forecasts. The ROMS output (for the physics-only model runs) was provided at both the Jet Propulsion Laboratory ROMS web site (<http://ocean.jpl.nasa.gov/SCB>) and the SCCOOS web site ([www.sccoos.org/data/roms](http://www.sccoos.org/data/roms)).

The ROMS configuration consisted of a single domain covering the SC coastal ocean from Santa Barbara to San Diego at a resolution of 1 km. The vertical discretization used a stretched terrain-following coordinate (S-coordinate) on a staggered grid over variable topography (Song and Haidvogel 1994). The stretched coordinate allowed increased resolution in areas of interest, such as the thermocline and bottom boundary layers. ROMS used a sigma-type vertical coordinate in which coordinate surfaces followed the bottom topography. In the SCB configuration, there were 40 unevenly spaced sigma surfaces used, with the majority of these clustered near the surface to better resolve processes in the mixed layer. The horizontal discretization used a boundary-fitted, orthogonal curvilinear formulation. Coastal boundaries were specified as a finite-discretized grid via land and sea masking. The SCB configuration of ROMS has been tested and used extensively (Dong et al. 2009).

Boundary conditions for the SCB domain were provided from a separate data-assimilating ROMS domain that covered the entire coast of California and northern Baja California at a resolution of 3 km. The tidal forcing was added through lateral boundary conditions that were obtained from a topography experiment—Poseidon (TOPEX POSEIDON) global barotropic tidal model (TOPEX POSEIDON global barotropic tidal model.6; Egbert et al. 1994), which had a horizontal resolution of  $0.25^\circ$  and used an inverse modeling technique to assimilate satellite altimetry crossover observations. There were eight major tide constituents used at the diurnal and semidiurnal frequencies (M2, K1, O1, S2, N2, P1, K2, and Q1). The atmospheric forcing required by the ROMS model was derived from hourly output from forecasts performed with a regional atmospheric model, the Weather Research and Forecasting System (WRF). This model has been used in the SCB region (Conil and Hall 2006). The horizontal resolution was 4 km and the lateral boundary forcing and initial conditions were derived from the National Centers for Environmental Prediction 12-km North American model daily Greenwich mean time forecasts. The surface latent and sensible heat fluxes, as well as surface evaporation rates, were derived from WRF surface air temperatures, surface relative humidity, 10-m winds, solar and terrestrial radiation, and ROMS sea-surface temperatures, using the bulk formula proposed by Kondo (1975). The freshwater flux was computed as the calculated evaporation rate minus the WRF precipitation rate (evaporation – precipitation). The wind stress was derived from the 10-m winds using the formula of Large and Pond (1981). The variables used for computing the ocean-model forcing have been evaluated against buoy data. The surface winds were accurate, with root mean square errors of 2–3  $\text{m s}^{-1}$  in speed and  $30^\circ$  in direction. Comparison of modeled vs. measured surface air temperatures and relative humidity showed good accuracy with errors of 1–2°C and 5–10%.

The biogeochemical model that was used in this ROMS configuration was an NPZD model based on Fasham et al. (1990). The model was optimized and validated for the U.S. West Coast coastal upwelling region by Gruber et al. (2006). This model has been validated and gave good results in the upwelling-dominated coastal zone, but it failed to reproduce observations farther offshore in more nutrient-depleted areas (Gruber et al. 2006). A full description of the model can be found in Gruber et al. (2006), but is described briefly here.

The NPZD model included a single limiting nutrient (N) and a diatom-like single phytoplankton class. Although the model output was only used to calculate  $\text{NO}_3$  and  $\text{NH}_4$  lateral and vertical fluxes, a total of 12 state variables is tracked including:  $\text{NO}_3$ ,  $\text{NH}_4$ , phytoplankton, zooplankton, small and large detritus (both N and carbon [C] concentrations due to varying C:N ratios), oxygen, dissolved inorganic carbon, calcium carbonate, and total alkalinity.

In the absence of a larger domain model with the same NPZD biogeochemical model characteristics, biogeochemical boundary conditions were based on the physical

Table 1. List of polynomial (polyn.) parameters for the biogeochemical boundary conditions in ascending order, e.g.,  $\text{NO}_3(\sigma_\theta > 26.8) = -20,258 + 1484.7\sigma_\theta - 27.1422\sigma_\theta^2$ . Chlorophyll *a* (Chl *a*), not applicable (na).

Variable	$\sigma_\theta$ range 1	Polyn. 1	$\sigma_\theta$ range 2	Polyn. 2	$\sigma_\theta$ range 3	Polyn. 3
Nitrate	Up to 24.99	-48.0343, 1.9910	25.0–26.79	-371.8125, 11.3264, 0.1449	Over 26.8	-20258, 1484.7, -27.1422
Chl <i>a</i> (top 50 m)	All values	-547.1559, 42.7240, -0.8334	na	na	na	na
Chl <i>a</i> (>50 m)	All values	17.4953, -0.7332	na	na	na	na
Ammonium	Up to 24.82	-1.9986, 0.0866	24.82–26.42	-265.6287, 20.7761, -0.4056	26.42–27.2	170.3260, -12.5235, 0.2302

boundary conditions, modeled at daily time steps, and the relationship between physical quantities (either temperature or potential density) and nutrients were used to derive initial and boundary conditions for  $\text{NO}_3$  and  $\text{NH}_4$ , as summarized in Table 1. There were not enough organic N or urea data to estimate the contribution of this form from upwelling. Therefore the total dissolved nitrogen (TN) flux for upwelling excludes organic N sources. Initial and boundary conditions for  $\text{NO}_3$  concentrations were determined with a polynomial regression that describes the relationship between  $\text{NO}_3$  and density ( $\sigma_\theta$ ), defined for the SCB from temperature, salinity, and  $\text{NO}_3$  data from the World Ocean Atlas 2005 (Garcia et al. 2006; Fig. 3).

Climatological biogeochemical boundary and initial conditions were used to determine a relationship between potential density and  $\text{NH}_4$  because there were no observed data available for  $\text{NH}_4$ . The scatter is much larger for this relationship than for  $\text{NO}_3$  (Fig. 3).

*Wastewater effluent discharge*—Nutrient loads from wastewater effluent discharged from outfalls to the SCB were estimated for both large (> 100 million gallons a day [MGD]) and small (< 25 MGD) publicly owned treatment works (POTWs) in each subregion (Table 2), where large POTWs contribute 90% of total discharges to SCB. Large POTW nutrient loads were determined for January–December 2010 by measuring effluent nutrient concentrations quarterly from December 2008 through December 2009; these quarterly concentrations were combined with monthly discharge flows from 2010 National Pollutant Discharge Elimination System (NPDES) monitoring reports from the Hyperion Treatment

Plant (HTP) operated by City of Los Angeles (LA), the Joint Water Pollution Control Plant (JWPCP) operated by LA County Sanitation District, the Treatment Plant No. 2 operated by Orange County Sanitation District, and the Point Loma Wastewater Treatment Plant operated by City of San Diego. Samples were analyzed for TN following Environmental Protection Agency (EPA) method SM4500-N, nitrate plus nitrite (herein referred to as  $\text{NO}_3$ ) following EPA 300.0 and SM4500, ammonia ( $\text{NH}_3$ ) following method EPA 350.1 and SM4500, and urea using Goeyens et al. (1998). Organic nitrogen (ON) was not measured for the large POTWs, only urea, which is a component of ON. An interlaboratory comparison was conducted for these analytes and the variability was determined to be negligible.

Effluent nutrient concentration data for small POTWs were determined using available data published for 2005 from NPDES monitoring reports (Lyon and Stein 2008). Small POTW effluent concentration data were available for  $\text{NO}_3$ ,  $\text{NH}_3$ , and TN; ON was reported from one POTW in Ventura. Details on methods were reported in Lyon and Stein (2008).

POTW N load (bight-wide) was estimated by multiplying nutrient concentrations ( $\text{mg L}^{-1}$ ) with annual flow volume (L) and POTW N fluxes for each subregion were estimated by dividing the N load by the area ( $\text{km}^2$ ).

The error associated with the N loads was determined by multiplying the standard deviation (SD) of nutrient concentrations by the total annual discharge. Total error was calculated as the square root of the squared sums of each of the individual estimates for each watershed.

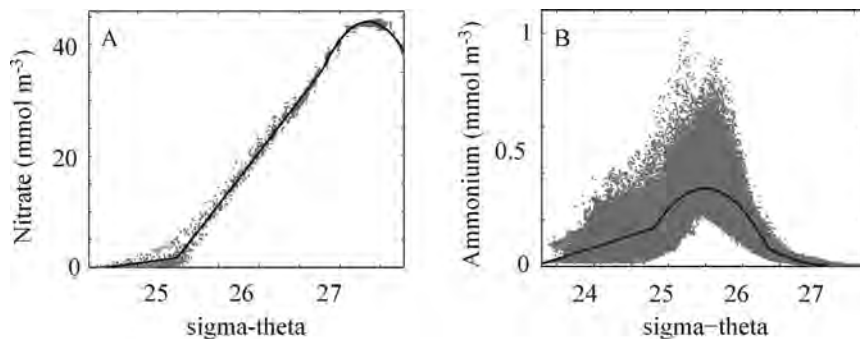


Fig. 3. Relationship between potential density ( $\sigma_\theta$ ) and (A) nitrate and (B) ammonium in the SCB. Nitrate and ammonium data (gray dots) are derived from the World Ocean Atlas (2005) and ROMS tests run with climatological boundary conditions, respectively. Black lines designate the stepwise polynomial fits.

Table 2. Location and relative size of POTWs used for effluent discharge load estimates by subregion. S, small; L, large; WWTP, wastewater treatment plant.

Subregion	POTW name	Size
Santa Barbara	Goleta WWTP	S
	El Estero WWTP	S
	Montecito WWTP	S
	Summerland WWTP	S
	Carpinteria WWTP	S
Ventura	Oxnard WWTP	S
Santa Monica Bay	HTP	L
	JWPCP	L
San Pedro	Treatment Plant No. 2	L
	Terminal Island WWTP	S
North San Diego	Aliso Creek Ocean Outfall	S
	San Juan Creek Ocean Outfall	S
	Oceanside WWTP	S
	Camp Pendleton WWTP	S
	Fallbrook Public Utility District WWTP	S
San Diego	Encina Ocean Outfall	S
	San Elijo Water Pollution Control Facility	S
	Point Loma Wastewater Treatment Plant	L
	Hale Ave. Resource Recovery Facility	S
	South Bay Water Reclamation Plant	S
	International Wastewater Treatment Plant	S

$$\text{Total load SD} = \left( \sum_1^{10} [C_e Q]^2 \right)^{1/2} \quad (2)$$

where  $C_e$  is the standard deviation in nutrient concentration for each large POTW effluent.  $Q$  is the total annual discharge.

*Riverine loads*—Riverine nutrient loads to the SCB were estimated using empirical wet-weather and dry-weather data for monitored watersheds in combination with modeled wet-weather loads for unmonitored watersheds for the period of October 2008–October 2010.

Discharge and nutrient samples were collected at 34 wet-weather and 57 dry-weather mass emission stations by Ventura, Los Angeles, Orange, and San Diego counties under their NPDES permits or by SCB Regional Monitoring Program partners during the period of October 2008–October 2010. Howard et al. (2012) provides methodological details including summary of the wet- and dry-weather monitoring and the 91 mass loading stations utilized for the study.

A spreadsheet model based on the rational method (O’Loughlin et al. 1996) was used to generate freshwater runoff  $Q$  ( $\text{m}^3 \text{d}^{-1}$ ) and the N loads associated with wet-weather events. Modeled storm discharge ( $Q$ ) was calculated as a function of drainage area ( $A$ ,  $\text{km}^2$ ), mean rainfall intensity ( $I$ ,  $\text{mm d}^{-1}$ ), hydraulic runoff coefficient ( $C$ ), and conversion constant ( $k$ ):

$$Q = AICk \quad (3)$$

Hydraulic runoff coefficient ( $C$ ) varied as a function of land use and cover type (Howard et al. 2012). The Ackerman and Schiff model (2003) was improved by refining land use-specific runoff concentrations for  $\text{NO}_3$  (excluding nitrite) and  $\text{NH}_4$ , on the basis of published values from previously published studies (Stein et al. 2007) and TN runoff concentrations were derived from empirical data for this study (Howard et al. 2012).

Within each watershed,  $Q$  was then calculated as the sum of discharge associated with six land-use categories: agriculture, commercial, industrial, open space (natural), residential, and other urban. The daily nutrient loads were estimated as the sum of the product of the runoff concentration ( $c$ ) and  $Q$  for each land use, using Eq. 3.

The error associated with the N loads was determined by multiplying the standard deviation of nutrient concentrations by the total discharge (wet- or dry-weather discharge, respectively, for the watershed). Total error was calculated as the square root of the squared sums of each of the individual estimates for each watershed, as given in Eq. 3.

The drainage area was delineated for each watershed on the basis of hydraulic unit code boundaries. The model domain included all SC coastal watersheds in San Diego, Orange, Riverside, Los Angeles, San Bernardino, Ventura, and Santa Barbara counties with an initial total watershed area of 27,380  $\text{km}^2$ . Watershed areas larger than 52  $\text{km}^2$  upstream of dams were excluded in the model domain, to mimic the retention of water by dams (Ackerman and Schiff 2003). The final model domain was comprised of 98 watersheds with a total area of 14,652  $\text{km}^2$ . Each of the watersheds was populated with land-cover data from Stein et al. (2007), and aggregated into the six land-use categories.

Daily precipitation data for approximately 200 rain gauge stations were obtained from the National Oceanic and Atmospheric Administration (NOAA), National Environmental Satellite, Data and Information Service, National Climatic Data Center, and Climate Data Online database. Data were transformed to estimate mean precipitation over the 98 watersheds relevant to the study. Precipitation data were interpolated within each watershed on a regular grid using a biharmonic spline interpolation method (Sandwell 1987).

A model scenario was run to estimate the anthropogenic influence on nutrient fluxes to the SCB using 100% open-space land use for the entire Bight, representing a “preurbanization” baseline. The model domain was expanded to include areas above existing dams because there were no dams withholding potential runoff in the modeled preurbanized state. Rainfall data were not available for the period representing the preurbanized state; therefore, current rainfall data (2008–2009) were used to estimate loads. This enabled a comparison of pre- and posturbanization loads without any bias due to differences in precipitation (Howard et al. 2012).

*Atmospheric deposition*—Atmospheric deposition rates were estimated for both wet-weather and dry-weather deposition. The wet deposition rates were calculated from the average annual rates for 2009 and 2010 at two National

Atmospheric Deposition Program sites: Site 42, Los Angeles County (Tanbark Flat, 34.2071, -117.7618) and Site 94, San Bernardino County (Converse Flats, 34.1938, -116.9131). Wet deposition rates for NO<sub>3</sub> and NH<sub>4</sub> from these two sites were averaged across sites and years (kg km<sup>-2</sup> d<sup>-1</sup>), then applied to the total number of wet days for the January–December 2010 study year.

Sampling for dry deposition was conducted three times over a 6-month period at rooftop location at the HTP and the City of Oceanside Library. Techniques using surrogate surfaces for estimating N dry deposition in semiarid environments, including a water surface sampler and filter samplers, were used (Moumen et al. 2004; Raymond et al. 2004). Both of these techniques use aerodynamic discs, are of short duration (2 to 4 d), and produce reproducible results when evaluated against the atmospheric concentrations and each other. Samplers were deployed in duplicate for the water collector and in triplicate for the filter collectors. Filter samplers and water surface samplers were analyzed for NH<sub>4</sub> and NO<sub>3</sub>. Concentrations were converted to deposition rates by incorporating the surface area of the sampler and the duration of the sampling event (kg km<sup>-2</sup> d<sup>-1</sup>). The average deposition rate for the three sampling events was multiplied by the number of dry-weather days during the January–December 2010 study year for a bight-wide estimation of dry deposition. Results from the HTP site were applied to the Santa Monica Bay and San Pedro Bay subregions, and results from the Oceanside sampler were applied to all other subregions.

*Estimates of contribution of anthropogenic activities to SCB nutrient loads*—The contribution of anthropogenic activities to SCB nutrient loads was calculated from the total flux of N from natural sources (upwelling, atmospheric deposition, and preurbanization rivers) compared with the TN flux of all nutrient sources (upwelling, atmospheric deposition, posturbanization rivers, and wastewater effluent discharge).

## Results

*Bight-wide regional nitrogen loads*—Summed across the entire SCB scale, TN loads differed by an order of magnitude, with upwelling contributing the largest load and riverine runoff the smallest (Fig. 4, Table 3). Upwelling consisted almost entirely of NO<sub>3</sub> (98.7%), and little NH<sub>4</sub> (1.3%), whereas effluent loads consisted mostly of NH<sub>4</sub> (92%) with minor percentages of NO<sub>3</sub> (7.0%) and ON (1.0%). The riverine runoff was comprised mostly of ON (60%) and NO<sub>3</sub> (35%), with a smaller contribution from NH<sub>4</sub> (6.0%). The NO<sub>3</sub> loads from riverine runoff and effluent were equivalent (3.5 × 10<sup>6</sup> and 3.4 × 10<sup>6</sup> kg N yr<sup>-1</sup>, respectively), even though NO<sub>3</sub> comprised only 7.0% of the TN from effluent. The error analysis of TN loads for the riverine runoff and effluent ranged from 3.3% to 17.6% for effluent and 2.4% to 37.8% for riverine runoff (Table 4).

*Subregional nitrogen fluxes*—TN for each source varied by subregion. Effluent and upwelling had similar annual TN fluxes for the three subregions with large POTW outfall

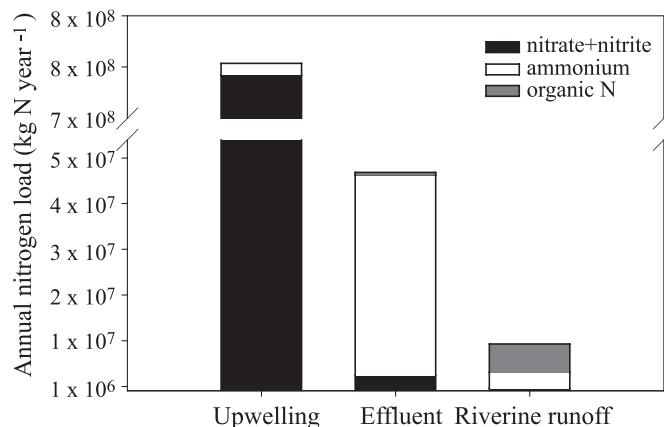


Fig. 4. Annual total nitrogen loads (in kg N yr<sup>-1</sup>) to the SCB for each nutrient source, with total nitrogen components separated into nitrate plus nitrite shown by the black bars, ammonium shown by the white bars, and organic nitrogen shown by the gray bars.

discharges (Santa Monica Bay, San Pedro, and San Diego; Fig. 5, Table 5). These were 9.9 × 10<sup>3</sup> and 1.0 × 10<sup>4</sup> kg N km<sup>-2</sup> yr<sup>-1</sup>, respectively, for Santa Monica Bay, 1.2 × 10<sup>4</sup> and 2.3 × 10<sup>4</sup> kg N km<sup>-2</sup> yr<sup>-1</sup>, respectively, for San Pedro Bay, and 7.4 × 10<sup>3</sup> and 2.4 × 10<sup>3</sup> kg N km<sup>-2</sup> yr<sup>-1</sup> for San Diego subregion. Note that the upwelling flux estimated for San Diego is at the edge of the model boundary; therefore, it has a large amount of uncertainty. For these three regions, riverine runoff and atmospheric deposition were one to two orders of magnitude less than upwelling and effluent, respectively, with annual fluxes ranging from 7.0 × 10<sup>1</sup> to 6.0 × 10<sup>3</sup> kg N km<sup>-2</sup> yr<sup>-1</sup> for riverine runoff and 4.3 × 10<sup>2</sup> to 8.7 × 10<sup>2</sup> kg N km<sup>-2</sup> yr<sup>-1</sup> for atmospheric deposition.

The Santa Barbara and Ventura subregions both had net annual downwelling rather than net upwelling, ranging from 2.1 × 10<sup>4</sup> to 1.0 × 10<sup>5</sup> kg N km<sup>-2</sup> yr<sup>-1</sup>, respectively. In these subregions, the dominant sources varied from effluent and atmospheric deposition in Santa Barbara (1.6 × 10<sup>2</sup> and 4.3 × 10<sup>2</sup> kg N km<sup>-2</sup> yr<sup>-1</sup>, respectively) to roughly equivalent fluxes of effluent, riverine runoff, and atmospheric deposition in Ventura (5.1 × 10<sup>2</sup>, 4.1 × 10<sup>2</sup> and 8.7 × 10<sup>2</sup> kg N km<sup>-2</sup> yr<sup>-1</sup>, respectively). Only in North San Diego County was upwelling (3.6 × 10<sup>4</sup> kg N km<sup>-2</sup> yr<sup>-1</sup>) dominant by an order of magnitude over effluent (1.4 × 10<sup>3</sup> kg N km<sup>-2</sup> yr<sup>-1</sup>) and by two orders of magnitude over riverine runoff (6.0 × 10<sup>2</sup> kg N km<sup>-2</sup> yr<sup>-1</sup>) and atmospheric deposition (4.7 × 10<sup>2</sup> kg N km<sup>-2</sup> yr<sup>-1</sup>).

Table 3. Annual nitrogen loads for each nutrient source and constituent. All loads are 10<sup>6</sup> kg N yr<sup>-1</sup>. The form of nitrogen expressed as a percentage of total nitrogen for each source is given in parentheses.

	Total N	Nitrate + nitrite	Ammonium	Organic N
Upwelling	750	740 (98.7)	10 (1.3)	na*
Effluent	48	3.4 (7.0)	44 (92.0)	0.5 (1.0)
Riverine runoff†	10	3.5 (34.0)	0.6 (6.0)	6.2 (60.0)

\* na, not analyzed for this source.

† Data for January through October 2010.

Table 4. Summary of the standard error calculated for nitrogen components of riverine runoff and effluent. Absolute and standard error are reported as  $10^4$  kg N  $\text{yr}^{-1}$ .

Component	Riverine runoff				Effluent	
	Wet weather		Dry weather		Standard error	% error
	Absolute error	% error	Absolute error	% error		
Total N	22	8.8	3.0	2.4	200	4.6
Nitrate	8.4	7.5	2.7	3.6	55	17.6
Ammonium	9.4	37.8	0.8	11.6	130	3.3

The flux of individual forms of nitrogen ( $\text{NO}_3$  and  $\text{NH}_4$ ) were estimated for each source in every subregion, whereas ON was estimated when data were available (Table 6). In the Santa Barbara subregion, the largest source of  $\text{NO}_3$  is from atmospheric deposition ( $2.1 \times 10^2$  kg N  $\text{km}^{-2}$   $\text{yr}^{-1}$ ), whereas effluent and atmospheric deposition deliver equivalent amounts of  $\text{NH}_4$  ( $1.6 \times 10^2$  and  $2.1 \times 10^2$  kg N  $\text{km}^{-2}$   $\text{yr}^{-1}$ , respectively). Riverine runoff and atmospheric deposition deliver the largest fluxes of  $\text{NO}_3$  ( $3.5 \times 10^2$  and  $2.1 \times 10^2$  kg N  $\text{km}^{-2}$   $\text{yr}^{-1}$ , respectively) in Ventura, whereas  $\text{NH}_4$  fluxes were dominated by effluent and atmospheric deposition ( $4.0 \times 10^2$  and  $2.1 \times 10^2$  kg N  $\text{km}^{-2}$   $\text{yr}^{-1}$ , respectively). The highly urbanized areas of Santa Monica Bay and San Pedro exhibited similar flux patterns, with upwelling providing the highest flux of  $\text{NO}_3$  ( $9.3 \times 10^3$  and  $2.2 \times 10^4$  kg N  $\text{km}^{-2}$   $\text{yr}^{-1}$ , respectively), effluent providing the highest flux of  $\text{NH}_4$  ( $8.4 \times 10^3$  and  $1.2 \times 10^4$  kg N  $\text{km}^{-2}$   $\text{yr}^{-1}$ , respectively), and riverine runoff providing the highest flux of ON ( $1.3 \times 10^2$  and  $5.0 \times 10^2$  kg N  $\text{km}^{-2}$   $\text{yr}^{-1}$ , respectively). The North San Diego

subregion had an  $\text{NO}_3$  flux from upwelling that was two to four orders of magnitude higher than any other source, whereas upwelling and effluent contributed most of the  $\text{NH}_4$  flux ( $3.1 \times 10^3$  and  $1.4 \times 10^3$  kg N  $\text{km}^{-2}$   $\text{yr}^{-1}$ , respectively). In the San Diego subregion, upwelling and riverine runoff provided the highest flux of  $\text{NO}_3$  ( $1.7 \times 10^3$  and  $1.5 \times 10^3$  kg N  $\text{km}^{-2}$   $\text{yr}^{-1}$ , respectively), whereas effluent provided most of the  $\text{NH}_4$  flux ( $7.3 \times 10^3$  kg N  $\text{km}^{-2}$   $\text{yr}^{-1}$ ) and ON was mostly provided by riverine runoff ( $4.2 \times 10^3$  kg N  $\text{km}^{-2}$   $\text{yr}^{-1}$ ).

*Estimates of contribution of anthropogenic activities to SCB nutrient loads*—The contribution of anthropogenic activities to SCB nutrient loads was estimated from the TN flux from natural sources (upwelling, atmospheric deposition, and preurbanization rivers) compared with the TN flux of all nutrient sources (upwelling, atmospheric deposition, posturbanization rivers, and wastewater effluent discharge). The increase in TN due to anthropogenic sources was largest for the more heavily urbanized areas of Santa Monica Bay

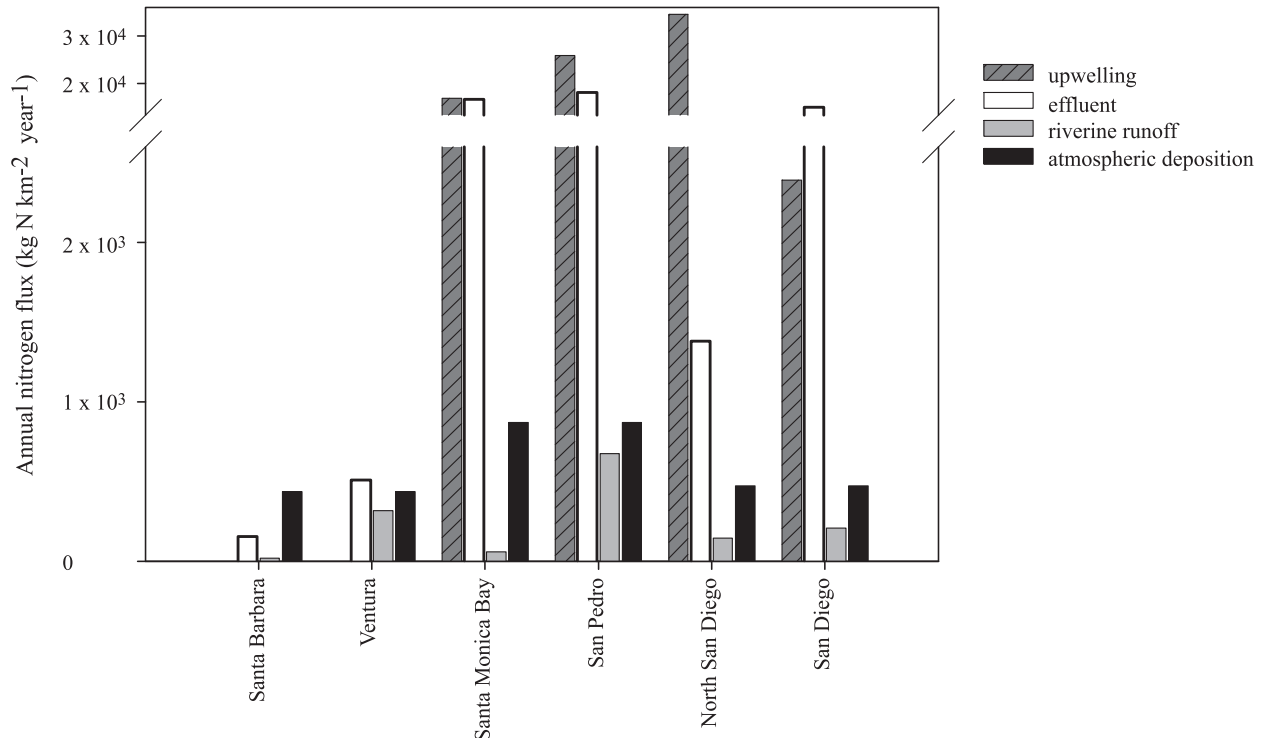


Fig. 5. Total annual nitrogen flux for each subregion in the SCB for each source including upwelling shown by dark gray bars with lines, effluent shown by white bars, riverine runoff shown by light gray bars, and atmospheric deposition shown by black bars.

Table 5. Annual total nitrogen flux for each subregion ( $10^2$  kg N km<sup>-2</sup> yr<sup>-1</sup>).

Source	Santa Barbara	Ventura	Santa Monica Bay	San Pedro	North San Diego	San Diego
Upwelling	-210	-1071	102	238	367	24
Effluent	1.6	5.1	99	121	14	74
Riverine runoff*	0.7	4.1	1.4	12	6	60
Atmospheric deposition	4.3	4.3	8.7	8.7	4.7	4.7
Total N	-203	-1057	211	380	392	163

\* Data for January through October 2010.

and San Pedro subregions, with increases of 2- and 1.5-fold (110% and 52%), respectively. The less urbanized subregions of Santa Barbara, Ventura, and North San Diego only had slight changes of 5% or less (Table 7).

Discussion

*Regional nitrogen loads and subregional nitrogen fluxes—* At the scale of the entire SCB region, the results of this study support the hypothesis that natural N sources (i.e., upwelling) dominated anthropogenic sources of N by an order of magnitude (Table 3, Fig. 4). However, at a subregional scale and proximal to the coastline (~20 km),

anthropogenic N sources, particularly wastewater effluent discharged through ocean outfalls, were equivalent to natural N sources in five of the six subregions (Table 5, Fig. 5). In the highly urbanized subregions of Santa Monica Bay and San Pedro, anthropogenic N inputs (mainly wastewater effluent) doubled the amount of TN flux in these subregions. The upwelling and effluent sources combined comprised 95% of the TN load in these subregions. The Santa Monica Bay subregion had equivalent contributions from upwelling and wastewater effluent to the TN flux (each was 47% to the TN flux). In San Pedro, the TN contribution from upwelling was the same order of magnitude as wastewater effluent, but the actual upwelling flux comprised 60% of the TN, whereas the

Table 6. Flux of each nitrogen form in each subregion of the SCB ( $10^2$  kg N km<sup>-2</sup> yr<sup>-1</sup>).

	Total N	Nitrate + nitrite	Ammonium	Organic N (urea only)
<b>Santa Barbara</b>				
Upwelling	-210	-198	-11	na
Effluent	1.6	na	1.6	na
Riverine runoff	0.7	0.1	0.04	0.6
Atmospheric deposition	4.3	2.1	2.1	na
<b>Ventura</b>				
Upwelling	-1071	-995	-75	na
Effluent	5.1	0.4	4.0	0.7
Riverine runoff	4.1	3.5	0.1	0.4
Atmospheric deposition	4.3	2.1	2.1	na
<b>Santa Monica Bay</b>				
Upwelling	102	93	8.6	na
Effluent	99	13	84	(0.9)
Riverine runoff	1.4	0.001	0.1	1.3
Atmospheric deposition	8.7	6.1	2.4	na
<b>San Pedro</b>				
Upwelling	238	220	18	na
Effluent	121	5.8	121	1.0
Riverine runoff	12	6.3	1.0	5.0
Atmospheric deposition	8.7	6.1	2.4	na
<b>North San Diego</b>				
Upwelling	367	336	31	na
Effluent	14	0.06	14	na
Riverine runoff	6.0	2.2	0.35	3.4
Atmospheric deposition	4.7	2.1	2.1	na
<b>San Diego</b>				
Upwelling	24	17	6.5	na
Effluent	74	2.1	71	(0.6)
Riverine runoff	60	15	3.1	42
Atmospheric deposition	4.7	2.1	2.1	na

na, not analyzed for this source.

Table 7. The total nitrogen flux ( $10^2 \text{ kg N km}^{-2} \text{ yr}^{-1}$ ) for natural nutrient sources (upwelling, atmospheric deposition, and preurbanization riverine runoff) and for natural and anthropogenic sources (upwelling, atmospheric deposition, posturbanization riverine runoff, and wastewater effluent discharge) to the SCB.

	Natural sources	Natural and anthropogenic sources	% change
Santa Barbara	−200	−203	1
Ventura	−990	−1057	7
Santa Monica Bay	100	211	110
San Pedro	250	380	52
North San Diego	370	392	6
San Diego	30	163	nd

nd, not determined due to subregional area at the edge of the ROMS model boundary.

POTW effluent was 33% of TN contribution (Table 5, Fig. 5). The TN flux from riverine runoff and atmospheric deposition was one to two orders of magnitude less than upwelling and effluent in both of these subregions (Table 5, Fig. 5). There are POTWs in these subregions that discharge directly into the major rivers and those discharges were included in the riverine runoff component, thereby making the total contribution of effluent slightly underestimated. In contrast, the North San Diego subregion had least amount of anthropogenic N inputs and the upwelling flux had the highest contribution to TN by two to four orders of magnitude compared with effluent, riverine runoff, and atmospheric deposition (Table 5, Fig. 5). The TN flux in Santa Barbara and Ventura was mostly driven by downwelling, as the TN flux from other sources differed by two to three orders of magnitude. In Santa Barbara, the riverine inputs were relatively insignificant compared with the other sources (Table 5, Fig. 5). In Ventura, effluent, riverine runoff, and atmospheric deposition contributions to TN were an equivalent order of magnitude and differed by three orders of magnitude from downwelling (Table 5, Fig. 5). The San Diego subregion had a large contribution of TN from effluent and riverine runoff; the upwelling is at the edge of the model boundary and is likely underestimated.

The absolute and standard error estimates were calculated to determine the amount of uncertainty in the nutrient source loads and fluxes (Table 4). The standard error determined for riverine runoff and effluent loads was less than 20% with one exception, the riverine runoff (wet weather)  $\text{NH}_4$  loads (37.8%). Effluent loads from POTWs are monitored on a monthly basis and have been tracked over the last 30 yr with a high level of quality assurance (Lyon and Stein 2008). There were insufficient data to calculate the error for the atmospheric deposition estimates, but this appears to be a very small source at the subregional scale. The coupled ROMS and NPZD model has been validated at the 15-km resolution for the entire U.S. West Coast by comparing model results with either remote-sensing observations (from advanced very-high-resolution radiometer, sea-viewing wide field-of-view sensor) or in situ measurements from the California Cooperative Oceanic Fisheries Investigations Program

(Gruber et al. 2006). Although we have a high level of confidence in our results at an annual and bight-wide scale, the 1-km ROMS model and NPZD used for the subregional scales has not yet been fully validated; therefore it is not possible at this time to calculate the error associated with the upwelling estimates from this study.

The two most urbanized subregions, Santa Monica Bay and San Pedro, had the largest percent change in TN flux due to anthropogenic sources (110% and 52%, respectively), whereas the less urbanized regions of Santa Barbara, Ventura, and North San Diego had much smaller changes in TN flux (1%, 1%, and 5%, respectively) due to anthropogenic inputs (Table 7). These findings contradict the current perception that anthropogenic nutrient inputs are negligible in upwelling-dominated regions. Other studies in Central California have focused on terrestrial runoff as the main source of anthropogenic nutrients (Kudela and Cochlan 2000; Kudela et al. 2008), but the results from this study show that wastewater inputs comprise a much higher contribution to the overall TN fluxes in the SCB, whereas the riverine contributions were relatively insignificant.

*The importance of nutrient forms and ratios*—Nitrogen is considered to be the primary limiting macronutrient for the growth of algae in many coastal ecosystems (Dugdale 1967; Ryther and Dunstan 1971), including California (Eppley et al. 1979). Previous studies have shown that the form of N, not just the quantity, is important for algal community composition, giving rise to algal blooms and HABs in particular (Howard et al. 2007; Cochlan et al. 2008; Kudela et al. 2008). The sources of N to the SCB are comprised of different forms of N, mainly  $\text{NO}_3$ ,  $\text{NH}_4$ , and ON, which includes urea. When we examined the forms of N that comprised each of the sources examined in this study on a bight-wide scale, upwelling was mostly comprised of  $\text{NO}_3$  (98.7% of TN), effluent was mostly comprised of  $\text{NH}_4$  (92% of TN), and riverine runoff was comprised of a mixture of inorganic and organic N forms (34% and 60%, respectively; Table 3). ON was mostly derived from riverine runoff (60% on a bight-wide scale).  $\text{NO}_3$  comprised only 7% of the TN load for effluent on a bight-wide scale (Table 3). However, examination of the forms of N from each source on a subregional scale provided surprising results (Table 6). In the heavily urbanized areas of Santa Monica Bay and San Pedro, effluent actually contributed a larger or equivalent  $\text{NO}_3$  flux than riverine runoff or atmospheric deposition (Table 6, Fig. 5). These findings contradict the perception that the contribution of effluent  $\text{NO}_3$  is insignificant, and show that effluent does provide an equivalent or larger contribution of  $\text{NO}_3$  compared with riverine and atmospheric deposition sources. Upwelling was one to two orders of magnitude larger than all of the sources and thus clearly provided the largest contribution of  $\text{NO}_3$  to the SCB (Table 6).

Urea, an organic form of N used as an indicator of coastal runoff in agricultural regions (Kudela and Cochlan 2000), has been found to sustain HABs in Central and Southern California (Kudela and Cochlan 2000; Kudela et al. 2008), and California HAB species have been shown to utilize urea for growth (McCarthy 1972; Howard et al.

2007). Despite these studies, urea concentrations in California's coastal waters and the importance of urea as an N source for algal growth is often overlooked and understudied. The main source of urea to the SCB was determined to be riverine runoff. Although it was a measurable source of N in the SCB, it was a minor component of the TN load (Tables 3, 6; Figs. 4, 5).

The nutrient fluxes estimated for the four major sources in this study were calculated at annual timescales. However, it is important to recognize that nutrient delivery to the coastal ocean on short, daily to weekly timescales is more ecologically relevant for primary productivity and HAB development. The timing of these nutrient inputs should be considered as some sources are chronic (daily wastewater effluent discharge into oceans and into rivers), whereas other sources are seasonal or episodic (riverine runoff and upwelling). Therefore, seasonal differences exist in both the TN flux as well as the proportion of N forms from each source. Riverine runoff is generally prevalent in the winter; upwelling occurs primarily in the spring and early summer; and effluent is chronic. Therefore, although upwelling clearly provided the largest source of  $\text{NO}_3$  (Table 6, Fig. 5), effluent probably provided most of the  $\text{NO}_3$  during nonupwelling and low riverine flow time periods. Other studies in SC have shown that stormwater runoff has at times been the dominant source of N inputs during nonupwelling periods and that those processes provided different proportions of N forms than upwelling (Warrick et al. 2005; McPhee-Shaw et al. 2007). In Monterey Bay, a more extensive study of this dynamic has shown similar results where riverine inputs of  $\text{NO}_3$  exceeded upwelling inputs across short, daily to weekly, timescales (but not monthly or annual scales), as often as 28% of the year (Quay 2011).

Another aspect to consider from this study is the importance of N:P ratios. Although the conventional Redfield ratio of N:P is 16:1, the effluent sources in this study have disproportionate N:P ratios that widely varied by POTW. The two large POTWs located in the San Pedro subregion have the highest N:P ratios of 60:1 (JWPCP) and 21:1 (Treatment Plant No. 2). Given the large contribution of effluent to the TN flux in this subregion (Table 6, Fig. 5), these ratios suggest that effluent provides a disproportionate amount of N relative to P compared with natural sources.

*Implications for primary production and algal blooms*—Nitrogen is the primary limiting macronutrient in the coastal waters in the SCB (Eppley et al. 1979); consequently, any N inputs to the coastal oceans will likely increase biological productivity. The results from the subregional spatial scale of this study are more ecologically relevant to the development of algal blooms, and show that anthropogenic nutrients can provide a significant source of N for algal blooms, including HABs (Table 6, Fig. 5). Recent studies have identified chronic algal bloom hot spots that coincide with areas in the SCB that have major anthropogenic sources of nutrients (Nezlin et al. 2012), suggesting that at local spatial scales, anthropogenic nutrients may provide favorable growth conditions for algal bloom development. On a more refined spatial scale, terrestrial freshwater

discharge and wastewater effluent discharges via ocean outfalls have been shown to increase phytoplankton biomass and affect patterns of phytoplankton productivity and community composition (Corcoran et al. 2010; Reifel et al. 2013). A 2006 study in Santa Monica Bay documented an effluent plume and urban riverine runoff that stimulated an algal bloom for which several HAB species dominated the community composition (Reifel et al. 2013). Other SCB studies in Santa Monica Bay and San Diego have been unable to attribute chlorophyll variability in the nearshore environment with upwelling and have concluded that nearshore productivity and chlorophyll are not always driven by classical coastal upwelling (Kim et al. 2009; Corcoran et al. 2010; Nezlin et al. 2012). The Scripps Pier time series in La Jolla, California (San Diego subregion) documented increased annual mean chlorophyll over the last 18 yr, but there was no obvious simultaneous increase in upwelling (Kim et al. 2009). Although anthropogenic nutrient sources (especially wastewater effluent) have traditionally been ignored as a significant source of N when evaluating algal biomass and community composition in the nearshore environment, the results from this study show that effluent contributes a significant portion of the TN flux, and therefore could explain nearshore chlorophyll variability that is not correlated to natural oceanographic conditions.

In summary, the results from this study contradict the currently held perception that anthropogenic nutrient inputs are negligible in upwelling-dominated regions and are consistent with a growing number of studies that suggest a linkage between anthropogenic N sources and HABs in California nearshore waters (Kudela and Cochlan 2000; Beman et al. 2005; Kudela et al. 2008). Although this study was designed to be a first-order estimation of nutrient sources, the results suggest that anthropogenic nutrients are not negligible compared with natural nutrients and can have ecological effects at local spatial scales. In the urbanized SCB, treated effluent has altered the quantity and composition of the N pool, which may have ecological consequences reflected in changes in algal community composition and has likely increased nearshore primary productivity and the duration of algal blooms. Although there are global examples of increased primary productivity with increased N inputs, quantification of such increases due to anthropogenic sources and determination of the spatial scale for which anthropogenic sources remain a significant component of overall TN in the SCB will be important to evaluate further in future research. The combination of physical and biogeochemical models will provide an important next step toward addressing these aspects of the effects of anthropogenic nutrients in the coastal waters of the SCB. Given that the forms of N can be biologically transformed, an important aspect of future studies should be to determine rates of nitrification and the timescales by which effluent  $\text{NH}_4$  is transformed into  $\text{NO}_3$ , as these processes will alter the forms of N present. Future studies should also include a multiyear source analysis to determine the interannual variability for each source.

#### *Acknowledgments*

We express our gratitude to Becky Schaffner for assistance with map preparation. We thank the two anonymous reviewers as our

manuscript was greatly improved from their suggestions and feedback.

This research was supported by funding provided by the California Ocean Protection Council (Grant Agreement 08-095), the State Water Resources Control Board (Agreement 08-060-250), and NOAA Monitoring and Event Response for HABs (NA05NO54781228).

## References

- ACKERMAN, D., AND K. SCHIFF. 2003. Modeling stormwater mass emissions to the Southern California Bight. *J. Am. Soc. Civ. Eng.* **129**: 308–323, doi:10.1061/(ASCE)0733-9372(2003)129:4(308)
- ANDERSON, D. M., P. M. GLIBERT, AND J. M. BURKHOLDER. 2002. Harmful algal blooms and eutrophication: Nutrient sources, composition, and consequences. *Estuaries* **25**: 704–726, doi:10.1007/BF02804901
- BEMAN, M., K. ARRIGO, AND P. MATSON. 2005. Agricultural runoff fuels large phytoplankton blooms in vulnerable areas of the ocean. *Nature* **434**: 211–214, doi:10.1038/nature03370
- BURKOV, V. A., AND Y. V. PAVLOVA. 1980. Description of the eddy field of the California Current. [Translated from Russian.] *Oceanology* **20**: 272–278.
- CARON, D. A., AND OTHERS. 2010. Harmful algae and their potential impacts on desalination operations off southern California. *J. Water Res.* **44**: 385–416, doi:10.1016/j.watres.2009.06.051
- CHISHOLM, J. R. M., F. E. FERNEX, D. MATHIEU, AND J. M. JAUBERT. 1997. Wastewater discharge, seagrass decline and algal proliferation on the Cote d'Azur. *Mar. Poll. Bull.* **34**: 78–84, doi:10.1016/S0025-326X(96)00072-0
- COCHLAN, W. P., J. HERNDON, AND R. M. KUDELA. 2008. Inorganic and organic nitrogen uptake by the toxigenic diatom *Pseudo-nitzschia australis* (Bacillariophyceae). *Harmful Algae* **8**: 111–118, doi:10.1016/j.hal.2008.08.008
- CONIL, S., AND A. HALL. 2006. Local regimes of atmospheric variability: A case study of Southern California. *J. Clim.* **19**: 4308–4325, doi:10.1175/JCLI3837.1
- CORCORAN, A. A., K. M. REIFEL, B. H. JONES, AND R. F. SHIPE. 2010. Spatiotemporal development of physical, chemical, and biological characteristics of stormwater plumes in Santa Monica Bay, California (USA). *J. Sea Res.* **63**: 129–142, doi:10.1016/j.seares.2009.11.006
- DAILEY, M. D., J. W. ANDERSON, D. J. REISH, AND D. S. GORSLINE. 1993. The Southern California Bight: Background and setting, p. 1–18. *In* M. D. Dailey, D. J. Reish, and J. W. Anderson [eds.], *Ecology of the Southern California Bight*. Univ. of California Press.
- DONG, C., E. Y. IDICA, AND J. C. MCWILLIAMS. 2009. Circulation and multiple-scale variability in the Southern California Bight. *Prog. Oceanogr.* **82**: 168–190, doi:10.1016/j.pocean.2009.07.005
- DORMAN, C. E., AND C. D. WINANT. 1995. Buoy observations of the atmosphere along the west coast of the United States. *J. Geophys. Res. Oceans* **100**: 16029–16044, doi:10.1029/95JC00964
- DUGDALE, R. C. 1967. Nutrient limitation in the sea: Dynamics, identification and significance. *Limnol. Oceanogr.* **12**: 685–695, doi:10.4319/lo.1967.12.4.0685
- EGBERT, G. D., A. F. BENNETT, AND M. G. G. FORE. 1994. Topex/Poseidon tides estimated using a global inverse model. *J. Geophys. Res.* **99**: 24821–24852, doi:10.1029/94JC01894
- EPPLEY, R., E. RENGER, AND W. HARRISON. 1979. Nitrate and phytoplankton production in California coastal waters. *Limnol. Oceanogr.* **24**: 483–494, doi:10.4319/lo.1979.24.3.0483
- FASHAM, M. J. R., H. W. DUCKLOW, AND S. M. MCKELVIE. 1990. A nitrogen-based model of plankton dynamics in the oceanic mixed layer. *J. Mar. Res.* **48**: 591–639, doi:10.1357/002224090784984678
- GARCIA, H. E., R. A. LOCARNINI, T. P. BOYER, AND J. I. ANTONOV. 2006. Nutrients (phosphate, nitrate, and silicate), p. 396. *In* S. Levitus [ed.], *World Ocean Atlas 2005*, V. 4. NOAA Atlas NESDIS 64, U.S. Government Printing Office.
- GLIBERT, P. M., J. HARRISON, C. HEIL, AND S. SEITZINGER. 2006. Escalating worldwide use of urea—a global change contributing to coastal eutrophication. *Biogeochemistry* **77**: 441–463, doi:10.1007/s10533-005-3070-5
- , S. SEITZINGER, C. A. HEIL, J. M. BURKHOLDER, M. W. PARROW, L. A. CODISPOTI, AND V. KELLY. 2005. The role of eutrophication in the global proliferation of harmful algal blooms. *Oceanography* **18**: 198–209, doi:10.5670/oceanog.2005.54
- GOEYENS, L., N. KINDERMANS, M. ABU YUSUF, AND M. ELSKENS. 1998. A room temperature procedure for the manual determination of urea in seawater. *Est. Coast. Shelf Sci.* **47**: 415–418, doi:10.1006/ecss.1998.0357
- GRUBER, N., AND OTHERS. 2006. Eddy-resolving simulation of plankton ecosystem dynamics in the California Current System. *Deep Sea Res. I* **53**: 1483–1516, doi:10.1016/j.dsr.2006.06.005
- HALLEGRAEFF, G. M. 2004. Harmful algal blooms: A global overview, p. 25–49. *In* G. M. Hallegraeff, D. M. Anderson, and A. D. Cembella [eds.], *Manual on harmful marine microalgae*. UNESCO Publishing.
- HAMILTON, P., M. A. NOBLE, J. LARGIER, L. K. ROSENFELD, AND G. ROBERTSON. 2006. Cross-shelf subtidal variability in San Pedro Bay during summer. *Cont. Shelf Res.* **26**: 681–702, doi:10.1016/j.csr.2006.01.009
- HEISLER, J., AND OTHERS. 2008. Eutrophication and harmful algal blooms: A scientific consensus. *Harmful Algae* **8**: 3–13, doi:10.1016/j.hal.2008.08.006
- HICKEY, B. M. 1979. The California Current system: Hypotheses and facts. *Prog. Oceanogr.* **8**: 191–279, doi:10.1016/0079-6611(79)90002-8
- . 1992. Circulation over the Santa Monica–San Pedro basin and shelf. *Prog. Oceanogr.* **30**: 37–115, doi:10.1016/0079-6611(92)90009-0
- HOWARD, M. D. A., W. P. COCHLAN, R. M. KUDELA, AND N. LADIZINSKY. 2007. Nitrogenous preference of toxic *Pseudo-nitzschia australis* (Bacillariophyceae) from field and laboratory experiments. *Harmful Algae* **6**: 206–217, doi:10.1016/j.hal.2006.06.003
- , AND OTHERS. 2012. Southern California Bight 2008 Regional Monitoring Program: Volume IX. Water Quality. Technical Report 710. Southern California Coastal Water Research Project. Costa Mesa, CA.
- HOWARTH, R. W. 2008. Coastal nitrogen pollution: A review of sources and trends globally and regionally. *Harmful Algae* **8**: 14–20, doi:10.1007/BF02804898
- JAUBERT, J. M., J. R. M. CHISHOLM, A. MINGHELLI-ROMAN, M. MARCHIORETTI, J. H. MORROW, AND H. T. RIPLEY. 2003. Re-evaluation of the extent of *Caulerpa taxifolia* development in the northern Mediterranean using airborne spectrographic sensing. *Mar. Ecol. Progr. Ser.* **263**: 75–82, doi:10.3354/meps263075
- KIM, H. J., A. J. MILLER, J. MCGOWAN, AND M. L. CARTER. 2009. Coastal phytoplankton blooms in the Southern California Bight. *Prog. Oceanogr.* **82**: 137–147, doi:10.1016/j.pocean.2009.05.002
- KONDO, J. 1975. Air–sea bulk transfer coefficients in diabatic condition. *Bound.-Layer Meteor.* **9**: 91–112.

- KUDELA, R. M., AND W. P. COCHLAN. 2000. The kinetics of nitrogen and carbon uptake and the influence of irradiance for a natural population of *Lingulodinium polyedrum* (Pyrrophyta) off Southern California. *Aquat. Microbial Ecol.* **21**: 31–47, doi:10.3354/ame021031
- , J. Q. LANE, AND W. P. COCHLAN. 2008. The potential role of anthropogenically derived nitrogen in the growth of harmful algae in California, USA. *Harmful Algae* **8**: 103–110, doi:10.1016/j.hal.2008.08.019
- LANGE, C. B., F. M. H. REID, AND M. VERNET. 1994. Temporal distribution of the potentially toxic diatom *Pseudo-nitzschia australis* at a coastal site in Southern California. *Mar. Ecol. Prog. Ser.* **104**: 309–312, doi:10.3354/meps104309
- LARGE, W. G., AND S. POND. 1981. Open ocean momentum flux measurements in moderate to strong winds. *J. Phys. Oceanogr.* **11**: 324–336, doi:10.1175/1520-0485(1981)011<0324:OOMFMI>2.0.CO;2
- LAPOINTE, B., P. J. BARILE, M. M. LITTLER, AND D. S. LITTLER. 2005. Macroalgal blooms on southeast Florida coral reefs II. Cross-shelf discrimination of nitrogen sources indicates widespread assimilation of sewage nitrogen. *Harmful Algae* **4**: 1106–1122, doi:10.1016/j.hal.2005.06.002
- LAPOINTE, B. E., P. J. BARILE, AND W. R. MATZIE. 2004. Anthropogenic nutrient enrichment of seagrass and coral reef communities in the lower Florida keys: Discrimination of local versus regional nitrogen sources. *J. Exp. Mar. Biol. Ecol.* **308**: 23–58, doi:10.1016/j.jembe.2004.01.019
- LEWITUS, A. J., AND OTHERS. 2012. Harmful algal blooms along the North American west coast region: History, trends, causes and impacts. *Harmful Algae* **19**: 133–159, doi:10.1016/j.hal.2012.06.009
- LYON, G. S., AND E. D. STEIN. 2008. Effluent discharges to the Southern California Bight from small municipal wastewater treatment facilities in 2005, p. 1–14. *In* S. B. Weisberg and K. Miller [eds.], Southern California coastal water research project 2008 annual report. Southern California Coastal Water Research Project.
- MARCHESIELLO, P., J. C. MCWILLIAMS, AND A. F. SHCHEPETKIN. 2003. Equilibrium structure and dynamics of the California Current system. *J. Phys. Oceanogr.* **33**: 753–783, doi:10.1175/1520-0485(2003)33<753:ESADOT>2.0.CO;2
- MCCARTHY, J. J. 1972. The uptake of urea by natural populations of marine phytoplankton. *Limnol. Oceanogr.* **17**: 738–748, doi:10.4319/lo.1972.17.5.0738
- MCPHEE-SHAW, E. E., D. A. SIEGEL, L. WASHBURN, M. A. BRZEZINSKI, J. L. JONES, A. LEYDECKER, AND J. MELACK. 2007. Mechanisms for nutrient delivery to the inner shelf: Observations from the Santa Barbara Channel. *Limnol. Oceanogr.* **52**: 1748–1766, doi:10.4319/lo.2007.52.5.1748
- MOUMEN, N., S.-M. YI, H. A. RAYMOND, Y. J. HAN, AND T. M. HOLSEN. 2004. Quantifying the dry deposition of ammonia in ammonia-rich and ammonia-poor environments using a surrogate surface approach. *Atmos. Environ.* **38**: 2677–2686, doi:10.1016/j.atmosenv.2004.02.010
- NEZLIN, N. P., M. A. SUTULA, R. P. STUMPF, AND A. SENGUPTA. 2012. Phytoplankton blooms detected by SeaWiFS along the central and southern California Coast. *J. Geophys. Res.* **117**: C07004, doi:10.1029/2011JC007773
- O'LOUGHLIN, G., W. HUBER, AND B. CHOCAT. 1996. Rainfall-runoff processes and modeling. *J. Hydr. Res.* **34**: 733–751, doi:10.1080/00221689609498447
- PAERL, H. W., AND M. F. PIEHLER. 2008. Nitrogen and marine eutrophication, p. 529–567. *In* D. Capone, D. Bronk, M. Mulholland, and E. Carpenter [eds.], Nitrogen in the marine environment. Elsevier.
- QUAY, J. 2011. New tools and insight for the recognition of *Pseudo-nitzschia* blooms and toxin incidence. Ph.D. thesis. Univ. of California, Santa Cruz.
- RAYMOND, H. A., S.-M. YI, N. MOUMEN, Y. J. HAN, AND T. M. HOLSEN. 2004. Quantifying the dry deposition of reactive nitrogen and sulfur-containing species in remote areas using a surrogate surface analysis approach. *Atmos. Environ.* **38**: 2687–2697, doi:10.1016/j.atmosenv.2004.02.011
- REIFEL, K. M., A. A. CORCORAN, C. CASH, R. SHIPE, AND B. H. JONES. 2013. Effects of a surfacing effluent plume on a coastal phytoplankton community. *Cont. Shelf Res.* **60**: 38–50, doi:10.1016/j.csr.2013.04.012
- RYTHER, J., AND W. DUNSTAN. 1971. Nitrogen, phosphorus and eutrophication in the coastal marine environment. *Science* **171**: 1008–1112, doi:10.1126/science.171.3975.1008
- SANDWELL, D. T. 1987. Biharmonic spline interpolation of GEOS-3 and SEASAT altimeter data. *Geophys. Res. Lett.* **14**: 139–142, doi:10.1029/GL014i002p00139
- SCHNETZER, A., AND OTHERS. 2007. Blooms of *Pseudo-nitzschia* and domoic acid in the San Pedro Channel and Los Angeles harbor areas of the Southern California Bight, 2003–2004. *Harmful Algae* **6**: 372–387, doi:10.1016/j.hal.2006.11.004
- , AND ———. 2013. Coastal upwelling linked to toxic *Pseudo-nitzschia australis* blooms in Los Angeles coastal waters, 2005–2007. *J. Plankton Res.* **35**: 1080–1092, doi:10.1093/plankt/fbt051
- SEUBERT, E. L., AND OTHERS. 2013. Seasonal and annual dynamics of harmful algae and algal toxins revealed through weekly monitoring at two coastal ocean sites off southern California, USA. *Environ. Sci. Pollut. Res.* **20**: 6878–6895, doi:10.1007/s11356-012-1420-0
- SHCHEPETKIN, A. F., AND J. C. MCWILLIAMS. 2005. The regional oceanic modeling system (ROMS): A split-explicit, free-surface, topography-following-coordinate oceanic model. *Ocean Mod.* **9**: 347–404, doi:10.1016/j.ocemod.2004.08.002
- SONG, Y., AND D. B. HAIDVOGEL. 1994. A semi-implicit ocean circulation model using a generalized topography-following coordinate system. *J. Comp. Phys.* **115**: 228–244, doi:10.1006/jcph.1994.1189
- STEIN, E. D., L. L. TIEFENTHALER, AND K. C. SCHIFF. 2007. Sources, patterns and mechanisms of storm water pollutant loading from watersheds and land uses of the greater Los Angeles area, California, USA. Technical Report 510. Costa Mesa: Southern California Coastal Water Research Project.
- SVERDRUP, H. U., AND R. H. FLEMING. 1941. The waters off the coast of southern California, March to July 1937. *Bulletin of the Scripps Institution of Oceanography* **4**: 261–378.
- THOMPSON, P., AND A. WAITE. 2003. Phytoplankton responses to wastewater discharges at two sites in Western Australia. *Mar. Freshw. Res.* **54**: 721–735, doi:10.1071/MF02096
- TRAINER, V., AND OTHERS. 2000. Domoic acid production near California coastal upwelling zones, June 1998. *Limnol. Oceanogr.* **45**: 1818–1833, doi:10.4319/lo.2000.45.8.1818
- WARRICK, J., L. WASHBURN, M. BRZEZINSKI, AND D. SIEGEL. 2005. Nutrient contributions to the Santa Barbara Channel, California, from the ephemeral Santa Clara River. *Est. Coast. Shelf Sci.* **62**: 559–574, doi:10.1016/j.ecss.2004.09.033

Associate editor: Mary I. Scranton

Received: 02 March 2013

Accepted: 03 September 2013

Amended: 02 November 2013

## Nutrient Loading through Submarine Groundwater Discharge and Phytoplankton Growth in Monterey Bay, CA

Alanna L. Lecher,<sup>\*,†</sup> Katherine Mackey,<sup>‡,‡</sup> Raphael Kudela,<sup>§</sup> John Ryan,<sup>||</sup> Andrew Fisher,<sup>†</sup> Joseph Murray,<sup>§</sup> and Adina Paytan<sup>†,⊥</sup>

<sup>†</sup>Department of Earth and Planetary Sciences, University of California Santa Cruz, 1156 High Street, Santa Cruz, California 95064, United States

<sup>‡</sup>Earth System Science, University of California Irvine, Irvine, California 92617, United States

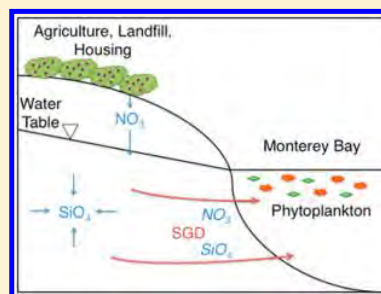
<sup>§</sup>Department of Ocean Sciences, University of California Santa Cruz, Santa Cruz, California 95064, United States

<sup>||</sup>Monterey Bay Aquarium Research Institute, Moss Landing, California 95039, United States

<sup>⊥</sup>Institute of Marine Sciences, University of California Santa Cruz, Santa Cruz, California 95064, United States

### Supporting Information

**ABSTRACT:** We quantified groundwater discharge and associated nutrient fluxes to Monterey Bay, California, during the wet and dry seasons using excess  $^{224}\text{Ra}$  as a tracer. Bioassay incubation experiments were conducted to document the response of bloom-forming phytoplankton to submarine groundwater discharge (SGD) input. Our data indicate that the high nutrient content (nitrate and silica) in groundwater can stimulate the growth of bloom-forming phytoplankton. The elevated concentrations of nitrate in groundwater around Monterey Bay are consistent with agriculture, landfill, and rural housing, which are the primary land-uses in the area surrounding the study site. These findings indicate that SGD acts as a continual source of nutrients that can feed bloom-forming phytoplankton at our study site, constituting a nonpoint source of anthropogenic nutrients to Monterey Bay.



### INTRODUCTION

Immense quantities of nutrients are injected into the euphotic zone in eastern boundary upwelling systems, resulting in high levels of primary productivity.<sup>1,2</sup> Our study region, Monterey Bay, California (Supporting Information Figure 1), lies in the California Current System, the eastern boundary upwelling system of the North Pacific. Climatological conditions in outer Monterey Bay show seasonally modulated upwelling and associated high productivity between approximately March and November.<sup>3</sup> Regional wind driven upwelling exhibits strong variability on not only seasonal, but also interannual and intraseasonal time scales. Interannual variability is linked to larger scale phenomena, such as El Niño.<sup>4,5</sup> Intraseasonal variability occurs through alternation of upwelling and relaxation/downwelling on time scales of days to weeks,<sup>6–8</sup> with consequences for phytoplankton bloom ecology.<sup>9–11</sup> The advective supply of nutrients to Monterey Bay from regional upwelling originates at upwelling centers north and south of the bay.<sup>7,8</sup> Upwelling can also occur within the bay, in response to diurnal sea-breeze forcing.<sup>12</sup> In addition to wind-forced upwelling, internal oscillations over Monterey Canyon can force nutrient fluxes from the canyon onto the shelf.<sup>13</sup> Blooms of algae in general and particularly of harmful algal species in Monterey Bay have been directly linked to canyon upwelling and regional wind-driven upwelling.<sup>11,14</sup>

The purpose of this study is to examine the potential role of submarine groundwater discharge (SGD) in affecting phyto-

plankton blooms in Monterey Bay. Extensive agriculture is prevalent near the bay's coast, and nutrients from fertilizers and other land based sources (sewage, landfills) may affect coastal phytoplankton ecology through land-sea nutrient fluxes, by surface or submarine transport pathways.<sup>15</sup> Nitrate is the primary limiting nutrient in this environment and during rain-induced land flushing events, the supply of nitrate from local rivers can exceed that from upwelling.<sup>16–18</sup> For example, a harmful algal bloom that caused mass stranding of seabirds in Monterey Bay started as a small but intense bloom near the outlet of a river, days after the first land flush of the rainy season.<sup>19</sup> These observations suggested a role of land-derived nutrients in bloom inception. Statistical description of exceptionally dense dinoflagellate "red tide" blooms, detectable by remote sensing, shows maximum frequency and intensity in near coastal waters of Northern Monterey Bay (NMB).<sup>20</sup> Alternative hypotheses for the near-coastal blooms include oceanographic forcing of nutrient fluxes into near-coastal habitat and near-coastal convergence in which motile phytoplankton accumulate.<sup>9,20,21</sup> Atmospheric deposition is a relatively small contributor to the bay's nutrient budget during most of the year.<sup>17</sup> One additional source of nutrients that has

Received: February 19, 2015

Revised: May 3, 2015

Accepted: May 6, 2015

Published: May 19, 2015



not been quantified is that associated with SGD, particularly along the northern margin of the bay where these blooms occur repeatedly. Indications of ecological impacts from land drainage motivate better understanding of terrestrial nutrient sources from both surface land drainage and SGD. Two primary aquifers (Aromas Sands and Purisima) and a more limited alluvial aquifer outcrop within NMB, and may act as preferential flow paths for SGD into the bay.<sup>22</sup> We characterize the nutrient composition of SGD flowing into NMB and phytoplankton responses to SGD amendments in incubation experiments to develop a better understanding of SGD and its potential influences on phytoplankton ecology in Monterey Bay.

SGD is a mix of fresh groundwater and seawater that has circulated through the coastal aquifer because of tide and wave action before discharging to the ocean.<sup>23</sup> SGD can account for a considerable fraction of nutrient loads to water bodies.<sup>24–28</sup> While upwelling and stream flows occur during defined and restricted times of the year, SGD may be a consistent source of nutrients to NMB throughout the year because of slow aquifer response and relatively consistent tidal and wave pumping.<sup>23</sup> Radium isotopes are often used as effective natural tracers of SGD because of their enrichment in brackish and saline coastal groundwater compared to receiving seawater and their relatively well-constrained behavior after discharge.<sup>29</sup> Specifically, <sup>224</sup>Ra with a half-life of ~3.5 days is useful to quantify SGD in coastal areas where water residence time is short because of extensive wave action and mixing.

## ■ MATERIALS AND METHODS

**Study Area, Sampling Procedures, and Sample Analyses.** Sunset State Beach (36° 52.790' N, 121° 49.685' W) is located in NMB, well within the area of bloom formation (map in Supporting Information Figure 1). Land use in the area surrounding Sunset State Beach is largely agricultural with a year-round growing season because of central California's Mediterranean climate and irrigation in the dry season. Rural residential units with septic tanks and a landfill are also located near the study site.

Discrete seawater and groundwater samples were collected twice, at the end of the wet season (May 2012) and at the end of the dry season (October 2012). Groundwater samples were collected on the beach using temporary well points installed to a depth that allowed sampling of the coastal unconfined aquifer. Samples were also collected farther inland from established nested monitoring wells screened in the upper Aromas, lower Aromas, and the alluvial aquifers.<sup>30</sup> No samples were collected from the Purisima aquifer, which is not thought to contribute to SGD as much as the Aromas aquifer because of its formation properties.<sup>30</sup> Surface seawater samples were collected from the surf-zone and along transects extending off-shore perpendicular to the beach (up to 3.1 km).

Large volume water samples (80–120 L for seawater and 13–120 L for groundwater) were collected using either submersible pumps or buckets (for surface water). Water samples were passed through columns containing MnO<sub>2</sub>-impregnated acrylic fiber at a rate of <1.5 L min<sup>-1</sup> for collection of Ra isotopes.<sup>31</sup> Samples were analyzed at the University of California Santa Cruz (UCSC) on a radium delayed coincidence counter (RaDeCC) for measurement of <sup>224</sup>Ra activities.<sup>32</sup> Samples were analyzed on the RaDeCC again 3–5 weeks after collection for <sup>224</sup>Ra to correct for <sup>224</sup>Ra that is produced from <sup>228</sup>Th decay.<sup>31</sup> Standards were run on a monthly

basis as part of the quality control for maintenance of the instrument. Analytical error of the instrument was calculated and is typically <10%.<sup>33</sup>

Brackish and saline groundwater discharge (for our purposes salinity ≥ 5) was calculated using a well-established mass balance model:<sup>34–36</sup>  $SGD = (Ra_{\text{box}} - Ra_{\text{off}})(V/R)/(1/Ra_{\text{gw}})$ . Groundwater radium activity ( $Ra_{\text{gw}}$ ) was calculated from an average of the saline and brackish groundwater samples, and ocean Ra activity ( $Ra_{\text{box}}$ ) was calculated from a weighted average of the near shore and transect samples, where surf-zone samples were averaged first, the result of which was averaged with the transect values. This prevents artificially high SGD fluxes due to preferential sampling of the surf zone. The residence time of water in the coastal area (R) studied (8 days) was taken from the literature.<sup>37</sup>  $Ra_{\text{off}}$  is the activity of radium offshore. Discharge (SGD) was normalized per meter of shoreline. Thus, a volumetric unit (V) of the area studied was defined by the length of the transect (3.1 km), 1 m of shoreline, and depth of the thermocline in the near shore (4 m),<sup>4,20</sup> which confines the majority of phytoplankton to the mixed layer. A deeper mixed layer, as occurs further offshore, would increase the calculated SGD (as more SGD would be needed to balance more radium in the larger mixed layer), hence our calculations are conservative.

For nutrient analysis, water was collected in 500 mL HPDE acid-cleaned sample rinsed bottles and stored on ice in a cooler until filtering (within 12 h). Forty milliliter aliquots were filtered (0.45 μm) into acid-cleaned centrifuge tubes and frozen until analysis. Nitrate, silica, and soluble reactive phosphate were measured by colorimetric methods on a flow injection auto analyzer (FIA, Lachat Instruments Model QuickChem 8000).

**Bioassay-Incubation Experiments.** Two bioassay incubation experiments were conducted to determine if SGD can support bloom-forming species of Monterey Bay. The first incubation experiment was conducted in June 2011 (hereafter referred to as EX1), and the second experiment was conducted in November 2012 (hereafter referred to as EX2). Bay water for both experiments was collected from within NMB (collection locations shows on Supporting Information Figure 1); water was collected so as to avoid ongoing blooms.

Groundwater for the incubations was collected from the upper Aromas Sand Aquifer (same well as for Ra) the day before each experiment. Groundwater was collected via a pumping system installed in the monitoring well into acid-cleaned carboys, and kept in the dark during transport. The groundwater was filtered through a 0.2 μm cartridge into an acid-cleaned container and stored at 8 °C until use in the experiments the next day. Aliquots were taken for nutrient concentrations of nitrate, ammonium, soluble reactive phosphate, and soluble reactive silica.

NMB water was filtered through 105 μm mesh to remove zooplankton grazers into 20 L acid-cleaned sample-rinsed carboys, which were kept in the dark during transport to the UCSC. Aliquots were taken for nutrient concentrations of nitrate, ammonium, soluble reactive phosphate, and soluble reactive silica prior to amendments (baseline) and processed as previously described. The water was distributed randomly into acid-cleaned sample-rinsed 500 mL clear polycarbonate bottles to which nutrients or groundwater was added (see below). Three bottles were processed from each treatment immediately following additions (time zero,  $t_0$ ) for the following analyses: chlorophyll *a*, nutrient concentrations, flow cytometry, and

phytoplankton species abundance. Remaining bottles were placed into a flow-through tank at Long Marine Lab through which Monterey Bay water was continuously pumped to maintain surface ocean temperature. The tank was covered with shading (50% attenuated irradiance) material to simulate mixed layer light levels. Three bottles from each treatment were removed from the tank and processed for chlorophyll *a*, nutrient concentrations, flow cytometry, and species abundance after 24, 48, and 72 h, for a total of 12 bottles per treatment and control for each experiment.

Treatments included a control (no additions), additions of nitrate (target concentration = 30  $\mu\text{M}$  for both experiments), ammonium (10  $\mu\text{M}$  for both experiments), urea (5  $\mu\text{M}$ , EX1 only), phosphate (1  $\mu\text{M}$  for both experiments), silica (20  $\mu\text{M}$ , EX 2 only), dissolved organic phosphorus (5  $\mu\text{M}$ , EX1 only), iron (5  $\mu\text{M}$ , EX1 only), vitamin B12 (100 pM, EX1 only), and a combination of nitrate and silica (30 and 20  $\mu\text{M}$ , respectively, EX2 only). Amendments were based on nutrient concentrations in upwelled water in Monterey Bay.<sup>3</sup> Groundwater additions were 50%, 20%, and 10% by volume (EX1) and 10%, 5%, and 1% by volume (EX2). We deliberately added more groundwater (as a percent contribution) to the treatment bottles than would be found naturally in the bay to elicit a response that could be observed in 3 days.

**Chlorophyll *a*.** Samples for chlorophyll *a* were collected by filtering 200 mL aliquots under gentle vacuum onto Whatman GF/F filters and stored frozen until analyzed. Filters were extracted for 16 h in 90% acetone at 6 °C in the dark. Fluorescence was measured with a Turner Fluorometer (Turner Designs 10-AU-005 CE). Groundwater treatment samples were multiplied by a coefficient to account for dilution of the original seawater volume used in the groundwater treatments.

**Flow Cytometry.** Flow cytometry samples (1.5 mL) were collected and fixed with glutaraldehyde to a final concentration of 0.1%, and stored at -80 °C until analysis on a Cytospeia Influx flow cytometer. FlowJo software was used for data analysis (TreeStar Inc.). Cells were classified as *Synechococcus* or Picoeukaryotes based on size and on autofluorescence characteristics. Total cell counts were normalized to sample volume.

**Phytoplankton Abundance.** Samples for determining phytoplankton abundances were collected by fixing 50 mL aliquots with formalin to a final concentration of 0.4% and stored in the dark at 6 °C. Phytoplankton ( $\geq 15 \mu\text{m}$ ) were enumerated according to previously established methods,<sup>38</sup> using Utermöhl settling chambers for 24 h. Counts were completed on an Olympus IX 70 Inverted microscope equipped with epi-fluorescence, with 400 cells counted from each sample at 200 $\times$  magnification.

## RESULTS AND DISCUSSION

**SGD Nutrient Fluxes.**  $\text{Ra}^{224}$  activity (Supporting Information Tables 1 and 2) was highest in saline/brackish (here defined as salinity  $\geq 5$ ) groundwater (wet season,  $138 \pm 12$  dpm  $100 \text{ L}^{-1}$ ; dry season,  $138 \pm 32$  dpm  $100 \text{ L}^{-1}$ ), followed by fresh (here salinity  $< 5$ ) groundwater (wet season,  $12 \pm 2$  dpm  $100 \text{ L}^{-1}$ ; dry season,  $18 \pm 2$  dpm  $100 \text{ L}^{-1}$ ), then coastal seawater within the NMB (wet season,  $2.3 \pm 2.6$  dpm  $100 \text{ L}^{-1}$ ; dry season,  $3.8 \pm 4.5$  dpm  $100 \text{ L}^{-1}$ ), and the lowest activities were seen in off-shore water (wet season,  $0.17$  dpm  $100 \text{ L}^{-1}$ ; dry season,  $0.69$  dpm  $100 \text{ L}^{-1}$ ).  $^{228}\text{Th}$  activity was typically less than 5% of  $^{224}\text{Ra}$ . These averages represent weighted averages

of the near shore and transect samples, where surf-zone samples were averaged first, the result of which was averaged with the transect values. The same weighted average was used for nutrient concentrations following. Brackish/saline groundwater was statistically different from fresh groundwater and seawater using ANOVA ( $F = 25.85$ ,  $p \leq 0.01$ ) and Tukey's ( $p \leq 0.01$ ). Using the same analysis,  $\text{Ra}^{224}$  activities in fresh groundwater and seawater were not statistically different. Differences between seasons for each water type were also not statistically different. These results indicate  $^{224}\text{Ra}$  is a good tracer of brackish/saline groundwater at this site. Brackish/saline groundwater is likely to be the dominant type of SGD at this site because of the lack of fresh water near the shoreline. SGD calculated using the mass balance box model in the wet season is  $24 \pm 19 \text{ m}^3 \text{ m}^{-1} \text{ day}^{-1}$  ( $17 \pm 13 \text{ L m}^{-1} \text{ min}^{-1}$ ); the SGD in the dry season is calculated to be  $35 \pm 22 \text{ m}^3 \text{ m}^{-1} \text{ day}^{-1}$  ( $24 \pm 15 \text{ L m}^{-1} \text{ min}^{-1}$ ). Errors were determined following the general rule for error propagation,<sup>39</sup> and are based on natural sample variability, which was greater than analytical error. These fluxes are consistent with fluxes observed in other beaches of similar geology in central California.<sup>25,40</sup> Although the dry season SGD flux is slightly higher than the wet season flux, wet and dry season SGD values are within error relative to each other. This is consistent with our hypothesis that submarine groundwater discharges continuously throughout the year. The persistent SGD flux during the late summer and early fall (when inputs from other nutrient sources are generally lower compared to other times of the year) suggests that SGD nutrient flux may be particularly important for sustaining the phytoplankton because its relative contribution to the total nutrient pool is higher at that time.

In the wet season, nitrate, silica, and phosphate concentrations (Supporting Information Tables 1 and 2) were highest in the fresh groundwater ( $330 \pm 320$ ,  $350 \pm 14$ , and  $7.5 \pm 5.2 \mu\text{M}$ , respectively), were lower in the saline/brackish groundwater ( $110 \pm 68$ ,  $96 \pm 38$ , and  $2.2 \pm 0.3 \mu\text{M}$ , respectively), and lowest in the coastal NMB water ( $3.6 \pm 1.6$ ,  $3.8 \pm 1.2$ , and  $0.8 \pm 0.1 \mu\text{M}$ , respectively). Offshore concentrations were higher than those in NMB (12.8, 15.9, and  $1.09 \mu\text{M}$ , respectively), most-likely due to upwelling of nutrient-rich water further offshore, which is common in May.<sup>3</sup>

In the dry season, nitrate, silica, and phosphate concentrations were highest in the fresh groundwater ( $200 \pm 100$ ,  $280 \pm 20$ , and  $3.9 \pm 1.2 \mu\text{M}$ , respectively), lower in the saline/brackish groundwater ( $110 \pm 24$ ,  $106 \pm 47$ , and  $2.4 \pm 0.4 \mu\text{M}$ , respectively), and lowest in seawater of NMB ( $4.1 \pm 1.9$ ,  $6.3 \pm 1.9$ , and  $0.7 \pm 0.1 \mu\text{M}$ , respectively). Offshore values (outside the bloom area) were similar to those in NMB waters for phosphate ( $0.7 \mu\text{M}$ ) and lower for nitrate and silica ( $1.1$  and  $5.7 \mu\text{M}$ ). These data suggest there was no offshore source (such as upwelling) during this sampling period. There was no significant difference across seasons and water types for nutrient concentrations using ANOVA ( $p \geq 0.05$ ) except for silica in the wet season when the fresh groundwater was statistically different from other water types.

Multiplying the SGD volume flux of each season by the corresponding saline/brackish groundwater end-member nutrient concentrations yields estimated nutrient fluxes. Nitrate fluxes were similar for the wet season ( $2.6 \text{ mol m}^{-1} \text{ day}^{-1}$ ) and dry season ( $3.9 \text{ mol m}^{-1} \text{ day}^{-1}$ ). Silica fluxes were higher in the wet season ( $8.3 \text{ mol m}^{-1} \text{ day}^{-1}$ ) than the dry season ( $3.7 \text{ mol m}^{-1} \text{ day}^{-1}$ ) because of the higher silica concentration in the groundwater in the wet season. Phosphate fluxes were similar in

the wet season ( $0.05 \text{ mol m}^{-1} \text{ day}^{-1}$ ) and dry season ( $0.08 \text{ mol m}^{-1} \text{ day}^{-1}$ ). Overall it appears nutrient fluxes are relatively consistent across seasons. The nitrate and silica fluxes are higher than the nearby San Francisco Bay ( $\leq 0.7 \text{ mol m}^{-1} \text{ day}^{-1}$  nitrate and  $0.25\text{--}0.5 \text{ mol m}^{-1} \text{ day}^{-1}$  silica). However, these differences may be due to less wave activity, and therein less SGD volume flux in San Francisco Bay since it is more protected than Monterey Bay.<sup>27</sup> SGD-associated nutrient fluxes at Stinson Beach, a beach ~6 miles north of San Francisco, has similar nutrient fluxes ( $1.4\text{--}2.4 \text{ mol m}^{-1} \text{ day}^{-1}$  nitrate,  $3.3\text{--}5.4 \text{ mol m}^{-1} \text{ day}^{-1}$  silica, and  $0.08\text{--}0.14 \text{ mol m}^{-1} \text{ day}^{-1}$  phosphate) to Monterey Bay.<sup>40</sup>

A persistent flux of nutrients through SGD contributes to an environment conducive to phytoplankton growth. Specifically, the coupled nitrate and silica SDG fluxes in a ratio of near 1:1, provide optimal conditions for diatom-based blooms, consistent with the observed repeated occurrences of *Pseudo-nitzschia* blooms in NMB.<sup>41,42</sup> SGD phosphate fluxes are below the Redfield ratio (required, N/P 16:1; observed, N/P ~30–75:1). Previous studies have shown that nitrogen is the limiting nutrient in NMB and phosphate is likely supplied through efficient recycling by phytoplankton and utilization of organic phosphorus compounds within this region.<sup>21,42,43</sup>

**Incubation Experiment Results. Chlorophyll *a*.** For EX1, the control showed little change in chlorophyll *a* over the duration of the experiment: phosphate, iron, vitamin B12, dissolved organic phosphorus, and the 50% groundwater treatments did not differ significantly from the control (Figure 1) using ANOVA (EX1,  $F = 35.7$ ,  $p \leq 0.01$ ) and Tukey's ( $p \leq 0.05$ , here and hereafter). The 10% groundwater treatment showed the most significant increase in chlorophyll *a* with time, followed by the 20% groundwater treatment. Additions of

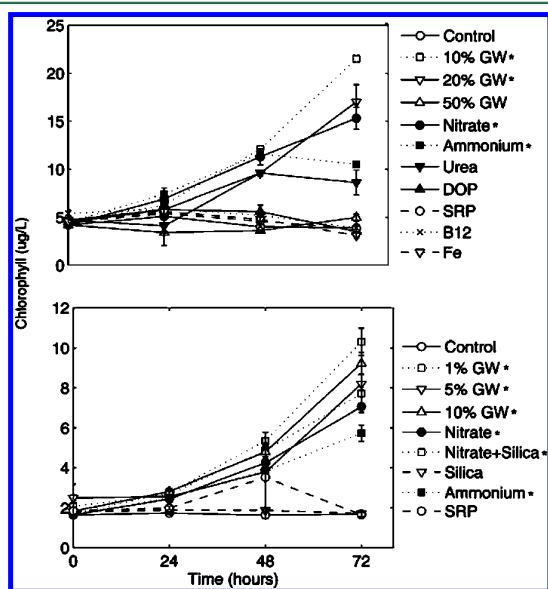


**Figure 1.** Chlorophyll at each time point for each treatment for EX1 (top) and EX2 (bottom). In EX1 the 10% groundwater treatment showed the most growth, followed by 20% groundwater, nitrate, ammonium, and urea treatments. In EX2, the nitrate plus silicate treatment showed the most growth, followed by the 10% groundwater, 5% groundwater, 1% groundwater, nitrate, and ammonium treatments. Treatments statistically different from the control are denoted with an asterisk.

nitrogen (nitrate, ammonium) also resulted in statistically significant chlorophyll *a* increases, although not as much as the groundwater treatments.

For EX2 (EX2  $F = 47.55$ ,  $p \leq 0.01$ ), the control showed no change in chlorophyll *a* concentration with time and the sole amendments with phosphate or silicate did not differ significantly from the control (Figure 1). The combined nitrate+silica treatment showed the most increase in chlorophyll *a* with time, followed by the 10% groundwater, 5% groundwater, 1% groundwater, and nitrogen (nitrate and ammonium) treatments in that order (Figure 1).

The nitrate + silica treatment group in EX2 was designed to simulate the nutrient combinations in groundwater that we suspected spurred growth observed in the groundwater treatments of EX1. Indeed the growth response to the nitrate + silica addition (even more than the growth with the groundwater treatments) in EX2 supports our hypothesis that it was the combination of these two nutrients together which spurred the growth observed in the groundwater treatments. The diatom dominance in many of the blooms in NMB also points to a need for both silica and nitrogen to sustain these blooms.

**Nutrients.** Initial nutrient concentrations in groundwater and ocean water were similar for ammonium for both EX1 and EX2 (shown in table form Supporting Information Table 3). More ammonium was present in the groundwater ( $0.9 \mu\text{M}$ ) in EX1 than the ocean water ( $0.6 \mu\text{M}$ ), while more ammonium was present in the ocean water ( $1.0 \mu\text{M}$ ) than the groundwater ( $0.5 \mu\text{M}$ ) for EX2. Groundwater phosphate (EX1,  $3.7 \mu\text{M}$ ; EX2,  $1.0 \mu\text{M}$ ) for both experiments was higher than the ocean water (EX1,  $0.5 \mu\text{M}$ ; EX2,  $0.3 \mu\text{M}$ ). Nitrate and silica concentrations were much higher in the groundwater (EX1, 1186.6 and  $750.1 \mu\text{M}$ , respectively; EX2, 629.1 and  $459.1 \mu\text{M}$ , respectively) than the ocean water (EX1, 2.6 and  $3.5 \mu\text{M}$ ; EX2, 0.7 and  $2.7 \mu\text{M}$ ) for both experiments. Relatively low concentrations of ammonium (e.g., similar to seawater) suggest groundwater is not an important source of nitrogen in the form of ammonium to NMB. In contrast, nitrate concentrations in groundwater are orders of magnitude higher than in seawater. Our incubation experiments indicate that to maximize algal growth (chlorophyll *a*) in the water collected from NMB both nitrate and silica are needed, consistent with the expectation that diatoms grow at a molar ratio of ~1:1 N/Si.<sup>44</sup>

Changes in concentration of phosphate, silica, nitrate, and ammonium over the 3 day incubation are shown in Figure 2. Values were calculated by subtracting the initial nutrient concentration of each treatment (Supporting Information Table 4) from the final nutrient concentrations. Negative values indicate a decrease in concentration (nutrient drawdown assumed to be uptake by phytoplankton), while positive values indicate an increase in nutrient concentration in the bottles (due to excretion, cell lysis, or microbial or chemical transformations). Negative values extending beyond the dotted line in Figure 2 indicate nutrient drawdown in excess of the concentrations present in the ocean water used for the experiment, indicating phytoplankton utilized nutrients provided by either the groundwater or nutrient additions.

Phosphate concentration decreased for all treatments in EX1. All decreases in phosphate concentration for EX1 were statistically significant using the two-sample *t* test ( $p \leq 0.05$ ) where initial phosphate concentrations of each treatment group were tested against final phosphate concentrations of the same treatment, except for the decrease observed in the phosphate

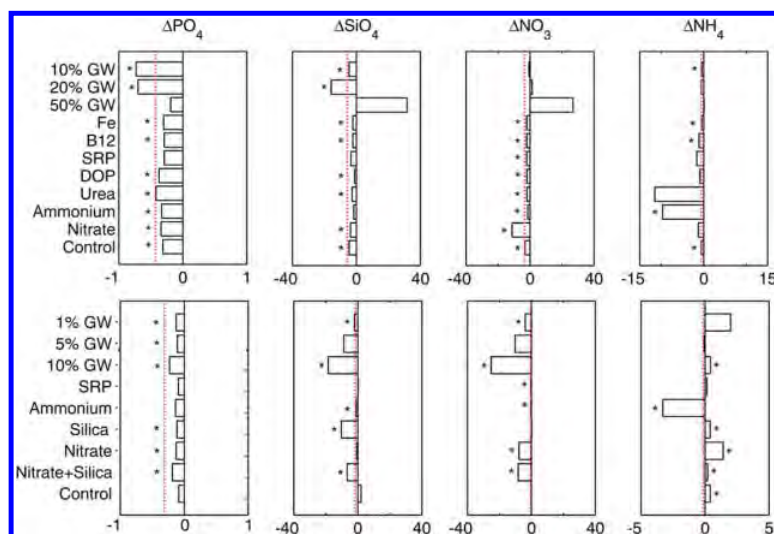


**Figure 2.** Change in phosphate, silicate, and nitrate concentration in the water of each treatment over each 3 days for with EX1 (top row) and EX2 (bottom row). Negative values indicate uptake by phytoplankton. The dotted line indicates the portion of uptake that could have been supplied by pretreatment Monterey Bay water. Negative values beyond this line indicate use of nutrients supplied by treatments. Drawdown of nitrate and silicate in EX2 correspond to the greatest chlorophyll increases observed. Units are in  $\mu\text{M}$ . An asterisk denotes the change is statistically significant.

and 50% groundwater treatments, both containing much higher phosphate than the other treatments and thus the fraction utilized ( $\pm 0.4$  and  $0.2 \mu\text{M}$ ) is very small with respect to phosphate decreases in other treatments, which were all larger (Figure 2) and similar to the analytical error ( $\pm 0.2$  and  $\pm 0.1 \mu\text{M}$ ). Only the 10% groundwater and 20% groundwater treatment groups showed a decrease in phosphate concentration beyond what could have been supplied by the ocean water, indicating phytoplankton drawdown of phosphate supplied by the groundwater. The phosphate concentration similarly decreased for all treatments in EX2. These decreases for EX2 were statistically significant, except for the decrease observed in the control and the treatment receiving high phosphate addition (again likely because of error in the latter case). Unlike EX1, none of the treatment groups showed a decrease in phosphate concentration beyond what could have been supplied by the ocean water. These results are consistent with the phytoplankton community in NMB being phosphate replete. However, when nitrate and silica are provided and growth is extensive phosphate may become limiting. Phosphate from SGD is then utilized and may enable further drawdown of nitrate and silica.

The silica concentration decreased for nearly all of the treatment groups in EX1, with a decrease of  $4.6 \pm 0.7 \mu\text{M}$  for the control and ranged between  $16 \pm 3 \mu\text{M}$  for the 20% groundwater treatment (largest decrease observed) and  $1 \pm 1 \mu\text{M}$  for the phosphate treatment (smallest decrease observed). All of these decreases were statistically significant, except for the decrease observed in the ammonium and the phosphate treatments. Only the 20% groundwater treatment group showed a decrease in concentration beyond what could have been supplied by the ocean water. The 50% groundwater treatment showed an increase of  $30 \pm 20 \mu\text{M}$ ; we attribute this to experimental error as there was no other source of silica in the treatment bottles; a 2% error in the amount of groundwater added to the bottles of the treatment groups would account for the increase seen, which was not statistically significant. The initial silica concentrations of this treatment group ( $416.6$ ,

$359.4$ , and  $348.0 \mu\text{M}$ ) have a range larger than all other treatment groups ( $< 5 \mu\text{M}$  silica) which also stems from analytical error in the amount of groundwater added to this treatment. This could result in a calculated increase which is not real (final silica concentrations for this treatment  $414.2$ ,  $398.7$ , and  $406.0 \mu\text{M}$ ).

In EX2, the 10% groundwater treatment showed the largest decrease in silica concentration,  $18 \pm 4 \mu\text{M}$ , and the nitrate treatment showed the smallest decrease,  $0.6 \pm 0.3 \mu\text{M}$ . The 10% groundwater, 5% groundwater, 1% groundwater, nitrate+silica, and silica treatment groups showed a decrease in silica concentration beyond what could have been supplied by the ocean water, indicating phytoplankton utilized silica supplied by the groundwater or nutrient additions. The decrease observed in these treatments, as well as the ammonium treatment, were statistically significant. The control and SRP treatments showed increases of  $2 \pm 3$  and  $0 \pm 1 \mu\text{M}$ , respectively, neither of which were statistically significant at the  $p \leq 0.05$  level. These results suggest that when nitrate is available silica is drawn down and groundwater becomes an important source of silica.

In EX1, the nitrate treatment showed the largest decrease in nitrate concentration,  $11.2 \pm 0.6 \mu\text{M}$ , and the 10% groundwater treatment showed the smallest decrease,  $0 \pm 2 \mu\text{M}$ . The control showed a decrease of  $3.1 \pm 0.1 \mu\text{M}$ . All of these decreases were statistically significant. Only the nitrate treatment group showed a decrease in nitrate concentration beyond what could have been supplied by the ocean water, indicating that nitrate could be limiting growth as previously reported for Monterey Bay.<sup>16,21</sup> Nitrate in the 20% and 50% groundwater treatments increased ( $1 \pm 2$  and  $30 \pm 40 \mu\text{M}$ , respectively). However, the increase observed in the 20% and 50% and the small change in 10% groundwater treatments were likely due to analytical errors associated with respect to adding the groundwater, similar to the silicate increases observed in EX1. Initial and final ranges for the 20% treatment ( $228.9$ – $231.7$  and  $228.3$ – $234.2 \mu\text{M}$ , respectively) show that this initial range is encompassed in the final range of almost  $5 \mu\text{M}$ . Similarly for the 50% treatment, the initial ( $507.8$ – $556.0 \mu\text{M}$ ) and final

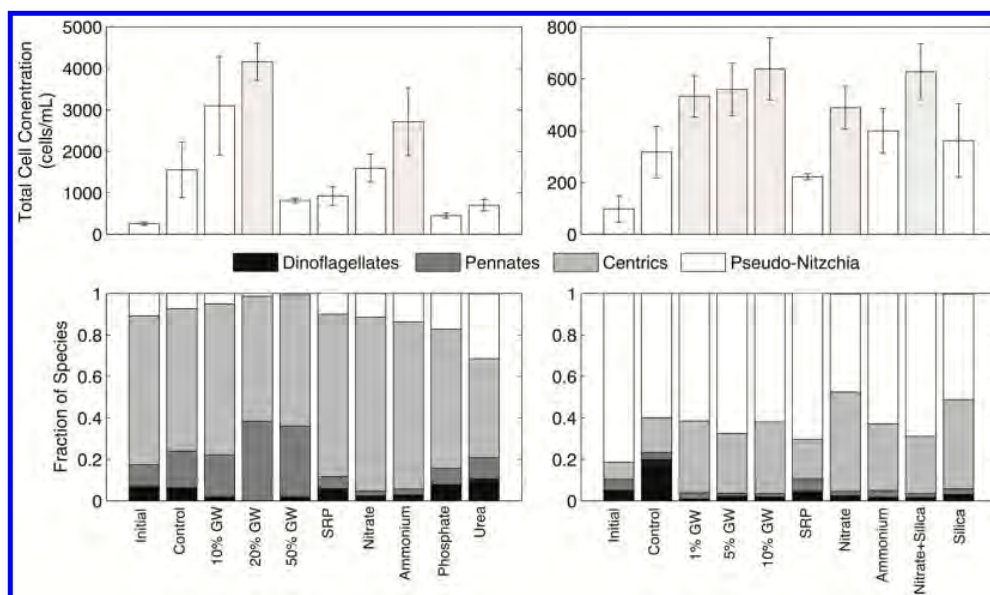


**Figure 3.** Cell abundances for diatoms (pennates, centrics, and *Pseudo-nitzschia*) and dinoflagellates for EX1 (top left) and EX2 (top right), and diatom and dinoflagellate relative cell abundances for EX1 (bottom left) and EX2 (bottom right). *Pseudo-nitzschia*, a dominant bloom forming species in Monterey Bay, responded well to groundwater treatments (statistically significant against initial using ANOVA and Tukey's  $p \leq 0.05$ ) in EX2 and the silicate plus nitrate treatment. While the cell abundances in EX2 followed the trends seen in chlorophyll. Shaded column in total cell concentration denote statistical significance (ANOVA and Tukey's  $p \leq 0.05$ ) from the initial. See Supporting Information Figure 2 for significance of each group from the initial.

(504.9–598.8  $\mu\text{M}$ ) concentration ranges overlap with a maximum range in the final treatment  $>90 \mu\text{M}$ . Error associated with analyzing very high nitrate concentrations (5% error above 300  $\mu\text{M}$ ) can also account for these observed increases, which were not statistically significant.

In EX2, the 10% groundwater treatment showed the largest decrease for nitrate,  $25 \pm 9 \mu\text{M}$ , and the ammonium treatment showed the smallest decrease ( $0.22 \pm 0.05 \mu\text{M}$ ). The control decreased  $0.05 \pm 0.19 \mu\text{M}$ . The 10% groundwater, 5% groundwater, 1% groundwater, nitrate, and nitrate + silica treatments all decreased more than could be accounted for by ocean water, indicating phytoplankton utilized nitrate supplied by the groundwater and nutrient additions. All of the decreases in nitrate were statistically significant except for the 5% groundwater treatment.

Ammonium decreased in all treatments for EX1, except for the 50% groundwater treatment, which showed a nonsignificant increase. Change in concentration of ammonium was statistically significant for the control, ammonium, vitamin B12, iron, and 10% groundwater treatments. In EX2, decreases in ammonium were observed only in the ammonium and 5% groundwater treatments. All other treatments showed an increase in ammonium concentration. Changes observed in the control, nitrate + silica, nitrate, silica, ammonium, and 10% groundwater treatments were significant. Changes observed in ammonium are likely due to the combined effects of excretion, cell lysis, and consumption of ammonium by phytoplankton during growth.

Overall, phytoplankton in our experiments were nitrogen limited and nitrate (but generally not ammonium) supplied by the treatments, either as nutrient additions or from groundwater, was utilized by the residing phytoplankton and supported growth. The largest decreases in nitrate were observed when silica was also provided and both nutrients

were drawn down simultaneously, suggesting colimitation of Si and N for the diatom population that is utilizing the nitrate. Like nitrate, silica concentrations often decreased beyond what could have been supplied by ocean water, indicating that SGD is likely supplementing the biological nutrient demand, particularly during blooms of diatoms.

N/Si drawdown ratios observed in the 1% groundwater, 5% groundwater, 10% groundwater, and nitrate + silica treatment groups of EX2 are very similar to Redfield ratios expected for diatoms (1:1). Ammonium and nitrate treatment groups (which had similar silica concentrations to those in Monterey Bay water) exhibited an N/Si drawdown ratio higher than that expected for diatoms. The lower silica concentrations in Monterey Bay water and these treatments likely limited the growth of diatoms in these treatment groups. Interestingly the ratio of N/Si in groundwater is very similar to the ratio required by diatoms, and to the N/Si drawdown ratios observed in the 1% groundwater, 5% groundwater, 10% groundwater, and nitrate+silica treatment groups. SGD at our study site provides nitrogen and silica in optimal ratios for Monterey Bay sourced diatoms used in our experiments, whereas ocean water from Monterey Bay was depleted in silica relative to nitrogen, potentially limiting the growth of bloom-forming diatoms.<sup>42</sup>

**Phytoplankton Abundance.** Phytoplankton abundance of the most common groups *Pseudo-nitzschia*, dinoflagellates, centric diatoms, and pennate diatoms (other than *Pseudo-nitzschia*) in our incubation experiments are shown in Figure 3 (concentration data and statistical significance for each group show in Supporting Information Figure 2). *Pseudo-nitzschia* is of particular interest to this study due to its tendency to form blooms in Monterey Bay, and is therefore given its own category. The increase in total cell abundances of these phytoplankton groups observed in both EX1 and EX2 is consistent with the chlorophyll *a* results (although more

robustly for EX2). The response of the phytoplankton to the groundwater (except for 50% groundwater) and groundwater-like (nitrate+silica) treatments suggests that the phytoplankton concentration increased more when both high concentrations of nitrate and silica were provided. This is supported by the statistically significant increases in total cell concentrations (Figure 3) with the nitrate and silica containing treatments. Phytoplankton growth was also seen in treatments receiving only nitrogen, but with a muted response compared to treatments with both nitrogen and silica. While the nitrate + silica treatment is statistically different from the nitrate treatments, the other nitrogen and silica containing treatments (groundwater treatments) were not statistically different from the nitrate treatment.

Phytoplankton relative abundance present in Monterey Bay (and in our baseline incubation water) was different in EX1 and EX2, with centric diatoms more dominant in EX1 and *Pseudo-nitzschia* more dominant in EX2. This is probably due to seasonal changes in phytoplankton abundance within Monterey Bay. However, despite the differences in initial phytoplankton composition, both experiments showed a shift toward increased abundance of diatoms with time, although not all diatom increases are not statistically significant (Supporting Information Figure 2). The shifts observed are consistent with the nutrient drawdown results that indicate growth of diatoms (e.g., drawdown of both nitrate and silica coupled with increasing chlorophyll *a*). Interestingly, in EX2 all of the nitrate and silica containing treatments showed a significant increase in *Pseudo-nitzschia* with time, while other centric diatoms only significantly increase in the nitrate treatment (Supporting Information Figure 2). This supports that the total cell concentration increase for the nitrate and silica containing treatments are due to an increase in *Pseudo-nitzschia* while the increase in the nitrate only treatment was due to increases in centric diatoms (Figure 3).

**Flow Cytometry.** Flow cytometry results are shown in Supporting Information (Figure 3). For both EX1 and EX2 the increases in chlorophyll *a* observed did not correspond with increases in picoplankton concentrations, indicating *Synechococcus* and Picoeukaryotes were not responsible for the chlorophyll *a* increases observed in the nitrogen and groundwater treatments. In contrast, these species showed the most positive response to ammonium, urea, and phosphate additions, which are less enriched in groundwater and thus SGD is not expected to increase the growth of these nonbloom-forming taxa.

**SGD Fluxes and Phytoplankton Demand.** The growth of bloom forming phytoplankton *Pseudo-nitzschia* is enhanced by nitrate and silica addition as shown by our bioassay incubation experiments. These nutrients are elevated in groundwater compared to seawater at Sunset State Beach, located in the heart of NMB. The extremely high levels of nitrate in the fresh groundwater (up to 1186.6  $\mu\text{M}$ ), prior to its dilution by low nutrient seawater forming the brackish to saline groundwater, suggest an anthropogenic source of nitrate. This is further supported by the presence of agriculture and extensive urban/suburban development on the land above the aquifer from which the groundwater was collected. The elevated silica concentrations in groundwater are likely due to dissolution of aquifer rock material and are typical of many groundwater samples.<sup>45</sup> Radium mass balance models indicate submarine groundwater is consistently discharging in this area throughout the year, providing nitrate and silicate to NMB,

even when other nutrient sources (upwelling and rivers) are at a minimum.

To put this study into context, we performed a scaling analysis to estimate the distance from shore that SGD could substantially influence NMB. For this analysis we used the 1% groundwater treatment as our benchmark, as it represents the most conservative addition of both nitrate and silica to still elicit a positive growth response from phytoplankton. The initial concentrations of nitrate and silica in the 1% groundwater treatments were 7.0 ( $7.0 \times 10^{-3} \text{ mol m}^{-3}$ ) and 7.7  $\mu\text{M}$  ( $7.7 \times 10^{-3} \text{ mol m}^{-3}$ ). Dividing the SGD nutrient fluxes (2.6–3.9  $\text{mol m}^{-1} \text{ day}^{-1}$  nitrate and 3.7–8.3  $\text{mol m}^3 \text{ day}^{-1}$  silica) by the depth of the mixed layer (4 m) and the nutrient concentrations, yields the distance from shore SGD increases the nutrient concentrations to the 1% treatment level. This yields distances of 90–140 m for nitrate and 120–270 m for silica, at least for our study site.

The implication of the scaling analysis is that the influence of SGD is limited to very close to shore, a spatial scale smaller than would be detectable by satellite remote sensing. We suggest that there are three possible ways that SGD could impact phytoplankton ecology in NMB. The first is that nutrients sourced from SGD maintain a seed population of phytoplankton which bloom when supplemented by other nutrient sources such as pumping of deep nutrient-rich water from Monterey Canyon, inflow of a wind-driven upwelling filament, or a flush of nutrients from runoff from the first seasonal rains. A second possibility is that some (spatially restricted) parts of NMB mix less (have longer residence times) or experience more focused flow of SGD (higher discharge), which would contribute greater nutrient inputs relatively to the volume of water affected. A third possibility is that while not providing enough nutrients to initiate a bloom, SGD can spur growth of diatoms (including *Pseudo-nitzschia*, which need not bloom to result in negative impacts), as observed in the incubation experiments. Regardless of the mechanism, our results are consistent with the hypothesis that SGD can contribute to the persistent formation and maintenance of algal blooms within the NMB by providing a persistent source of nutrients throughout the year.

## ■ ASSOCIATED CONTENT

### 📄 Supporting Information

Map of the sampling sites overlaid on a land use map, cell concentrations of each of the major groups of diatoms and dinoflagellates, cell concentrations of *Synechococcus* and Picoeukaryotes in each experiment, water quality data used for the box models, nutrient concentrations for groundwater and bay water used in each experiment, and initial nutrient concentrations after treatment additions. The Supporting Information is available free of charge on the ACS Publications website at DOI: 10.1021/acs.est.5b00909.

## ■ AUTHOR INFORMATION

### Corresponding Author

\*E-mail: alecher@ucsc.edu. Phone: 727.421.4080.

### Notes

The authors declare no competing financial interest.

## ■ ACKNOWLEDGMENTS

This project was funded by the California Sea Grant award 035-CONT-N to A.P., A.F., J.R., and R.K. Technical support for the

incubation experiments was provided by the UCSC Long Marine Lab, and access and equipment required to sample the monitoring wells was provided by the Pajaro Valley Water Management Agency. We would also like to thank the undergraduate, graduate, and post graduate researchers who assisted with the field work, and Ryan Harmon who acquired and processed the data for Supporting Information Figure 1.

## REFERENCES

- (1) Wooster, W. S.; Reid, J. L. Eastern boundary currents. *The Sea*; Hill, M. N., Ed.; Interscience: New York, 1963; Vol. 2, pp 253–280.
- (2) Barber, R.; Smith, R. L. Coastal upwelling ecosystems. In *Analysis of Marine Ecosystems*; Longhurst, A. R., Ed.; Academic Press: New York, 1981; pp 31–68.
- (3) Pennington, J. T.; Chavez, F. Seasonal fluctuations of temperature, salinity, nitrate, chlorophyll and primary production at station H3/M1 over 1989–1996 in Monterey Bay, California. *Deep Sea Res., Part II* **2000**, *47*, 947–973.
- (4) Kudela, R. M.; Chavez, F. P. Modeling the impact of the 1992 El Nino on new production in Monterey Bay, California. *Deep Sea Res., Part II* **2000**, *47*, 1055–1076.
- (5) Chavez, F.; Strutton, P.; Friederich, G.; Feely, R.; Feldman, G.; Foley, D.; McPhaden, M. Biological and chemical response of the equatorial pacific ocean to the 1997–98 El Nino. *Science* **1999**, *286*, 2126–2131.
- (6) Breaker, L. C.; Broenkow, W. W. The circulation of Monterey Bay and related processes. *Oceanogr. Mar. Biol.* **1994**, *32*, 1–64.
- (7) Rosenfeld, L. K.; Schwing, F. B.; Garfield, N.; Tracy, D. E. Bifurcated flow from an upwelling center: A cold water source for Monterey Bay. *Cont. Shelf Res.* **1994**, *14*, 931–964.
- (8) Ramp, S. R.; Paduan, J. D.; Shulman, I.; Kindle, J.; Bahr, F. L.; Chavez, F. Observations of upwelling and relaxation events in the northern Monterey Bay during August 2000. *J. Geophys. Res., C: Oceans Atmos.* **2005**, *110*, 1–21.
- (9) Ryan, J. P.; Fischer, A. M.; Kudela, R. M.; Gower, J. F. R.; King, S. a.; Marin, R.; Chavez, F. P. Influences of upwelling and downwelling winds on red tide bloom dynamics in Monterey Bay, California. *Cont. Shelf Res.* **2009**, *29*, 785–795.
- (10) Ryan, J. P.; McManus, M. a.; Kudela, R. M.; Lara Artigas, M.; Bellingham, J. G.; Chavez, F. P.; Doucette, G.; Foley, D.; Godin, M.; Harvey, J. B. J.; et al. Boundary influences on HAB phytoplankton ecology in a stratification-enhanced upwelling shadow. *Deep Sea Res., Part II* **2014**, *101*, 63–79.
- (11) Ryan, J.; Greenfield, D.; Marin, R., III; Preston, C.; Roman, B.; Jensen, S.; Pargett, D.; Birch, J.; Mikulski, C.; Doucette, G.; et al. Harmful phytoplankton ecology studies using an autonomous molecular analytical and ocean observing network. *Limnol. Oceanogr.* **2011**, *56*, 1255–1272.
- (12) Woodson, C. B.; Eerkes-Medrano, D. I.; Flores-Morales, A.; Foley, M. M.; Henkel, S. K.; Hessing-Lewis, M.; Jacinto, D.; Needles, L.; Nishizaki, M. T.; O'Leary, J.; et al. Local diurnal upwelling driven by sea breezes in northern Monterey Bay. *Cont. Shelf Res.* **2007**, *27*, 2289–2302.
- (13) Shea, R. E.; Broenkow, W. W. The role of internal tides in the nutrient enrichment of Monterey Bay, California. *Estuarine, Coastal Shelf Sci.* **1982**, *15*, 57–66.
- (14) Ryan, J. P.; Johnson, S. B.; Sherman, A.; Rajan, K.; Py, F. P.; Thomas, H.; Harvey, J. B. J.; Bird, L.; Paduan, J. D.; Vrijenhoek, R. C. Mobile autonomous process sampling within coastal ocean observing systems. *Limnol. Oceanogr. Methods* **2010**, *8*, 394–402.
- (15) Kudela, R. M.; Lane, J. Q.; Cochlan, W. P. The potential role of anthropogenically derived nitrogen in the growth of harmful algae in California, USA. *Harmful Algae* **2008**, *8*, 103–110.
- (16) Kudela, R. M.; Dugdale, R. C. Nutrient regulation of phytoplankton productivity in Monterey Bay, California. *Deep Sea Res., Part II* **2000**, *47*, 1023–1053.
- (17) Mackey, K. R. M.; van Dijken, G. L.; Mazloom, S.; Erhardt, A. M.; Ryan, J.; Arrigo, K. R.; Paytan, A. Influence of atmospheric nutrients on primary productivity in a coastal upwelling region. *Global Biogeochem. Cycles* **2010**, DOI: 10.1029/2009GB003737.
- (18) Quay, J. E. New tools and insight for recognition of pseudonitzschia bloom and toxin incidence. PhD. Dissertation, University of California Santa Cruz, Santa Cruz, CA, 2011.
- (19) Jessup, D. A.; Miller, M. A.; Ryan, J. P.; Nevins, H. M.; Kerkering, H. A.; Mekebr, A.; Crane, D. B.; Johnson, T. A.; Kudela, R. M. Mass stranding of marine birds caused by a surfactant-producing red tide. *PLoS One* **2009**, *4*, No. e4550, DOI: 10.1371/journal.pone.0004550.
- (20) Ryan, J. P.; Gower, J. F. R.; King, S. A.; Bissett, W. P.; Fischer, A. M.; Kudela, R. M.; Kolber, Z.; Mazzillo, F.; Rienecker, E. V.; Chavez, F. P. A coastal ocean extreme bloom incubator. *Geophys. Res. Lett.* **2008**, *35*, No. L12602.
- (21) Mackey, K. R. M.; Mioni, C. E.; Ryan, J. P.; Paytan, A. Phosphorus cycling in the red tide incubator region of Monterey Bay in response to upwelling. *Front. Microbiol.* **2012**, *3*, 33.
- (22) Eittrheim, S.; Anima, R.; Stevenson, A. Seafloor geology of the Monterey Bay area continental shelf. *Mar. Geol.* **2002**, *181*, 3–34.
- (23) Moore, W. S. The subterranean estuary: A reaction zone of ground water and sea water. *Mar. Chem.* **1999**, *65*, 111–125.
- (24) Shellenbarger, G.; Monismith, S.; Genin, A.; Paytan, A. The importance of submarine groundwater discharge to the nearshore nutrient supply in the Gulf of Aqaba (Israel). *Limnology* **2006**, *51*, 1876–1886.
- (25) Black, F. J.; Paytan, A.; Knee, K. L.; De Sieyes, N. R.; Ganguli, P. M.; Gray, E.; Flegal, A. R. Submarine groundwater discharge of total mercury and monomethylmercury to central California coastal waters. *Environ. Sci. Technol.* **2009**, *43*, 5652–5659.
- (26) Knee, K.; Street, J. H.; Grossman, E. G.; Paytan, A. Nutrient inputs to the coastal ocean from submarine groundwater discharge in a groundwater-dominated system: Relation to land use (Kona coast, Hawaii, U.S.A.). *Limnol. Oceanogr.* **2010**, *55*, 1105–1122.
- (27) Null, K. a.; Dimova, N. T.; Knee, K. L.; Esser, B. K.; Swarzenski, P. W.; Singleton, M. J.; Stacey, M.; Paytan, A. Submarine groundwater discharge-derived nutrient loads to San Francisco Bay: Implications to future ecosystem changes. *Estuaries Coasts* **2012**, *35*, 1299–1315.
- (28) Hosono, T.; Ono, M.; Burnett, W. C.; Tokunaga, T.; Taniguchi, M.; Akimichi, T. Spatial distribution of submarine groundwater discharge and associated nutrients within a local coastal area. *Environ. Sci. Technol.* **2012**, *46*, 5319–5326.
- (29) Taniguchi, M.; Burnett, W. C.; Cable, J. E.; Turner, J. V. Investigation of submarine groundwater discharge. *Hydrol. Processes* **2002**, *16*, 2115–2129.
- (30) *Geohydrologic Framework of Recharge and Seawater Intrusion in the Pajaro Valley, Santa Cruz and Monterey Counties, California*, Water Resources Investigation Report 03-4096; United States Geological Survey: Sacramento, CA, 2003; <http://pubs.usgs.gov/wri/wri034096/pdf/wri034096.pdf>.
- (31) Moore, W. S. Fifteen years experience in measuring <sup>224</sup>Ra and <sup>223</sup>Ra by delayed-coincidence counting. *Mar. Chem.* **2008**, *109*, 188–197.
- (32) Moore, W.; Arnold, R. Measurement of <sup>223</sup>Ra and <sup>224</sup>Ra in coastal waters using a delayed coincidence counter. *J. Geophys. Res.* **1996**, *101*, 1321–1329.
- (33) Garcia-Solsona, E.; Garcia-Orellana, J.; Masqué, P.; Dulaiova, H. Uncertainties associated with <sup>223</sup>Ra and <sup>224</sup>Ra measurements in water via a delayed coincidence counter (RaDeCC). *Mar. Chem.* **2008**, *109*, 198–219.
- (34) Paytan, A.; Shellenbarger, G. Submarine groundwater discharge: An important source of new inorganic nitrogen to coral reef ecosystems. *Limnology* **2006**, *51*, 343–348.
- (35) Moore, W. Using the radium quartet for evaluating groundwater input and water exchange in salt marshes. *Geochim. Cosmochim. Acta* **1996**, *60*, 4645–4652.
- (36) Moore, W. S. Sources and fluxes of submarine groundwater discharge delineated by radium isotopes. *Biogeochemistry* **2003**, *66*, 75–93.

- (37) Graham, W. M.; Largiert, J. L. Upwelling shadows as nearshore retention sites: the example of northern Monterey Bay. *Cont. Shelf Res.* **1997**, *17*, 509–532.
- (38) Karlson, B., Cusack, C., Bresnan, E., Eds. *Microscopic and Molecular Methods for Quantitative Phytoplankton Analysis*, IOC Manuals and Guides, No. 55.; Intergovernmental Oceanographic Commission, UNESCO: Paris, 2010.
- (39) Taylor, J. R. *An Introduction to Error Analysis*; University Science Books: Sausalito, CA, 1997.
- (40) De Sieyes, N.; Yamahara, K.; Layton, B.; Joyce, E.; Boehm, A. Submarine discharge of nutrient-enriched fresh groundwater at Stinson Beach, California is enhanced during neap tides. *Limnol. Oceanogr.* **2008**, *53*, 1434–1445.
- (41) Lane, J.; Raimondi, P.; Kudela, R. Development of a logistic regression model for the prediction of toxigenic *Pseudo-nitzschia* blooms in Monterey Bay, California. *Mar. Ecol.: Prog. Ser.* **2009**, *383*, 37–51.
- (42) Mackey, K. R. M.; Chien, C.-T.; Paytan, A. Microbial and biogeochemical responses to projected future nitrate enrichment in the California upwelling system. *Front. Microbiol.* **2014**, *5*, 1–13.
- (43) Nicholson, D.; Dyhrman, S.; Chavez, F.; Paytan, A. Alkaline phosphatase activity in the phytoplankton communities of Monterey Bay and San Francisco Bay. *Limnol. Oceanogr.* **2006**, *51*, 874–883.
- (44) Brzezinski, M. A. The Si:C:N of marine diatoms: Interspecific variability and the effect of some environmental variables. *J. Phycol.* **1985**, *21*, 347–357.
- (45) Haines, T.; Lloyd, J. Controls on silica in groundwater environments in the United Kingdom. *J. Hydrol.* **1985**, *81*, 277–295.



## OFFICE OF THE GOVERNOR

February 9, 2016

The Honorable Penny Pritzker  
Secretary, U.S. Department of Commerce  
1401 Constitution Ave NW  
Washington, D. C. 20230

Dear Secretary Pritzker:

California is experiencing an economic disaster to our fishing industry and communities due to a public health concern that has caused the closure of State-managed Dungeness crab and rock crab fisheries.

In 2015, a massive and persistent toxic algal bloom of phytoplankton caused Dungeness crab and rock crab from Santa Barbara to the Oregon border to accumulate dangerous levels of domoic acid. When ingested by people, this potent neurotoxin can cause nausea, diarrhea, vomiting, and in higher levels, memory loss, seizures, and even death.

In early November 2015, the California Office of Environmental Health Hazard Assessment and California Department of Public Health determined the unsafe levels of domoic acid found in crab tissue posed a human health risk and recommended delaying the opening of the Dungeness crab season and closing the rock crab season. In response, the California Department of Fish and Wildlife and California Fish and Game Commission took emergency regulatory action, closing the commercial and recreational fisheries in the affected areas until conditions improved to safe levels. Although we have reopened a limited number of sectors of the fisheries in the southern part of California, this is a small portion of the overall species' ranges. Persistent unsafe levels of domoic acid have resulted in the continued closure of the entire commercial Dungeness crab fisheries statewide and the commercial rock crab fisheries in the Channel Islands and northern part of the State.

Dungeness crab is one of the highest valued commercial fisheries in California. The direct economic impact from the commercial closures to date is estimated to be at least \$48.3 million for Dungeness crab and \$376,000 for rock crab, representing 71 percent of the total estimated commercial value of Dungeness crab and 37 percent of the total estimated value of the affected area of rock crab for the period from November 6, 2015 through June 30, 2016. This initial estimate is based on the average ex-vessel value of

GOVERNOR EDMUND G. BROWN JR. • SACRAMENTO, CALIFORNIA 95814 • (916) 445-2841



The Honorable Secretary Pritzker  
February 9, 2016  
Page 2

commercial landings over the previous five years and does not account for other commercial impacts or those of the fishing industry beyond commercial fisheries. Further, it is unclear when it will be safe to open the fisheries, and there is a growing possibility the commercial Dungeness crab season may remain closed for most or all of the 2015-16 season. Therefore, these initial estimates of impact are likely to increase.

Given the significant impacts to date, I request you declare a fishery resource disaster under section 308(d) of the Interjurisdictional Fisheries Act of 1986 (16 U.S.C. § 4107(d)), and a commercial fishery failure under section 312(a) of the Magnuson-Stevens Fishery Conservation and Management Act of 1976 (16 U.S.C. § 1861a(a)).

As you know, declaring a commercial failure will enable the fishing communities affected by the closure to receive essential economic assistance. Crabs are a vital component of California's natural resources and provide significant aesthetic, recreational, commercial, cultural, and economic benefits to our state. Economic assistance will be critical for the well-being of our fishing industry and our state. I also ask National Oceanic and Atmospheric Administration Fisheries to work directly with the California Department of Fish and Wildlife to expeditiously complete the required review process.

Thank you for your consideration of this critical issue.

Sincerely,

A handwritten signature in black ink, appearing to read "Edmund G. Brown Jr.", with a large, sweeping flourish at the end.

Edmund G. Brown Jr.